Electron Spin Resonance of Free Radicals formed from DNA and its Constituents on X-ray Irradiation: Influence of Matrices, Additives, Dose, Temperature and Time

Dissertation

zur Erlangung des Grades
des Doktors der Naturwissenschaften
der Naturwissenschaftlich-Technischen Fakultät III
Chemie, Pharmazie, Bio-und Werkstoffwissenschaften
der Universität des Saarlandes

von

Chandrima Pal

Saarbrücken

2008

Tag des Kolloquiums:	26.02.2009
Dekan:	Prof. Dr. Uli Müller
Berichterstatter:	Prof. Dr. J. Hüttermann
	Jun.-Prof. Dr. G. Jung

Contents

Abstract

Electron spin resonance (ESR) studies were performed on free radicals formed upon X ray irradiation on DNA, its constituents and model compounds like fluorouracil and its derivatives. One aim of this thesis was to understand the much debated mechanism of radical formation in irradiated frozen aqueous solutions of DNA. In things matrix, DNA separates from the bulk ice as an inhomogeneous mass and mimics biological conditions. Fluorouracil (FU) and its derivatives were used as model compounds utilizing the large fluorine hyperfine splitting as a tool of radical identification. Glassy low temperature matrices were employed for comparison with frozen aqueous solutions. Electron scavengers like $Na_2S_2O_8$ and $K_3Fe[CN]_6$ were used to enhance the contribution of oxidized radicals. This study gave evidence of direct irradiation action in the frozen aqueous system. The study was extended to frozen aqueous solutions containing DNA; where irradiation dose as well as electron and hole scavengers were used to modulate the formation of radicals. From spectra reconstruction utilizing isolated component patterns the formation of sugar based radicals and guanine cation radicals at low temperatures were observed which supports the direct effect of irradiation. Another aim was to study the hypothesis of electron transfer from DNA anions to the doped additives in post irradiation time phase. Time dependent quantitative ESR studies were done on DNA and on its complexes with mitoxantrone and riboflavin, deoxy ribonucleotides of thymine and cytosine and their complexes with mitoxantrone in 7 M LiBr glass. No transfer of electrons was observed but differential decay behavior with time of the radicals on DNA and the additive, respectively, was found.

Zusammenfassung

Elektronen Spin Resonanz (ESR) Untersuchungen wurden an den freien Radikalen durchgeführt, die nach Röntgenbestrahlung an der DNA, ihren Komponenten und an Modell-Substanzen, wie Fluoruracil und seinen Derivaten, gebildet werden. Ein Ziel dieser Arbeit war es, den vielfach diskutierten Radikalbildungsmechanismus in gefrorenen wässrigen DNA-Lösungen besser zu verstehen. In dieser Matrix separiert sich die DNA als inhomogene Masse vom Eis und bildet so biologische Bedingungen nach. Fluoruracil (FU) und seine Derivate stellten Modellsysteme dar, deren große Fluor-Hyperfeinaufspaltung zur Radikalidentifizierung genutzt wurde. Tieftemperatur-Gläser wurden zum Vergleich mit den gefrorenen wässrigen Lösungen bearbeitet. Elektronenfänger wie $Na_2S_2O_8$ und $K_3Fe[CN]_6$ wurden eingesetzt, um den Anteil oxidierter Radikale zu vergrößern. In dieser Untersuchung ergaben sich Hinweise auf eine direkte Strahlenwirkung im gefrorenen wässrigen System. Sie wurde auf gefrorene wässrige Lösungen von DNA ausgeweitet, wobei durch die Strahlendosis und den Einsatz von Elektron- und Loch-Fängern die Radikalbildung moduliert wurde. Aus der Spektrenrekonstruktion mit isolierten Mustern der Komponenten wurde auf die Bildung von Zuckerradikalen und Guanin Kationradikalen bei tiefen Temperaturen geschlossen, was auf die direkte Wechselwirkung der Strahlung hinweist. Ein weiteres Ziel war es, die Hypothese eines Elektronentransfers von den DNA-Anionen zu den zudotierten Additiven in der Zeit nach der Bestrahlung zu untersuchen. Zeitabhängige quantitative ESR-Untersuchungen wurden an DNA und ihren Komplexen mit Mitoxantron und Riboflavin, an Desoxyribonukleotiden des Thymins und Cytosins und deren Komplexen mit Mitoxantron in 7 M LiBr Glas durchgeführt. Es wurde kein Elektrontransfer beobachtet, sondern vielmehr ein zeitabhängiger differentieller Zerfall der Radikale an der DNA und am Additiv gefunden.

Summary

In this work continuous wave (CW) X-band electron spin resonance (ESR) spectroscopic investigations were performed on the free radicals formed upon X-ray irradiation at low temperatures on deoxyribonucleic acids (DNA), its constituents, complexes of DNA-chemical additives and other model compounds like fluorouracil (FU) and its derivatives. Different solvent matrices were used like frozen glasses e.g., 5 M Sulfuric acid (H_2SO_4), 7 M Beryllium fluoride (BeF_2), 7 M Lithium bromide (LiBr) and frozen aqueous (H_2O) solutions. One aim of the thesis was to gain more insight into the mechanism of DNA radical formation in frozen aqueous solutions. This has been approached by a comparative study of the model compound fluorouracil and its derivatives in glasses (5 M H_2SO_4, 7 M BeF_2) and in frozen aqueous solutions. The study was then extended to DNA in frozen aqueous solutions. Electron or hole scavenging additives and different irradiation doses were used to modulate the formation of free radicals upon irradiation. A detailed isolation of the ESR patterns for the free radicals formed allowed to estimate their relative distribution and their correlation with radical structures. Another aim of this study was to evaluate the possibility of electron transfer from DNA radicals to doped electron scavenging moieties (Mitoxantrone or Riboflavin) in frozen glass (7 M LiBr) solutions in post irradiation phase as a function of time.

Frozen aqueous solutions have often been used in ESR spectroscopic investigations but the mechanism of free radical formation in this matrix owing to its biphasic nature is under debate. Gregoli and coworkers (Gregoli, S., Olast, M. and Bertinchamps, A., *Radiation Research*, 1982, *89*, 238) emphasized the direct effect of irradiation in frozen aqueous solutions. Many subsequent studies have shown that indirect (via solvent matrix), quasi direct (via immediate hydration layer) or direct (to the substrate) mechanisms of radiation might be possible in frozen aqueous solutions containing DNA or its constituents. The overlapping natures of the ESR radical patterns from DNA and its constituents have often prohibited understanding of the radical structures. In this study Flurouracil (FU) and its derivatives 5-Fluoro-2′-deoxyuridine (FUdR), 5-fluorouridine (FUR) and 5-Fluoro-2′-deoxyuridine 5′-monophosphate (Na salt) (FdUMP) were used utilizing the large hyperfine splitting of fluorine nucleus. Formation of oxidized radicals on base and deoxyribose moieties provides information regarding

the direct type of radiation effects; thus, several electron scavengers were used here to enhance the contribution of the oxidized species. In 5 M H_2SO_4 glass containing $Na_2S_2O_8$, the N1 deprotonated neutral radical derived from the cation was observed in FU at 77 K. In FUdR and FdUMP deprotonation is not possible at N1 position owing to the presence of bulky groups; thus the base cation radical was formed at 77 K. Upon annealing to about 165 K an ESR pattern is observed in FUdR, FUR and FdUMP which can be correlated to a radical formed by $SO_4^{-•}$ additon at the C6 position of the FU base. Formation of sugar radicals like the C2'$^•$ radical or, tentatively, C5'$^•$ via H- abstraction from the C2' or C5' position of the deoxyribose part were observed for the first time in the FU derivatives dissolved in this glass matrix after annealing to 165 K. An asymmetric doublet pattern strongly correlating with O4 protonated FU anion radical was observed in all cases. In 7 M BeF_2 OH$^•$ radicals were trapped at 77 K; the radicals formed on FU were anions and 5-yl radicals. Upon annealing (> 165 K), a minor presence of OH addition radical at the C6 position of the FU base was observed. The final radical pattern (170-175 K) was the asymmetric doublet (tentatively from the O4 protonated anion) as described above. In FUdR and FdUMP formation of C1'$^•$ and C2'$^•$ radicals by loss of hydrogen from C1' and C2' position of the deoxyribose moiety could be ascribed to OH$^•$ attack at higher annealing temperatures. Addition of the electron scavenger $K_3Fe[CN]_6$ prevented the anion formation at 77 K and C1'$^•$ and C2'$^•$ sugar radicals pattern were isolated at 165-175 K. H-addition to C6 (5-yl radical) and OH$^•$ addition radical at C6 of FU base were also observed in FUdR and FdUMP upon annealing to higher temperatures (>140 K). FU could not be investigated in frozen aqueous solution owing to its poor solubility in water. Irradiation of FUdR and FdUMP in that matrix showed formation of the FU anion radical and 5-yl radicals along with OH$^•$ radicals at 77 K. Clear evidence of formation of C1'$^•$ radical from deoxyribose moiety was observed at 77 K in both FUdR and FdUMP unlike in 7 M BeF_2 glasses. Upon annealing to 140 K the OH addition radical at C6 position of FU was observed in contrast to its observation in 7 M BeF_2 only after annealing to 170 K. On addition of high concentrations of the electron scavenger $K_3Fe[CN]_6$ the formation of the FU anion was diminished strongly. The presence of neutral C1'$^•$ and C2'$^•$ sugar radicals was clearly observed at 77 K. The sugar radical patterns could be confirmed from their outer lines in FUdR/ FdUMP containing electron scavenger at 77 K. This difference in observation at 77 K between 7 M BeF_2

and frozen aqueous DNA points to the direct or quasi-direct effect of irradiation in frozen aqueous solutions unlike in frozen glasses.

The formation of free radicals on DNA irradiated in frozen aqueous solutions has been a topic of debate for about two decades. In this matrix DNA gets separated from the bulk ice forming an inhomogeneous mass; which might mimic the biological conditions in the nucleus of eukaryotic cells. Using electron scavengers like $K_3Fe[CN]_6$ (ESR silent) and Mitoxantrone (ESR active) as well as the hole scavenger $K_4Fe[CN]_6$ (ESR silent) the formation of radicals on DNA was modulated. In addition, the effect of dose and temperatures was probed as it was in pure DNA. As a result oxidized radicals were detected at low temperature upon irradiation on the DNA: guanine cations ($G^{+\bullet}$) and neutral radicals via loss of hydrogen from C1', C3' and C4'/C5' position of the deoxyribose moiety ($C1'^{\bullet}$, $C3'^{\bullet}$ and $C4'^{\bullet}/C5'^{\bullet}$). As reduced radicals at low annealing temperatures mainly cytosine anions or, more favorably, N3 protonated cytosine anion ($C^{\bullet}$ / $C(N3H^+)^{-\bullet}$) and thymine anions ($T^{-\bullet}$) were formed. A separation of these two radical patterns was not possible. Upon annealing secondary radicals like the 5-thymyl radical ($TH^{\bullet}$), the thymine allyl radical ($TCH_2^{\bullet}$) and peroxyl radicals (minor quantities, $ROO^{\bullet}$) were observed. Also, minor quantities of the guanine based $GN^{\bullet}$ radicals (successor of the guanine cation by deprotonation at N1) were observed but only in pure DNA upon irradiation with high doses and on annealing to high temperatures. The ESR patterns of most of these radicals could be isolated. Pure ESR component patterns representing the reduced base radicals like $C^{-\bullet}/C(N3)^{-\bullet}$ and $T^{-\bullet}$, neutral radicals from deoxyribose moieties ($C4'^{\bullet}/C5'^{\bullet}$) and allyl radicals ($TCH_2^{\bullet}$) could not be extracted from frozen aqueous system although traces of their formation were observed in the experimental spectra. These patterns were instead obtained from DNA in 7M LiBr glass/H_2O, 76% hydrated (H_2O) DNA and frozen aqueous solution of deuterated DNA respectively. The relative contribution of each radical with temperature, dose and with different additives could be analyzed. Contributions of charged radical species were found to decrease with increasing dose while neutral radicals remained constant in weight or were enhanced in pure DNA. Electron adducts were not formed on DNA in the presence of $K_3Fe[CN]_6$; the guanine cation radical and sugar radicals were present in major proportion instead. With increasing dose the guanine cation contribution was found to decrease much faster than in pure DNA. Sugar derived radicals were dominantly observed at higher doses. With $K_4Fe[CN]_6$ (1 Fe^{2+}:20 DNA nucleotide) the formation guanine cation radical was

diminished but the sugar radicals remained largely unscavenged. MX acted as a strong electron scavenger even when present in small concentrations (1MX:800 DNA nucleotides) and showed the expected effects on reduction of anion radicals. With increase in MX concentration (1MX:200 DNA nucleotides) formation of guanine cation radical also diminishes drastically; this cannot be explained properly. At high doses and high temperatures (260 K) the formation of allyl radicals is clearly observed in the experimental spectrum in frozen aqueous (H_2O) solutions.

Initial studies by Gregoli and coworkers (Gregoli, S., Olast, M. and Bertinchamps, A., *Radiation Research*, 1982, *89*, 238) postulated the formation guanine cations and thymine anions as two radical components in irradiated frozen aqueous DNA at 77 K. Many other studies since then and the results obtained from this thesis revealed the formation of many other radical components on frozen aqueous DNA. The formation of guanine cation and sugar radical patterns at low temperature shows a similarity of results between DNA and derivatives of FU in frozen aqueous solutions. This observation emphasizes on the existence of quasi direct or direct effect of irradiation. Two sugar derived radical patterns (C1'$^{\bullet}$, C3'$^{\bullet}$) could be isolated and traces of C4'$^{\bullet}$/C5$^{\bullet}$ could be observed from this study. Formation of some other radicals like N4 protonated cytosine anion $C(N4H^+)^{\bullet-}$ (Weiland, B. and Hüttermann, J., *International Journal of Radiation Biology*, 1998, *74*, 341), a radical formed by dephosphorylation at the C3' carbon of the deoxyribose (C3'$^{\bullet}_{dephos}$) and phosphate radical of type $ROPO_2^{\bullet}$ (Becker, D., Bryant-Friedrich, A., Trzasko, C. A. and Sevilla, M. D., *Radiation Research*, 2003, *16*, 174, Shukla, L. I., ,Pazdro, R., Becker, D. and Sevilla, M. D., *Radiation Research*, 2005, *163*, 591) which were reported in other studies were not observed in this work.

The hypothesis of electron transfer from DNA, e.g, to mitoxantrone as proposed earlier in the post irradiation phase (Messer, A., Carpenter, K., Forzley, K., Buchanan, J., Yang, S., Razskazovkii, Y., Cai, Z. and Sevilla, M. D., *The Journal of Physical Chemistry B*, 2000, *104*, 1128) was tested. A reinvestigation of free radical formation in DNA and in colyophillized mixtures of DNA with the additives mitoxantrone and riboflavin was performed in frozen glasses (7M LiBr/D_2O) at 77 K. Particularly the post irradiation time course of the respective free radical intensity residing at DNA or on the additive was probed. For both additives, different additive loadings and irradiation doses were employed. The observed relative change in contributions of DNA radicals and those from the additive to the experimental spectra with time could be described due to independent

differential decay of component radicals in both cases. Transfer of electrons from DNA to the additive moiety via electron tunneling mechanism as proposed earlier could not be supported from the results obtained from the detailed quantitative analysis of the experimental spectra using reconstruction techniques. Additional studies were performed with the nucleotides Thymidine 5'-monophosphate (TMP) and 2' deoxycytidine 5'-monophosphate (dCMP) and its mixtures with mitoxantrone in order to describe the time course in systems as they were expected to behave independently; the results supported the conclusions as obtained from DNA/ additive system. It was proposed that the post irradiation radical fading mechanisms involved liberation of radiation induced matrix trapped defects with time. These defects were ESR mute under the measured conditions and react with radicals by net radical destruction. The influence of decreasing the temperature on the decay favored the proposal but a clear quantitative description is still needed to be explored.

1. Introduction

Studying the effect of ionizing radiation on DNA has remained a subject of immense interest for last many decades. There are multiple reasons behind it. Living organisms in this earth are no longer exposed only to the natural ionizing radiations like from cosmic rays or through the radioactive elements present in the natural rocks but human beings have started harnessing ionizing radiation sources for several purposes. There has been a continuously increasing use of radiation in modern society especially in the fields of medicine, agriculture, food preservation, industries, power generation and in military. Along with the utilities of ionizing radiation it is needed to count its risks too. Ionization is a process by which a fast moving quantity of energy transfers through few atoms of a material and in turn creates electrically charged ions. In living matter, the nucleic acid moieties are most drastically affected by Ionizing radiation, it takes a fraction of seconds for the ionizing sources to ionize the atoms but this process can cause several physico-chemical changes which include initial energy deposition in the living matter causing excitation of the electrons to the higher energy levels and further ionization of several atoms/molecules thus creating free radicals. These radicals undergo through several chemical changes and consequently leading to the severe biological damages namely a) structural damage leading to a breakage of phosphodiester bonds and subsequent single-strand break (ssb) or double strand break (dsb) and b) changes in information caused by the radiation chemical modification of individual bases (von Sonntag 1987). Both types of damages can be lethal and may lead to mutagenesis, cell death and cancer. Identification and quantification of these risks becomes particularly difficult in cases where radiation exposure is at a low dose rate for a long period of time. To understand, determine and predict the long term biological endpoints and effects it becomes significant to unveil the entire pathway of interaction of ionization radiation with the nucleic acid entities in the biophysical, chemical, biochemical and in biological levels.

In this perspective it becomes important to identify all the free radicals on DNA bases and on the sugar moieties formed upon irradiation, the mechanism of formation of free radicals on DNA in a cellular medium and in model systems, the effect of the surrounding medium, how and to what extent the electrons and hole produced during irradiation migrate in the DNA double helix before being trapped and the distribution of

the trapping sites. Eventually decoding the primary events which takes place during and within few seconds (biochemical time phase) after irradiation can plays a crucial role in understanding many biological effects of ionization in a living body.

Along with the biological relevance, the topic of charge transfer in DNA in recent scientific advancements plays a growing role in the development of DNA chips detecting single base mismatches or various DNA lesions by electrochemical readout methods. Most recently, investigations are going on to elucidate how DNA can be modified in order to enhance its electron transfer capacities for new nano technological devices based on DNA or designs inspired by DNA like artificial molecular switches (Wagenknecht 2005).

The main obstacle for studying the primary events caused due to ionization in living matter is the immensely short time frame (10^{-12}-10^{-6}s) of their existence. To simplify the situation and to access the very short lived radicals, model system study in very low temperatures has become a popular approach to gather ample amount of information about the topic of early effects of radiation on DNA. Cryogenic (low-temperature) electron spin resonance (ESR) spectroscopy has been a major technique in deciphering the free radical reactions that follow the irradiation of DNA in model systems.

1.1. Outline of the Thesis

This thesis deals with the cryogenic X- band (9.5 GHz) ESR spectroscopic investigation of the effect of X irradiation on DNA and its constituents in different frozen matrices namely frozen aqueous solutions and frozen glass solutions. Both matrices are considered to be good models for understanding the effect of irradiation and for identification of free radicals formed on DNA and other bio molecules.

ESR spectroscopy of irradiated DNA and its constituents at low temperatures has always remained a topic of continuous interest owing to the overlapping nature of the spectral fingerprints of the free radicals formed in the system. The ambiguity also lies on understanding the mechanism of irradiation on matrix for example in frozen aqueous solutions and on the behavior of the DNA based radicals formed after irradiation. In this

thesis a further approach is taken to gain more insight on the present status of the subject.

This thesis consists of details (chapter 2) on theoretical backgrounds of the radiation biology (section 2.1), basics of ESR spectroscopy (section 2.2) and its application on identifying organic free radicals on irradiated DNA systems with some basics about structure of DNA (section 2.3). The literature review (chapter 3) explains the different developmental steps in the field of DNA study by using different techniques of ESR spectroscopy and irradiation sources. More specific review of literature is also provided for the themes particularly about mechanism of radiation in frozen aqueous system containing DNA model components or DNA (Section 3.1.1 and 3.1.2) itself and the extent or possibility of electron transfer from DNA to doped chemical additives after irradiation is completed in time scale (Section 3.1.3). These are the main topics which have been further dealt with in this thesis. Section 3.2 provides the motivation and the approach to deal with these two specific problems. Chapter 4 is about the materials and methods, it gives a list of all the chemicals used for carrying the different projects considered in this thesis and details about different experimental methodologies and computer simulation processes which were used. Chapter 5 consists of the results and is divided into four sections starting from the results in section 5.1 obtained from the comparative study of 5-Fluorouracil (used as a model system) and its components in frozen aqueous and frozen glass solutions, in section 5.2 results from ESR spectroscopy on frozen aqueous solutions containing pure DNA or DNA and various additives ($K_3Fe[CN]_6$, Mitoxantrone and $K_4Fe[CN]_6$) are given. Effect of different doses of X-ray and increase in temperature through stepwise annealing on the formation of radicals and on the modulation of radical balance has also been detailed in this section. The results are compared between fluorouracil and its derivatives and DNA systems in frozen aqueous system. Results on the probability of electron transfer reaction from irradiated DNA radicals to the intercalated or non intercalated doped electron scavengers with increasing time at low temperatures has been given in section 5.3 and models are provided which contradicts the results as obtained from other study (Messers et. al. 2000.). Each section ends with detailed discussion about the results obtained and has been correlated or compared with other studies which has been reported on these topics. Conclusions on the observations of above mentioned themes are provided in chapter 6 and a short outlook has been provided at the end explaining about further

perspectives and experiments which can be carried out in these topics. An appendix is added giving a short literature review, results and discussions about the formation of primary radicals formed on the DNA nucleotides upon irradiation in 7 M LiBr frozen glass. Information is given on further studies done to know whether any secondary reactions occur upon annealing via oxidation from mobilized holes of the matrix. These systems were studied to understand how the solvent matrix influences the radical balance in the irradiated substrates upon increasing temperatures.

2. Theoretical Background

2.1. Radiation Biology

2.1.1. Basic Concepts of Radiation

Radiation can be defined as the process of emission of energy in the form of waves or particles. Various types of radiation can be distinguished, depending on the properties of the emitted energy/matter, the type of the emission source, properties and purposes of the emission, etc. Sources of irradiation are broadly classified as non ionizing radiation and ionizing radiation. Ionization is the physical process of converting an atom or molecule into an ion by changing the difference between the number of protons and electrons. A positive electric charge or ion is produced when an electron bound to an atom or molecule absorbs enough energy from an external source to escape from the electric potential barrier that originally confined it. The amount of energy required being equal to the Ionization potential. A negative electric charge or ion is produced when a free electron collides with an atom and is subsequently trapped inside the electric potential barrier, releasing any excess energy which in turn is known as electron affinity.

Non Ionizing Radiation

Non-ionizing radiation are referred to any type of electromagnetic radiation that does not carry enough energy to ionize atoms or molecules. Examples of non-ionizing radiations are visible light, near ultraviolet, infrared, microwave and radio waves. Though to some extent visible and near ultraviolet can ionize some molecules. The light from the sun that reaches the earth is largely non-ionizing radiation, with the notable exception of some ultraviolet rays. The absorption of energy from non-ionizing radiation depends in general on the molecular structure of the medium and only indirectly on the atomic composition.

Ionizing Radiation

Radiation produced by highly energetic particles or photons which can remove electron from the outer orbit of an atom or molecule with which they interact are known as ionizing radiation.
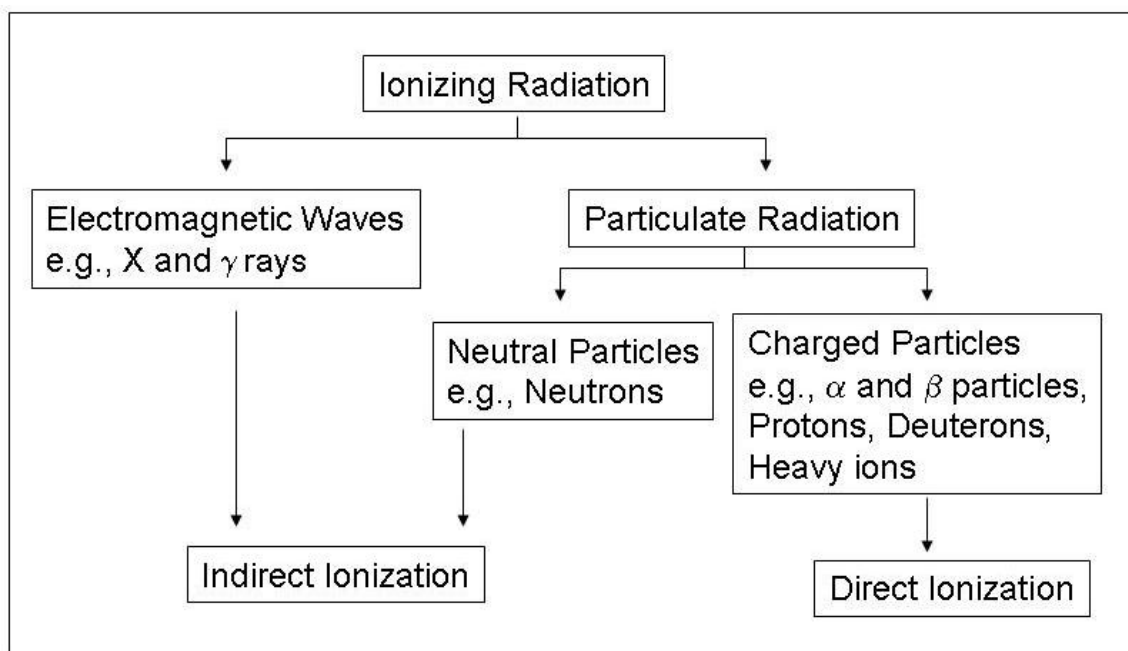
Scheme 2.1.1. Different categories of radiation and their examples.

In this type of radiation most of the energy is absorbed in the medium to eject electrons from the atoms of the material and the process is almost entirely dependent on the atomic composition and not on the molecular structure of the medium. Energetically charged particles capable of causing ionization are electrons, protons, neutrons, alpha (doubly charged ^{4}He ion) and other heavy particles. Electromagnetic radiations (high energy photons) which can ionize atoms or molecules are X rays and γ rays. They form the high frequency portion of the electromagnetic radiation spectrum. Ionization caused by X rays, γ rays and neutrons are known as indirect ionization as these species are electrically neutral. Ionizing radiation can also be specified as densely ionizing such as heavy particle radiation which produces a large number of ions, secondary electrons, and excited molecules in the medium through which it passes, and as sparsely ionizing, for example electromagnetic radiation which produces excited molecules and secondary electrons by processes such as the photoelectric effect, Compton scattering, and pair production. **Scheme 2.1.1** shows different categories of ionizing radiations with examples. The rad is a unit of radiation dose. It stands for "radiation absorbed dose". It is superseded in the SI by the gray (1 rad = 0.01 gray (Gy) = 0.01 joule of energy absorbed per kilogram of tissue).

There are several processes by which ionizing radiation interacts with matter, through these processes the energy is transferred to the medium and this energy absorption consequently leads to the biological effects. These ionizations, if occurs frequentky, can be very destructive to living tissue, and can cause DNA damage and mutations.

In spite of dual nature (wave and particle) of electromagnetic radiation the phenomenon of ionization deals with the particle nature of electromagnetic radiation. The particle nature of light is visualized in the form of wave packet or a quantum of radiation (defined as photon) whose energy is given by the relation as shown below.

$$E = h\nu \tag{2.1.1}$$

Where h is Planck's constant (6.62 x 10^{-34}Js) and ν is frequency. Also from Einstein's equation

$$E = mc^2 \tag{2.1.2}$$

Combining the two equations gives the momentum of a photon and can be given as below.

$$mc = \frac{h\nu}{c} \tag{2.1.3}$$

2.1.2. Formation of High Energy Photons

X rays and γ rays are electromagnetic radiations consisting of streams of energetic photons with the capacity to produce ionizations. X ray is a term for high-energy electromagnetic radiation produced by energy transitions due to accelerating electrons with wavelengths of around 10^{-10} meters. The basic production of X rays is by accelerating electrons in order to collide with a metal target (usually tungsten, but sometimes molybdenum). Here the electrons suddenly decelerate upon colliding with the

metal target and if enough energy is contained within the electron it is able to knock out an electron from the inner shell of the metal atom and as a result electrons from higher energy levels then fill up the vacancy and X ray photons are emitted. This causes the spectral line part of the wavelength distribution. There is also a continuum bremsstrahlung (German; meaning breaking) which arises when an incident electron undergoes a Coulombic interaction scattering due to close collision with the target nucleus. In these types of collision considerable accelerations occur and the electron may be scattered through large angles. The electron loses energy by electromagnetic radiation, the energy of which depends on the electron-nucleus interaction. Photons with a range of energies are obtained and consequently a continuous spectrum. When medical X rays are being produced, a thin metallic sheet is placed between the emitter and the target, effectively filtering out the lower energy (soft) X rays. The resultant X ray is said to be hard. Soft X rays overlap with the range of extreme ultraviolet. The frequency of hard X rays is higher than that of soft X rays, and the wavelength is shorter. Because it is possible for some electron transitions to be of higher energy than some nuclear transitions, there is an overlap of hard X rays (high energy) with the range of "long"-wavelength (lower energy) gamma rays. Gamma rays form the highest-energy end of the electromagnetic spectrum. They are high-energy electromagnetic radiation produced from transition of a nucleus from an excited state to a more stable one. Since they are emitted during allowed, discrete transitions, γ ray spectra are line spectra, with no continuous background, as is found for X rays. Apart from the differences in their origins, X ray and γ ray interact similarly with matter. X ray has been utilized as ionization tool in this thesis.

2.1.3. Interactions of Photons with Matter

The interaction of X rays and γ rays with matter is divided into three main categories, whose importance depends on the energy of the photons. They are known as photoelectric effect, Compton scattering and pair production. The first two involve interactions of the photons with the electrons of the traversed material, whilst the last is an absorption event occurring within the strong nuclear field of the atom.

The Photoelectric Effect

This is the predominant mode of absorption for photons of low energy (less than 0.5 MeV[1]) where the photons interacts with a bound electron and is absorbed causing the ejection of the electron from its shell with energy given by the following relation.

$$E_e = h\nu - E_b$$

<div align="right">(2.1.4)</div>

Where hν is energy of photon in the beam; E_b is binding energy of the electron in atom and E_c, kinetic energy of the electron.

As various electrons in an atom have different binding energies (depending upon the energy levels), the energy of the ejected electrons (photoelectrons), will vary. For this effect to take place the electron to be ejected must be bound in a molecule or atom for conservation of the momentum carried by the photon, the nucleus has to act as third body. The probability for this process reaches its maximum when energy of photon coincides with the binding energy of the electron with which it interacts. **Fig. 2.1.1** shows the schematic representation of photoelectric effect in tungsten.
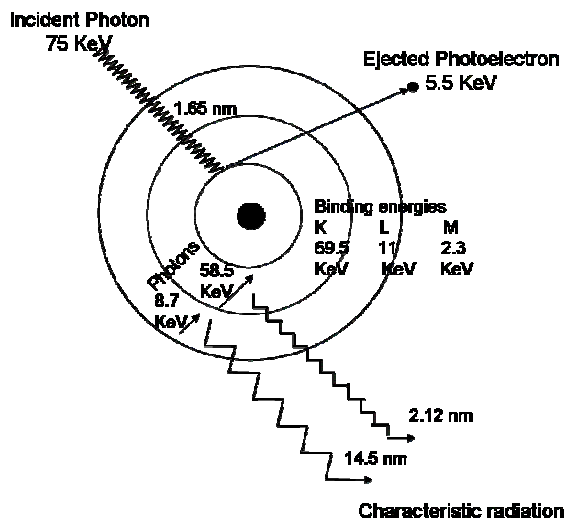
Fig. 2.1.1. Photoelectric effect in tungsten (von Sonntag 1987).

---

[1] The electronvolt (**eV**,) is the amount of kinetic energy gained by a single unbound electron when it passes through an electrostatic potential difference of one volt, in vacuum, (1 eV = 1.602 176 53 (14)$\times 10^{-19}$ J).

The Compton Effect

As the energy of incident photon beam increases from 0.5 MeV to ~ 10 MeV the most important type of interaction producing attenuation and absorption is Compton scattering. In contrast to the photoelectric effect, the characteristics of the Compton Effect are such that only a part of the incident energy is absorbed to eject an electron, usually called Compton electron. As a result of this interaction, the incident photon disappears; the energy is given to recoil the electron and a secondary photon is created with reduced energy propagating in a changed direction in order to conserve the energy and momentum before and after interaction. Here, the photon interacts with the outer electrons of the atom, which have low binding energy. By applying the principle of conservation of energy and momentum the change in photon wavelength, $\Delta\lambda$ is given as below.

$$\Delta\lambda = \left(\frac{h}{m_0 c}\right)\left(1 - \cos\theta^{'}\right) \qquad (2.1.5)$$

The energy of the scattered photon is given by the following equation.

$$h\nu^{'} = \frac{h\nu}{1 + (h\nu/m_0 c^2)(1 - \cos\theta^{'})} \qquad (2.1.6)$$

Here m_0 is the rest mass of an electron, ν and $\nu^{'}$ are, respectively, the frequencies of the incident and scattered photons, c is the velocity of light, h is the Planck's constant and $\theta^{'}$ is the angle of the scattered photon measured from its original direction. The scattered photon may interact further with matter either by Compton scattering or the photoelectric effect depending on its residual energy. **Fig. 2.1.2** shows the effect of Compton scattering.

$$E_1 = \frac{1}{2}MV^2$$

$$h\upsilon_1 = \frac{hc}{\lambda_1}$$

$$h\upsilon_2 = \frac{hc}{\lambda_2}$$
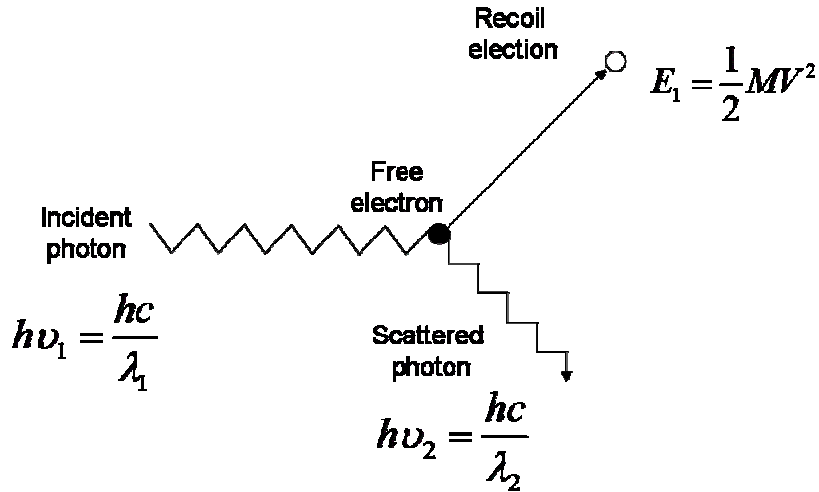
Fig. 2.1.2. Compton Scattering (von Sonntag 1987)

Pair Production

When the rest mass of an electron is 0.51 MeV c^2 and at photon energies in excess of 1.02 MeV, pair production occurs. In the cases of photoelectric and Compton effects, the interaction of the photons is always with electrons of the atoms. Pair production as shown in **Fig. 2.1.3** involves interaction of photons with the nucleus of the atom. Such an interaction results in complete disappearance of the incident photon and the appearance of a positron and an electron pair. This is an example of a physical process where energy is converted into mass.

The rest mass energy of an electron or positron is 0.511 MeV, hence for pair production to occur, the minimum photon energy must be 1.02 MeV. In pair production, no net electronic charge is created as the positron and electron have opposite charges. For photons of energy larger than 1.02 MeV, the excess energy is shared by the positron and electron in the form of kinetic energy.

$$h\nu = 1.02 MeV + E_{electron} + E_{positron} \qquad (2.1.7)$$

The positrons surrounded by a sea of electrons, are prone to annihilation and after several interactions (similar to those of electrons) which slow it down, it collides with electron and is annihilated. This process occurs mainly in the neighbourhood of the nucleus.
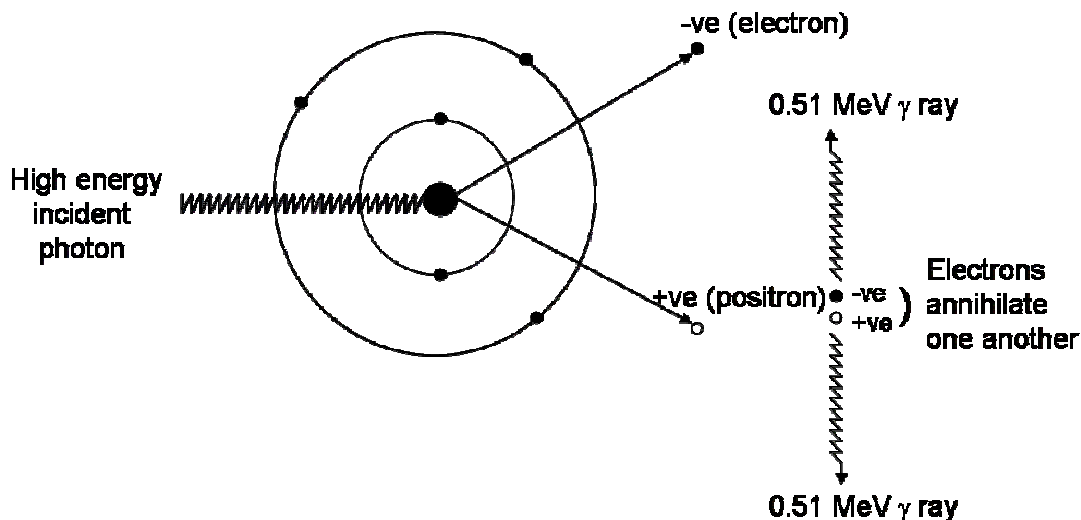
Fig. 2.1.3. Pair Production (von Sonntag 1987)

Auger Emission

On absorption of ionizing radiation when an electron is removed from a core level of an atom, leaving a vacancy, an electron from a higher energy level may fall into the vacancy, (known as Auger electron) resulting in a release of energy. Although sometimes this energy is released in the form of an emitted photon, the energy can also be transferred to another electron, which is then ejected from the atom. Upon ejection the kinetic energy of the Auger electron corresponds to the difference between the energy of the initial electronic transition and the ionization energy for the shell from which the Auger electron was ejected. These energy levels depend on the type of atom and the chemical environment in which the atom was located. It is a minor effect.

The probability of the various processes mentioned above depends on the energy of the photon and may require the nucleus as a third body. The contribution of the three processes to the absorption of the photon energy is not only a function of photon energy but also of the atomic number of the stopping matter (the probe for irradiation). **Fig. 2.1.4** shows the energy dependence of the various effects when carbon (which is a major component in biomolecules) is used as a stopping matter.
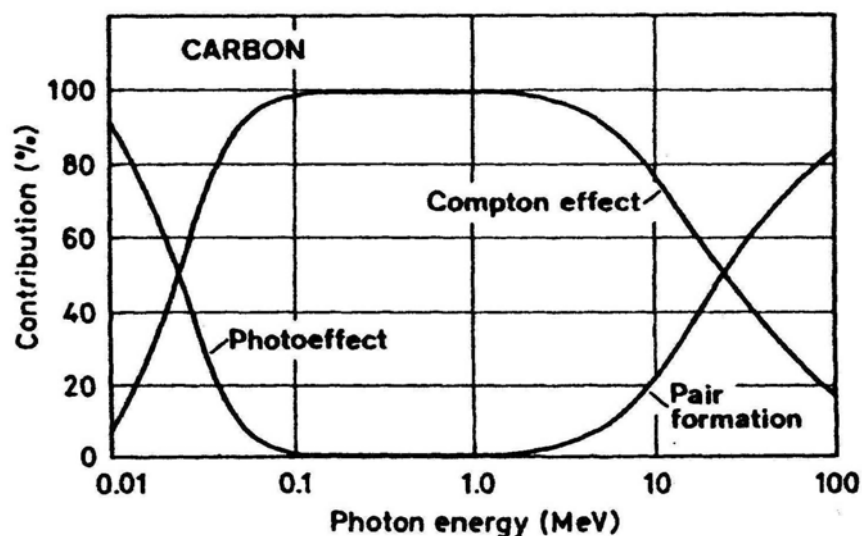
Fig. 2.1.4. Contributions of the Compton effect, photo effect and pair formation as a function of photon energy with carbon as stopping matter (von Sonntag, 1987).

When high energy radiations (e.g., X irradiation) traverses a solvated DNA molecule, the immediate effect is the ionization and excitation of the moieties of the molecules mainly via direct absorption and the Compton effect. The initial ionizations from the radiation result in release of high energy electrons which then cause further ionizations and excitations producing secondary electrons. Energetic secondary electrons then are the cause of most of the ionizations and subsequent damages to carbon containing biomolecules like DNA. The ionizations results in DNA anions and cation radicals as well as excitations.

2.1.4. Interaction of Charged Particles with Matter

The energy of the incident photon plays a decisive role about which of the above mentioned processes will dominate in their absorption. Regardless of the mechanism of the interaction involving protons, generation of secondary ionizing electron is an essential phenomenon. This production of electrons forbids the photons to travel straight through the matter without any penetration. All the chemical changes in a medium following photon irradiation are attributed to these electrons. The biological and biochemical effects thus observed in a system due to ionization are result of the processes lead by these electrons and their subsequent electron cascade.

2.1.5. Direct and Indirect Effect of Radiation

Direct Effect

The direct action of radiation as showed in **Fig.2.1.5A** involves the simple interaction between the ionizing radiation and critical biological molecules. In case when the critical target for irradiation is DNA, the direct effect involves, in principle, ionization of the DNA itself. The direct effect makes a significant contribution to DNA damage under the prevailing conditions in the nuclei of eukaryotic cells. This is because chromatin is tightly packed, the amount of unbound water is relatively small, and diffusible radical intermediates are efficiently scavenged. It has been estimated that the direct effect contributes 40-50% of the DNA damage responsible for viral or cell death (Purkayastha et. al. 2005b)
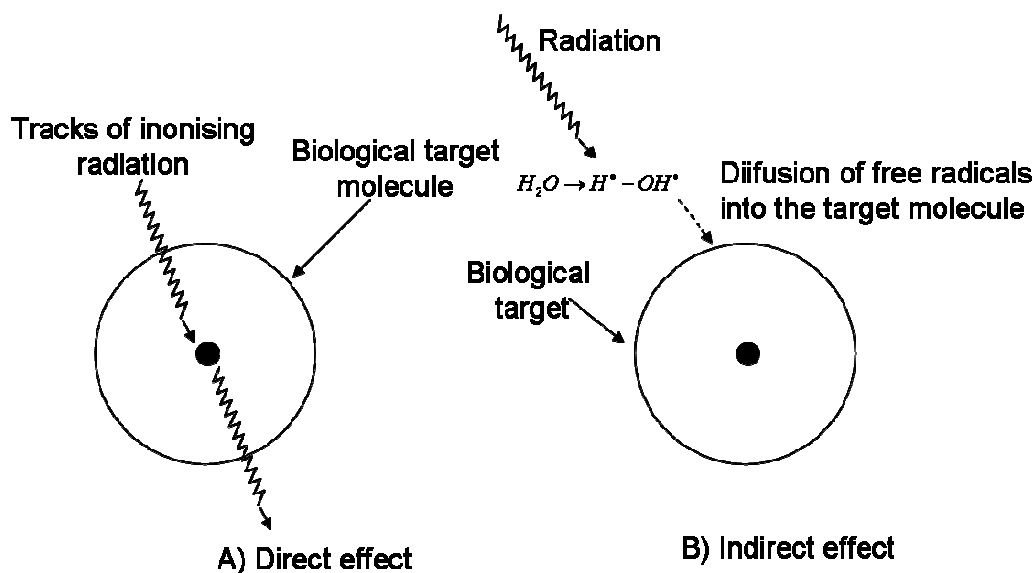
Fig.2.1.5. A) Direct and B) indirect actions of ionizing radiation.

Indirect Effect

Radiation produces excitations and ionisations at random, so that in a complex system such as living matter, those molecules that are most abundant are those most likely to become ionized. Living system as is constituted of 70-90% water the maximum impact of irradiation falls on the water molecules. These irradiated aqueous free radicals formed as a result of water radiolysis then react with biologically important molecules and this mode of interaction of radiation with the critical target i.e., bio molecules through an immediate medium is known as indirect effect as shown in **Fig.2.1.5B**.

2.1.6. Radiolysis of Water

For a proper understanding of indirect effect of radiation on biomolecules the radiation chemistry of water is of extreme importance. **Scheme 2.1.2** presents an overview of the effect of X ray ionisation on water molecules. (von Sonntag, 1987). Beside the shown reactions free radicals formed from water radiolysis may also react with organic biological molecules or they may react with oxygen. This kind of reactions further produces organic radicals or peroxy radicals producing indirect effect of ionisation in biomolecules. The extent of direct and indirect effect of ionization on DNA or on model fluorouracil components are specifically discussed in **section 5.1 and 5.2**.
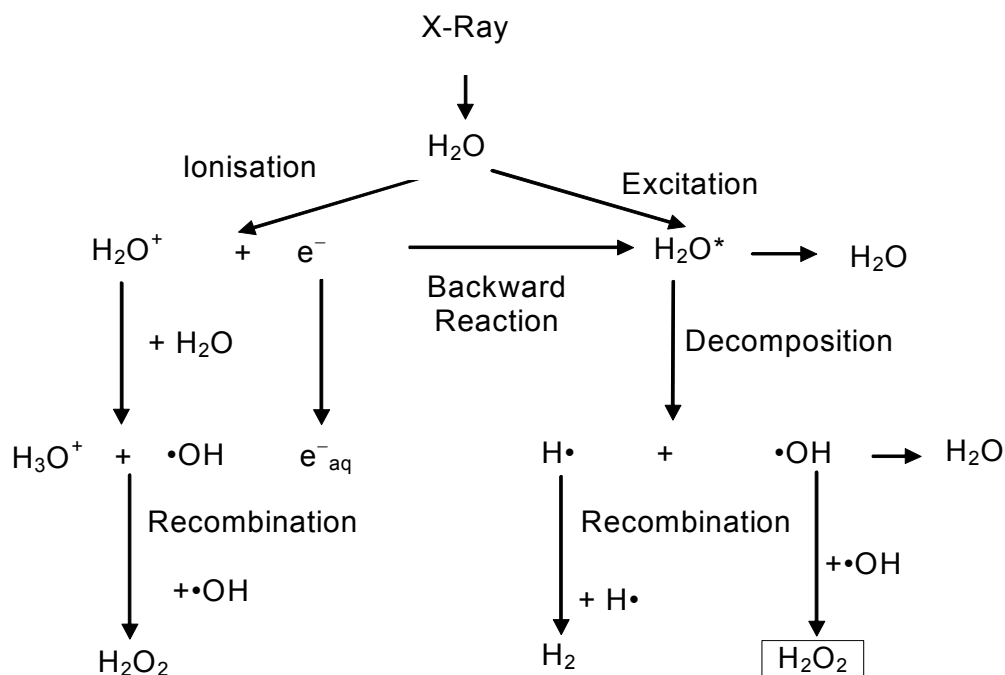
Scheme 2.1.2. Radiolysis of water (Weiland 1999)

2.1.7. Radiation Damage: Time Course

The biological consequences of exposure to ionizing radiation are mediated by a series of physical, chemical, biochemical, and cellular responses initiated after the deposition of the radiation in the medium (**Scheme 2.1.3**). Radiation produces ionization through the generation of secondary electrons which cause secondary ionizations, this physical process occurs in extremely short time period of 10^{-17} to 10^{-15} seconds. The time

scale of the initial steps of energy deposition and bond scission i.e., chemical damage is in the order of 10^{-13} seconds. The energy associated with ionizing radiation is significantly greater than the bond energies of many molecules and can cause homolytic bond scission.
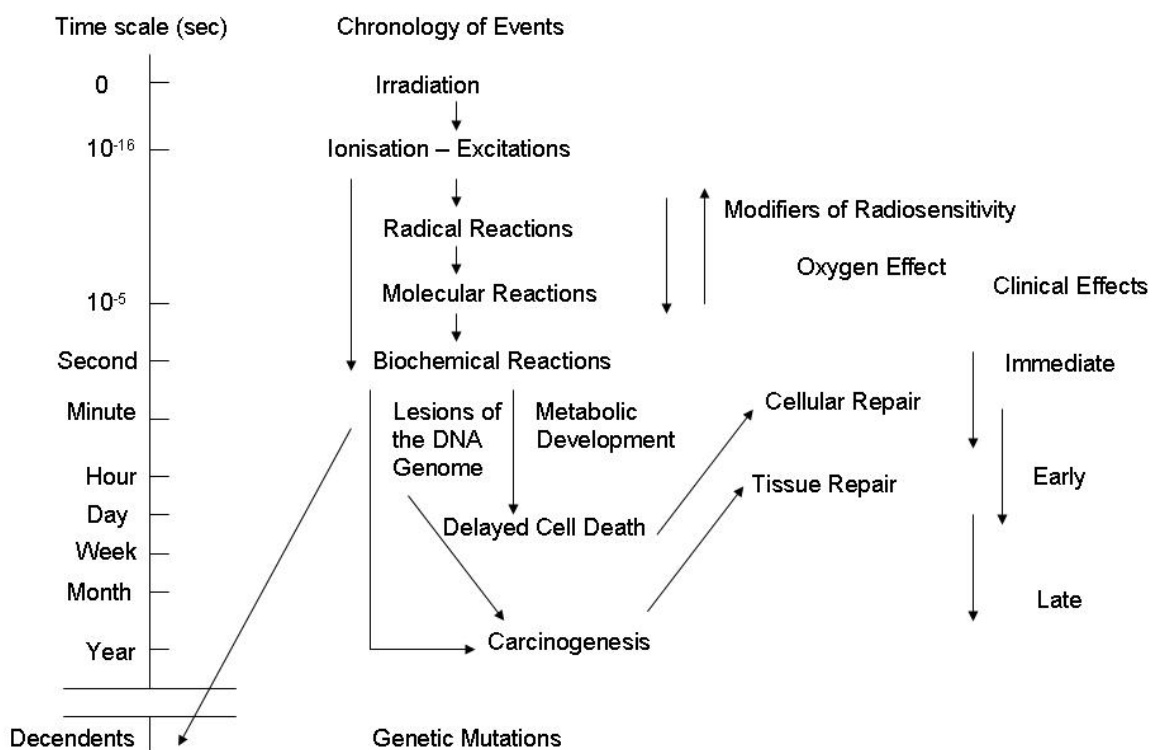
Scheme 2.1.3. Time scales of events initiated by deposition of ionizing radiation in biological matter (Tubiana et. al. 1990).

Since water is the main constituent of cellular matter, ionization of water to produce secondary species with high reactivity and short life times (10^{-10}–10^{-9}s) such as the $OH^{\bullet}$ radical, hydrated electrons, or H atoms, would be expected to mediate the chemical reactions which damage biologically important molecules (BIMs). The phase of chemical damage to the BIMs like cellular membranes, proteins/enzymes and DNA can be broadly defined to take time in the range of 10^{-14}-10^{-3}s. In this period excited molecules as well as free radicals are created which in turn can behave as electron acceptors (oxidising species) or electron donors (reducing species) and consequently can result

16

into bio molecular damage in the time range of seconds to hours which further extends into biological damage causing carcinogenesis or genetic mutation taking time of years or decades.

In order to understand the mechanisms undergoing in biological phase specifically for the subject of irradiated DNA several techniques play a very important role. Optical and mass spectroscopy can give a deep insight for the ionized model substances at room temperatures. Nuclear magnetic resonance spectroscopy has proved to be a very useful method for structure determination; further knowledge about single or double strand can be obtained by gel–electrophoresis, pulse-field-gel –electrophoresis. High performed liquid chromatography (HPLC) is also utilised to understand the mechanisms in product formation of model irradiated DNA constituents. More information about chromosome aberration (deletion and translocation) can be accumulated by processes like fluorescence in situ hybridisation (FISH).

For studying physico - chemical and chemical phase in aqueous solutions pulse radiolysis studies have proved very useful. Electron spin resonance spectroscopy (ESR) has been utilised in order to understand the paramagnetic species formed after irradiation by stabilising them at low temperatures or by adding spin labels at room temperatures. This field has evolved almost forty years ago with the analysis of irradiated crystals of DNA components at low temperatures and has developed with the study of DNA in amorphous media, then DNA-protein complexes.

2.2. Basics of Electron Spin Resonance (ESR) Spectroscopy

2.2.1. Introduction

Molecular spectroscopy is defined as the study of interactions of electromagnetic radiations with matter. Electromagnetic radiation in free space is regarded classically as coupled electronic and magnetic field perpendicular to each other and to the direction of propagation. Both oscillate at some frequency. Among two types of molecular spectroscopy; optical spectroscopy involves studies of interaction between electric field components of electromagnetic radiation with matter ranging from microwave to visible region of electromagnetic radiation. On the other hand in radio frequency region and in long wavelength edge of microwave region the spectroscopic studies are dominated by the interaction of magnetic field of electromagnetic waves with the matter and named as magnetic resonance spectroscopy. Magnetic resonance spectroscopy is categorized as Nuclear Magnetic Resonance (NMR) and Electron Spin/Paramagnetic Resonance (ESR/EPR) spectroscopy. The principal ideas behind both types of spectroscopy are common but there are differences in the magnitudes and signs of the magnetic interactions involved. This leads to divergence in the experimental techniques involved and the applicability of the methods. NMR deals with the interaction of electromagnetic waves with the magnetic moments arising from the nuclei of the molecules. The NMR technique can be used to detect the presence of particular nuclei in a compound and since for a given nuclear species the strength of NMR signal is directly proportional to the number of resonating nuclei and hence they can be estimated quantitatively. It is one of the major tools for structural determination of mainly organic substances.

The ESR spectroscopy deals with the phenomena of absorption of electromagnetic radiation by the molecules or atoms containing electrons with unpaired spins. ESR spectroscopy deal with paramagnetic species (species containing unpaired electrons) alternatively known as free radicals which occur in redox reactions or can be produced by ionization. They can be organic radicals, transition metal ions or inorganic complexes. In this thesis X-band (9.5 GHz) ESR spectrometer is used as a tool for isolation and analysis of radicals formed on DNA and its components upon X ray irradiation in different matrices.

2.2.2. Zeeman Splitting and g factor of Free Electrons

Electrons (S= ½) being a spinning charged particle behave as a tiny bar magnet placed along the spin axis producing a permanent magnetic moment. The magnetic moment will point along the direction z perpendicular to the plane of the circle. Magnetic moment μ_s is related to the spin angular momentum ($|S|$) by the equations given below.

$$|S| = \sqrt{S \cdot (S+1)} \, \hbar \qquad\qquad (2.2.1)$$

$$|\mu_s| = -g \cdot \mu_B \cdot |S| \qquad\qquad (2.2.2)$$

As shown above $\hbar$ is atomic angular momentum and equals to Planck's constant h (6.626 x 10^{-34} Js) divided by 2π. μ_B (= $eh/4\pi m_e$) is Bohr magneton for electrons (9.27x10^{-24}JT^{-1}) and g is a dimensionless constant known as Lande splitting factor, this value is ≈ 2.002319 for the free electrons. This value is valid for electron present in hydrogen atom at ground state and is approximately same for unpaired electrons present in free radicals.

According to quantum mechanics, the angular momentum vector cannot have any arbitrary direction but can point only along certain directions (space quantization of angular momentum vector). These directions are such that the component of angular momentum vector along a certain reference axis, known as z-axis, has only quantized values. This reference axis is usually taken to be the direction of an external magnetic field. The z component of spin angular momentum, S_z can be denoted as $m_s(h/2\pi)$ can have only two values corresponding to the magnetic quantum numbers m_S = + ½ and m_S = - ½ and these two values are also called spin states. Thus the angular momentum can have only two orientations in the presence of magnetic field. The orientation angle δ is given by the relation below.

$$m_S = |S| \cdot \cos\delta . \qquad\qquad (2.2.3)$$

In the absence of an external magnetic field the spins of the unpaired electrons present in a paramagnetic substance are aligned in random direction. The spin magnetic

moments will be degenerate in energy. The application of an external static magnetic field B_0 breaks the degeneracy of the two magnetic moment quantum states. The extent of interaction between the magnetic dipole and a field strength applied along the z axis is equal to the product of the two. The potential energy E of an electron when placed in a magnetic field is given by the expression below.

$$E = -\left|\mu_S\right| \cdot B_0 \cdot \cos\delta \qquad (2.2.4)$$

Putting the values of μ_s, above equation can be written as below.

$$E = g \cdot \mu_B \cdot B_0 \cdot m_s \qquad (2.2.5)$$

For the values of +1/2 and -1/2 for m_s following energy levels can me obtained.

$$E^- = -1/2 \cdot g \cdot \mu_B \cdot B_0 \qquad (2.2.6)$$

$$E^+ = +1/2 \cdot g \cdot \mu_B \cdot B_0 \qquad (2.2.7)$$

This splitting of degenerate energy levels of free electrons in two different levels in the present of an external magnetic field (B_0) is known as Zeeman splitting and the energy difference between the two states is given below.

$$\Delta E = g\mu_B B_0 \qquad (2.2.8)$$

2.2.3. Resonance, Boltzmann Distribution and Larmor Precession

An unpaired electron can move between the two energy states by either absorbing or emitting electromagnetic radiation (hν) only when the condition of resonance is obeyed as given in the equation below and **Fig. 2.2.1**.

$$\Delta E = h\nu = g\mu_B B_0 \qquad (2.2.9)$$
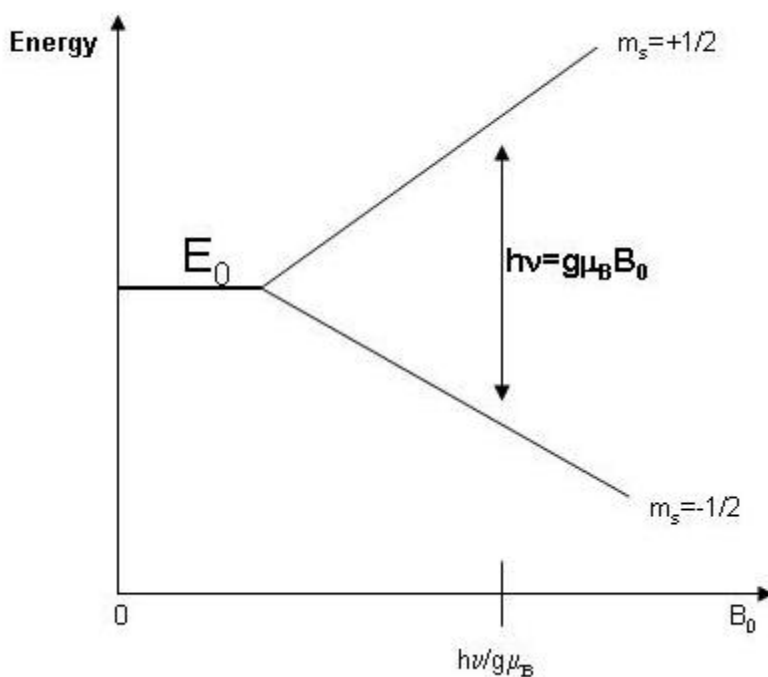
Fig.2.2.1. Schematic representation of the electron Zeeman splitting versus field strength. When the resonance condition is fulfilled an EPR signal in absorption is detected corresponding to the resonance magnetic field.

During an EPR experiment a macroscopic assembly containing a generic number of electrons is analyzed and not only a single spin. In thermal equilibrium the distribution of spins over the possible states is statistical and governed by the Boltzmann's distribution law, which for a two spin level system is given by the following relation.

$$n^+ = n^- \cdot e^{-\frac{\Delta E}{k \cdot T}} \quad . \tag{2.2.10}$$

Where n^- and n^+ are the number of spins in the lower and upper energy states, ΔE is the energy difference given in equation, k is the Boltzmann's constant and T is the absolute temperature. For electrons in a field of 9.5 GHz (X band) and at room temperature (298 K), it can be calculated that the populations of the two spin states differ by only 1.5 parts in 10^3. At low temperature the difference between the two states can be enhanced and thus the intensity of ESR spectra can be increased.

In most systems, electrons occur in pairs such that the net magnetic moment is zero. Hence only species that contain one or more unpaired electrons possess the net

spin necessary for suitable interaction with an electromagnetic field. EPR transitions between the electron spin levels occur only when there is a population difference between the spin states, the magnetic component of the electromagnetic radiation is perpendicular to the steady field $\mathbf{B_0}$ and the following selection rule needed for spin transitions is fulfilled.

$$\Delta m_s = \pm 1 \tag{2.2.11}$$

The behavior of a spinning electron can be considered analogous to that of a gyroscope revolving in friction free bearings. Experiments have convinced that the application of couple to a gyroscope does not cause its axis to tilt but merely induces a precession of the axis about the direction of the couple. Essentially the same occurs with the spinning particle where the magnetic moment vectors of spin dipoles starts precessing around the magnetic field in a cone in anticlockwise direction to the field at a uniform angular velocity ω_0 making a constant angle with the field. This motion is called the Larmor precession of the spin.

$$\omega_0 = \gamma \mathbf{B}_0 \tag{2.2.12}$$

ω_0 is known as the Larmor frequency and γ is the gyromagnetic ratio). The potential energy of the spinning particles remains constant in this precession. This potential energy can be changed by changing the orientation angle of the magnetic moment vector to the other permitted angle. This can be achieved by applying a secondary magnetic field rotating around the main field with a frequency equal to Larmor frequency. Under this condition the rotating magnetic field is in resonance with the precessing magnetic field and thus induces a transition from one level to the other level. This is a mechanism by which particle spins can interact with a beam of electromagnetic radiation. If the beam has the same frequency as that of the precessing particle, it can interact coherently with the particle and energy can be exchanged.

The ESR signals can be achieved by two ways; one is by varying the field strength keeping the frequency of the oscillator constant, and another by varying the frequency of the oscillator, keeping the external magnetic field constant. Until recently second method is experimentally more favourable because it is relatively easy to vary the magnetic field

(i.e., the current in the electromagnet) than to vary the frequency of radiation beam. So an ESR spectrum is observed by placing the paramagnetic centre in a magnetic field and the electrons caused to resonate between the two states; the energy absorbed as it does so is monitored. The magnetic field where this absorption occurs is known as resonance field as shown in **Fig. 2.2.1**.

2.2.4. Relaxation, Line Shapes, Line width and Line Intensity

Considering an ensemble of spins with (e.g., electrons, protons, with S=1/2) a constant uniform microwave frequency is assumed to be present. Now if the system is subjected to a sudden external magnetic field range then at certain field resonance will occur and it will result energy absorption which will cause a change in population of the energy levels in the system. Since the spin system has gained energy, it can be considered as hot as compared to the surroundings. In order to restore the normal temperature the spin system in practice undergoes interactions with the surroundings.

The mechanism by which excess spin energy of a system is shared either with the surroundings or with other nuclei is referred to as relaxation process; the time taken for a fraction $1/e = 0.37$ of the excess energy to be dissipated is called relaxation time. Two different relaxation processes can occur both for nuclei and electrons.

Spin-Lattice Relaxation

In this case, the excess spin energy equilibrates with the surroundings (the lattice) by spin-lattice relaxation time (or longitudinal relaxation time) denoted as T_1. This is a non - radiative transfer of energy from spins to the other degree of freedom (lattice). Such relaxation comes about by lattice motions for example atomic vibrations in a solid lattice, or molecular tumbling in liquids and gases. Spin-Lattice relaxation is efficient at room temperature (10^{-6}s) but becomes progressively less at reduced temperature, often becomes several minutes at the temperature of liquid nitrogen.

Spin-Spin Relaxation

There is sharing of excess spin energy directly between spins of nuclei or electrons via spin-spin relaxation (or transverse relaxation), the symbol for the time of which is T_2. The relative energies of the spin levels are varied and not their lifetimes. This kind of relaxation is very effective even at low temperature, unless the system is extremely dilute and gives a relaxation of 10^{-8}-10^{-6}s.
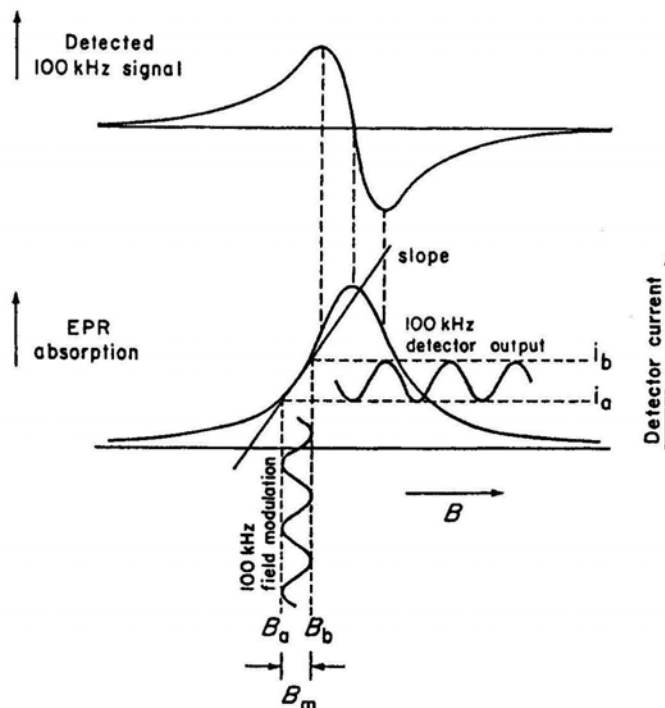
Fig.2.2.2. Effect of small amplitude 100 kHz field modulation on the detector output current. The static magnetic field B is modulated between the limits B_a and B_b. The corresponding detector current varies between the limits i_a and i_b. The upper diagram shows the recorded rectified 100 kHz signal as a function of B (Wertz and Bolton 1972).

In actual practice, the ESR signals have finite width because of the larger relaxation time (time required for the electron to revert from the excited level to the ground level). In order to improve accuracy, the signals are recorded as the derivative as shown in of the absorption curve with respect to the magnetic field. The derivative of a curve is simply its slope at a given point; in calculus notation, the derivative of the spectral trace is $dA/d\nu$, where A is the energy absorbed or emitted. To do this the magnetic field strength is modulated sinusoidally at a certain modulation frequency (usually 100 kHz). The effect of modulation is depicted in **Fig. 2.2.2**. This technique allows amplification of ESR signal using AC techniques, elimination of most of the noise-contributing components and enhanced spectral resolution.

The shapes of ESR lines are usually described by Lorentzian and Gaussian line shapes and their derivatives.

Lorentzian line shapes are usually observed for ESR lines of systems, if there is no hyperfine broadening, if the concentration of paramagnetic centers is low and if there is dynamic averaging, for example in liquid solution. Lorentz line can be described by the distribution given below and is shown in the **Fig.2.2.3**.

$$g(\omega) = \frac{T_2}{\pi} \cdot \frac{1}{1 + T_2^2 \cdot (\omega - \omega_0)^2} \tag{2.2.13}$$

Where $g(\omega)$ is function of frequency, ω_0 is resonance frequency and T_2 is transverse relaxation time.

Gaussian shapes for lines are observed if the line is a superposition of many components. Generally the unpaired electrons in a sample are not all subjected to exactly same magnetic field. Thus at any time, only a small fraction of the spins is in resonance as the external magnetic field is swept. The observed line is then a superposition of a large number of individual components each slightly shifted from the others thus giving rise to Gaussian curve. This phenomenon is also called inhomogeneous broadening and may be caused due to inhomogeneous external magnetic field, unresolved hyperfine structure, and anisotropic interactions in randomly oriented systems in the solid state giving rise to highly unsymmetrical line shapes, dipolar interactions with other fixed paramagnetic centers. The expression is given as below.

$$g(\omega) = \frac{T_2}{\sqrt{2\pi}} e^{-\frac{1}{2}T_2^2 (\omega - \omega_0)^2} \tag{2.2.14}$$

Where meaning for each term is already given before. The Gaussian curve along with its derivative is shown in **Fig.2.2.3**.

The main parameters describing these line are; the maximum amplitude (Y_{max}) or the maximum height of the observed line, this factor depends on the experimental factors such as power level, detector sensitivity, amplifier settings, sample composition and temperature and the half width at half height (Γ). In ESR spectroscopy the line shapes can therefore be described as Lorentzian, Gaussian or a mixture of both and

spectral line widths are popularly given by peak to peak distance of first derivative spectrum which is denoted as ΔH_{PP}.
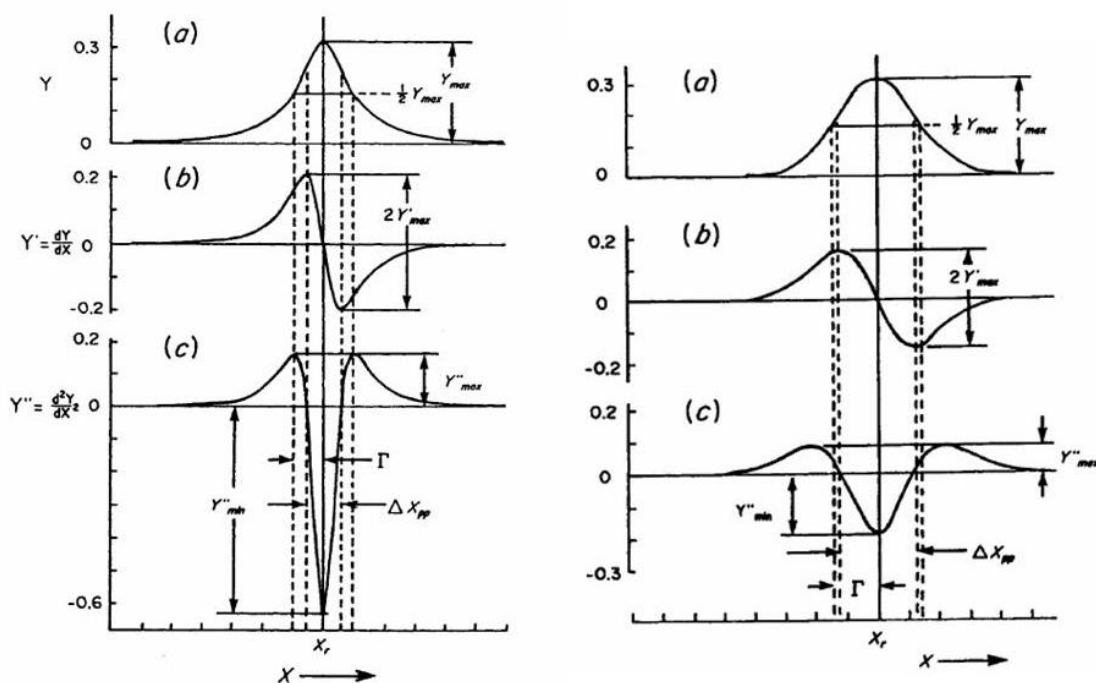
Fig.2.2.3. Line shapes from Lorentzian function (left) and Gaussian function (right) and the respective a) absorption, b) First derivative, and c) second derivative spectrum
(Wertz and Bolton 1972).

The spin-lattice relaxation causes the spins to achieve thermal equilibrium according to the Boltzmann law, so that the population difference between the spin energy levels is re-established. On the other hand, if during continuous wave irradiation the microwave power becomes high enough, so that the relaxation is slow compared with the transition rate, finally an equal population of the spin energy levels will occur. This is known as saturation.

In the non-saturating regime the square of the double integral over the intensity I of a derivative signal is proportional to the microwave power irradiated. If the line width does not change, one can write this as below.

$$I \propto \sqrt{P} \qquad (2.2.15)$$

As the line is saturating the signal intensity does not grow as fast as P anymore and finally decreases. The power, where the quotient out of I and P has been reduced to one half of its non-saturating value, is called half saturation power $P_{1/2}$. The saturation curve usually obeys the empirical law as given below.

$$\frac{I}{\sqrt{P}} = c \frac{1}{\left(1 + \dfrac{P}{P_{1/2}}\right)^{b/2}} \qquad (2.2.16)$$

Where c is a constant, b = 1 in case of an inhomogeneous line broadening and b = 2 for a homogeneously broadened line.

Intensities of the spectra obtained are not only dependent on the microwave power but on the concentration of the EPR active species (spins) in the sample. The integrated intensity of an EPR absorption signal is directly proportional to the spin concentration and can therefore be used as estimation for the concentration of the paramagnetic species (ref). Thus this is a technique to estimate the amount of free radical present; the method is extraordinarily sensitive, in favorable cases some 10^{-13} mol of free radical being detectable.

2.2.5. Characteristics of Dipole Interactions

Along with the interaction of unpaired electrons with externally applied homogenous magnetic fields (as given by g factor) the ESR technique also provides information about interaction of free electrons with other dipoles.

Spin-Orbit Coupling

The intrinsic spin angular momentum of a free electron is associated with a g factor of 2.00232. Although ground state of most molecules (including free radicals) has zero orbital angular momentum but there are spin orbit interaction between the hypothetical pure spin ground state with certain excited states and causes a small

amount of orbital angular momentum to appear in the actual ground state. The orbital angular momentum couples coherently with the spin angular momentum, giving rise to extra magnetic field (local effect) that adds vectorially to the external magnetic field. As a consequence a change in effective g factor is observed. This results in anisotropy to the g value of the paramagnetic species. The anisotropic g tensor can be expressed as symmetric tensor, with for example three principle values g_{xx}, g_{yy}, g_{zz}. Spin-orbit coupling is also observed to some extent in the organic free radicals when they are studied in frozen (solid) state.

In this thesis the paramagnetic species are the DNA base radicals and as most of them are carbon centered organic radicals so the anisotropy of g value is not overwhelming giving rise to a complex spectrum highly overlapping spectral components at low frequency e.g., at X-band. Few radicals formed on oxygen and nitrogen centers can because of higher spin orbit coupling gives rise to spectra with deviated g values from free electrons and can be studied specifically.

The Hyperfine Structure in ESR Spectra

The interaction of the magnetic moment of an electron with those of surrounding magnetic active nuclei (having non zero spin) results in the hyperfine structures in the ESR signals, i.e., a single absorption splits into more than one signal. Hyperfine patterns provide the principle evidence for the identification of radicals.

Nuclei individually associated with the electron spin system often have a magnetic moment I and magnetic quantum number m_I which also has different allowed orientations (2I + 1) (ranging from m_I= I, I-1, I-2…-I) in the presence of external magnetic field. The magnetic field associated with the nuclear moment then can add to or subtract from the applied field experienced by the electron spin system associated with it. In the bulk sample some electrons will therefore be subjected to an increased field and some to a reduced field. Consequently, the original electron resonance line is split into (2I+1) components. The phenomenon is known as hyperfine splitting. The selection rules for the electron magnetic transitions are Δm_s=1 and Δm_I=0. **Fig.2.2.4** shows the energy level diagram showing the interaction of an electron with neighbouring nitrogen nuclei (with I =1).
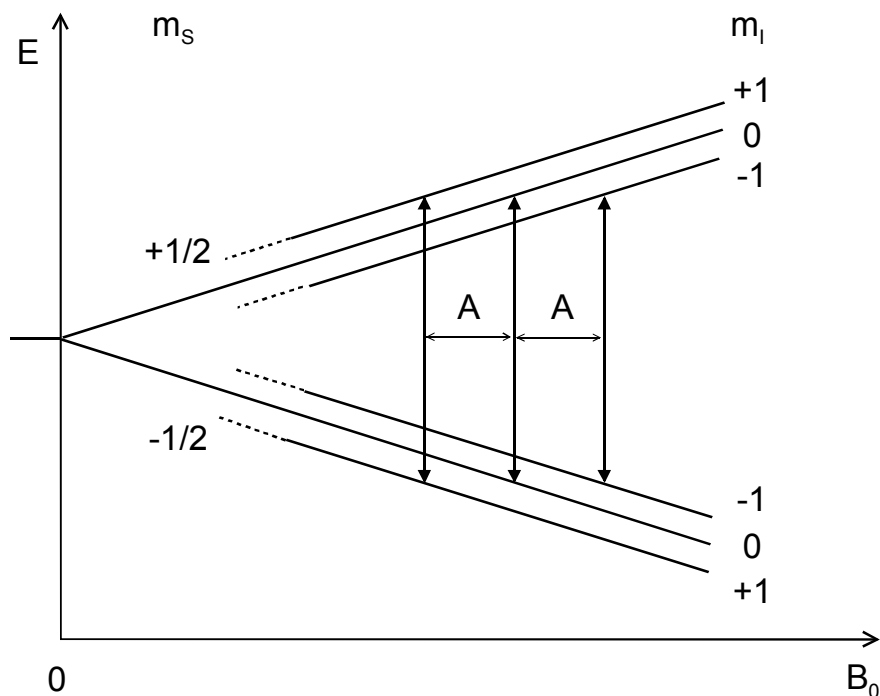
Fig. 2.2.4. Energy level diagram of hyperfine interactions on a system with one unpaired electron (S = 1/2) and one nucleus with I = 1 (for example ^{14}N). Dotted line indicates the electron-Zeeman interaction when there is no hyperfine interaction.

Similarly **Fig. 2.2.5** depicts an example for the coupling of an electron (S=1/2) with two equivalent protons (I=1/2) and the respective ESR spectrum. The respective ESR spectrum originating from these transitions are also shown here. It can be seen from the allowed transitions that the ESR pattern will be a triplet where the intensity of the splittings will vary in 1:2:1 ratio in isotropic conditions.

Hyperfine interactions can be quantum mechanically explained by hyperfine tensors denoted as **Ã**. The hyperfine interaction is electromagnetic and consists of two parts. It may be either isotropic also called Fermi-contact interaction. It is a pure quantum mechanical term and occurs only when the electron has a finite probability density; it is orientation independent hence contact interaction can only occur when the electronic wave function has some s orbital character.
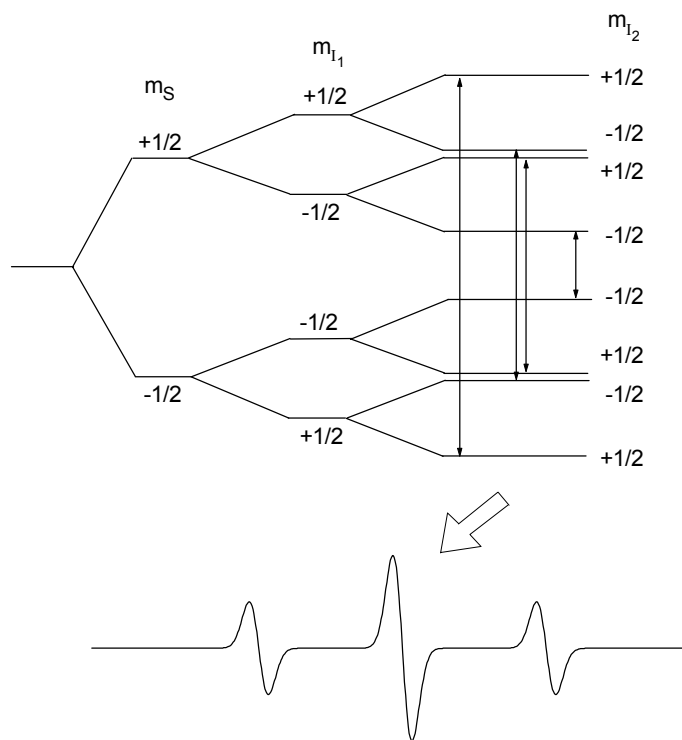
Fig. 2.2.5. Energy level diagram and spectrum showing hyperfine splitting due to interaction between an electron with S=½ and two equivalent protons with I=½.

The dipole-dipole interaction arising due to the spin density in p or higher orbital results into anisotropic hyperfine interactions. Anisotropic hyperfine interaction is dependent on the orientation of molecular axis with respect to the external magnetic field. In most of the cases an anisotropic hyperfine interaction can be accompanied by isotropic components and both are measurable. The anisotropic hyperfine interaction term vanishes when averaged over all orientations, as it is usually the case in liquids due to the rapid tumbling of molecules.

2.2.6. Static Spin Hamiltonian and its Components

The transition energies of an electron spin S_1 in a constant magnetic field $\mathbf{B_0}$, interacting with n magnetic nuclei with spin $\mathbf{I}$ and with another electron spin $\mathbf{S_2}$, can be calculated from the static spin Hamiltonian operator;

$$\hat{H} = \mu_B \cdot B_0 \cdot \widetilde{g} \cdot \hat{S} + \hat{S} \cdot \widetilde{A} \cdot \hat{I} + \hat{I} \cdot \widetilde{P} \cdot \hat{I} - \mu_N \cdot B_0 \cdot \widetilde{g}_N \cdot \hat{I} \qquad (2.2.17)$$

<div align="center">a)   b)   c)   d)   e)</div>

Whereby

a) Electron-Zeeman-Term	μ_B: Bohr´s Magneton
b) Hyperfine InteractionTerm	μ_N: Nuclear magneton
c) Quadrupole Term	B_0: Magnetic Field
d) Nuclear-Zeeman Term	$\widetilde{g}$: g-Tensor
	$\widetilde{A}$: A Tensor
	$\widetilde{P}$: Quadrupole Tensor
	$\hat{S}$: Elektronspin Operator
	$\hat{I}$: Nuclearspin Operator

Electron - Zeeman and Hyperfine interactions are the interactions contributing to the transition frequencies of the systems described in this work and will be further analyzed in the coming contexts.

2.2.7. Measurement Technique: Continuous Wave (CW) ESR Spectrometer

All the spectra presented in this thesis are recorded with a conventional CW X-band spectrometer working at $\nu \sim 9.5$ GHz. The main advantage of utilising this tool is the relative simplicity and fastness of the method. The investigation of radical systems is done at low temperature ranging from 4 K-77 K. A typical CW spectrometer as blocked out in **Fig.2.2.6** is consisted of three parts. i) Source contains components that produce the electromagnetic waves, the cavity system holds the sample, and direct and control the microwave beam to and from the sample. ii) The modulation and detection system

monitor, amplify and record the signal. iii) The magnet system provides a stable, homogenous and linearly variable magnetic field within the desired range.
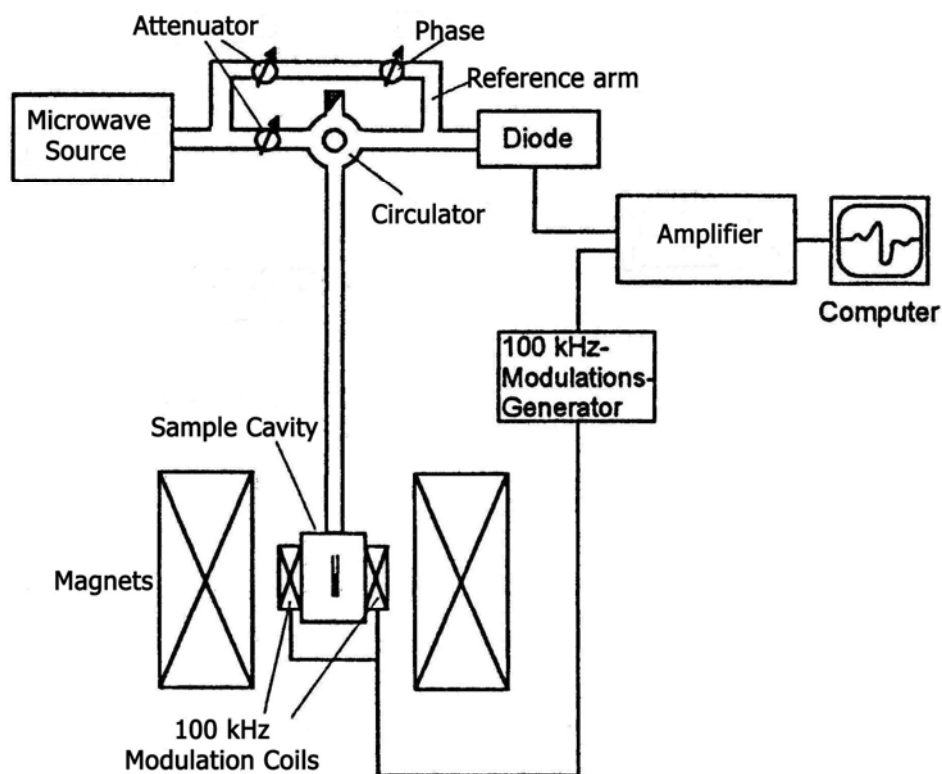
Fig. 2.2.6. Block diagram of a typical X-band ESR spectrometer employing 100 kHz phase-sensitive detection (adapted from Weiland 2000).

The microwave system consists of a microwave power supply consisting of a klystron. The output of the microwave power supply is connected via rectangular waveguide and through a circulator to a high-Q resonant cavity. The samples to be investigated are mounted in the middle of the cavity, where magnetic component of the microwave power has a maximum and is oriented perpendicular to the static field. A microwave diode, which detects the microwaves, resides inside the same box as the power supply. The higher the quality of the resonant cavity the greater the microwave field can be obtained on the sample. Very polar solvents like water absorb efficiently on microwave frequencies themselves. Because of that, water samples have to be made in narrow capillaries and carefully located in the center of the cavity.

2.2.8. Interpretation of the ESR Spectra of Organic Radicals

In this work the DNA and its constituents have been dealt with after irradiation (radicals) in frozen aqueous or glassy matrices (rigid solutions) which can be treated as amorphous systems. Powder spectrum are obtained from these systems which consist of a random distribution of orientations of molecular axes, a spectrum which consists of a super position of spectra from the three principal axes and all intermediate orientations are obtained. The g values are not resolvable. The hyperfine splitting is also in most cases measurable only in the single crystals. In the following sections the mechanisms of hyperfine structure in some specific cases especially for organic systems have been dealt with. These cases will prove to be useful for explaining the analysis given in the result and discussion section.

For most organic molecules with an unpaired spin the coupling constants are of the order 10^{-4}-10^{-3} tesla (2-20 MHz); these are smaller than in the hydrogen atom because an unpaired electron in a molecule is never confined to just one nucleus and seldom even to one bound, but can move over several bonds with relative ease, spending only part of its time at any one nucleus.

Free radicals can often be distinguished as π radicals and σ radicals. A σ molecular orbital has maximum probability density in the bonding plane and is symmetric with respect to reflection through the plane. In a σ radical the unpaired electron occupies a σ molecular orbital. A π molecular orbital has a node in the bonding plane of the molecule and is anti symmetric with respect to reflection through the bonding plane. In a π radical the unpaired electron occupies a π molecular orbital. The distinction between π and σ radicals can often be carried over to non polar radicals by considering only that part of the paramagnetic molecule where the probability of finding the unpaired electron is maximum. The systems studied in this thesis are mainly consisting of carbon centered or nitrogen centered organic radicals which can be categorized as π radicals where the unpaired electrons are situated at 2p orbital. The organic radicals studied in this thesis showed interaction of unpaired spin with protons, nitrogen, and fluorine atoms.

Interaction with Protons

In aliphatic radical systems the maximum hyperfine interaction is observed mainly with the nuclei positioned at α and β positions to the atom (carbon atoms here) which is primarily associated with the unpaired electron. The proton positions can be defined as
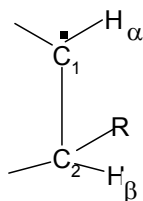
Scheme 2.2.1. Notation of position of protons in an aliphatic system

follows;

The proton bonded with C_1 where the probability of finding the unpaired electron is 100% is designated as α proton. The classification of the x, y and z axis are shown in the **Fig. 2.2.7**.
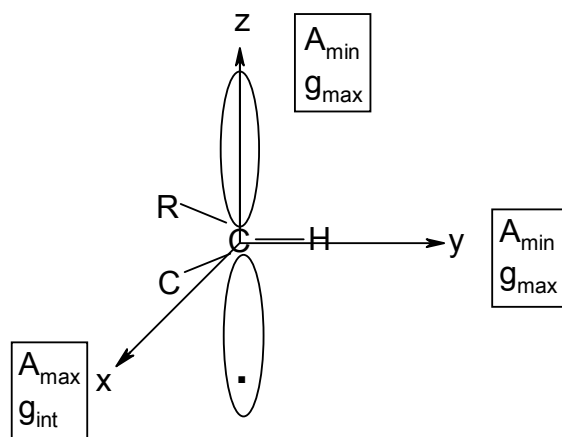
Fig. 2.2.7. Classification of x, y and z axes of the radical structure and the principle value of the hyperifine splitting and g tensors.

The α proton is bonded with σ binding with one of the three sp^2 hybridized orbital of carbon atom which is planar. The unpaired electron is orthogonal to this plane in a $2p_z$

orbital of carbon atom and contains a nodal point on the sp^2 bonding plane which means that the probability of electron density is zero at this point. As isotropic proton hyperfine splitting arises when a net unpaired electron density exists at the proton so theoretically no hyperfine splitting should be observed in this case. But in reality there are many π radicals which show proton hyperfine splitting. This can be explained by spin polarization effect. A basic assumption for conjugated molecules is that the electrons do not influence the other electrons but in real situations the electrons are affected by each other. For example in a C-H fragment of a conjugated system as shown in **Fig. 2.2.8**, there are two possibilities for assigning the spins in the C-H σ bonds. It is assumed that here C atom has its $2p_z$ orbital perpendicular to the C-H bond; the $2p_x$ and $2p_y$ and the 2s orbital of the C atom form trigonal sp^2 hybrids. The hydrogen atom bonds with one of these three coplanar hybrids. If there were no electron in the $2p_z$ orbital both B and C in **Fig. 2.2.8** would be equally probable but introduction of an odd electron in $2p_z$ orbital gives rise to an energetically more favorable situation when the electron in sp^2 orbital is aligned parallel to the unpaired electron (B) than when the electrons are anti parallel (C) as per Hund´s principle.
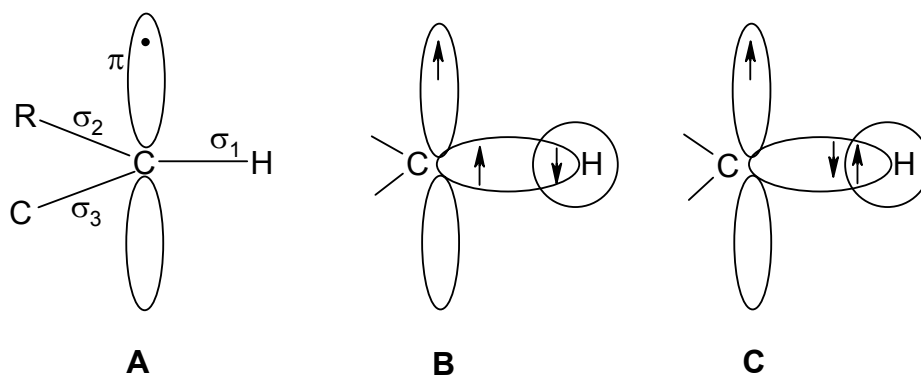
Fig. 2.2.8. Mechanism for the production of isotropic hyperfine interaction with an α proton. A Carbon centered radical fragment with one α proton. B Spins parallel in the σ bonding orbital and the 2pz orbital of carbon. C Corresponding spins anti parallel.

By the Pauli's exclusion principle for a bond formation the electron formally in the H (1s) orbital must be anti parallel to that in sp^2 orbital and hence also anti parallel to the unpaired electron thus consequently there will be a net unbalance in spin. A negative spin density will be observed on hydrogen and a positive spin density at carbon centre or vice versa depending on the spin state of electron at p_z orbital of C atom. There is

relation between spin density on the carbon atom and the proton hyperfine splitting parameter (Scheffler and Stegmann 1970) as given below. The equation is known as McConell relationship and Q_{CH} is known as McConell constant expressed in magnetic field units, $A_{H,iso}$ is isotropic proton hyperfine splitting parameter and ρ_C is the unpaired π electron population at the adjacent carbon atom of the proton.

$$A_{H,iso} = Q_{CH} \cdot \rho_C \qquad (2.2.18)$$

The McConnell-Constant values Q_{CH} are between -2.2 mT and -2.8 mT. Analogous values are for OH protons, the Q_{OH} is between 1.2 mT and 1.9 mT and for NH protons Q_{NH} is between -3.5 and -3.9 mT).

Along with isotropic hyperfine interaction the α proton also possesses an anisotropic component through the dipole-dipole interaction between the unpaired electron and the α proton. The dipolar tensor shows the minimum dipolar interaction in parallel to π orbital and the maximum in the direction of C-H bonding. This gives the system a rhombic symmetry. Through the addition of isotropic coupling constant ($A_{H,iso} \cong$ -2.3 mT) with the dipole tensor, following principle values can be obtained (Scheffler and Stegmann 1970).

$$\begin{pmatrix} A_{xx} \\ A_{yy} \\ A_{zz} \end{pmatrix} = -2.30 \text{ mT} + \begin{pmatrix} -1.38 \text{ mT} \\ +1.55 \text{ mT} \\ -0.17 \text{ mT} \end{pmatrix} = \begin{pmatrix} -3.68 \text{ mT} \\ -0.75 \text{ mT} \\ -2.47 \text{ mT} \end{pmatrix} \qquad (2.2.19)$$

Due to the spin-orbit coupling the values of g tensors will be shifted from the value of free electron i.e., 2.002319. The influence is more in x and y direction due to slight amplification of g factors and is also dependent on several other factors which are specific for radical under consideration.

The proton bonded with C_2 in **scheme 2.2.1** which is also two bond lengths away from the spin centre at C_1 is designated as β- proton. The effect of dipole – dipole interaction is negligible in this case. The hyperfine interaction between the unpaired electron present on carbon atom and a β proton can be explained by the phenomena

known as hyperconjugation. As shown in **Fig. 2.2.9** when there is overlap between one or more of the σ (C-H) bonds and the p-orbital of the unpaired electron, there will be some redistribution of electron spin on the β-protons. Quantum mechanically considering the example of methyl hydrogen atoms with electrons in the π system it can be said that the atomic orbitals of the three hydrogen atoms may have combined in such a way that the molecular orbital is obtained which has same symmetry as π orbital. Such an interaction is said to be maximum when the density axis of the p orbital and the C-H bond are co planar, and should be reduced to zero when the C-H bond lies in the radical plane. The interaction follows the relation as given for methyl protons.

$$A_{CH_3} = \rho_C \cdot B \cdot \cos^2 \vartheta \qquad (2.2.20)$$

The magnitude of hyperfine splitting in the case of β proton coupling is dependent from the spin density ρ_C on the C atom and the dihedral angle θ.
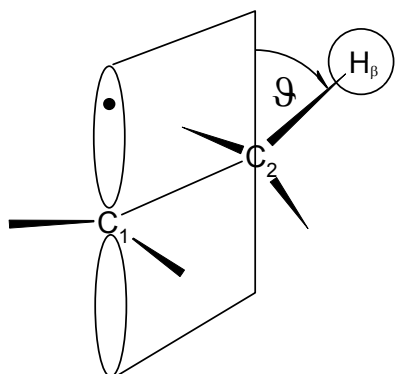
Fig. 2.2.9. Model of hyperconjugative interaction with β protons.

Coupling to Deuterium

Due to the nuclear spin I=1 a triplet splitting is observed when a hydrogen is replaced in a molecule by its isotope deuterium. The magnetic moment of deuterium is 6.5 times smaller than that of hydrogen thus narrowing the total splitting as seen with hydrogen. Easily approachable hydrogen atoms are therefore sometimes replaced by deuterons organic radicals to see the isotopic effects. Some organic radicals show better resolution and distinguishable spectra on isotopic substitution. In this thesis some works are conducted in D_2O matrix for the same purpose.

Coupling to Nitrogen (N^{14}) Nucleus

Nitrogen centered radicals with unpaired electron situated on the p_z orbital will give a triplet anisotropic splitting because of the dipole - dipole interaction with nuclear spin of N^{14} i.e. 1. The anisotropic hyperfine tensor of N^{14} nuclei depends mainly on the unpaired electron density in the 2p atomic orbital of the same atom, whereas the isotropic part measures the 1s or 2s character of the odd electron. The tensors are usually close to being axially symmetric. The g anisotropy shows mainly in x axis varying from 2.006 to 2.009 and in z axis the g value is similar to free electrons. This system can be designated as axial system where the principle values in the x and y axes can be replaced as ⊥ (perpendicular) and z axis can be replaced as ∥ (parallel). Additionally through the induction from the spin density of s-orbital nitrogen atom also experiences a isotropic hyperfine splitting which is common to the anisotropic contribution in the ⊥ direction. A nitrogen hyperfine tensor with 100% spin density approximately has the principle values as ~0 mT/ ~0 mT/ ~6 mT. The g anisotropy is about 2.006 to 2.009 in x direction while in z direction it is more close to the free electrons. The assignment of principle axes x, y and z for a nitroxide radical is shown in **Fig. 2.2.10**.
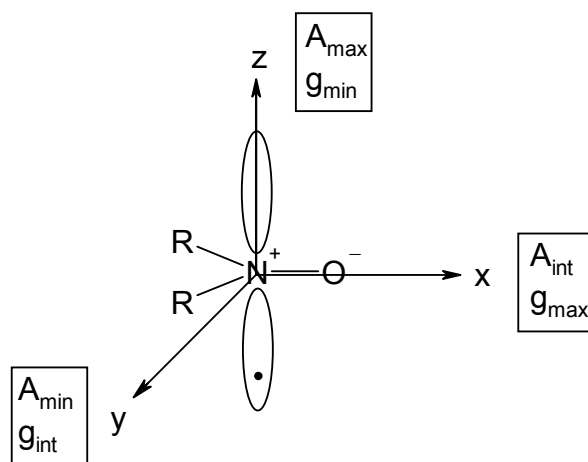
Fig. 2.2.10. Classification of x, y and z axes of the R$_2$N$^•$O radical fragment and the principle value of the hyperfine splitting and g tensors (Galla 1988).

Coupling to Halogen Nucleus

The nuclear spin of F^{19} is ½ and its natural abundance is 100%. There are three main contributions to the fluorine dipolar tensor. The carbon centered α-halogen radical is one of the main radicals dealt with in this thesis as shown in **Fig. 2.2.11**. There is no induction of spin density in the p_y halogen orbital. The biggest portion of halogen spin

density comes from contribution of unit spin density in the halogen π orbital resulting from direct polarization by the carbon π orbital spin density. There is contribution from the halogen p_z density and from the dipolar interaction between the carbon π spin density and halogen nucleus. A very small effect also comes due to the small s orbital spin density arising from the isotropic term of hyperfine coupling. The most prominent contribution to the a-halogen hyperfine interaction stems from the halogen π orbital spin density. The β-fluorine hyperfine coupling are also quite large in fluorine containing organic radicals. The coupling tensor is again close to axial symmetry indication delocalization of the odd electron into fluorine $2p_\pi$ orbital. The hyperfine splitting values for ^{19}F are 16.67 mT/ -0.46 mT/ 2.065 mT (Oloff and Hüttermann 1980).
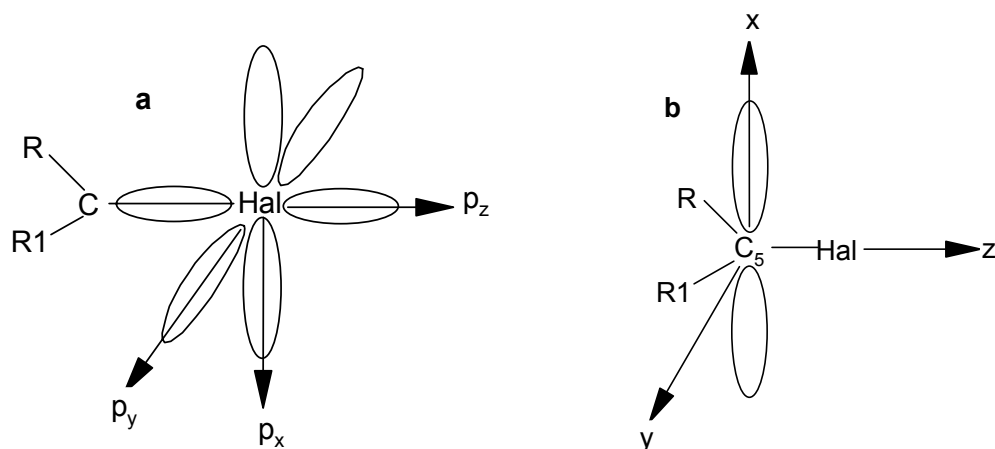
Fig.2.2.11. a) Axis system of halogen p orbital in 5-halouracils. b) Axis system for spectral parameters in α- halogen radicals (Oloff and Hüttermann 1980).

2.3. DNA and its Constituents

2.3.1. The DNA Double Helix: Structure

The study of nucleotides and nucleic acid structure has remained a field of immense interest from last many decades as the hereditary material of all living cells and many viruses known as DNA is a linear polymer built up of monomeric units, the nucleotides. A nucleotide is made up of three molecular fragments: heterocyclic nitrogenous base, sugar and phosphate as shown in **Fig. 2.3.1**.
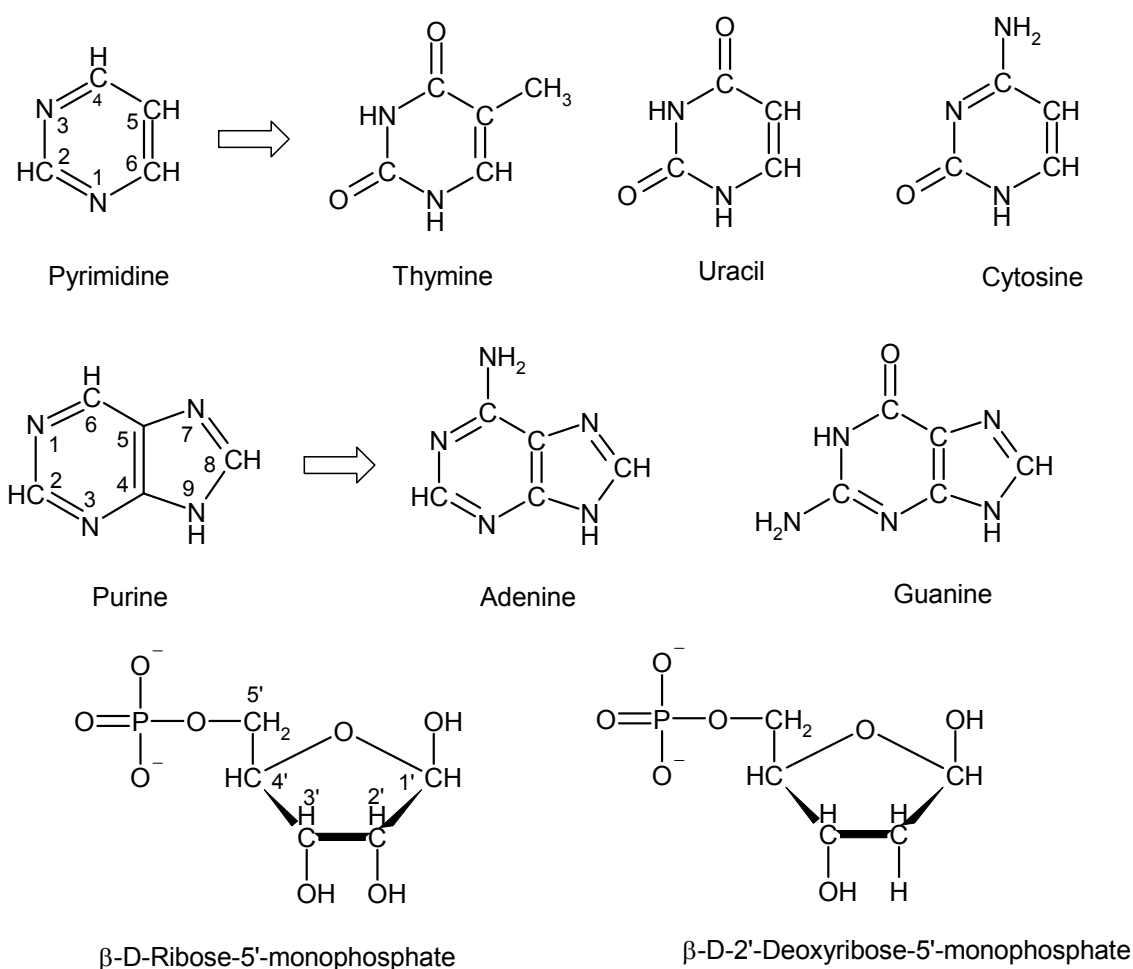
Fig.2.3.1. Chemical structures of bases and the sugar phosphate groups constituting RNA and DNA.

The heterocyclic base can be a purine, namely adenine (A) and guanine (G), or a pyrimidine, namely thymine (T) or uracil (U) (in RNA) and cytosine (C) (in DNA). The

sugar moiety can either be ribose (for RNAs) or deoxyribose (in DNA and this sugar lacks one oxygen atom that is present in ribose) (**Fig. 2.3.2**). A nucleoside consists of a purine or pyrimidine base bonded to a sugar. In a deoxyribonucleoside, N-9 of a purine or N-1 of a pyrimidine is attached to C-1 of a deoxyribose. The configuration of this N-glycosidic linkage is β (the base lies above the plane of the sugar). A nucleotide is a phosphate ester of a nucleoside. The most common site of easterification in naturally occurring nucleotides is the hydroxyl group attached to C-5 of the sugar.
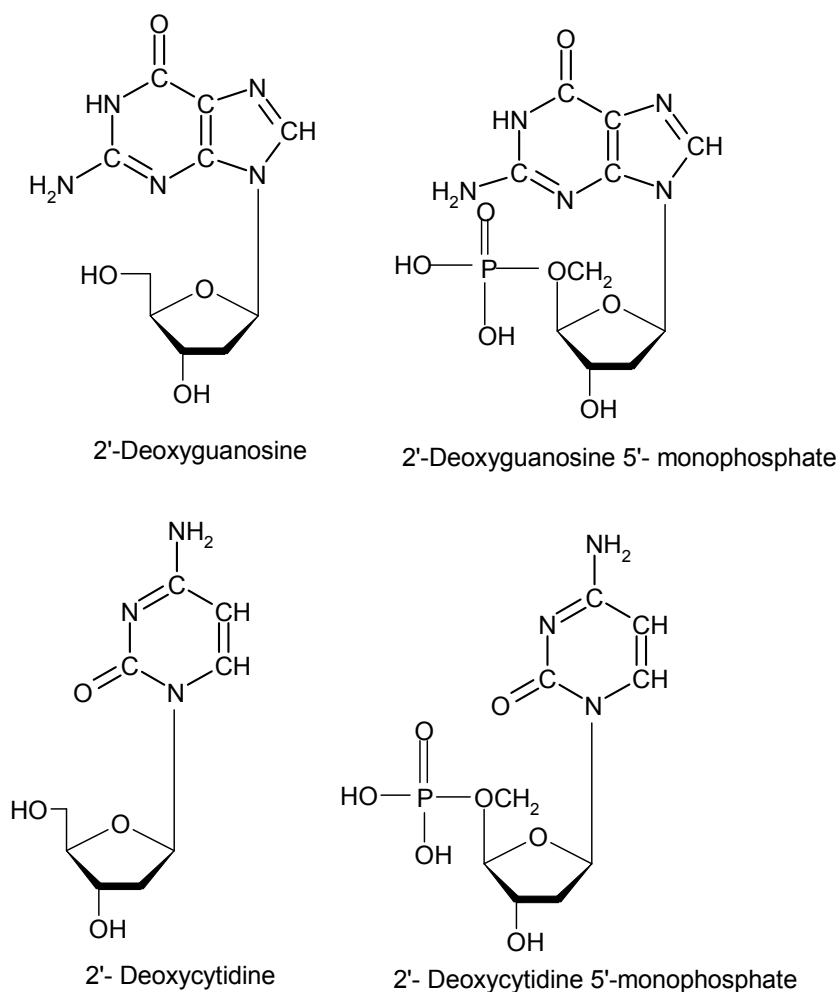
Fig. 2.3.2. The structure of nucleoside and nucleotides

The backbone of DNA consists of deoxyribose moiety linked by phosphate groups. The 3'-hydroxyl of the sugar moiety of one deoxyribosenucleotide is joined to the 5'-hydroxyl of the adjacent sugar by a phosphodiester bridge. The bases act as variable in

a DNA chain. A DNA chain has polarity. One end of the chain has a 5'-OH group and the other a 3'-OH group, neither of which is linked with another nucleotide.

The DNA double helical structure contains two polynucleotide chains which are coiled around a common axis and run in opposite direction to each other. In this helix the purines and pyrimidine bases are present at the inner positions and the phosphate and dioxyribose units are outside. The planes of the bases are perpendicular to the helix axis and the planes of the sugars are nearly at right angles to that of bases. The diameter of the DNA double helix is 20 Å. Separation between the adjoining bases are 3.4 Å along the helix and related by a rotation of 36 degrees. The helical structure therefore repeats itself after 10 residues on each chain and that is at interval of 34 Å. The nucleotides guanine is always paired with cytosine by three hydrogen bonds and thymine with adenine by two hydrogen bonds. The intertwined strands make two grooves of different widths, named major and minor groove, which may facilitate binding of specific proteins. This base stacking and braided architecture provides an excess stiffness to it. The phosphates in DNA's backbone make it one of the highly charged polymers known. Moreover hydrophobic interactions, van der Waals forces, and neutralizations of the electrostatic repulsive forces of the phosphate groups by cations do stabilize the helix as well.

The conformation of the sugar phosphate in a nucleotide unit is defined by torsion angle α, β, γ, δ, ε, ζ in alphabetical order. The orientation of the base relative to the sugar is given by χ as shown in **Fig. 2.3.3**. The torsion angle γ of the exocyclic C4'-C5' bonding identifying the position between sugar plus base unit with the phosphate group is explained with trans (~ 180°) and gauche (~± 60°) (Saenger 1984)

The sugar backbone is basically in a cyclic furanoside form and is connected by a β-glycosyl linkage with one of the four heterocyclic bases to produce nucleosides. The five-membered furanose ring is generally nonplanar. It can be puckered in an envelope (E) form with four atoms in a plane and the fifth atom is out by 0.5 Å; or in twist (T) form with two adjacent atoms displaced on opposite sides of a plane through the other three atoms. Atoms displaced from these three-or four-atom planes and on the same side as $C_{5'}$ are called endo; those on the opposite sides are called exo as shown in **Fig. 2.3.3**. The deviation from the planar structure induces puckering in the sugar molecule.

Relative to the sugar moiety, the base can adopt two main orientations about the glycosyl C_1'-N link, called syn and anti. They are defined by torsion angle χ.
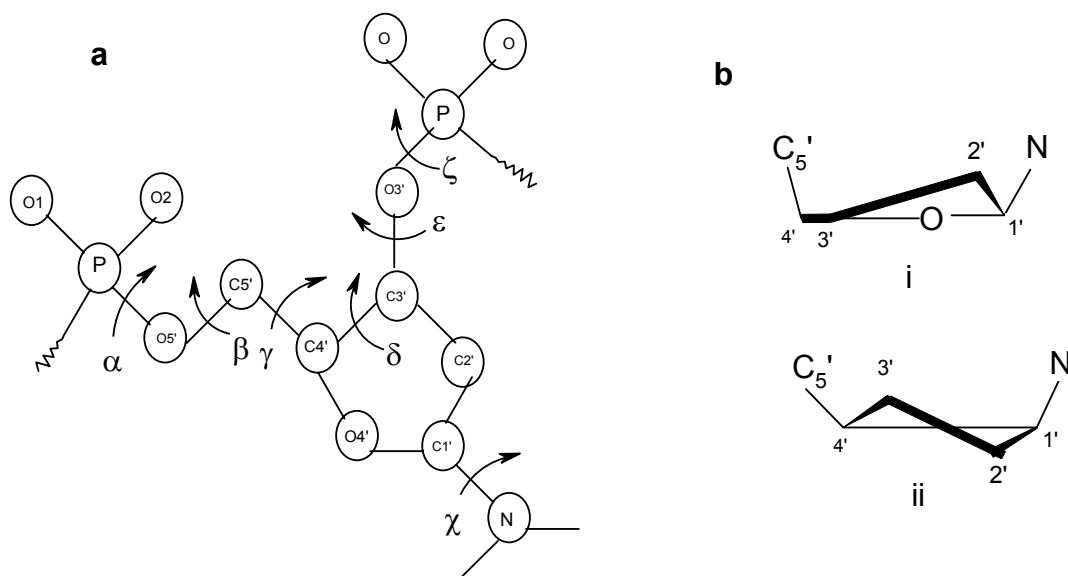
Fig. 2.3.3.a) Atomic numbering scheme and definition of torsion angles for a poly nucleotide chain. B) Sugar conformation structure i) Envelope C_2' endo and ii) Symmetrical twist of half chair C2'-exo –C3'- endo (Saenger 1984).

Polynucleotides in helical arrangement display order which can be expressed by helical parameters. In a double helix, the two polynucleotide chains are connected with complimentary base pairing. The A:U and G:C base pairs are similar in shape, or isomorphous and have identical C1'-C1' distances. The base pairs are usually displaced and are not centred on the helix, instead of being perpendicular to the helix axis they are inclined with twist angle θ_T and roll angle θ_R. Bases are not always co-planar; they can have propeller twist θ_p defined by a rotation about the roll axis or by a dihedral angle between the normals to the base planes as shown in **Fig. 2.3.4**.

DNA can assume different helical structures like A, B, C, D, E and Z. The degree of hydration of DNA plays a key role in its conformation. High relative humidity prefers the B form i.e. also the case in physiological conditions and reduced humidity or increased ionic strength leads to a transition from B form to C-, A-, and if it is possible through the sequence then D- and Z-DNA. DNA structure is found to be sensitive to cation types and temperature. Sodium and lithium salts of natural and synthetic DNA

adopt different helical structure in the fibre state while different anions do not show any such measurable effect.
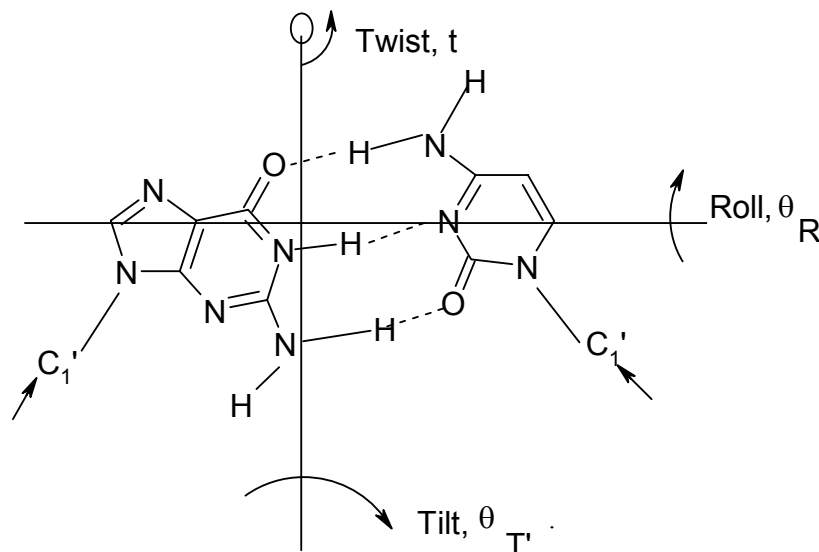
Fig.2.3.4. Helical parameters, Twist, Roll and Tilt in a double helical polynucleotide, (Saenger 1984)

2.3.2. Interactions of DNA with other molecules

The highly anionic nature of DNA makes it prone to interact with monovalent or bivalent cations. The complex functioning of DNA double helix depends strongly on presence of several metal ions in the near vicinity for example Mg^{2+}, Na^+, Ca^{2+}, K^+ etc. Some of the metals interact directly with DNA while others act as cofactors for a number of nuclear proteins. In general it has been found that cations get settled in major or minor grooves of DNA. Cations share the grooves with water and water mediated contacts are an integral component of how the grooves coordinate cations.

In the field of studying radical structure of solid state DNA by EPR spectroscopy at low temperature, several electron scavengers containing metal ions (Fe^{3+}, Ti^{3+}) (Weiland and Hüttermann 1998, Shukla et. al. 2004) have been used. The metal cations in these studies have shown strong electrostatic interaction with DNA structure hence have modulated the radical balance to a large extent by scavenging the electrons produced in the system and prohibiting formation of DNA anions. This kind of study has enabled the

ESR spectroscopist to understand the oxidative pathway of radical formation in irradiated amorphous DNA at low temperatures.

A large number of aromatic molecules influence the biological function of nucleic acids by binding to them. These include pyrimidine and purine bases, aromatic amino acids, polycyclic hydrocarbons, dyes, antibiotics and many others kinds of aromatic drugs. Small aromatic ligand molecules can bind to DNA double helical structures by groove binding. It is a weak mode of ligand binding. It causes little distortion of the DNA backbone. Groove binding is dominated by cooperative and electrostatic interactions for attaining stabilization of the weak complexes. The ligand molecules are externally bound to the DNA helix by electrostatic forces and aggregate on the sugar-phosphate backbone. The strong binding mode of aromatic ligands with DNA is known as intercalation which occurs between stacked base pairs thereby distorting the DNA backbone conformation and interfering with DNA-protein interaction. Both interactions work through non covalent interaction. A large class of molecules intercalates into DNA - in the space between two adjacent base pairs. These molecules are mostly polycyclic, aromatic, and planar, and therefore often make good nucleic acid stains. Intensively studied DNA intercalators include ethidium bromide, proflavin, acridine orange. DNA intercalators are also used as chemotherapeutic agents (for example Mitoxantrone, Daunomycin) to inhibit DNA replication in rapidly growing cancer cells. Intercalation changes the physical properties of double helix. ESR spectroscopic studies have been done to understand the formation of free radicals after irradiation of DNA-organic molecule/intercalator system at low temperatures in frozen glass and frozen aqueous solutions. Another theme was to study the distance traveled by electrons through DNA double helix during irradiation in the presence of such additives.

3. Literature Review and Aim of the Thesis

As DNA plays a fundamental role in the radiation induced biological inactivation of cells therefore the field of analyzing the radical formation (both qualitative and quantitative) and their reaction pathway in DNA and its constituents in model systems upon irradiation is a topic of persistent curiosity for the last almost four decades. ESR spectroscopy has significantly contributed to this subject due to its specificity and sensitivity in free radical detection and characterization specifically at low temperatures. However, the ESR investigation of DNA and its components after irradiation at low temperatures remained a topic of continuous debate and conflicts because of several reasons; as accounted below;

- Most of the radicals formed on DNA give an overlapping spectral signature of in a very narrow field range at typical X-band (9.5 G Hz) ESR conditions.

- Chemically identical radical structures may give variable ESR spectra in different environments.

- A strong influence of matrices i.e., depending on the system in which DNA or its constituents were observed, e.g. single crystals of oligonucleotides, oriented fibers, freeze dried amorphous samples or frozen aqueous solutions or glasses, different types of radicals were obtained and comparisons between the systems were not possible.

- Difficulties in detecting the sugar radicals formed on DNA in powder or aqueous systems although there presence was predicted by hole scavenging mechanism due to irradiation.

- The contribution of direct or indirect effect of irradiation in frozen aqueous matrix which is a widely used system in this field is still not clear.

- The electrons and holes produced during irradiation do migrate through DNA double helix before being trapped by and base or by any doped additive but the extent of charge transfer after irradiation at very low temperature is again a topic of controversy raised in last few years.

In order to improve the existing picture there has been an implementation of different experimental conditions. Pioneering work in this field was done by using single crystal systems (Pruden et al. (1965), Hüttermann 1970) mainly because of the fact that radicals formed in the crystal environment are selectively oriented, the well established directional properties of anisotropic hyperfine coupling tensors and dipolar interaction helps to identify the specific magnetic nuclei in the compound interacting with unpaired spins. Single crystal works also show the effect of direct irradiation on the samples and thus help to understand direct ionization mechanism (Close 1993, Hüttermann 1982, Hüttermann 1991, Sevilla and Becker 1994). More recent approaches are mainly dealing with the mechanisms of radical formation and extent of electron transfer specifically in mixed crystals like co crystals, doped crystals and oligonucleotide crystals (Herak and Hüttermann 1991, Herak et al, J., 1991, Bernhard 1989, Sankovic et.al. 1991, Sagstuen et.al 2006). The main disadvantage of using single crystals is the inherent difficulty to alter the conditions of the system and, moreover the polymer DNA itself cannot be crystallized. This prompted the investigators to utilize other matrix systems like oriented DNA fibers (Zell 1989), lyophillized dry or hydrated DNA, aqueous glasses and frozen aqueous systems in which it was easy to alter the conditions and DNA itself can be easily studied in these matrices. Among these the oriented fibers, lyophillized dry and hydrated systems containing DNA are models for studying direct effect of irradiation while frozen aqueous glasses show the free radical formation through indirect mechanism. The extent of direct and indirect mechanism in frozen aqueous solutions is still under debate.

Among all these benefits one main drawback in this case was the composite nature of ESR spectra obtained from these systems due to overlap of many spectra in a small region of g-factors specifically in X band frequency. In order to overcome this drawback ESR methods with several higher frequencies especially Q band ESR spectroscopy (34 GHz) on oligonucleotides have been done in last many years (Bernhard 2000 and references therein). Weiland and co workers have for the first tim,e utilized a much higher frequency (245 GHz) spectrometer for irradiated nucleotides and DNA (lyophillized systems) and tried to separate the overlapping spectroscopic signatures as obtained by X-band ESR spectroscopy (Weiland et. al. 1997a, 1997b). One other innovative method was first study of a pulsed EPR spectroscopic study of the free radicals formed in irradiated oriented DNA fibers at 77 K. Electron spin echo ESR

employed in this work allowed relaxation time resolution of not all but some component of spectra (Gatzweiler et. al. 1994).

Other approaches taken for a better understanding of the free radical mechanism in irradiated DNA and its components were utilization of specific electron scavenging and electron donating additives. These molecules can change the contribution of radicals in a specific manner. Several electron scavenging additives like iodoacetamide (Ormerod 1965). Gregoli and co workers (1970, 1974, 1976, 1977, 1979), nitro compounds (Boon et. al. 1985), intercalators like proflavin and mitoxantron (Cullis et. al. 1990, Messer, 2000 and references therein) and ESR silent metal ions at 77 K like Fe^{3+} and Ti^{3+} (Lange et. al. 1995, Weiland and Hüttermann 1998, Shukla et. al. 2004) were used to quench the formation of reduced radicals on DNA and therefore helped understanding the oxidative pathway as well as sugar phosphate backbone reactions.

The quality and quantity of irradiation plays a crucial role in the formation of radicals on DNA and its constituents. Structural and quantitative analysis of the radicals in solid state DNA bases and nucleosides both at room and low temperature after irradiating with heavy ions from different elements with different energies was initiated by Schaefer and Hüttermann (1993a, 1993b). It was observed for the first time that the G-values (free radicals normalized to the energy given) are strongly dependent on the lower energy transfer (LET) of the particle. Further analysis of Bragg peaks in heavy ion irradiated lyophilized dry DNA (by Weiland et. al. 1999) as well as hydrated DNA (by Becker et. al. 1996, Becker et. al. 2003) has shown an increasing amount of sugar radical formation in heavy ion irradiated DNA in comparison to X or γ rays. The highly dense ionization produced by high LET ions may be the cause of such differences. These investigations have provided a good source for studying the structures of different sugar radicals formed on DNA. It has been found that the nature of radicals formed depends also on the quantity of dose used. All DNA radicals shows an initial increase with increasing dose, the base cation and anion radicals gets saturated after a particular dose but the neutral radicals specially the neutral sugar radicals don't show such saturation behavior at the same dose point and becomes main radical centers in higher dose region. This phenomenon that different chemical species demonstrate a different dose saturation behavior is known as saturation asymmetry was previously observed by Spaletta and Bernhard (1992) became more evident in recent dose dependent studies and has also been dealt theoretically by Nelson (2005). Variable saturation behavior of

radicals provides additional information about their nature and has become a subject of recent study (Purkayastha and Bernhard 2004, Shukla et.al. 2005) and has provided helpful information regarding the formation of sugar radicals.

3.1. State of Art on the Topics Related to this Thesis

3.1.1. Understanding the Effects of Irradiation in Frozen Aqueous Solutions in DNA Model Systems

Among the various matrices investigated to get knowledge about mechanism of radiation and the radical formation in irradiated DNA and its constituents in frozen aqueous system has remained a theme of vivid interest for the last few decades. Frozen aqueous solutions of DNA or its constituents are prepared by freezing their aqueous solutions to 77 K (in liquid nitrogen). The system was first used as early as in 1965 (Omerod). Since then the system has been employed extensively as matrix for ESR spectroscopic investigations of spectral features of free radicals produced from substrate molecules by ionizing radiation, typically at 77 K and subsequent annealing. Gregoli and co workers studied model DNA systems like single nucleotides, costacking nucleotide mixtures as well as DNA in pure form and along with the electron scavenger Iodoacetamide (1974, 1976, 1977a, 1977b, 1979). They pointed out that in frozen aqueous systems containing nucleotides (dAMP, dGMP or TMP) there is a linear relationship between the solute radical yield and solute concentration as observed in dry systems. They reported that when an aqueous solution containing DNA constituents (bases, nucleosides or nucleotides) which are having higher degree of association with each other are frozen they tend to exclude from the ice crystals and settle down as large aggregates in the interstices of the solvent crystallite; this phenomenon was termed as phase separation. Assumption of the spatial separation between the ice and the solute phase lead to a hypothesis that in a frozen aqueous matrix the formation of oxidised and reduced species of the substrate caused by ionisation follows the pattern of direct radiation action. The water radicals produced heterogeneously as clusters with high local density get mutually deactivated before reaching to any solute molecule by diffusion. The mechanism for γ radiolysis of nucleotides in frozen aqueous as corroborated by Gregoli and coworkers can be represented as shown in **Scheme 3.1.1** (Gregoli et.al. 1976). In the frozen aqueous solution of nucleotide thymidine 5'-monophosphate (TMP) for example it was postulated that after irradiation Thymine cations and anions (T$^{+\bullet}$ and

T$^{-\bullet}$) (**Fig. 3.1.1**) were produced and got converted into TOH$^\bullet$ (**Fig. 3.1.1**) as a quintet and TH$^\bullet$ (**Fig. 3.1.1**) as an octet pattern, respectively, upon annealing. The other nucleotides (dAMP and dGMP) were treated accordingly. This model of direct irradiation in frozen aqueous solution lead to many controversies as the spectral features assigned to thymine cation were observable in frozen aqueous system only after addition of sizable amount of electron scavengers and the pattern had no resemblance with the T$^{+\bullet}$ formed in glass upon photolysis (Gregoli et. Al. 1976 and Sevilla 1972, Sevilla 1976). The quintet pattern was reproduced by Wang and Sevilla (1994) and accepted as TOH$^\bullet$ but formation of this radical was also was questioned against its identification by other working groups.

Nucleotides $\xrightarrow{\gamma\ \text{rays}}$ Anions + Cations (primary radicals)

Anions + H_2O $\longrightarrow$ H-addition radicals + OH$^-$

Cations + H_2O $\longrightarrow$ OH-addition radicals + H$^+$ thermally induced secondary radicals
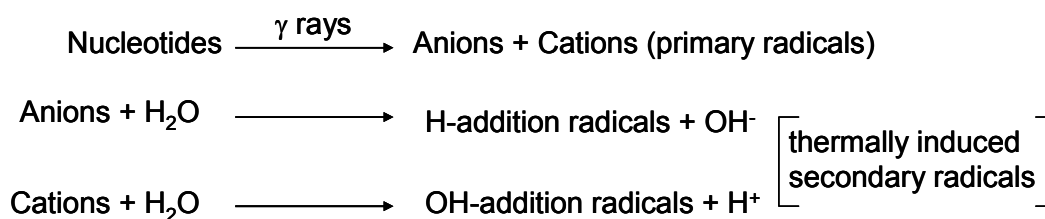
Scheme 3.1.1. Model for direct irradiation mechanism in frozen aqueous system as proposed by Gregoli and coworkers (1976).

Hüttermann and co workers revisited the case of nucleotide thymidine 5' monophosphate in frozen aqueous solution (Hüttermann et. al. 1992) and reached the conclusion that the radical identified as cation on thymine (labelled as T$_4$) in the previous work (Gregoli et. al. 1976) was actually allyl radical (TCH$_2$$^\bullet$) as reported previously in single crystals (Hüttermann 1970, Hüttermann et. al. 1971). In the single crystals the radical was considered to result from deprotonation of the base cation at the methyl group, and in glasses or in aqueous solutions it must have formed from the reaction of OH$^\bullet$ radical upon thermal decay. The characterization of TCH$_2$$^\bullet$ was done by comparison with analogous C(CH$_2$$^\bullet$) (**Fig. 3.1.1**) allylic radical formed in 5-methyl cytosine. In this work they observed by using 5-chloro-2'-deoxyuridine (ClUdR) in frozen aqueous system no phase separation was observed. The large extent of reduced species found at 77 K in irradiated TMP was assigned due to selective transparency of the bulk ice phase for the electrons and not for the OH$^\bullet$ radicals. The quintet patterns were observed but a conclusive mechanism for its formation was not provided. In a continuation of this effort (Lange et. al. 1995) the authors studied irradiated TMP in both BeF$_2$ glass where OH$^\bullet$ species are stabilised at 77 K just like as in frozen aqueous solutions and found the allyl radical to be predecessor of the quintet pattern which was a

major component at higher temperature (240 K) even in the presence of electron scavengers.
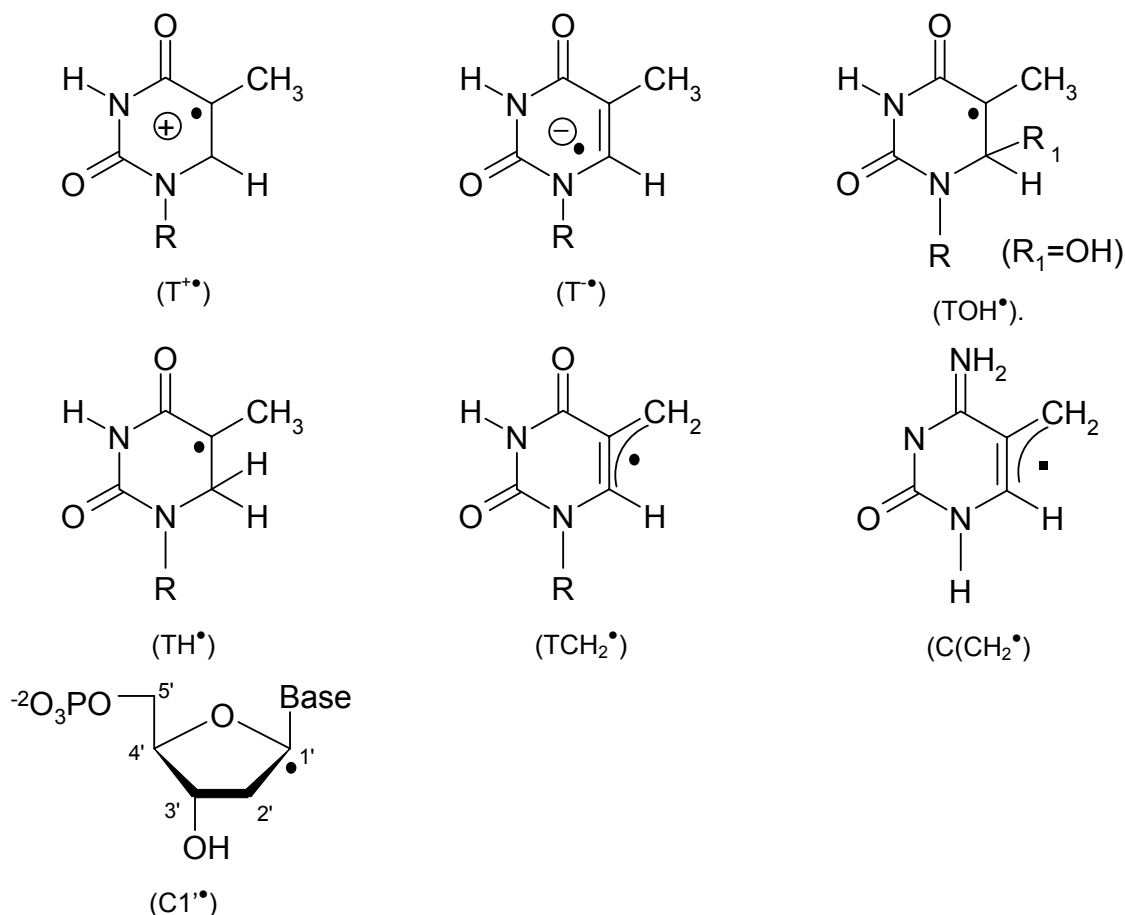
Fig. 3.1.1. Structures of the radicals formed on TMP, 5-methyl cytosine and a C1' based sugar radical on dCMP (see text).

They also pointed out by comparing other DNA constituents like 5-methyl uridine, 5-methyl-2'-deoxycytidine monophosphate, 5-methyl-2'-deoxycytidine, thymine and 4-O-methyl-thymidine in the same conditions that although the allyl radical was formed in all cases but presence of a sugar (or sugar phosphate group) and a C4 - carbonyl group were necessary prerequisites for subsequent quintet pattern formation. The mechanism of quintet formation as a result of dimerization or cyclization at C6 of thymine base moiety as postulated by Malone et. al. (1993) was put to a question here. They compared for the first time the effect of irradiation on DNA in both frozen aqueous and frozen glass (LiCl) solutions in the presence of different concentration of electron scavenger. For both TMP and DNA they concluded that in frozen aqueous system the

oxidised radical species at 77 K are formed only at minor concentrations and therefore the conclusion was drawn that direct irradiation model cannot be the only model to explain the mechanism of irradiation in frozen aqueous solutions. In spite of these postulates a question remained about the mechanism of formation of allyl radical in TMP nucleotide in frozen aqueous solutions as there are evidences of its formation by both direct and indirect type of irradiation.

In order to gain more insight on this problem Weiland and co workers (Weiland et. al. 1996) studied cytosine base containing derivatives in BeF_2 /D_2O and LiCl /D_2O glasses and in frozen aqueous systems. In BeF_2 glasses the $OD^\bullet$ addition reactions are important therefore they carefully distinguished between the quartet ESR spectrum that raised from $OD^\bullet$ addition to the 5,6 double bond in cytosine and the quartet that is produced from C1' deoxyribose sugar radical (**Fig. 3.1.1**) which was also identified by Malone et. al. 1995. In BeF_2 at 77 K the ESR spectrum obtained from irradiated 5'-dCMP was explained as a mixture of radicals containing 50% $C(N3)D^\bullet$, 40% $OD^\bullet$ and 10% $C1'^\bullet$. On warming to 150 K the $OD^\bullet$ pattern disappears while the relative amount of $C1'^\bullet$ increases to 25% of the radical concentration while the total radical concentration did not change showing that the formation of the $C1'^\bullet$ radical is due to H abstraction by mobile $OD^\bullet$ at elevated temperatures. In LiCl glass where $OD^\bullet$ were not stabilised showed no increase in $C1'^\bullet$ on warming the system to 150 K. In frozen solutions of D_2O, on annealing to 150 K, no concomitant increase in $C1'^\bullet$ was observed with disappearance of the $OD^\bullet$ species. In BeF_2 the formation of $C1'^\bullet$ sugar radical was attributed to immediate deprotonation of a cation formed by hole transfer from $D_2O^{+\bullet}$ to the substrate before they deprotonate to form $OD^\bullet$ or by hydrogen abstraction at C1' by $OD^\bullet$ radicals that are mobile at 77 K. On annealing the increase in $C1^\bullet$ concentration were because of H abstraction from deoxyribose moiety by $OD^\bullet$ which became mobile after 150 K. In LiCl glass the different hole trapping mechanism and $Cl_2^{-\bullet}$ being a very strong hole trap may be the reason of no increase in $C1'^\bullet$ radical with annealing. In frozen aqueous system three possible mechanisms for formation of C1' radical in cytosine nucleosides and nucleotides were discussed. First as proposed earlier by Gregoli and co workers the direct ionization of the substrate forms a cation and subsequent deprotonation at C1' of deoxyribose sugar moiety. Though it was not possible to distinguish but the authors also gave emphasis to the hole migration from glass like water of solvation and mobile $OD^\bullet$ radicals (at 77 K) formed due to ionization of water of hydration. In spite of all these

studies the question of mechanism of irradiation in frozen aqueous solutions remained open owing to the formation of same radical species through both indirect and direct pathways in the model system like in TMP.

Another DNA model system which has been previously probed to understand the effect of radiation in frozen aqueous solutions is the class of halouracils. Specifically 5-Flurouracil and its nucleoside i.e. 5-Fluoro-2′-deoxyuridine (FUdR) are assumed to clarify the effect of direct and indirect oxidation as the FU cation formation via direct oxidation and OH addition radical formed by solvent matrix can be well differentiated owing to characteristic large fluorine hyperfine coupling.

Solid state ESR and electron nuclear double resonance (ENDOR) studies of 5-halouracils in single crystals of bases and nucleosides did not show any difference in the anion reactions between thymine and the halo substituted compounds and indicated that matrix effect like solvation energy or lattice parameters might have a directing role in the reactions of radiation induced free radicals (Flossmann et. al. 1979, Neumüller and Hüttermann 1980). Additionally in these substrates a systematic investigation of radiation effects on halouracils and its derivatives in different solid systems has been done providing information about several radical structures and condition needed for their formation. A large range of reports can be found in the literature for the halo components at the level of single crystals of bases and nucleosides (-tides) which can provide a base for gaining more information on formation of free radicals in frozen glass or aqueous solutions. In single crystals of a molecular complex containing 1-methyl cytosine and 5-fluorouracil (FU), X irradiated and ESR measured at 77 K a primary oxidized radical was found to form by deprotonation at N1 position of FU (**Fig. 3.1.2 (I)**) (Close et. al. 1978), another precursor radical was found to be FU anion (**Fig. 3.1.2 (III)**) formed upon irradiation of single crystal of FU at 77 K (Neumüller and Hüttermann 1980). The secondary radicals who were observed to be formed at about 220 K and were stable even at room temperatures were resulted from H addition to the 5, 6-pyrimidine double bond (**Fig. 3.1.2 (V)**) and from the enolization of the C4-carbonyl group (**Fig. 3.1.2 (VI)**) (Close et. al. 1978, Neumüller and Hüttermann 1980) and were also observed in other halo uracils (Oloff and Hüttermann 1977). In frozen glass solutions the primary π cation radical (**Fig. 3.1.2 (II)**) and its neutral deprotonated form was difficult to distinguish spectroscopically because of similar spin density distributions on both radical but when FU and its nucleoside (FUdR) were treated in aqueous glass

(H_2SO_4) medium containing high concentrations of electron scavenger $Na_2S_2O_8$ (Riederer and Hüttermann 1982) it was observed that the two radicals could be differentiated by an enhanced halogen splitting as observed in FUdR where formation of radical II is the only possibility due to the presence of bulky deoxyribose group at N1. Not so significant in solid crystals but in solid glasses and frozen ice systems with increasing temperature the cations were found to react with anion moieties (SO_4^{2-} in H_2SO_4 glass or OH^- in BeF_2 glass) and produces a radical where one of the methylene proton was replaced. The anions produced at 77 K in glass or frozen matrices were found to get protonated at C6 or at O4 just as in single crystals with increase in temperature of the medium. In the halo nucleosides treated in H_2SO_4 glass medium no oxidation radical could be trapped or observed at the sugar moiety (Riederer and Hüttermann 1982) while in fluoro deoxyuridine (FUdR) treated in BeF_2 matrix a quintet structure was observed at high temperatures (~ 190 K) which was tentatively assigned to C2'(-H) radical of the deoxyribose moiety.
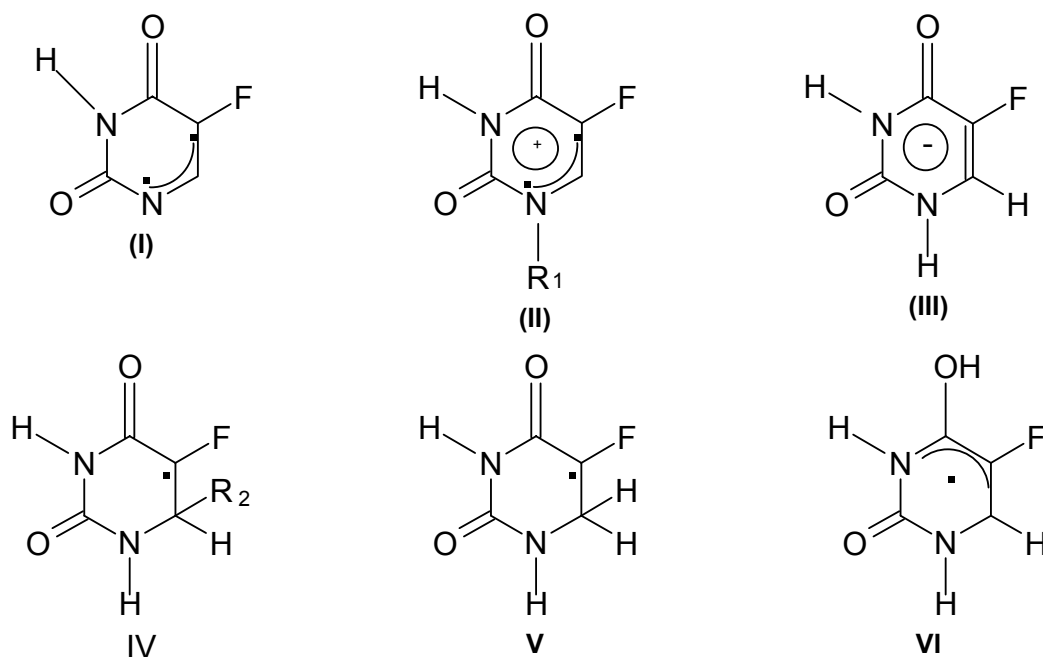
R_1= H, CH$_3$, deoxyribose, ribose, R_2= SO$_4$-, OH

Fig.3.1.2. Structural formulae of the radicals found to form in Fluorouracil and its derivatives upon direct or indirect ionization radiation in different matrices.

Geimer (1994) has tried to investigate and differentiate the radicals formed in frozen glass (LiCl or BeF_2) and aqueous solutions containing FU and FUdR as substrates as well as with other halouracils (like ClUdR) upon irradiation but to very low

solubility of the substrates in water resulted into very noisy spectra where perfect identification or differentiation of ESR spectral pattern from FU base cation or from OH addition radical on FU was not distinctively possible under the used conditions.

3.1.2. Understanding the Mechanism of Irradiation, Identification and Assignment of Free Radicals Formed in DNA in Frozen Aqueous Solutions

Symons and colleagues continued the investigation of free radicals formed on irradiated DNA in frozen aqueous system along with strand break measurements. They also used the additives like O_2 (Boon et. al. 1984), Iodoacetamide (Cullis et. al. 1985), H_2O_2 (Cullis et. al. 1986), nitrocompounds (Boon et. al. 1985), thiols (Cullis et. al. 1987a) and intercalators (Cullis et. al. 1990) and investigated their effect on the free radical balance. From these studies and along with infrared measurements Symons and co workers agreed with the biphasic nature of frozen aqueous system and also introduced an additional glass like water shell in the immediate vicinity of the substrate where most of the electrons and holes formed during irradiation migrate to the bases (Symons 1991, Symons 1997). This was called quasi direct effect of radiation. The $OH^\bullet$ radicals formed at 77 K by water oxidation were supposed to be confined to the bulk ice compartment in which they decay at about 130 K without interfering with the substrate radicals. It was also revealed from these studies that electrons and holes migrate to a large extent through the DNA double helix before they are being trapped, especially when intercalator like Mitoxantrone was added with DNA in frozen aqueous system.

Several ESR investigations were done to analyse the effect of hydration layer on the radical yields of DNA. Gregoli and coworkers (1982) studied DNA dry and as a frozen aqueous solution and found differences in the slope of dose/yield curves between the two, they also reported a two fold increase in the DNA radical yield in frozen aqueous solution in comparison to the dry DNA samples. Direct ionisation of the DNA and ionisation of the hydration layer and immediate transfer of the dry electrons and mobile holes to the DNA was accounted for this observation. Hüttermann and et. al. (1992) equilibrated lyophilized DNA (calf thymus, Na salt) at selected relative humidity of 15%, 32%, 45%, 66%, 76% and 95% which are equivalent to Γ's (degree of hydration i.e., mass ratio of water to nucleotide plus counter ion) of about 0.15, 0.20, 0.25, 0.30, 0.42 and 1.40 respectively (Mroczka and Bernhard 1993). They reported that water of hydration is an integral part of the DNA target up to 76% (~10 waters per nucleotide) of

relative humidity while the radiation chemistry changes to that of ice and hydrated DNA at 95% ($\Gamma > 1$) relative humidity. The total radical yield mainly of the anionic species which are formed on DNA almost doubles with increasing water content from 0% to 45% of the samples used which reaches saturation from 76% onwards. Similar efforts by Wang et. al. (1993) suggested that for frozen DNA solutions the hydration layer extends to about 15 waters per nucleotide and an increase in radical yield relative to the dry DNA was observed. The change in molecular packing and the change in water proximity was accounted for the observation. Both Wang et. al. (1993) and Mroczka and Bernhard (1993) found that beyond the first hydration layer radical yield drops significantly. Product analysis study on irradiated DNA (Swarts et. al. 1992) at ambient temperature also suggested that first 15 waters per nucleotide act to transfer dry charges to DNA whereas subsequent waters from hydroxyl radicals. The results so obtained were also supported by investigations on DNA using other techniques (Tao et. al. 1989). A detailed description of the OH$^\bullet$ as a function of the level of hydration (La Vere et. al. 1996) showed three regimes of behaviour for waters of hydration in DNA exposed to irradiation. For the approximately 0-9 waters/nucleotide, no significant OH$^\bullet$ was observed due to the fact that the migration of the hole formed during irradiation to DNA was favoured over proton transfer to water molecue to form OH$^\bullet$, in the next layer consisted of ~ 9-21 waters/nucleotide OH$^\bullet$ were found to be formed which had similarities with the OH$^\bullet$ formed in CsF glass and were termed as OH$^\bullet_{glass}$ and inferred to be formed from the holes which escaped recombination in spurs, the third layer consists of bulk water (in the form of ice) where OH$^\bullet$ radicals formed were similar to that formed in pure water (**Fig. 3.1.3**). Electrons ejected in the hydration layer during irradiation were proposed to be captured by the DNA both because trapped electrons were not observed in glassy phase and anions were found to be formed in DNA, an assumption was made that some electrons from bulk phase might also transfer to the DNA. Most of these reports used hydrated DNA systems (76% or 95%) to understand the effect of radicals formed in bulk water upon irradiation. Systematic studies on frozen aqueous solution of DNA or DNA-additive systems are very few and needs more investigation.

In order to understand the molecular mechanism of radiation damage to DNA, identification and assignments of free radicals formed on DNA by ESR spectroscopy has remained a subject of interest since many decades. From the large body of work done in this field it can be summarised that three types of matrices modelling the cellular

situation have been employed: oriented fibres equilibrated at 76% relative humidity, lyophilised powders containing different amounts of water of hydration and frozen aqueous solutions.

In the oriented fibres the orientation of the DNA fibre axis with respect to the magnetic field is utilized to obtain assignable spectra. In this system the guanine cation ($G^{+\bullet}$), cytosine and thymine anion ($C^{-\bullet}/T^{-\bullet}$) were observed at low temperatures. Upon annealing thymine -H-addition radical ($TH^{\bullet}$), thymine allyl ($TCH_2{}^{\bullet}$) radical and N1 deprotonated guanine cation ($GN^{\bullet}$) were found predominantly as secondary radicals (Gräslund et. al. 1971, Hüttermann et. al. 1984, Hüttermann and Voit 1987, Gatzweiler et. al. 1994). Additionally formation of adenine anion and guanine anion were also proposed to form in oriented fires of DNA (Gatzweiler et. al. 1994) (**Fig. 3.1.4**).
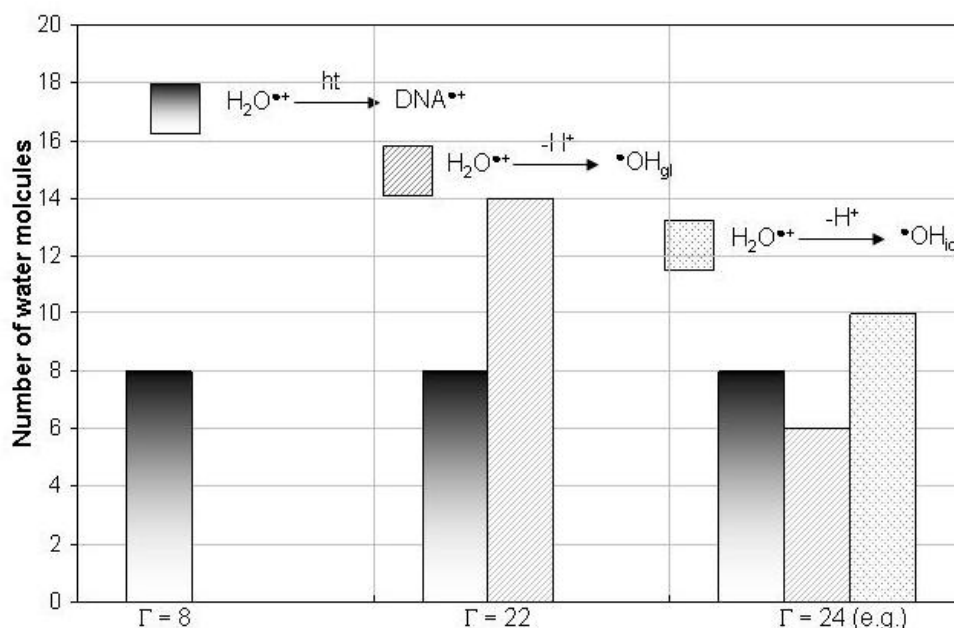
Fig. 3.1.3. The change in balance of radiation-induced holes formed in water hydration layers as a function of the nature of DNA hydration layer and number of waters of hydration/nucleotide (Γ) (adapted from Becker et. al. 2007)

In normal DNA owing to the problem of extensive overlap between radical component spectra in a narrow field range at typical X-band (9.5 GHz) conditions and because of the comparable hyperfine parameters of many species several approaches

were adopted to delineate the radical patterns obtained from irradiation of DNA. Several factors like temperature, presence of electron scavenger, the DNA hydration state, the total dose and the LET of the irradiation were taken into consideration to identify the specific primary electron loss and electron gain radicals and subsequently their successors.

In frozen aqueous DNA two primary radicals were mainly observed $T^{-\bullet}$ and $G^{+\bullet}$ and the secondary radicals were $TH^{\bullet}$ and also peroxy radical specifically in aerobic conditions (Gregoli et. al. 1982, Boon et. al. 1984) as shown in **Fig. 3.1.4**.
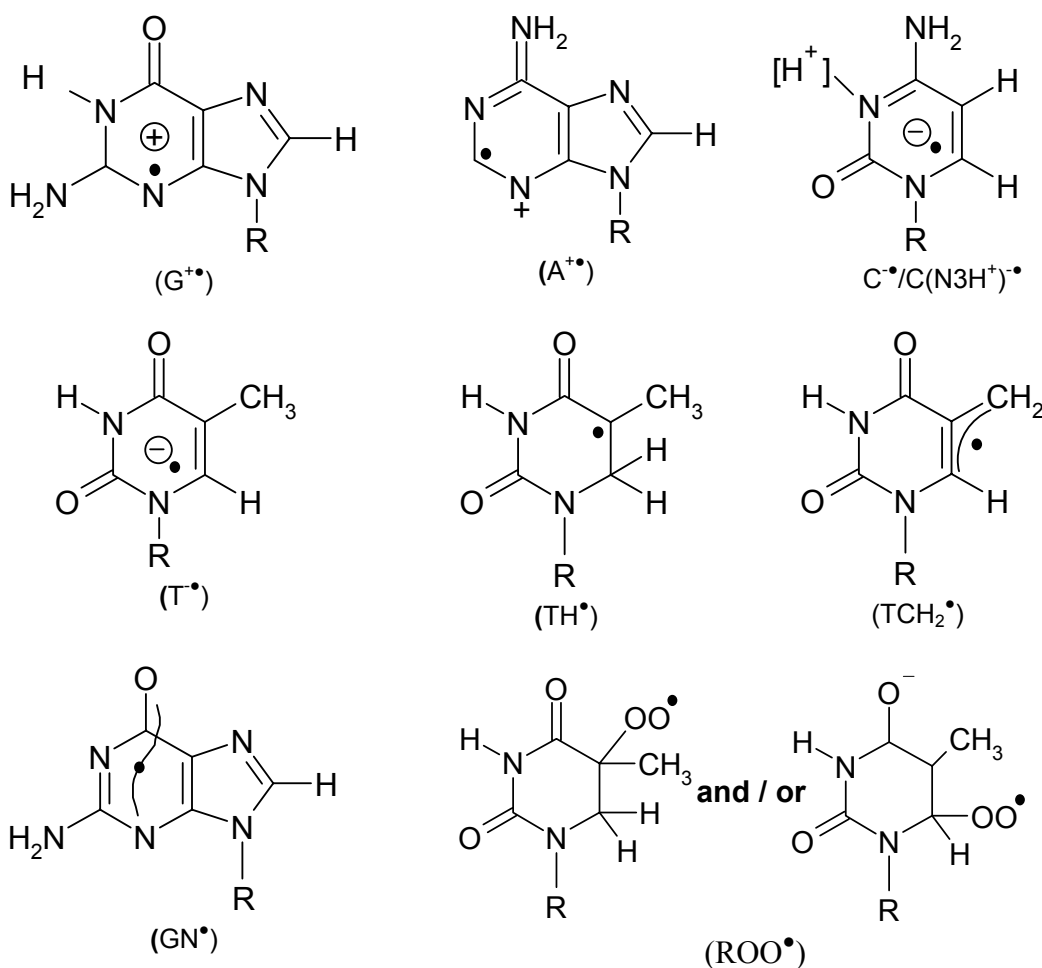
Fig. 3.1.4. Structural formulae of the charged and reversibly protonated base radicals proposed to form on irradiated DNA in different matrices like oriented fibers, or normal DNA.

Sevilla and co workers (Sevilla et. al. 1991, Yan et. al. 1992, Wang et. al 1994) investigated the distribution of oxidized and reduced species in hydrated DNA using reconstruction methods of experimental spectra by selected 'benchmark' components

obtained from suitable model compounds or from analysis of microwave saturation behaviour. For double stranded (ds) DNA equilibrated in 100% relative humidity of D_2O vapour, γ-irradiated at with a dose of 5 kGy at 77 K and then after annealing to 130 K they proposed presence of 41% $G^{+\bullet}$, 43% $C^{-\bullet}/CN3(H)^{\bullet}$, 16% $T^{-\bullet}$ and 3% $A^{+\bullet}$. On analysis of thermal annealing behaviour of the primary components, $TH^{\bullet}$ was found to be main secondary product and its large proportion (35%) as compared to the original signal was accounted due to electron transfer from cytosine to thymine in ds DNA irradiated with a dose of 5 kGy. Cullis et. al. (1992) investigated the formation of $TH^{\bullet}$ from $DNA^{-\bullet}$ in frozen aqueous DNA irradiated with 40 kGy and reported that the yield of $TH^{\bullet}$ maximises at 18% of the original signal and disagreed with the proposal of electron transfer from cytosine to thymine. Wang and Sevilla (1994) repeated the attempt with various doses for hydrated DNA and showed that the yield of $TH^{\bullet}$ at 190 K decreases with increase in irradiation dose and were suggested due to increased radical recombination owing to higher radical concentration at higher doses. They also studied the effect of dose and hydration on other individual radical yields as well and showed that effect of increasing dose is more intense in hydrated samples where $C^{-\bullet}$ are favoured at the expense of $T^{-\bullet}$. Formation of neutral sugar radicals ($S^{\bullet}$) were observed and were found to increase with hydration level and also with radiation dose. It was suggested that high dose might prefer the formation of $S^{\bullet}$ over $G^{+\bullet}$. Although the sugar radicals proposed to form in this work were not identified into individual sugar components. The imbalance in anion and cation radicals formed in DNA even after considering the formation of sugar radicals at higher doses were attributed to the artefact which might have resulted due to computer analysis using benchmark spectra or due to some untraced oxidised radical who could mimic the doublets formed by the anions or might have very broad ESR spectra.

In order to avoid potential transfer problems that were possible with model compound benchmark spectra, Hüttermann and co workers tried to isolate component spectra from DNA spectra themselves and investigated the influence of level of hydration in irradiated lyophilised DNA (Hüttermann et. al. 1992). Presence of $TCH_2^{\bullet}$ radical was proved first time in hydrated DNA in this work. Other major findings were reconfirmation of cytosine based anion along with reduced species of thymine, increase in amount of $TH^{\bullet}$ with increasing hydration level and the doublet character of the spectra enhanced with increasing hydration level. Weiland and Hüttermann (1998) extended

their work on lyophilised dry as well as hydrated DNA (76%) (in H_2O and D_2O) in neat form and containing additives with moderate dose of X ray radiation (~50 kGy). Annealing measurements were also done. In this effort many new ESR patterns were isolated and characterised to respective radicals. At low temperature the radicals suggested were $C^{-\bullet}$, $T^{-\bullet}$ (doublet pattern) $G^{+\bullet}$ (singlet), minute amounts of $TH^{\bullet}$ (octet) and $C(N4H^+)^{-\bullet}$(triplet). In the presence of ESR silent electron scavenging additive $K_3Fe[CN]_6$ quartet patterns consisting of $TCH_2^{\bullet}$ and $C1'^{\bullet}$ sugar radical (from deoxyribose part) were also isolated. In contrast to the reports given earlier the percentage of $G^{+\bullet}$ cation was found to be much smaller in this report (about 25% at 77 K). In hydrated system containing electron scavenger a new doublet species was identified which was also observed in frozen aqueous DNA containing high concentrations of electron scavenger (Lange et. al. 1995), though not sure but the authors suggested the pattern to be associated with $C5'^{\bullet}$ sugar radical and the proportion of the $G^{+\bullet}$ was found to reduce drastically to 5% at 77 K. The formation of about 10% of triplet pattern was found in the composite DNA patterns at 77 K in both dry and 76% hydrated DNA which was not reported earlier, and this was correlated to $C(N4H^+)^{-\bullet}$ radical. At higher temperature along with dominant presence of $TH^{\bullet}$ and peroxy radical (specifically in hydrated systems) a broad doublet pattern was obtained in dry DNA (H_2O) suggested to arise from purine C-8 adduct, this species was identified as $G(C8)OH^{\bullet}$ (**Fig. 3.1.5**) in model compounds but its exact nature in DNA is still not known. At 300 K sharp singlet was observed in all cases in DNA and was tentatively correlated to N1-deprotonated radical cation ($GN^{\bullet}$) after high magnetic field measurements, studies on RNA at 300 K and on correlation with previously found results (Voit and Hüttermann 1987), in other work using hydrated DNA and DNA containing Tl^{3+} additive in deuterated medium this sharp singlet is emphasised to be produced by 8-oxo-$G^{+\bullet}$ radical (Shukla et. a.l 2004). On comparing the dry and hydrated DNA in neat forms they found a decrease in singlet pattern arising from $G^{+\bullet}$ from 25% to 5% and pointed out that guanine might not be the primary spot for oxidation although it is believed to be so because of its lowest ionisation potential, in hydrated or frozen aqueous DNA systems. Another radical component (sextet pattern) was identified in this article was on application of high dose (> 300 kGy) in dry DNA (H_2O) at 240 K and was associated to the C3' or C4' sugar radical. Such pattern was also observed in hydrated DNA but on irradiation with oxygen ions (Becker et. al. 1996) and in cytosine containing nucleosides and –tides (Malone et. al. 1995, Weiland et. al. 1996) (**Fig. 3.1.6**).
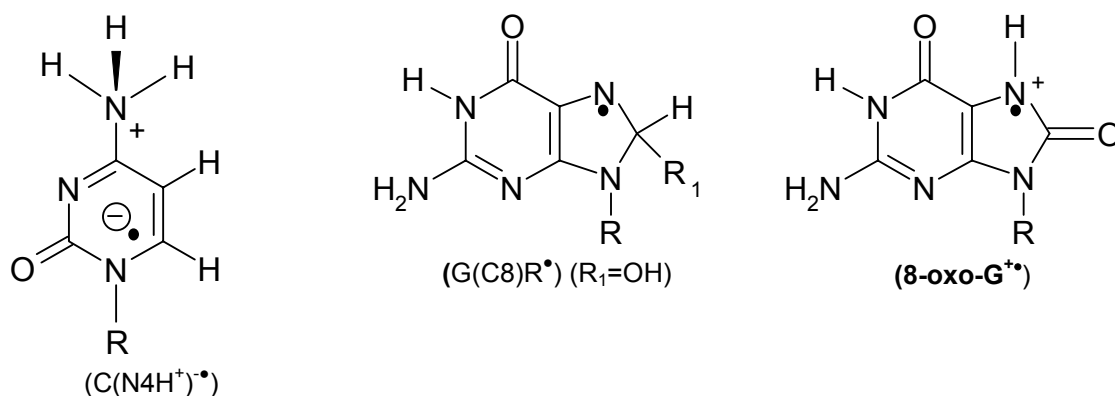
Fig. 3.1.5. Structural formulae of the charged and reversibly protonated base radicals proposed to form on irradiated dry or hydrated DNA.

Close (1997) pointed out in his work that even though 50% ionisation is faced by the DNA sugar phosphate backbone only 15% of that is trapped by them. Though successfully monitored in model compounds, it took long time for ESR scientists to identify the sugar radicals in DNA. This is an area of active interest also owing to the fact that damages in the sugar phosphate backbones are also responsible for double strand breaks in DNA upon radiation. Along with the efforts made by Weiland and Hüttermann (1998) as described above the authors also used heavy ion beams (having high LET) as a tool of irradiation for dry DNA (Weiland and Hüttermann 1999). They employed a number of ion beams including Ti^{50}, Zn^{68}, Au^{197}, Bi^{209} and reported similar radical formation as was observed by X ray irradiation with enhanced relative amount of C1' sugar and thymine allyl radicals. Becker et. al. (2003) performed ESR investigations on hydrated DNA on irradiating with Ar^{+18} ion beam and found neutral sugar radicals constituting 25% of the total radical yield which build up steadily with increase in dose as can be predicted due to the neutral charge of these sugar radicals. Along with the sugar radicals formed from deoxyribose moiety the authors proposed formation of two new radicals originating from strand cleavage at the phosphate deoxyribose linkage. Cleavage of a C-O bond at C3' forming $C3'^{\bullet}_{dephos}$ radical whereas cleavage of a P-O bond, at either or both C3' and/ C5, yielding a phosphorous centered radical, $ROPO_2^{-\bullet}$. The dry electrons were suggested to be the precursor for this strand break (**Fig. 3.1.6**).

Recent works have given emphasis on different pathways on formation of sugar radicals in DNA using low LET irradiation techniques. Shukla et. al. (2004) and Adhikary et. al. (2005) found that when frozen aqueous DNA (D_2O) in neat form or with electron

scavenger Tl^{3+} were irradiated with low dose of γ- rays and then treated with UV illumination in the range of 310-480 nm range $C1'^{\bullet}$ was reported to form due to hole transfer from excited $G^{+\bullet}$ to the proximate sugar moiety to form $S^{+\bullet}$ followed by its deprotonation to form $C1'^{\bullet}$.
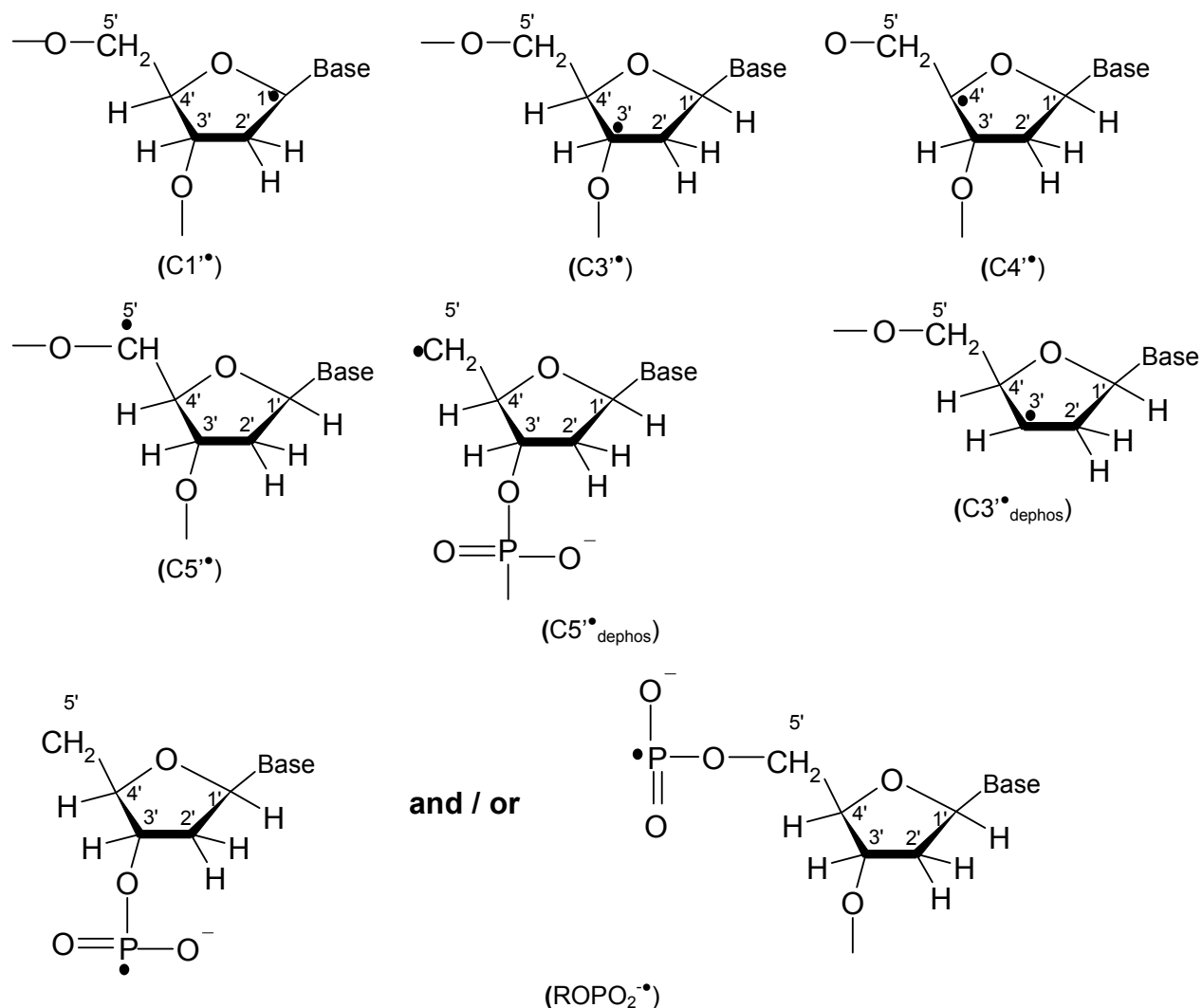
Fig. 3.1.6. The structures of the neutral sugar radicals proposed to be formed on the deoxyribose moieties of irradiated DNA in dry and hydrated lyophillzed samples on irradiation.

In another attempt Shukla et. al. (2005) investigated in hydrated DNA using $K_3Fe(CN)_6$ as an electron scavenger, $K_4Fe(CN)_6$ as an electron donor and combination of both in high molar concentration in frozen aqueous (D_2O) system to suppress the formation of both anions and cations and to obtain better view on the sugar radical formation using γ ray as the irradiation source. Dose dependence study was also performed and all the analysis was done only at 77 K. In this attempt authors claim to

obtain isolated cohort of neutral radicals i.e. mainly sugar radicals for the first time experimentally. The spectrum obtained from DNA containing one $K_3Fe(CN)_6$ per 10 base pairs and one $K_4Fe(CN)_6$ per 10 base pairs is estimated to be constituting of 15% $G^{+\bullet}$, 13% $C(N3)H^\bullet$, 6% $C1'^\bullet$, 8% $C3'^\bullet_{dephos}$, 4% $C3'^\bullet$, and $C5'^\bullet_{dephos}$ along with $C5'^\bullet \leq 30\%$. Authors show their doubts on accuracy of estimation of $C5'^\bullet_{dephos}$ and $C5'^\bullet$ because of the similarity in the line widths of these two radical patterns (structures in **Fig. 3.1.6**). This work also puts light on the mechanism of action of electron scavenger ($K_3Fe(CN)_6$) and electron donor ($K_4Fe(CN)_6$) on DNA.

In spite of all these efforts the topic of irradiation mechanism in frozen aqueous system in DNA and identification of all the radicals formed in DNA poses many open questions. The disagreement about the percentage of formation of $G^{+\bullet}$ radical in different studies on similar samples (Sevilla and co-workers 1991, Weiland and Hüttermann 1998, Burger 1999) remained unanswered. It is important to gain more insight on the oxidative processes in irradiated DNA at low temperatures. In the recent report of Shukla et. al. (2005) authors were unable to identify the almost half of the neutral radical cohort that gives a composite spectrum after the neutral sugar radicals are subtracted out. Thymine allyl radical was not identified in this study which is also a neutral radical and was observed predominantly in dry DNA and hydrated systems previously. A quartet pattern was used to reconstruct the composite DNA spectry in dry and hydrated systems in the previous study (Weiland and Hüttermann 1998) which was viewed as a super position of C1' sugar radical quartet and allyl radical features in a ratio of about 4:1 but a separation of the two patterns for the purpose of reconstruction was not possible. The question also remains about the formation of neutral radicals like $C3'^\bullet_{dephos}$, $C5'^\bullet_{dephos}$ and $ROPO_2^{-\bullet}$ which were first observed in dry DNA after irradiations with heavy ions and is reported to be formed in hydrated DNA on irradiation with high doses of γ-rays. The formation of these radicals in DNA (frozen aqueous systems) on irradiation with low LET sources needs further confirmation.

3.1.3. Post-irradiation Charge Transfer in DNA: Effect of Time and Temperature

Extent of charge transfer in DNA double strands has remained a subject of great interest for nano technological and medical purposes. Photochemical studies have intensely focussed on this theme since last ten years. There was incorporation of various

electron acceptors and donors with various mode of binding on DNA. These studies have established that long range electron transfer persists along DNA (Murphy et. al.1993, Kelly and Barton 1999). This molecular wire like character of DNA was soon under debate and new works showed that DNA can also behave as an insulator or semiconductors (Debije et. al. 1999, Porath et. al. 2004). Theoretical studies have suggested several models of electron transfer in DNA (Marcus and Sutin 1982, Ratner 1999, Jortner et. al. 1998). In the field of ESR spectroscopy this topic has also been studied by different scientists in different conditions. Cullis and co-workers had shown the long range migration of electrons in frozen aqueous system containing intercalators (Cullis et. al. 1990), in a further extension of this work it was found that in a frozen aqueous system of DNA containing Mitoxantrone (MX) or 1,4-bis{[2-(dimethylamino)ethyl]-amino-5,8-dihydroxyanthracene-9,10-dione} (AQ_4) electron affinic intercalating additives at separation of about 1 additive : 110 base pairs (bp) there was almost 50% scavenging of reduced species and the mean distance travelled by electrons prior to any permanent trapping was approximately 31 base pairs (Pezeshk et. al. 1996). Similar studies were also done with DNA doped with various levels of bromosubstituted bases (Razskazovskii et. al. 1997). Oligonucleotides of crystalline and polycrystalline deoxyoligonucleotides at temperatures 4-240 K, where the radical yields were compared with well known insulators like methyl mannoside and also with conductors like graphite. It was observed that oligonucleotides serve as excellent traps for electrons and holes at 4K which would not be the case if it behaved as a conducting molecular wire, the property which was shown by graphite and copper. It was concluded in this work that DNA behaves like insulator (Debije et. al. 1999), more investigations were done on the topic of charge transfer by the same group concentrating mostly on the base sequence, strand length, DNA conformation (A, B, Z form), counter ion, base stacking effect yields (Debije and Bernhard 2000). Sevilla and co-workers have studied electron transfer in DNA when complexed with several randomly intercalated electron scavengers like MX, ethidium bromide (EtBr) and 5-nitro-1,10-phenanthroline (Npa) in frozen glass (7M LiBr/ D_2O) system (Messers et. al. 2000). On irradiation of the system the holes were captured by the glass and electrons were exclusively trapped by DNA-additive complexes. A temporal ESR spectroscopic study was performed after irradiation and electron transfer from the DNA anion radicals to the intercalators was invoked by this study by process of single step electron tunnelling, the average value of the electron transfer rate constant was given as 0.8-0.9 Å. This work was further extended in frozen

aqueous (D_2O) (Cai et. al. 2000) systems also and a three dimensional tunnelling model was postulated that assumes electron transfer both along the intra and inter strand of the DNA duplexes. This work also suggested that at higher temperature the many other processes like hopping comes into play in moderation of charge transfer. Experiments were performed to establish the effect of hydration layer on the probability of electron transfer and it was found to decrease with increasing layer of hydration (Cai et. al. 2001). Further studies were done to see the effect of complexing agents like spermine cation (Cai et. al. 2001b), to observe the effect of different base sequences (Cai et. al. 2002) and effect of H_2O and D_2O (Cai et. al. 2000). These studies gave evidences that complexing agents (except spermine) increases inter duplex distances and therefore the electron transfer rates were decreased. The base sequences have strong effect on electron and hole transfer and gave analogous results in frozen glass and frozen aqueous solutions. It was also indicated that H_2O is a medium for faster deprotonation and protonation because of its small size than D_2O (Cai and Sevilla 2004, Sevilla and Becker 2004).

Spin transfer from histone and other related proteins to DNA has been studied since long (Alexander et. al. 1961, Kuwabara et. al. 1974) it was shown that the ESR spectra from DNA and DNA along with any kind of protein exhibits very little difference. This observation leads to the belief that there is transfer of electrons from proteins to DNA during ionisation. Other works in the same direction (Cullis et al 1987b, Faucitano et. al. 1992, Symons 1997) modified the idea with the postulation that electron transfer is a favourable process while holes remain trapped in the proteins. Weiland and Hüttermann (2000) have reconsidered the problem once more with intention to isolate radical structures in DNA–histone complex and chromatin in dry and hydrated state (76%) by utilising both X band and high frequency ESR spectroscopy. Temperature annealing was performed to chase the fate of primary radicals. The yield of radicals in DNA in chromatin was found to be twice that was found in neat DNA confirming the transfer of electrons from proteins to DNA on irradiation. This work also showed the differential charge transfer in the system with anionic sites stabilising more on DNA. Another important conclusion of this work was that on annealing no transfer of spins were observed between protein and DNA components. This work gave the hint that the transfer behaviour of radicals tend to vary during irradiation in comparison to after irradiation.

3.2. Aim of the Thesis

From the above discussion on the state of art in the field of ESR studies in frozen aqueous system it becomes clear that the direct or indirect models of irradiation effects are not sufficient to explain all the phenomena observed in the irradiated model compounds or DNA itself when present in this matrix. The quasi direct mechanism as adopted by Symons and co workers which includes a glassy capsule of water around the substrate separating it from the bulk does provide a logical extension but the role of the bulk water in irradiating the substrates is still not clear and needs to be ventured both for model system and DNA itself.

TMP which was used as a popular model system in frozen aqueous system has its own disadvantages as the formation of the well observed allyl radical can be pursued both from Thymine cation formed by direct irradiation or by H abstraction of methyl hydrogen from thymine by nearby $OH^\bullet$ radical implicating indirect mechanism (as mentioned previously). The investigations on dCMP in frozen glass (BeF_2) and aqueous solutions showed formation of $C1'^\bullet$ sugar radical in both matrices at 77 K. On increasing the temperature of the matrices by annealing, increase in the $C1'^\bullet$ radical contribution is observed in glasses owing to the mobilization of the $OH^\bullet$ but in frozen aqueous solution a clear increase in sugar radicals were not observed. An exact mechanism could not be derived to explain this finding. In order to know more on this line we have extended the theme in this thesis by using another DNA base model compound i.e. Fluorouracil and its derivatives. We have tried for the first time to study it systematically in different glasses and aqueous system as well, firstly to characterize the radicals formed after irradiation and then to compare their formation in 5 M H_2So_4, 7 M BeF_2 and in aqueous matrix. ESR mute electron scavenger $K_3Fe[CN]_6$ has been used to emphasize the oxidative pathway of the systems in frozen glass as well as frozen aqueous solutions. It is assumed that the large hyperfine splitting due to fluorine atom will help to distinguish the radicals formed on the substrate. Both oxidized radicals i.e., FU cation and radical formed due to $OH^\bullet$ addition on FU do have very different ESR signature and their formation is assumed to be tracked without ambiguity in both glass and frozen aqueous matrices thus will be providing more insight into the mechanism of irradiation in frozen aqueous system. The nucleoside (FUdR) and nucleotide (FdUMP) does have better solubility property in water than FU itself and this has been utilized to understand about

formation of oxidized radicals via direct radiation or through solvent in frozen aqueous solutions. In the present times with more knowledge about the formation of sugar radicals on DNA and its nucleotide models by using higher doses it also imposes a natural curiosity to us to probe the formation of neutral sugar radicals in Fluorouracil nucleoside and nucleotide derivatives after irradiation with moderate doses. Formation of sugar radicals if found can also offer additional information regarding the mechanism of irradiation in frozen aqueous system at low temperatures.

The results from these model studies can then be extended and compared to the mechanism of irradiation in frozen aqueous solutions containing DNA in pure form or along with additives.

In frozen aqueous DNA solution our aim was to improve the understanding of the effect of irradiation along with identification and isolation of radical patterns from the DNA spectra themselves for the reconstruction of the experimental spectra. The use of electron scavengers which has been done previously (Gregoli and coworkers) to strengthen the model of direct irradiation model can be discarded as electron scavengers are found to be capable of scavenging electrons during irradiation in dry DNA systems also. We have tried to probe the formation of guanine radical cation ($G^{+\bullet}$) which has been reported to be 41% and 5 % in hydrated DNA by two different groups (see before). Pure DNA in frozen aqueous solutions and along with several additives like $K_3Fe[CN]_6$, Mitoxantrone and $K_4Fe[CN]_6$ having diverse electron scavenging capacities and varied binding properties with DNA double strands have been used to understand the modulation of the total radical balance in DNA system. Samples were irradiated with different doses to understand the radical stabilities with increasing doses and how does the formation of more stable sugar radicals can affect the total radical cohort in DNA. For the first time temperature annealing studies are reported for frozen aqueous DNA samples which are irradiated with various doses. Similar studies are also reported with DNA-additive complexes with an aim to understand the role of guanine cation on the formation of sugar radicals in frozen aqueous solutions as many recent reports have suggested the formation of sugar radicals via hole transfer from excited guanine cation (Shukla et. al. 2004 and Adhikary et. al. 2005)

A further effort was to study the post irradiation single step electron tunneling process from DNA anions to intercalated Mitoxantrone as invoked by Sevilla and

coworkers (2000) in frozen glass system. As it is earlier mentioned that it has been previously observed that increase in temperature in an irradiated histone –DNA system did not show any transfer of spins from DNA to histone or vice versa after completion of irradiation because of compartmentalization of the radicals formed. Temperature increase could only induce some intramolecular changes mainly causing protonation and deprotonation. An overall independent decay of radicals was observed as a result of annealing. The apparent discrepancy in the *post irradiation* behavior of DNA radicals with temperature and time prompted us to reinvestigate this theme. For detailed insight DNA as well as single deoxyribonucleotides was utilized and riboflavin was used along with mitoxantrone because of different mode of interaction of two additives with DNA. A strong control system involved was stable free radical, TEMPOL (4-hydroxy-2,2,6,6-tetramethylpiperidin-*N*-oxyl).

4. Material and Methods

4.1. Chemicals

In this section of all the chemicals needed are listed sequentially. The chemicals are categorized in three tables consisting of list of substrates, additives and solvents used in this work. In each table the name of the chemicals, their abbreviated form as used in this thesis and the name of the suppliers are given in **Table 4.1.1**-**4.1.4**.

Table 4.1.1. List of substrates which are used in this thesis along with their abbreviations and manufacturing company names.

Substrates	Abbreviation	Suppliers
5-Fluorouracil	5-FU	Sigma
5-Fluoro-2′-deoxyuridine	FUdR	Sigma
5-Fluorouridine	FUrd	Sigma
5-Fluoro-2′-deoxyuridine 5′-monophosphate (Na Salt)	FdUMP	Sigma
Cytosine	C	Sigma
2′-Deoxycytidine 5′-monophosphate (Na Salt)	dCMP	Sigma
Thymidine 5′-monophosphate (Na Salt)	TMP	Sigma
2′-Deoxyguanosine 5′-monophosphate (Na Salt)	dGMP	Sigma
2′-Deoxyadenosine 5′-monophosphate (Na Salt)	dAMP	Sigma
Deoxyribonucleic acid (Na Salt) from salmon testes	DNA	Sigma

Table 4.1.2. List of additives used as electron scavengers or donors along with their abbreviations and manufacturing company names.

Additives	Abbreviation	Suppliers
Potassium hexacyanoferrate(III)	$K_3[Fe(CN)_6]$	Merck
Potassium hexacyanoferrate(II) trihydrate	$K_4[Fe(CN)_6]$ $3H_2O$	Sigma
Sodium persulfate	$Na_2S_2O_8$	Fluka
Riboflavin (Vitamin B12)	RF	Sigma
2-Nitroimidazole	Azomycin	Sigma
Mitoxantrone dihydrochloride	MX	Sigma

Table 4.1.3. List of solvents used in this work.

Solvents	Abbreviation	Suppliers
Berillium flouride	BeF_2	Sigma
Lithium chloride	LiCl	Sigma
Lithium bromide	LiBr	Sigma
Sulphuric acid	H_2SO_4	Sigma
Deuterium oxide	D2O	Sigma
Nitrogen in gas and liquid form	N_2	Messer Griesheim
Water	H_2O	Millipore Quality

Table 4.1.4. Other chemicals used during the process of experiments.

Substances	**Abbreviation**	**Suppliers**
4-Hydroxy-2,2,6,6-tetramethylpiperidine 1-oxyl	TEMPOL	Sigma
Sodium hydroxide	NaOH	Sigma

All the chemicals were bought in their highest purity from respective firms and were used without further purification.

4.2. Sample Preparation

4.2.1. Glass Matrices

Several glass matrices are used in this thesis. The glasses used are acidic glasses like 5 M H2SO$_4$, 7 M BeF$_2$ and neutral glasses like 7 M LiCl, and 7 M LiBr. 5 M H_2SO_4 was prepared by diluting concentrated H_2SO_4, 7 M BeF$_2$ was bought in liquid form and was used as it is. LiCl, LiBr, were prepared by dissolving their appropriate amount in water or in D_2O.

4.2.2. Preparation of Frozen Solutions

The main condition required for the preparation of frozen samples was exclusion of oxygen as good as possible. For this reason all the solutions used were degassed with Nitrogen gas for at least 20 minutes. The mixing of substrate and solvents and preparation of frozen samples were always performed inside an anaerobic glove box. Once the frozen samples were prepared, then all the further processes like irradiation, ESR measurement and future storage were performed inside liquid nitrogen.

DNA bases, Nucleosides and Nucleotides

Various bases, nucleosides and nucleotides used in this study were mixed with desired solvent (glass forming solvents, H_2O or D_2O). For additive-nucleotide systems needed amount of additives were also added into the solution. The solutions were prepared in concentration from 10mM to 1M depending on the solubility of the substrate and need of a particular experiment. The solutions were stirred for homogenous mixing. The DNA bases owing to their poor solubility required longer stirring and they could be prepared in lower concentrations. After homogenous mixing the solutions were dropped into liquid nitrogen with the help of Pasteur pipettes. As a result spherical transparent glassy beads were formed of approximately ~3 mm diameter. TEMPOL was used as standard probe for time dependent analysis and was prepared by taking 200 μl of 0.87 mM TEMPOL in an 4 mm X-band EPR tube.

DNA Samples

Dry DNA as well as additive-DNA complexes was obtained by freeze drying their homogenous solution in water or D_2O. The process of freeze drying was performed in an home made instrument. Sodium salt of DNA (Salmon testes) as obtained from Sigma were fibrous in nature, processing them by freeze drying gave them a paper like structure which were better in absorbing X rays equivalently. For additive-DNA (prepared in molar ratios) complexes freeze drying helped in an homogenous distribution of additive in DNA structure. The freeze dried samples were than mixed with deoxygenated solvents (7 M LiBr, 7 M LiCl, H_2O or D_2O) in anaerobic conditions. The concentration of DNA was 20 mg/1ml in glassy samples and 50 mg-100 mg in one milliliter of H_2O or D_2O. The viscous mixture so formed were stirred in regular interval and incubated inside the anaerobic tent for at least 24 hours for getting a homogenous gel like sample. In the case of DNA being solved in 7 M LiBr/7M LiCl small transparent glass beads were prepared by dropping the solutions with thin head Pasteur pipettes into liquid nitrogen. The frozen aqueous solution was on the other hand drawn into a quartz tube (approximately 4 mm in diameter) and was frozen into liquid nitrogen (Lange 1994). The resulting frozen aqueous DNA cylinder was then pushed with the help of a wooden stick into liquid nitrogen by little bit warming the glass tube.

4.3. Irradiation Technique

X ray irradiation source is used throughout in this work. All the irradiation was always done at 77 K as the glass samples and frozen aqueous samples are unstable at higher temperature. Irradiation at low temperature is also essential to stabilize the radicals formed on irradiation. X ray (95 kV, 25 mA) source has a Phillips tube employing a generator from Seifert. The samples inserted in a small glass vessel and then were kept in homemade isolated glass Dewar fitted at the bottom with 1mm Aluminum filter (to exclude the soft X rays) exactly above the X ray outlet window. X ray irradiation dose used were from 400 Gy to 30 kGy in glass solutions and 10 kGy–850 kGy in case of frozen aqueous samples. X ray irradiated samples were always stored in liquid nitrogen before measurement. Calibration of the X ray source was done by Fricke dosimetry at low doses (~800 Gy) and this value was used as basis for estimating higher doses via irradiation time.

4.4. ESR Measurement Technique

In the frame of this work two different X-band ESR spectrometer have been used, they are Bruker ESP 300 and ESP 300e (X-band, ~9.5 GHz with 100 kHz modulation). The first one is connected with Windows PC, and data were collected by using home made software named Lila_X, ESP 300e functions with integrated OS/9 computer with Bruker software. Both were connected with external frequency counters for getting exact values.

The parameters used in the spectrometer were magnetic field sweep 200G-1200 G, attenuation 5 dB-42 dB and modulation amplitude 1.6 G-2.5 G. Multiple scans were done to obtain high signal to noise ratio or better quality of the ESR spectrum.

For measurement at 77 K the glassy samples were transferred to ESR tubes (Spintec) (with diameter 4mm) after irradiation inside liquid nitrogen for time dependent studies. Frozen aqueous samples of DNA components or other glassy samples were either transferred to 5mm ESR tubes (Spintec) or directly to the quartz finger Dewar (Spintec) depending on their availability. As for qualitative analysis the quality of the spectra of radicals formed depend on their concentration. Frozen aqueous samples of DNA (in the form of cylinders ~2 cm) were measured in finger Dewar. The samples were

annealed to higher temperatures by emptying the finger Dewar and then the temperature rise of the sample was measured by placing a thermocouple on the top of the sample. When the required temperature was reached the Dewar was again quickly refilled. Some time dependent measurement were performed at lower temperature from 4-77 K by using ESR 900 cryostat (Oxford Instrument).

4.5. Analysis and Simulation of EPR Spectra

4.5.1. Qualitative Analysis of Spectra

The spectra obtained from X-band ESR spectrometer consists of the measurement parameter and 1024 measurement points per spectrum. They were then read and analyzed by home made software named APOLLO (Dosemund 1998)). In this software in the Bearbeiten (edit) mode several kinds of operation like baseline correction, subtraction and addition of two spectra as well as integration and differentiation can be done. In the Simulation mode of the software other operation like ESR simulation, Factor analysis, Target transformation and reconstruction of the spectrum are possible. The detailed review about the functioning of this software has been given in the earlier works from this laboratory (Dusemund 1998, Weiland1999). In this thesis the software APOLLO is mainly utilized for isolation of pattern spectra from the compound spectra obtained from frozen glass and frozen aqueous spectra. Comparison of spectra was done which were obtained with equivalent parameters to see the effect of temperature, scavengers and dose. The isolated spectral patterns were than utilized for deconvulation of the compound spectra to find out the relative distribution of each radical in those spectra. In some cases deconvolution or reconstruction of a compound spectrum is also done by using the patterns obtained from pure systems. This program provides a general Least-Square method for the determination of component contributions to composite spectra (denoted "reconstruction" (rec.)) which involves a Gauss-Jordan elimination algorithm (Moens et. al. 1993). The resulting weight of individual components normalized to their respective double integral was used to produce reconstructed spectra. The goodness-of-fit between experimental and reconstructed spectra was calculated according to the formula given by Moens et. al 1993.

4.5.2. Analysis of Spectra from Time Dependent Studies

For the time dependent ESR study in this thesis, the experiments were always done along with measurement of TEMPOL standard before and after the experimental sample measurement. TEMPOL standard remains unchanged with time and gives constant double integral value when the spectra are taken with identical measurement parameters. Experimental samples were also measured for a long range of time in identical measuring condition and the change in their double integral values were then compared with that of TEMPOL to investigate the rate of change of radical concentration. Along with APOLLO, WINEPR which is a software for spectral analysis from Bruker was also used for analysis of time dependent studies. This software was used for controlled baseline correction and double integral calculation for time dependent quantitative study. The development of component radical concentration with time was analyzed with the program ORIGIN (Originlab Corp., USA) using nonlinear least-squares fit procedures.

4.5.3. Simulation

Simulation of the X-band spectra were done by using software named as SIMFONIA (from Bruker). The data obtained on simulation (with an extension name of spc.) can be read in WINEPR or in APOLLO and can be used further for comparative purpose with experimental spectra.

To obtain the simulated spectrum the ESR parameters like the values for g tensors and hyperfine tensors are obtained from literature (especially from the crystal structure study). A specific pattern was chosen and then by manipulating different ESR parameters as well as the line widths a simulated spectrum was tried to develop. The simulated spectrum was then compared with the experimental spectrum to obtain knowledge about the radical structure.

5. Results and Discussion

5.1. Identification and Comparison of Radicals formed in Irradiated 5-Fluorouracil and its Derivatives in Frozen Glass and Frozen Aqueous Matrices

In order to investigate the extent of indirect effect of irradiation in frozen aqueous system we have carried out comparative investigation of xray induced radical formation in the group of 5-Fluoro substituted nucleic acid base uracil.
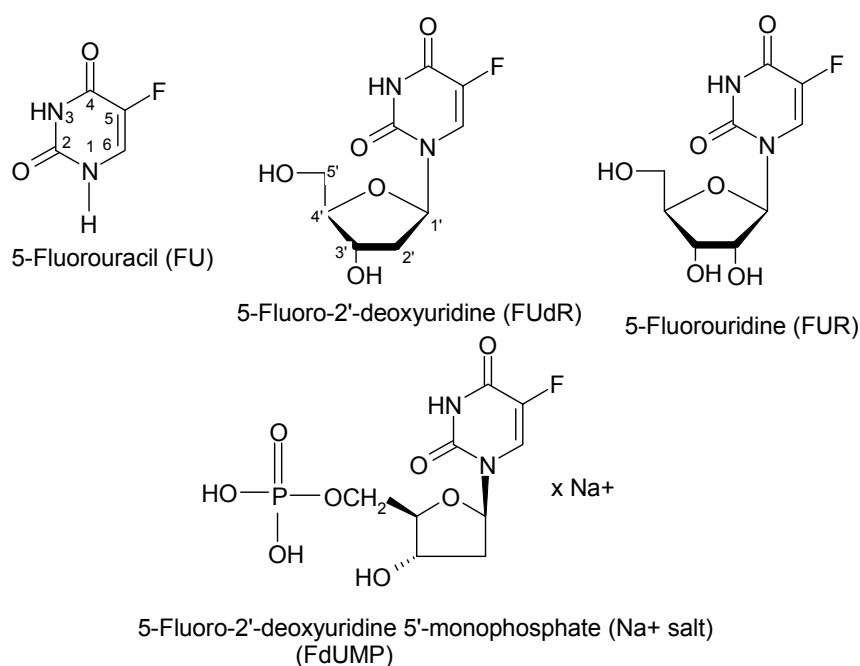
Fig. 5.1.1. Structures of the 5-Fluorouracil and its derivatives used in this study.

We have studied frozen glass solutions of 5-Fluorouracil (FU) in different frozen glass matrices, and 5-Fluoro-2′-deoxyuridine (FUdR), 5-fluorouridine (FUR) and 5-Fluoro-2′-deoxyuridine 5′-monophosphate (Na$^+$ salt) (FdUMP) in both frozen glass and aqueous matrices. The solubility of these substrates are of order FU<FudR~FUR<FdUMP in water and glass solutions. Their structures are shown in **Fig. 5.1.1**. The ESR measurements were performed for the irradiated frozen samples at 77 K and then annealed, step by step, up to the melting point. In a frozen aqueous system, it

has been postulated from previous studies (**see section 3.1.1**) that it is difficult to differentiate between reduction by electrons from the matrix or from the substrate, oxidation derived reactions on the other hand can provide crucial insight regarding the contribution of direct radiation action. An enhancement of the features arising from the oxidized radicals of the respective bases can be achieved by adding sizable amounts of electron scavengers to the system. This phenomenon has been utilized throughout the investigation of fluorouracil and its derivatives in various glasses as well as in frozen aqueous system. In Fluorouracil systems the ESR spectra obtained from the oxidized radicals produced by direct irradiation action or by hole scavenging from solvent matrix and by OH addition can be very well differentiated because of the characteristic large fluorine hyperfine coupling. This property of fluorouracil system is assumed to provide more details about the radiation mechanism in frozen aqueous system.

5.1.1. Reactions and Products in H_2SO_4/$Na_2S_2O_8$ Glasses

X ray irradiation of dilute H_2SO_4 glasses at 77 K produces both electrons and $OH^\bullet$ radicals. Electrons being mobile get converted into hydrogen atoms ($H^\bullet$) and $OH^\bullet$ transforms into $SO_4^{-\bullet}$ radicals predominantly (Riederer 1981). The $H^\bullet$ unequivocally attacks on C6 position of FU forming H-addition radicals which also overlap with the ESR signature produced by $SO_4^{-\bullet}$ attack (Riederer et. al. 1981). In order to suppress $H^\bullet$ and to increase $SO_4^{-\bullet}$ radicals, strong electron scavenging agents like sodium persulphate ($Na_2S_2O_8$) have been used in earlier studies (Riederer et. al. 1982) as the electrons produced in the matrix after irradiation cleaves the dioxygen bonds in $Na_2S_2O_8$ as shown in equation **5.1.1** and produces $SO_4^{-\bullet}$.

$$S_2O_8^{2-} + e^- \rightarrow SO_4^{-\bullet} + SO_4^{2-}$$
(5.1.1)

Small concentration of $OH^\bullet$ radicals which is produced at 77 K upon irradiation in pure H_2SO_4 glasses are also diminished by the presence of $Na_2S_2O_8$. Therefore this matrix system offers a strong environment for formation of oxidized radicals via indirect irradiation effect in fluorouracil systems at 77 K. A demerit of this system is the invariable formation of peroxy radical ($ROO^\bullet$) after the decay of $SO_4^{-\bullet}$. Its occurrence is independent of the presence of molecular oxygen in the system and is supposed to involve the undamaged $Na_2S_2O_8$ molecules which can be represented by the equation

5.1.2 (Riederer et. al. 1982). The relative concentration of ROO$^\bullet$ varies with the annealing rate and the $Na_2S_2O_8$ concentration in the matrix.

$$^-O_3SO^\bullet + {}^-O_3SOOSO_3^- \rightarrow {}^-O_3SOO^\bullet + {}^-O_3SOSO_3^-$$ (5.1.2)

5 - Fluorouracil (FU)

ESR spectra obtained from the temperature annealing measurements of 50 mM FU (solid lines) containing equivalent amount of $Na_2S_2O_8$ as an electron scavenger in 5 M H_2SO_4 glass matrix after x- ray irradiation for 2 hour (20 kGy) are shown in **Fig. 5.1.2**. At low temperatures (77-150 K) the central part of the ESR spectra is dominated by a radical pattern arising from $SO_4^{-\bullet}$, as also seen in ESR spectra obtained from 100 mM of pure $Na_2S_2O_8$ (shown by the dotted line spectra). The symmetrical triplet features are observed at the wings with a distance of about 16 mT in **Fig. 5.1.2 A** and **B** gives evidence of formation oxidized radical on FU base.
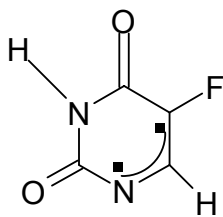
Str. 5.1.1. FU_CAT
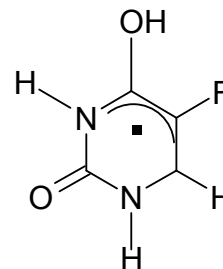
Str. 5. 1.2. FU_O4H

With increasing temperature of the sample upon annealing of the glass matrix to 165 K and on re cooling to 77 K the ESR spectrum shows complete loss of $SO_4^{-\bullet}$ pattern at the central region and of the triplets from the wings, a new doublet like pattern originates at the middle (**Fig. 5.1.2C**). The formation of peroxy radicals can also be observed owing to the large $Na_2S_2O_8$ concentration and becomes prominent on measurement at low attenuation (**Fig. 5.1.2D**). The pattern E obtained after subtraction of peroxy radical pattern from Fig. 5.1.2C shows a single pattern which remains alike till the sample melts (~ 175 K) with a very low radical yield of about 1% to that of total radical obtained at 77 K.

Oxidized radical formation after deprotonation of N1 hydrogen atom has been previously observed in single crystal studies and also in the same matrix at 77-160 K (Farley and Bernhard 1975, Neumüller and Hüttermann 1980, Riederer and Hüttermann
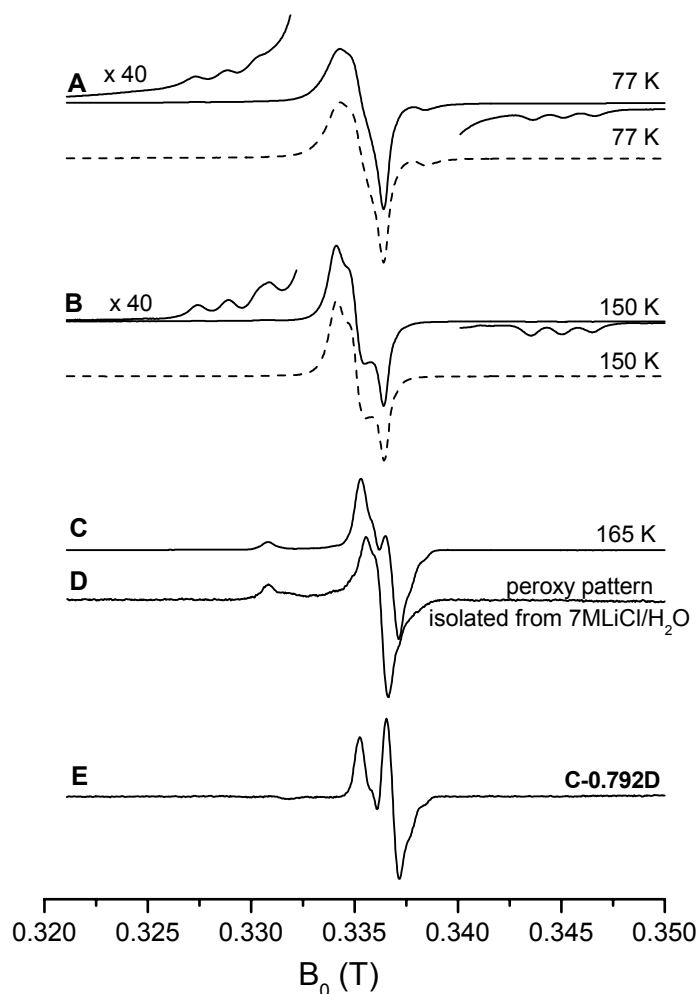
Fig. 5.1.2. A-D) ESR spectra of X irradiated (20kGy) 50mM 5-FU: $Na_2S_2O_8$ (1:1) (solid lines) and 100mM $Na_2S_2O_8$ (dotted lines) in 5 M H_2SO_4 glasses at different temperatures. The microwave power used was 42dB in all cases. D) Peroxy radical pattern isolated from subtraction of ESR spectra obtained at 165 K and 160 K respectively in 7M $LiCl/H_2O$ system containing FU. E) Isolated pattern for the radical produced may be because of enolisation of C4-carbonyl group (see text and simulations).

1982) and is attributed to **Str. 5.1.1**. When the magnetic field is perpendicular to pyrimidine plane a fluorine doublet of about 16 mT arises which further splits into 1:1:1 triplet with 1.5 mT spacing due to the interaction with N1.

This pattern is more clearly observed for FU in 7 M $LiCl/H_2O$ matrix containing $Na_2S_2O_8$ as electron scavenger at higher temperature as shown in **Fig. 5.1.3A**.This can
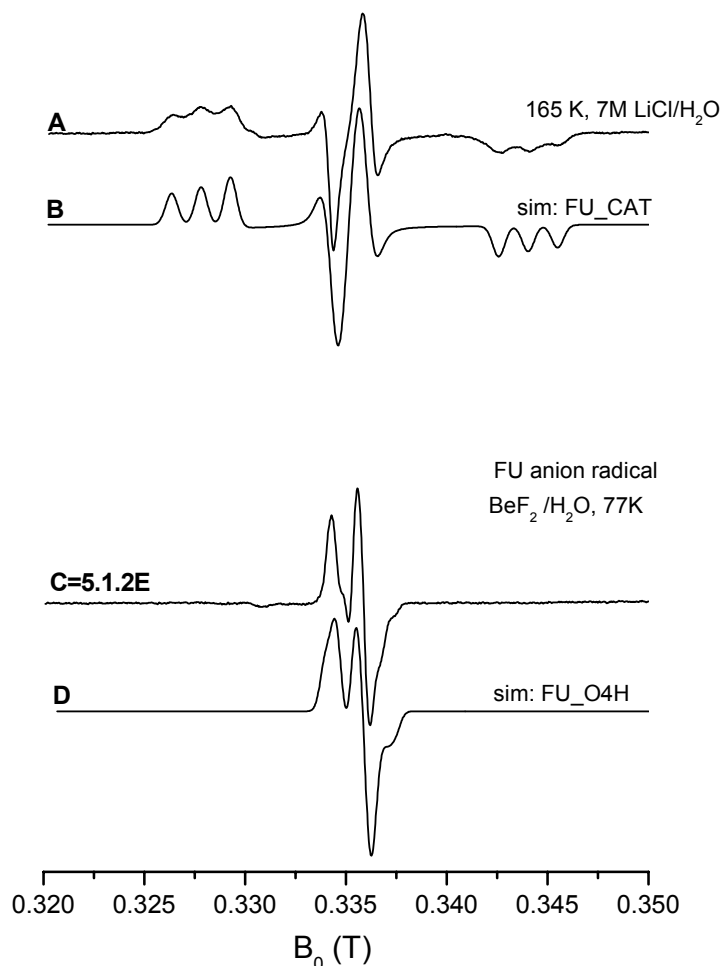
Fig.5.1.3. A) ESR spectrum obtained from 5-FU in 7M LiCl/ H_2O glass on annealing at 165 K where there is no influence from $SO_4^{-\bullet}$, B) simulated pattern of 5-FU base cation (str. 1). C is same as in figure 2E, D) simulated pattern for H addition radical on O4 of 5-FU.

be simulated (**Fig. 5.1.3B**) using the parameters which are given in **Table 5.1.1**. In 7 M LiCl matrix containing equimolar amount of FU and persulphate, upon radiation at 77 K the electrons and hole produced in the matrix which consequently gets trapped as $SO_4^{-\bullet}$ and $Cl_2^{\bullet-}$ respectively. Annealing (> 140 K) liberates the $SO_4^{-\bullet}$ to react with Cl⁻ and more $Cl_2^{\bullet-}$ are formed which diffuses at 165 K and react with the FU to form N1 deprotonated neutral radical as shown in **Fig.5.1.3A**.

The asymmetric doublet pattern observed at 165 K (**Fig. 5.1.3C**) shows close resemblance with the simulated pattern (**Fig. 5.1.3D**) obtained by using the parameters

given in **Table 5.1.1** which can be very well correlated to the O4 protonated radical (**Str. 5.1.2**) in crystal structure study (Neumüller and Hüttermann 1980). This pattern remains as a final pattern in all fluorouracil derivatives treated similarly in same glass matrix and also in 7 M BeF$_2$/H$_2$O, and frozen aqueous system. More on this pattern is discussed in later sections.

Table 5.1.1. Simulation parameters used for FU_CAT and FU_O4H.

FU_CAT (Sevilla et.al, 1984)				In this work			
A(mT); g F (C5) N(C1)	x -1.6 0	y -1.6 0	z 16.0 1.7	A(mT); g F(C5) N(C1) Line width	x -1.46 0 0.8	y -1.46 0 0.8	z -16.2 1.46 0.8
g	2.0060	2.0056	2.0011	g	2.0060	2.0056	2.0011
FU_O4H (Neumüller, Hüttermann, 1980)				In this work			
A(mT); g H (C6) F(C5)	x -0.52 0	y -1.49 0	z -1.12 1.12	A(mT); g H (C6) F(C5) Line width	x -0.52 0 0.6	y -1.49 0 0.5	z -1.12 1.12 0.5
g	2.0054	2.0084	2.0019	g	2.0054	2.0084	2.0019

5-Fluoro-2'-deoxyuridine (FUdR)

Fig. 5.1.4 presents the selected X band ESR spectra of annealing series of 400 mM FUdR along with equimolar Na$_2$S$_2$O$_8$ in 5 M H$_2$SO$_4$ treated with 20 kGy of x- ray irradiation at 77 K. Central region of the experimental spectrum at 77 K (**Fig. 5.1.4A**) is dominated by SO$_4^{-•}$, while the triplet features arising due to oxidation of the nucleoside base are observable at the wings (as is clear from the magnification). With increase in temperature a composite spectrum is observable at 165 K (**Fig. 5.1.4D**) with no influence of the additive radical, which on further annealing converts into a single component doublet like spectrum at 175 K (**Fig. 5.1.4G**).

In FUdR the presence of a deoxyribose moiety at N1 position prevents deprotonation at N1 position but oxidation is possible at 77 K and has been observed before (Riederer and Hüttermann 1982). The oxidized radical (**Str. 5.1.3**) in FudR at 77 K have more fluorine coupling than that in FU base and nitrogen splitting becomes smaller and can be simulated (**Fig. 5.1.4B**) using the parameters given in **Table 5.1.2**. Presence of traces of other inseparable radical pattern is observable at 77 K and becomes more prominent with increase in temperature (e.g., at 165 K) as shown by double arrows in **Fig. 5.1.4C**. This radical can be manifested by a large fluorine doublet and each of its line splits further into small doublet because of C6-β hydrogen interaction. This pattern is dealt with in earlier reports (Riederer and Hüttermann 1982)

and has been correlated to a radical formed by $SO_4^{-\bullet}$ addition at C6 position of the base moiety (**Str. 5.1.4**). **Fig. 5.1.4E** shows the simulation of the pattern using the parameters given in the **Table 5.1.2**. Additional peaks (as shown by the * in **Fig. 5.1.4C**) were also observed in FUdR at 165 K which was not found in ESR measurements of FUR at identical conditions. This gives a strong evidence of formation of radical at the deoxyribose moiety in FUdR.
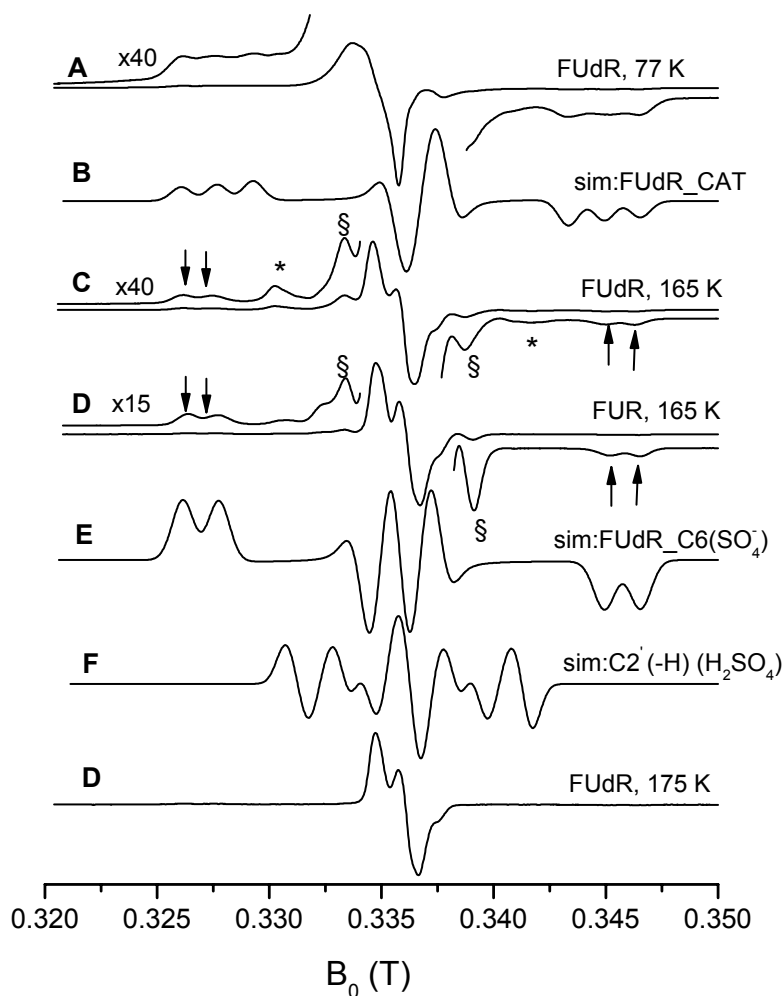
Fig. 5.1.4. X band ESR spectrum of 5-FUdR (400mM) irradiated with 20 kGy in 5 M H_2SO_4 containing equimolar $Na_2S_2O_8$ A) at 77 K, B) Simulated spectrum of FUdR base oxidized product, C) FUdR at 165 K D) FUR at 165 K, E) Simulation of OH/ SO_4^- adduct at C6 of FUdR, F) Simulation if C2' -H abstraction radical, G) FUdR at 175 K.

Simulated pattern of C2'(-H) (**Str.5.1. 5**) shows a good fit with the experimental result. The simulation parameters are provided in **Table 5.1.2** which shows coupling of the unpaired electron with one α proton and two β protons from C3' and C1' rspectively. In FUR presence of hydroxyl group on C2' position hinders the formation of C2' (-H) radical pattern. Another spectral feature (indicated with § in **Fig. 5.1.4C**) observed at 165 K with total splitting 5.4-5.7 mT is typically observed in nucleosides and needs to be discussed further. As with FU in FUdR also the spectrum obtained at 175 K is a single component (**Fig. 5.1.4G**) and has close correlation with O4 protonated anion radical.

R = deoxyribose
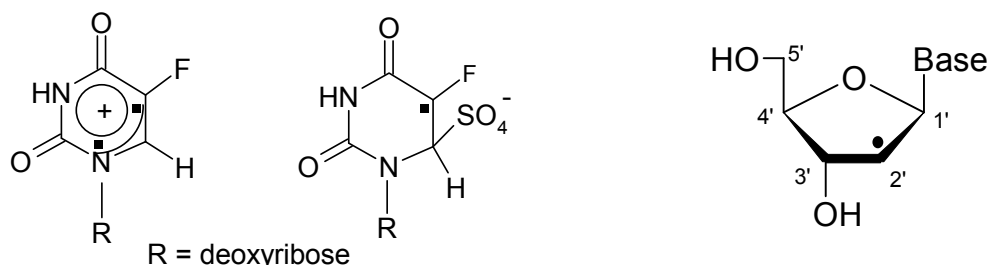
Str. 5.1.3. FUdR_CAT   **Str. 5.1. 4.** FUdR_C6(SO$_4^-$)   **Str. 5.1.5.** C2' (-H) radical

Table 5.1.2. Simulation parameters used for FUdR_CAT, FUdR_C6(SO$_4^-$) and C2'(-H) radicals

FUdR_CAT (Riederer, Hüttermann, 1982)				In this work			
A(mT); g	x	y	z	A(mT); g	x	y	z
F(C5)	-1.8	-1.8	17	F(C5)	-1.8	-1.8	17.26
N(C1)	0	0	1.5	N(C1)	0	0	1.6
H' (C1)	0	0	5	H' (C1)	0	0	5
				Line width	0.9	0.9	0.9
g	2.000	2.0045	2.0050	g	2.000	2.0045	2.0050
FUdR_C6(SO$_4^-$) (Riederer, Hüttermann, 1982)				In this work			
A(mT); g	x	y	z	A(mT); g	x	y	z
F(C5)	-1.5	-1.5	18.3	F(C5)	-1.5	-1.5	18.8
H(C6)	1.5	1.5	1.5	H(C6)	1.6	1.6	1.6
				Line width	0.95	0.95	0.95
g	2.0009	2.0046	2.0032	g	2.0009	2.0046	2.0032
C2'(-H) (Geimer,1994)				In this work			
A(mT); g	x	y	z	A(mT); g	x	y	z
H(C2)	-0.8	-2.8	-1.8	H(C2)	-0.8	-2.8	-1.8
H(C1)	2.9	2.9	2.9	H(C1)	3.1	3.1	3.1
H(C3)	3.8	3.8	3.8	H(C3)	4.9	4.9	4.9
				Line width	0.9	0.8	0.9
g	2.0037	2.0037	2.0020	g	2.0037	2.0037	2.0020

5-Fluoro-2'-deoxyuridine 5'-monophosphate (Na Salt) (FdUMP)

    Fig. 5.1.5 shows the selective spectra of annealing series of 380 mM FdUMP plus Na$_2$S$_2$O$_8$ in 5 M H$_2$SO$_4$ glass irradiated with 20 kGy of x-ray irradiation at 42 db. In this

case also at 77 K the substrate radical pattern is visible only at the wings and the middle of the spectrum remains masked by $SO_4^{-\bullet}$ radical from the scavenger, with decay of the scavenger radical at 165 K a composite spectrum is visible which again converts into a single component spectrum at 175 K similar to that observed in FU and FUdR. At 77 K the triplet splittings at a distance of about 16 mT were very pronounced in FU and were quite detectable in FUdR which inturn were correlated to N1 deprotonated neutral base radical in FU and to π cation in FUdR. In FdUMP the formation of π cation at 77 K is not clearly observed as it can be seen from the **Fig. 5.1.5B** that at temperature as low as 130 K FUdR_C6(SO_4^-) like patterns become evident. At 165 K the spectral features assures the formation of both the FUdR_C6(SO_4^-) (shown by the double arrows) and C2' (-H') (pointed by *) radicals are visible in FdUMP just as it was observed in FUdR (**Fig. 5.1.4**). The experimental peaks can be very well correlated with the simulated patterns (**Fig. 5.1.4E and F**). The non symmetry of the C2' (-H) pattern in experimental spectrum can be due to the presence of minute amount of peroxy radical which becomes prominant by measuring the same sample at 10 dB. Additional patterns (§) observed in FUdR and FUR were not found here gives a clue for its formation in C5' position of sugar part which is blocked by mono phosphate group in FdUMP. Finally the doublet like pattern tentatively correlated to FU_O4H is observed here just like in the previous case.

Discussion

Two mechanisms have been put forward for explaining the base oxidation process in FU in the previous works (Riederer and Hüttermann 1982) in 5 M H_2SO_4 glass containing persulphate as an electron scavenger. As the triplet features are present even at 77 K directly after irradiation and as the direct ionization of the solute is not possible in a glass matrix therefore scavenging of holes produced in matrix by the FU base may be probable where excited holes appear to migrate in the matrix to encounter a solute molecule and then the charge is transferred.

$$FU + h^{+\bullet} \rightarrow FU^{+\bullet} + h \tag{5.1.3}$$

With increasing temperature (> 120 K) as the $SO_4^{-\bullet}$ is thermally released from the matrix traps, further oxidation at the base moiety and consequently deprotonation can be observed.

$$FU + SO_4^{-\bullet} \rightarrow FU^{+\bullet} + SO_4^{2-} \tag{5.1.4}$$
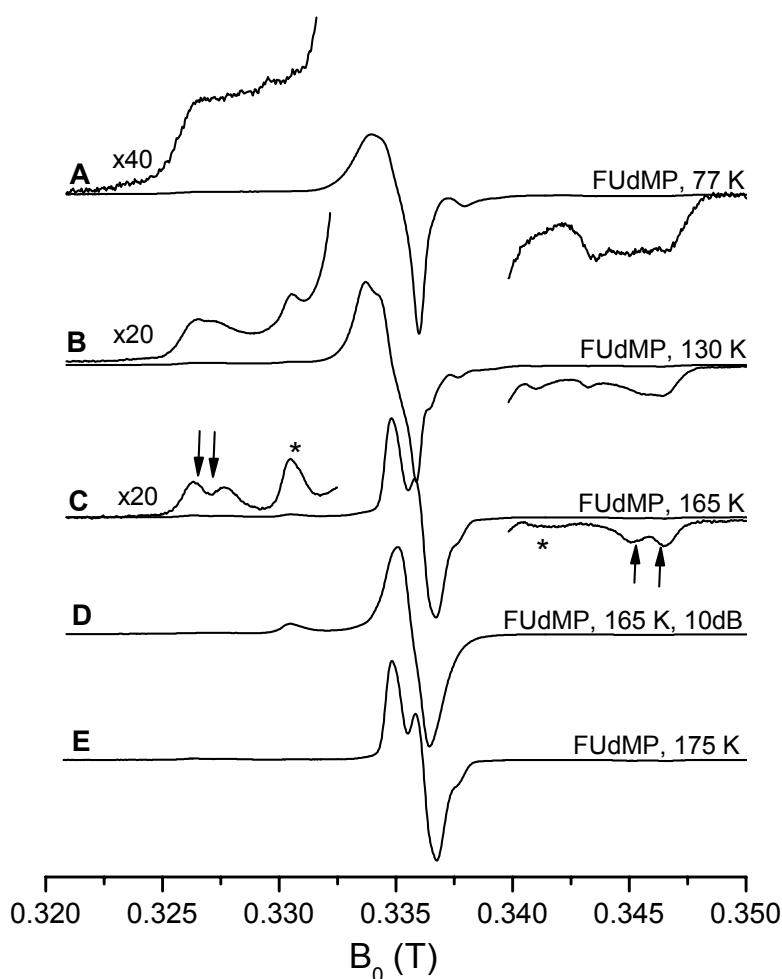
Fig.5.1.5. X band ESR spectrum of 5-FdUMP (380mM) irradiated with 20 kGy in 5 M H_2SO_4 containing equimolar $Na_2S_2O_8$ A) at 77 K, B) at 130 K C) at 165, D) FdUMP at 165 K measured at 10DB showing presence of mainly peroxy radical, E) FdUMP at 175 K showing only presence of thermostable O4 protonated radical.

In FUdR as well as in FdUMP owing to the presence of the big groups at N1 position, the base cations formed at 77 K because of hole scavenging does not converts into neutral radicals by deprotonation at N1 position. With increase in the temperature

(above 145 K) the $SO_4^{-\bullet}$ present in the matrix gets mobile and reacts with the base cations by adding to them at C6 position instead of oxidizing them as in the case of FU.

It is noteworthy to mention that in the previous work done on the same nucleoside system (Riederer and Hüttermann 1982) no oxidation product at the sugar moiety of nucleosides were observed in spite of the fact that the C2' (-H) radicals were formed by $SO_4^{-\bullet}$ attack in irradiated 5 M H_2SO_4 glass containing deoxyribose (300 mM) and 300 mM $Na_2S_2O_8$. The C2' (-H) radical observed here in both FUdR and FdUMP are a result of strong anaerobic conditions maintained during the preparation, irradiation and measurement of the samples. This radical is not detectable at 77 K which means that it is not formed by hole scavenging mechanism and at higher temperatures (> 145 K) it may be formed because of H abstraction by $SO_4^{-\bullet}$ from the matrix.

The patterns (§) found both in FUdR and FUR were not observed in FdUMP may originate from H abstraction of C5' position in FUdR and FUR. In a previous effort (Sieber and Hüttermann 1989), $H^\bullet$ were exclusively produced by photolysis of Fe^{2+} in 6M H_2SO_4 glass matrix and then $H^\bullet$ reactions were selectively studied with annealing studies for riboside as well as deoxyriboside derivatives of purine. A Formation of C5' sugar radical through H abstraction was depicted through a triplet pattern in both ribosides and deoxyribosides with anisotropic coupling of an α- proton (~2.0mT isotropic interaction) together with a nearly axial β-proton (2.1mT). Isolation of a neat triplet pattern was not possible here due to the presence of several other radical patterns in the composite spectra of FUdR or FUR obtained at 165 K but the probability of C5'(-H) radical in the FUdR or FUR systems cannot be ignored.

In all the fluorouracil systems studied in this glass an asymmetric doublet like pattern originating at about 165 K and remaining as the only pattern till the melting point of the sample is reached. The pattern perfectly fits with the simulated pattern of O4 protonated FU anion radical and has not been reported in the earlier works. Previous study on FU and FUdR with $Na_2S_2O_8$ in 5 M H_2SO_4 glass (Riederer and Hüttermann 1982) mainly reported that the deprotonated cations were formed at 77 K or via $SO_4^{-\bullet}$ reactions at higher temperatures in FU and cations gets converted into SO_4^- addition radical at C6 in FUdR and then they decay into non radical species with further increase in the temperature of the system.

In several glass matrices containing FU or its components, studied earlier (Geimer 1994) O4 protonated radical was detected at higher temperature. It has been observed that in all the cases formation of FU anion at 77 K or presence of reducing environment is necessary for the production of this radical. Another work considering irradiation of crystals of FU at 300 K showed direct formation of O4 protonated radical in major concentration (Neumüller and Hüttermann 1980). Though the experimental pattern (**Fig. 5.1.2E**) is a good fit with the simulated O4 protonated radical but the mechanism of its formation in an oxidizing environment is not clear.

From all the annealing series of nucleosides and nucleotides it is clear that there is no transfer of spins from sugar to base or vice versa. The two units reacted independently and decayed with annealing in separate compartments.

5.1.2. Reactions and Products in 7M BeF$_2$/H$_2$O Glasses

In order to understand whether there is any indirect mechanism of radical formation in irradiated frozen aqueous system it is necessary to have a model glass system which traps OH$^\bullet$ radicals directly on ionization at 77 K just as it happens in frozen aqueous system. For this purpose BeF$_2$ is an appropriate glass forming agent as it gives characteristics of OH$^\bullet$ species at 77 K (Riederer et. al. 1983) which is unique as in most glass matrices OH$^\bullet$ radical as soon as they are formed either deprotonates to O$^\bullet$ as in NaOH or oxidizes the anions (Cl$^-$ to Cl$^\bullet$, SO$_4^{2-}$ to SO$_4^{-\bullet}$) in LiCl or H$_2$SO$_4$ glasses. BeF$_2$ have been used before several times to probe the indirect effect of radiation either independently or for comparative purposes with frozen aqueous system (Ohlmann and Hüttermann 1993, Lange et. al. 1995, Weiland et. al. 1996). BeF$_2$ provides a suitable medium to study the reactions of OH$^\bullet$ radicals, electrons and H$^\bullet$ species simultaneously, so all the water radiolysis intermediates are formed in this system upon irradiation. All these intermediate radicals can interact with the substrate molecules during irradiation as well as after irradiation with rising temperature of the system. The ESR active species thus formed on the substrates can provide a close insight into the mechanism of their formation. To understand the reactions of OH$^\bullet$ species particularly additional studies are done using a strong electron scavenger (K$_3$Fe[CN]$_6$) along with the substrates which is assumed to scavenge the electrons from the system leaving oxidized radicals in the matrix. One drawback of this solvent is the relatively acidic pH of 2-3 which causes acid

hydrolysis of bulky biomolecules like DNA, but for the fluorouracil base and its derivatives used in this study there were no abnormalities observed.

5 - Fluorouracil (FU)

Fig. 5.1.6 shows the selective spectra of the annealing measurement of 10mM FU in 7M BeF$_2$/ H$_2$O irradiated with x- ray dose of 10 k Gy at 42 dB. Close inspection of the ESR spectrum at 77 K does not reveal any sign of formation of N1 deprotonated cation at 77 K which was observed in H$_2$SO$_4$/ Na$_2$S$_2$O$_8$. The spectrum consists of an OH$^\bullet$ radical formed from water oxidation and trapped in the matrix (as represented by the dotted spectrum in **Fig. 5.1.6A**) together with a doublet pattern formed from electron addition at the FU center. Minor amounts of other radical pattern are also detectable at the right side (on magnification) of the spectrum. With increasing temperature of the sample to 140 K and then re cooling to 77 K the OH$^\bullet$ radical decays while the high and low field region of the spectrum (**Fig. 5.1.6B**) shows prominent presence of peaks with same splitting of the outer lines as at 77 K (of about 4.0 mT). With continuous increase in the temperature the central doublet pattern slowly changes into a sharper doublet indicating formation of a new radical and formation of very small amount of another radical can also be predicted at 165 K (as shown by the arrows).

At 77 K the doublet pattern formed which can be associated to the base anion radical (**Str. 5.1.6**). The splitting of this pattern is equivalent to that formed in 7 M LiBr matrix with the same substrate after irradiation (**Fig. 5.1.7B**). The pattern can be simulated using the parameters given in the **Table 5.1.3** and is shown in **Fig. 5.1.7C**. On raising the temperature the radical pattern with a total spread of approximately 25 mT (**Fig.5.1.7D**) and with the outer line splitting of about 4 mT is due to α-halogen 5-yl radical (**Str.5.1.7**) and can be judged from the close correspondence with the simulated pattern (**Fig. 5.1.7E**). This radical is found to form in single crystals as well as in glass matrices of several halogenated nuclei acid bases like in Chlorouracil (ClU) and Bromouracils(BU) (Neumüller anh Hüttermann 1980, Riederer et. al 1981). Irreversible formation of another radical is visible at the middle of the spectra after 150 K can be easily explained by protonation of anion radical at O4, whose simulation has already been provided in the **Fig. 5.1.3D**. The small raise shown by arrows at 165 K may be the result of OH addition radical at C6 position of FU as OH$^\bullet$ becomes mobile in this temperature range but confirmed identification is not possible at this stage.
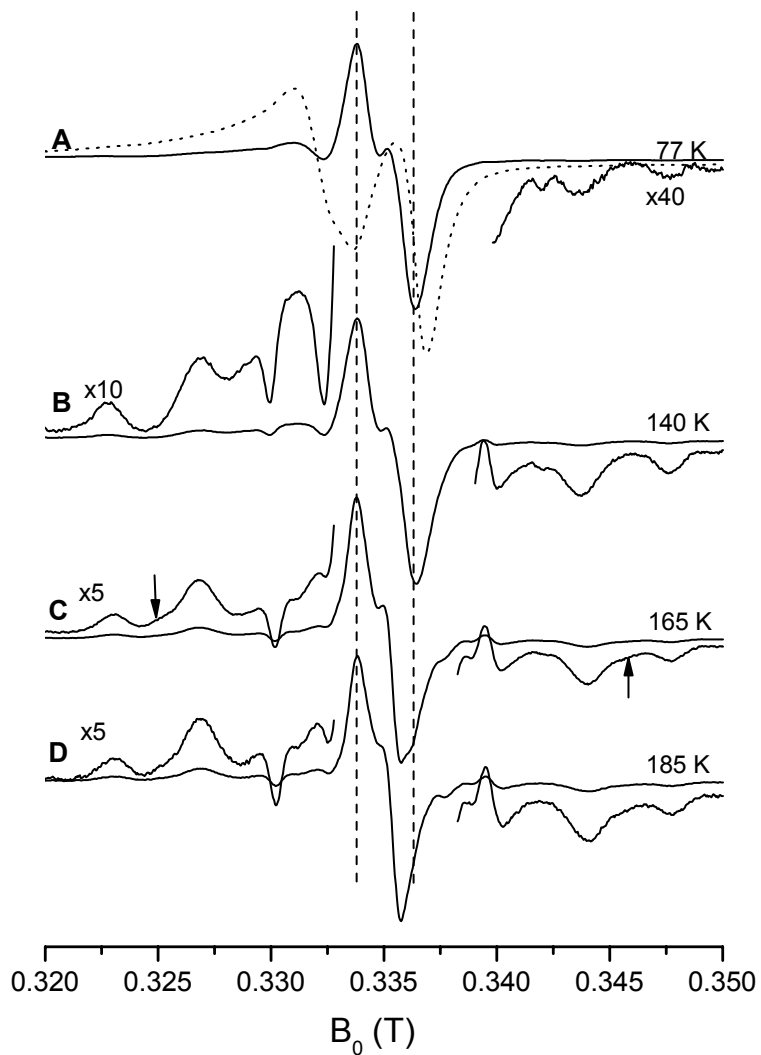
Fig. 5.1.6. ESR spectra of selected annealing steps of 10mM FU in 7M BeF2/ H2O irradiated with 10 kGy. A) Spectra at 77 K containing the OH$^\bullet$ radical formed in the matrix from water radiolysis (dotted spectrum) and the electron adducts at FU base, B) OH$^\bullet$ pattern decomposes at 140 K and more than one substrate radicals are formed as visible from the central and magnified wing regions, C) at 165 K, D) at 185 K.
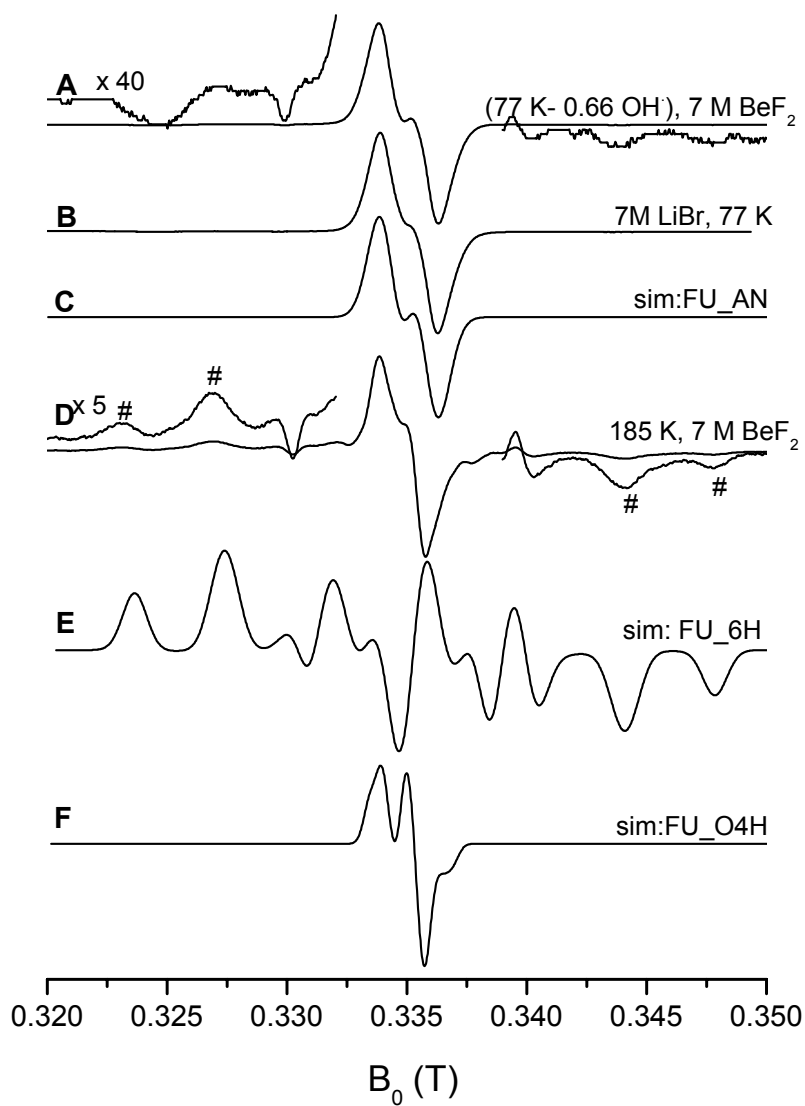
Fig. 5.1.7. A) ESR spectrum of FU in 7 M BeF$_2$ glass after subtraction of OH$^\bullet$ pattern as shown in Fig. 5.6 B) FU electron adduct formed in 7 M LiBr/ H$_2$0 matrix C) Simulation of FU_ anions (FU_AN) with the parameters from Table 5.3 D) FU at 185 K, E) Simulated spectrum of 5-yl radical from the parameters given in Table 5.3, E) Simulated pattern for H addition radical on O4 of FU.

Table 5.1.3. Simulation parameters used for FU_AN and FU_C6H radicals

FU_AN(Riederer et. al. 1981)				In this work			
A(mT); g	x	y	z	A(mT); g	x	y	z
H (C6)	1.6	1.6	1.6	H1 (C6)	1.3	1.3	1.3
				Line width	1.2	1.2	1.2
g	2.0029	2.0066	2.0052	g	2.0029	2.0066	2.0052
FU_C6H ((Riederer et. al. 1981)				In this work			
A(mT); g	x	y	z	A(mT); g	x	y	z
H1 (C6)	4.1	4.1	4.1	H1 (C6)	4.03	4.03	4.03
H2 (C6)	3.5	3.5	3.5	H2 (C6)	3.5	3.5	3.5
F(C5)	16.5	-0.9	-1.8	F(C5)	16.7	-0.9	-1.8
				Line width	1	1	1
g	2.0029	2.0066	2.0052	g	2.0029	2.0066	2.0052
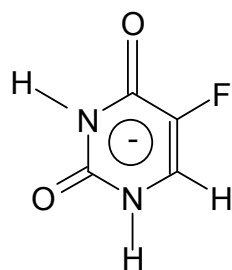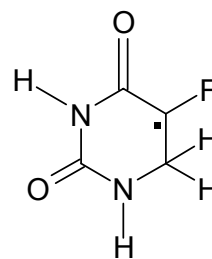
Str. 5.1.6. FU_AN   **Str. 5. 1.7.** FU_C6H

5-Fluoro-2'-deoxyuridine (FUdR)

Fig. 5.1.8 represents the annealing series of 25 mM FUdR X irradiated with 10 kGy in 7M BeF_2/ H_2O. At 77 K the OH$^\bullet$ pattern trapped in the matrix was observed along with the electron adduct signals from solute molecules. Spectrum **A** is isolated after subtracting OH$^\bullet$ radical pattern from ESR spectrum of FUdR at 77 K. The distribution of radicals is same as was observed in FU under same condition. The central doublet pattern which is from base anion (**Fig. 5.1.7B and C**) do changes into a sharper doublet which has been attributed to O4 protonated anion (**Fig.5.1.7F**) with increasing temperature however formation of some other radical is evident from visual inspection of the middle region of the spectra at 155 and 175 K (see discussion below).
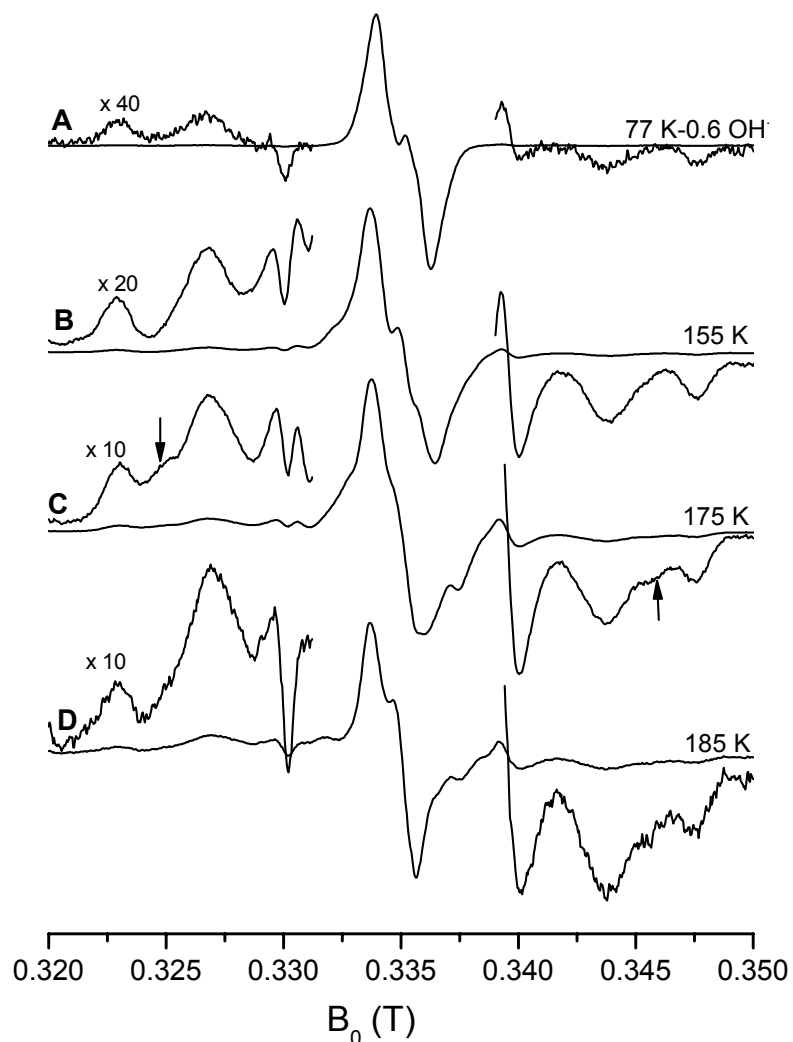
Fig 5.1.8. (A-D)Important annealing steps of 5-FUdR (25 mM) x-ray irradiated with dose of 10 kGy in 7M BeF$_2$/ H$_2$O where the outer lines are magnified as indicated for clarity.

Formation of the H addition at C6 of FUdR base is quite clear from the 4 mT splitting of the outer wings and also from its simulation (**Fig. 5.1.7E**). At 175 K the arrows probably indicates the upcoming of a radical because of OH$^•$ reactions.

5-Fluoro-2'-deoxyuridine 5'-monophosphate (Na Salt) (FdUMP)

Fig. 5.1.9 shows the ESR spectra representing the specific annealing steps of 50 mM FdUMP in 7M BeF$_2$/ H$_2$O irradiated with a dose of 35 kGy in liquid nitrogen. At 77 K

the spectrum reproduced after subtraction of OH pattern shows formation of anion as can be correlated with the simulated picture from **Fig. 5.1.7C** and the amplified wings shows formation of H addition radical at C6 position of FU and is also simulated earlier (**Fig. 5.1.7E**) by using the parameters given in **Table 5.1.3**. On increasing temperature of the sample and measuring again after re cooling to 77 K shows increase in formation H addition radical. After 140 K although OH radicals disappear from the obtained ESR signal but formation of OH addition radical from the substrate is not so well observed in this annealing series. At the last temperature point of the annealing series i.e., at 195 K the formation of the O4 protonated radicals is clearly observable and can be correlated to the simulated pattern (**Fig. 5.1.3D**) along with H addition radical at C6 position of FdUMP base and some flanges (indicated by arrows) are produced may be originating from OH$^\bullet$ addition radical but is too small to be analyzed before the sample starts melting. The change in the central doublet pattern with increasing temperature is more similar to that of FUdR and may be an indication of formation of any radical originating from the deoxribose moiety of the nucleotide (see discussion).

Discussion

The results obtained from the study of Fluorouracil bases and its derivatives are in good correlation with those obtained from annealing study of 5-bromouracil in the same glass matrix (Oloff et. al. 1984). Among the solvated electrons, H$^\bullet$ and OH$^\bullet$ produced in the BeF$_2$ matrix upon X irradiation at 77 K, the solvated electrons react instantaneously with the FU base or its derivatives at that temperature to produce π^* anions, which latter upon annealing, forms 5-yl radical, Some of the hydrogen atoms (H$^\bullet$) which are formed on irradiation and are mobile during the process of irradiation at 77 K may encounter with the solute anions and form 5-yl radicals at 77 K while most of them gets trapped in the glass matrix at 77 K. These trapped hydrogen atoms liberates after 130 K and produces the same 5-yl radical on reacting with the solute molecules. The mechanism of formation of this type of α halogen radical has been widely discussed in the literature. Two reactions for its formation have been established so far, addition of a hydrogen atom at the C6 position of base moiety and protonation of the previously formed π^*anion at same carbon position. The former mechanism was demonstrated by kinetic measurements in nucleosides in single crystals (Hüttermann et. al. 1977). In the glassy matrices however it was inferred that H-addition radicals arise through protonation of an anionic intermediate radical (Sevilla 1971).
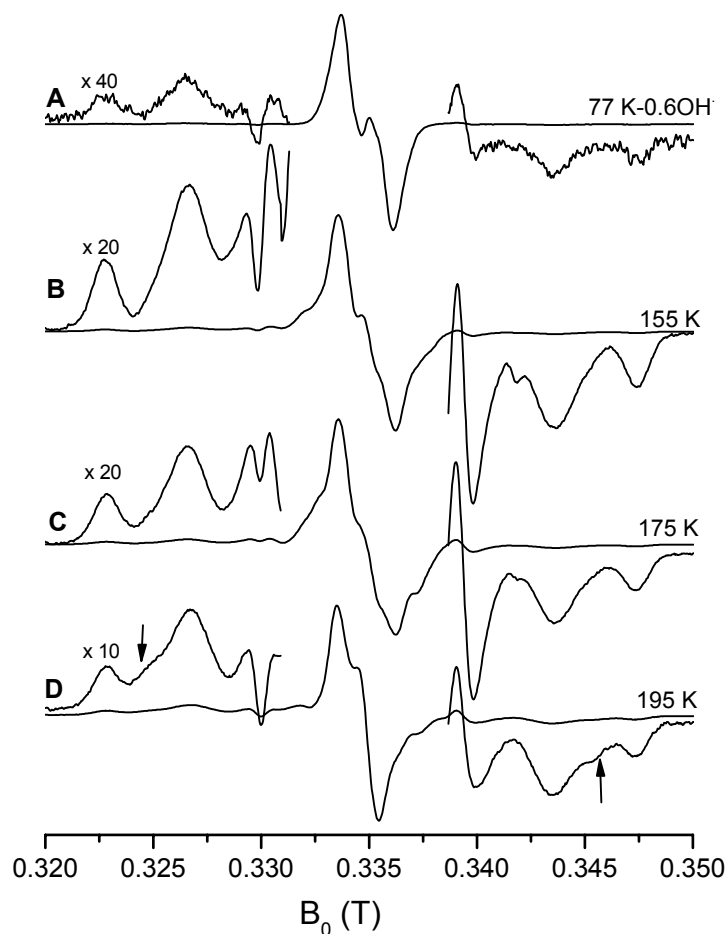
Fig. 5.1.9. (A-D)Important annealing steps of 5-FdUMP (50mM) in 7M BeF_2/H_2O after x-ray irradiation with a dose of 35 kGy. The magnification of lower and higher magnetic field regions shows the formation of H addition radical through protonation at C6 position of FdUMP base anion.

It is interesting to note that in the case of irradiated single crystals of FU upon warming protonation at O4 oxgen site is dominating and on comparative studies of single crystals of different halosubstituted bases a relation was established that qualitative tendency of O4 protonation increases from bromo to fluoro substituted bases. In the glassy matrices like in BeF_2 and also in 5 M H_2SO_4 , (Riederer 1981, Geimer 1994) however both 5yl radical and O4 protonated radical have been observed even in FU and in its derivatives. Finally, mobile hydroxyl radicals produced on irradiation are trapped in the matrix and give their ESR signature at 77 K and are assumed to react in

the temperature range 120-150 K by adding to carbon C6 at the 5,6-double bond of the halopyrimidine moiety. In all the three systems studied here showed the indication of formation of this radical at temperature range from 165-195 K, but there presence were not so much prominant like the 5-yl radicals. A noticeable point is that the 5 substituent fluoro component directs the site of addition reaction of both H$^\bullet$ and OH$^\bullet$ radicals to the 6-carbon site of the base moiety and as H$^\bullet$ is more mobile and is kinetically faster to protonate the C6 position. Alternatively the OH$^\bullet$ radical might be involved in producing some other radicals perhaps in the sugar moiety. In the previous works (Geimer 1994) an attempt was made to isolate the FU_C6OH radical pattern by substraction of the experimental spectra obtained at different temperatures. In this study high concentration of strong electron scavenger like $K_3Fe[CN]_6$ has been used which itself is ESR mute. It is assumed that by using this strong electron scavenger along with the solute will probably subside the H$^\bullet$ reactions to a great extent and pure OH addition radical pattern from the experimental spectra could be isolated.

On comparing the spectra obtained for FU, FUdR and FdUMP at the temperature range 140-175 K with each other and on substraction of FU spectra from that of FUdR and FdUMP recorded at same temperatures indicated the formation of additional radicals in nucleosides and –tides. **Fig. 5.1.9** shows presence of additional peaks (+) both on FUdR and FdUMP with a spread of about 5.8 mT. The specific presence of this pattern only in FUdR and FdUMP ensures its origin from the deoxyribose sugar moiety and can be correlated to C1'(-H) radical as has already been found in many other nucleic acid derivatives in single crystals and aqueous glasses and also in dry and frozen aqueous solutions of DNA in the previous studies (Hole et.al. 1992, Sieber and Hüttermann 1989, Malone et. al. 1995, Weiland et. al. 1996, Weiland and Hüttermann 1998, Shukla et.al. 2005). The spectral appearance of the C1' radical in deoxynucleosides and nucleotides (**Str.5.1.8**) is a quartet due to interaction of the unpaired electron with two β-protons at C2'. The simulated pattern for this radical is given in **Fig. 5.1.9** whose parameters are provided in **Table 5.1.4**.
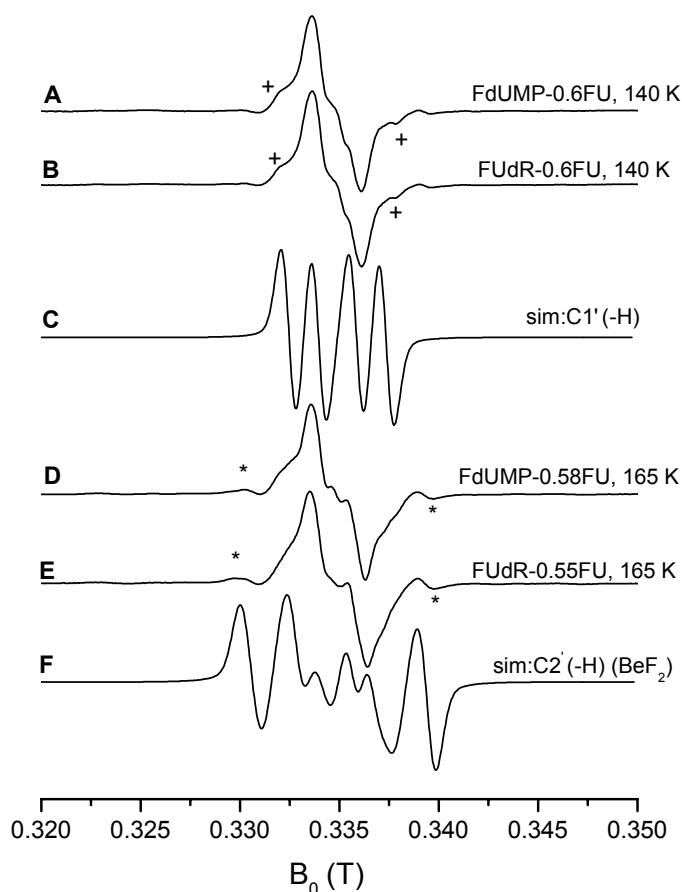
Fig. 5.1.9. A-B) Subtracted patterns from BeF_2/H_2O matrix obtained as indicated from FdUMP and FUdR at 140 K showing formation of C1' (-H) radical (+), C) Simulated pattern of C1' (-.H) radical, D-E) Subtracted patterns obtained as indicated from FdUMP and FUdR at 165 K indicating the presence of C2'(-H) (*), F) Simulated pattern of C2'(-H) specific for BeF_2/H_2O matrix.

With increasing temperature (becomes prominent at 165 K) one more radical pattern with a splitting of about 8.7 mT comes into play in FUdR and FdUMP, after subtraction of ESR spectrum of FU also measured at 165 K. This pattern has been also observed in the previous study done on FUdR in 7 M BeF_2/H_2O (Geimer 1994) and has been attributed to C2'(-H) radical. The spectrum of C2'(-H) in **Fig. 5.1.9F** is simulated using the parameters given in **Table 5.1.2**. The C2' (-H) radical pattern shows some differences in splitting in different matrices as can be noted here.

In the other studies done in the same glass with thymine nucleosides and nucleotides (Lange 1994, Lange et. al. 1995) it has been found that all of the OH$^\bullet$ reaction involved the formation of an allyl radical by abstraction of hydrogen from the 5-methyl group also at 77 K. The uracil and cytosine containing nucleosides and nucleotides on the other hand was a good probe for formation of sugar radicals. The investigations made on dCMP in BeF$_2$ showed the formation of C1' sugar radical directly at 77 K. Two mechanisms were thought to be responsible for this. One is that hole formed in the matrix on irradiation before getting trapped as OH$^\bullet$ produces a cation on base which deprotonates immediately to produce C1' or allyl radicals. Alternate way would be that a fraction of OH$^\bullet$ would be mobile at 77 K and react with the substrate. Though in ice matrix the mechanisms could be very fast because of hydrogen bonding network but in the acidic glasses like in BeF$_2$ there remains some reservations for deploying the above two mechanisms (Weiland and Hüttermann 1996). In the halouracil systems used here, a very close look into the spectra obtained from nucleosides and nucleotides did not show any indication of C1' radical pattern formation at 77 K. The OH$^\bullet$ gets liberated after 140 K and react with the solutes to deprotonate at the C1' position of the sugar part or hydroxylate at the active C6 site of the base.

5 - Fluorouracil (FU) and K$_3$Fe[CN]$_6$

X band ESR spectra obtained from temperature annealing study of FU in the presence of very high concentration of a strong electron scavenger K$_3$Fe[CN]$_6$ in 7M BeF$_2$/H$_2$O glass matrix (in a molar ratio of 1FU :4 K$_3$Fe[CN]$_6$) has been represented in **Fig. 5.1.10**. The irradiation dose used here is 30 kGy which is higher than that used for neat FU in the same matrix as the intensity of the spectra produced by 10 kGy dose in FU+ Fe^{3+} system was very weak specially at higher temperatures. Increase in dose from 10 to 30 kGy does not change the nature of the spectra in this system. It can be noticed from the **Fig. 5.1.10A** that at 77 K in the presence of K$_3$Fe[CN]$_6$ the solvated electrons from the matrix are completely scavenged by the additive and there is no electron adduct formation on the base which was observed so clearly in neat FU system (**Fig. 5.1.10B**). OH$^\bullet$ radicals are trapped at 77 K and on increase in temperature the radical formation on the base moiety can be observed. Just after decay of the OH$^\bullet$ radical at 140 K and then more clearly at 155 K the sharp assymetric doublet pattern is observed which remains till the sample melts and the magnification of the wings show presence of more than one radical pattern.
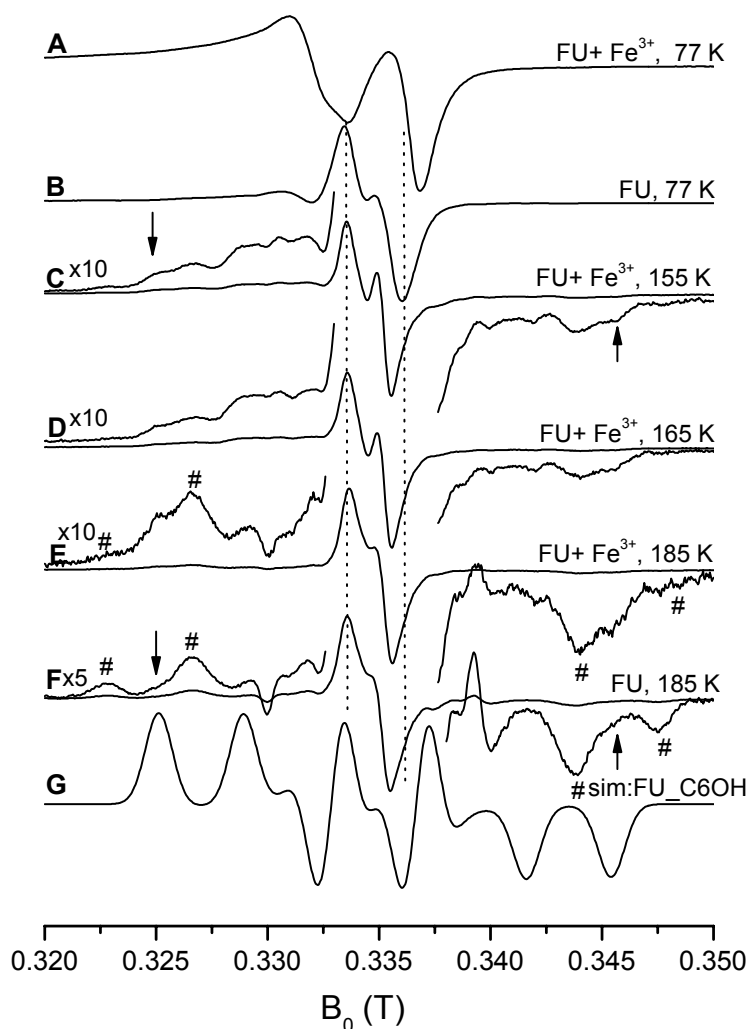
Fig. 5.1.10. ESR spectra taken in BeF_2 matrix after 30 kGy of irradiation for FU and $K_3Fe[CN]_6$ in a molar ratio of (1:4) at a) 77 K, C) 155 K, D) 165 K and E) 185 K. The spectra obtained from neat FU (From Fig. 5.1.6) are represented here for comparison, B) FU at 77 K, F) FU at 185 K. Simulated spectrum of OH addition radical at C6 position of FU base is show in G.

The sharp doublet pattern observed so strongly in the series has already been attributed to the O4 protonoted base anion radical and among the composite ESR signatures obtained on the wings at least at 185 K clear presence of H addition radical at C6 can be pointed by comparing the additive containing spectra of FU (**Fig. 5.1.10E)** with that of neat FU at same temperatures (**Fig. 5.1.10F**) (as shown by the #).

The OH$^\bullet$ radical reaction after its liberation from the matrix is more evident in this system and formation of OH addition radical formed by breaking the 5,6 double bond in FU through hydroxylation can be traced from 155 K (shown by the arrows) which becomes very clear at 185 K. After simulating the spectrum using the parameters from **Table 5.1.4** as shown in **Fig. 5.1.10G** it can be stated with confidence that the OH addition is at C6 position where a coupling with α fluor atom is evident (**Str. 5.1.9**).
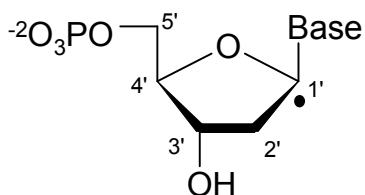
Str. 5.1.8. C1'(-H) radical
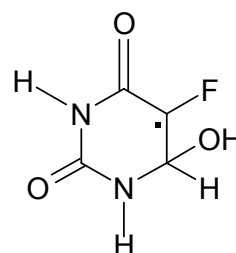
Str. 5.1.9. FU_C6(OH)

Table 5.1.4. Simulation parameters used for C1' sugar radical and FU_C6OH radicals

C1'-Deoxyribose radical (Weiland 1999)				In this work			
A(mT); g	x	y	z	A(mT); g	x	y	z
H (C2')	1.5	1.5	1.5	H (C2')	1.5	1.5	1.5
H(C2')	3.4	3.4	3.4	H(C2')	3.4	3.4	3.4
Line width	0.8	0.8	0.8	Line width	0.8	0.8	0.8
g	2.0032	2.0032	2.0032	g	2.0032	2.0032	2.0032
FU_C6OH (Riederer 1981)				In this work			
A(mT); g	x	y	z	A(mT); g	x	y	z
F (C5)	16.5	-0.9	-1.8	F(C5)	16.5	-0.9	-1.8
H(C6)	3.5	3.5	3.5	H(C6)	3.8	3.8	3.8
				Line width	1.3	1.3	1.3
g	2.0029	2.0066	2.0052	g	2.0029	2.0066	2.0052

5-Fluoro-2'-deoxyuridine (FUdR) and K$_3$Fe[CN]$_6$

Fig. 5.1.11 shows the selective spectra obtained from the annealing series of the system containing FUdR and K$_3$Fe[CN]$_6$ in a molar ratio of 1:1. The system was X irradiated with 10 kGy. At 77 K the spectrum obtained is identical to the OH$^\bullet$ radical pattern trapped in the matrix thus indicating that the solvated electrons are all scavenged by the electron scavenger and is not available to react with the nucleotide molecules. At 140 K after the OH$^\bullet$ species are released from the matrix and becomes available to the substrate to react. The spectrum shows almost no H addition radical formation. The peaks pointed by + symbol in **Fig. 5.1.11B** may appear from C1' sugar radical which

were detected in neat FUdR only after proper subtraction. With further raise of the temperature another radical pattern originates which was not detected in FU with additive. From the splittings, the peaks (as shown by * in **Fig.5.1.11C**) seems to be same as C2' sugar radical as was observed in neat FUdR with maximum spread of about 9.3 mT. Formation of the OH addition radical at C6 position of the FUdR base is observable from 140 K but distinguished peaks can be seen at 175 K as denoted by the arrows in **Fig. 5.1.11D**. At 185 K before the sample starts melting the H addition radical at C6 position of the base (shown by #) and O4 protonated anion radical patterns are observable which are formed due to $H^\bullet$ reactions again indicates that the matrix may have trapped some $H^\bullet$ radicals at 77 K.

5-Fluoro-2'-deoxyuridine 5'-monophosphate (Na Salt) (FdUMP) and $K_3Fe[CN]_6$

In order to increase the fraction of OH addition radical the reduced species in the system were successfully lowered by using $K_3Fe(CN)_6$ in the molar ratio of 2 to 1 to FdUMP (50mM) and the annealing series so obtained are shown in the **Fig. 5.1.12**. At 77 K the spectrum formed is from the trapped $OH^\bullet$ in the matrix. The anion formation is completely prohibited due to presence of strong electron scavenger in large amount in the matrix. With increase in temperature as OH radical pattern disappears at 155 K disappears some other spectral features originates from the substrate. At about 5.7 mT of spectral width the peaks observed (+) in the **Fig. 5.1.12B** may be due to C1' sugar radical from the deoxribose moiety of FdUMP. With increase in the temperature another radical pattern comes into play with a total spread of about 8.7 mT (denoted by * in **Fig. 5.1.12C**) which has been also observed in FUdR and therefore can be correlated with C2' (-H) radical from the deoxyribose moiety. As it is already observed in FU and FUdR, here also hydrogen addition radical do interfere with the formation of OH addition radical at C6 position of the base moiety of FdUMP. Outer lines of the two radical patterns overlap and broaden the peaks obtained at low and high field region of the spectra. Overlaying the experimental patterns with simulated spectra of the respective radicals enables to delineate the composite experimental spectra (**Fig. 5.1.12**) as shown by # and arrows).
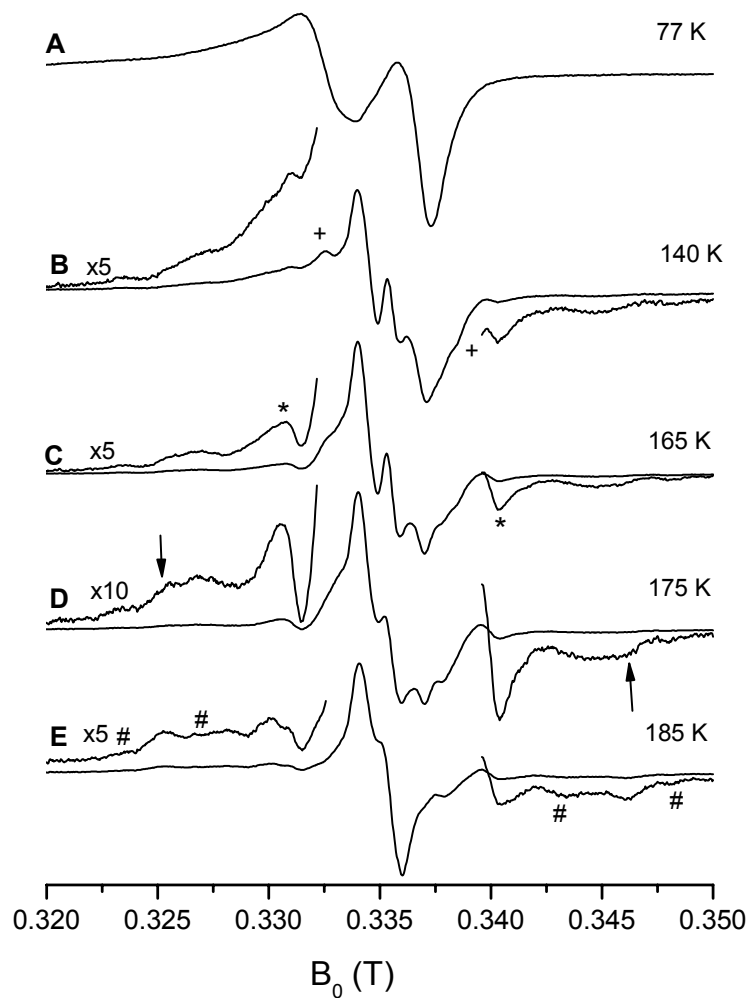
Fig. 5.1.11. Selected ESR spectra from the annealing series of FUdR and $K_3Fe[CN]_6$ (molar ratio 1:1) in 7M BeF_2/H_2O matrix after x- ray irradiation with 10 kGy at 77 K. A) At 77 K only $OH^•$ radicals are trapped in this magnetic field range, B) At 140 K, formation of radicals on the substrate due to $OH^•$ and $H^•$ reactions, C) 165 K. D) 175 K, E) 185 K (for details see text).
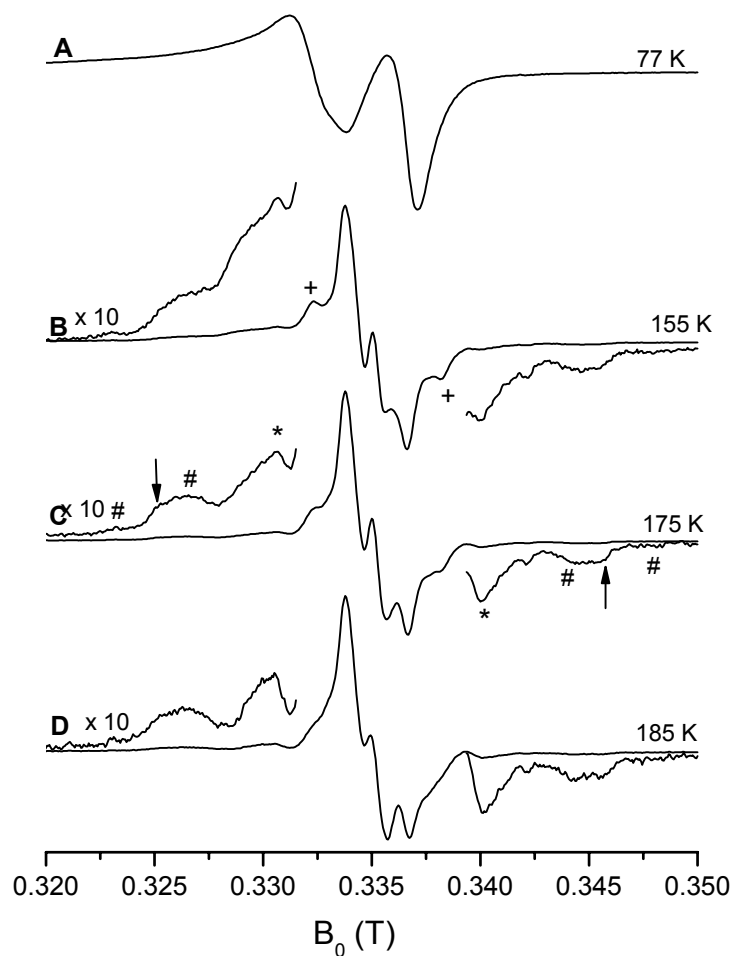
Fig. 5.1.12. ESR spectra from the annealing series of FdUMP and $K_3Fe[CN]_6$ (molar ratio 1:2) in 7M BeF_2/H_2O matrix after x- ray irradiation with 35 kGy at 77 K. A) Formation of $OH^\bullet$ radical at 77 K B) At 140 K, formation of radicals on the substrate due to $OH^\bullet$ and $H^\bullet$ reactions, C) 165 K. D) 175 K, E) 185 K (for details see text).

Discussion

In all the three systems investigated here (FU, FUdR and FdUMP) along with the high concentrations of ESR silent electron scavenger $K_3Fe[CN]_6$, the aim was to subside the electron adduct formation and enhance the oxidized radical balance in the system. From the spectra obtained at 77 K just after irradiation it is easily observed that all the solvated electrons formed during irradiation were directly scavenged by the oxidizing

agent and no electron adducts were formed on the substrate which could later interfare with the oxidative radical pathway. After annealing the systems to 140 K the OH$^\bullet$ pattern decayed showing that it was liberated from the matrix and reacted with the substrate. Considering each system one by one, it was found that in FU the OH$^\bullet$ attacks at the 5,6 double bond of the fluorouracil and formed OH addition radical at C6 of FU which was expected from the system. In FUdR and FdUMP the OH$^\bullet$ reacted not only with the base moieties and produced OH addition radicals at C6 position but also formed radicals on the sugar part of the nucleoside and the nucleotide. The C1'(-H) radical on the deoxyribose part of both FUdR and FdUMP was already traced in the neat substrates and now can be isolated from the annealing series of FdUMP plus K$_3$Fe[CN]$_6$. **Fig. 5.1.13A and B** shows the isolated spectrum of C1'(-H) radical from the subtraction of 93% of the experimental spectrum obtained at 185 K from that obtained at 175 K and its simulated spectrum respectively. From the annealing series of FUdR plus the additive, after subtraction of the 70% of the spectrum obtained at 185 K from that received at 175 K a composite spectrum is obtained as can be seen from the **Fig. 5.1.13C**, almost 16% of which is composed of the simulated spectrum of C2'(-H) radical pattern. The pattern C in **Fig. 5.1.13** might contain another radical pattern but could not be disentangled with the present results.

Formation of C5'(-H) radical which has been tentatively predicted for FUdR in 5 M H$_2$SO$_4$ glass was also expected to be observed here. The comparisons of the spectra from FUdR and FdUMP were made but a clear distinction was not possible in this case.

Apart from the OH$^\bullet$ reaction pathway observed in FU, FUdR and FdUMP the formation of H addition radicals on C6 position or on the O4 position in all the annealing series could not be ignored. This indicated that perhaps H$^\bullet$ radicals are being trapped at 77 K. On doing control experiments at 77 K with the irradiated FUdR and FdUMP probes containing electron scavengers with large magnetic sweep widths it was found to be indeed the case and at about 50.4 mT two spikes were observed which shows the presence of trapped H atoms. So that clarifies the scenario to a great extent. The H$^\bullet$ species which get trapped at 77 K are released on warming the sample to about 120 K and form addition radical via protonation of the anion intermediates. The anions however could not be observed here as perhaps they are extremely unstable at temperatures above 77 K and immediately gets protonated.

The BeF_2 matrix serves as an excellent trap for solvated electrons, $H^{\bullet}$ and $OH^{\bullet}$ species. In the neat systems reactions of the substrate with all three moieties could be very well followed and distinguished from one another. As in 5 M H_2SO_4 glass there was
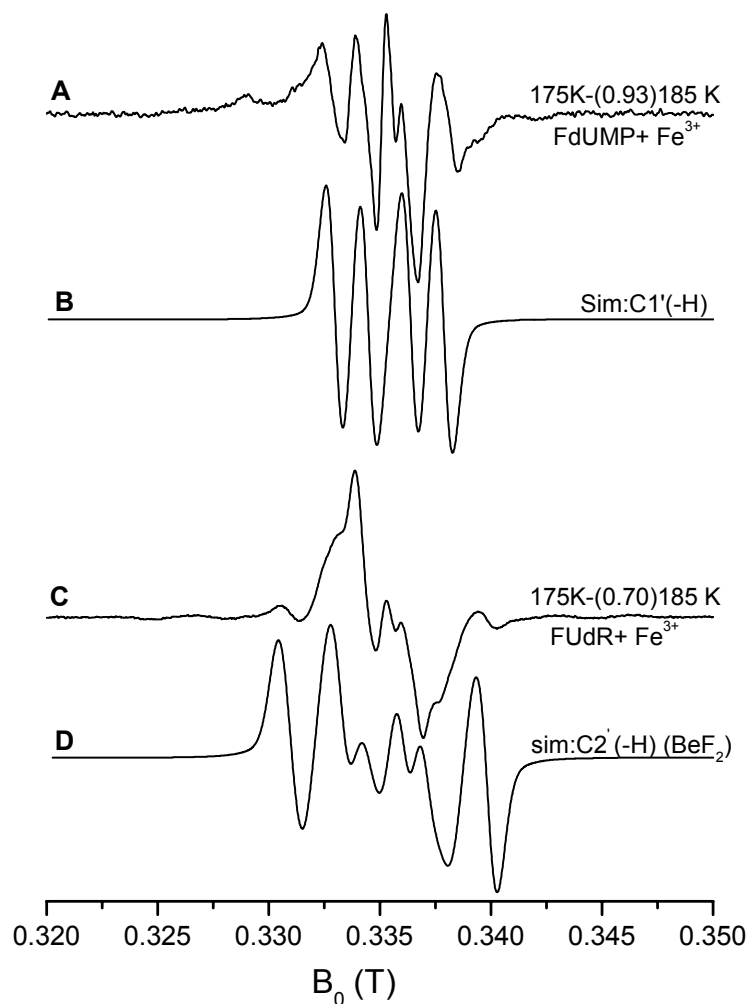
Fig. 5.1.13. A) The subtraction of 93% of spectrum E from spectrum D from Fig. 5.1.12 gives this quartet which can be correlated with the simulated pattern (B) of C1'(-H) (Table 5.1.4). C) This pattern is obtained from subtraction of 70% of spectrum E from the spectrum D as given in the Fig. 5.1.11. D) Simulated spectrum of C2'(-H) in BeF_2

no transfer of spins from sugar to base moieties and vice in 7 M BeF_2/H_2O glass matrix also.

5.1.3. Reactions and Products in Frozen Aqueous Solutions

In the frame of this work the reactions undergoing in frozen aqueous solutions will be investigated. In frozen aqueous system as an effect of ionizing radiation after radiolysis of water (details have been discussed before) solvated electrons, the OH$^\bullet$ radical and the H$^\bullet$ radicals are mainly produced. In ESR experiment of polycrystalline ice matrix at 77 K the OH$^\bullet$ radical can only be detected as a trapped species. The formation of solvated electrons and H$^\bullet$ radicals can in turn be detected by their reaction with any suitable substrate added to the aqueous matrix. The system of frozen aqueous system has been used widely as the matrix for ESR spectroscopic investigations of spectral features of free radicals produced from substrate molecules by ionization radiation, typically at 77 K, and on subsequent annealing. The mechanism of ionization of the substrates in the frozen aqueous system (**see section 3.1.1**) remained an open question to till date.

Fluorouracil and its derivatives used in this work may provide some additional knowledge to the present scenario, specifically because the radicals formed in the base moiety are easy to separate from each other due to the large hyperfine coupling of fluorine. On specifically looking on the oxidised species as has been already found from 5 M H_2SO_4 (plus $Na_2S_2O_8$) and 7M BeF_2/H_2O that the cations formed on the base moiety and the OH addition radicals gives distinctly different spectra and can be well differentiated. Formation of oxidised sugar species can also be verified from their broad structures. For FU, the solubility of the base is so low in H_2O that it was not possible to get reproducible results from this system, therefore data only from FUdR and FdUMP are documented here. The main aim of this particular study was to distinguish the formation of base cations formed upon direct irradiation and OH addition radical at C6 position of FU base via matrix in frozen aqueous solutions of FUdR and FdUMP.

5-Fluoro-2'-deoxyuridine (FUdR)

ESR spectra obtained from the annealing series of 200 mM FUdR in frozen aqueous system after irradiation with 200 kGy of x- ray are shown in **Fig. 5.1.14**. FUdR at 77 K (**Fig.5.1.14A**) (Solid line) shows the trapping of OH$^\bullet$ radical (as compared with the neat OH$^\bullet$ radical (dotted lines) pattern obtained by irradiating the pure ice matrix) at the left part of the spectrum along with the electron adduct formation on the substrate

molecules and shows similarity with the anion radicals formed in the 7M BeF_2 as well as 7M LiBr glasses at 77 K.
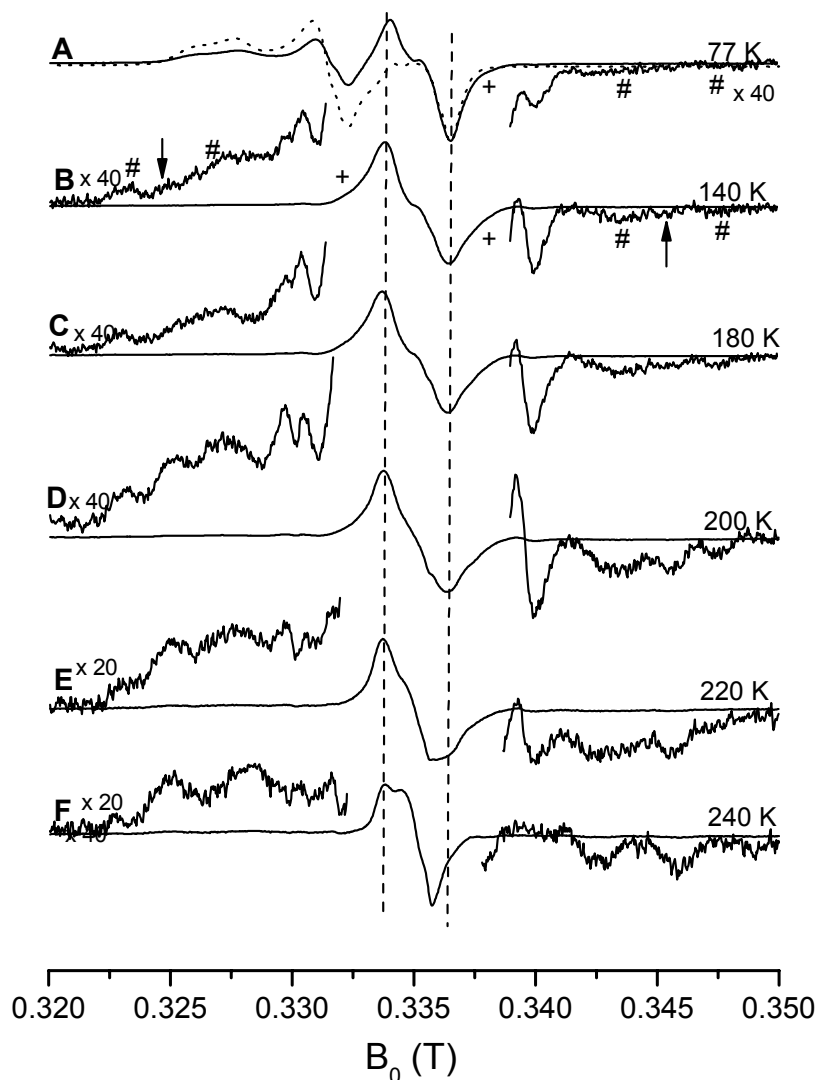
Fig. 5.1.14. ESR spectra obtained from the annealing series of 200 mM FUdR in frozen aqueous system after irradiation with 20 kGy of x- ray. A) FUdR at 77 K (Solid line) showing trapping of $OH^\bullet$ radical (as compared with the neat $OH^\bullet$ radical (dotted lines) pattern obtained by irradiating the pure ice matrix) along with the anion radical formed at FUdR, B) at140 K , C) 180 K, D) 200 K, D) 220 K, E) 240 K.

On magnification of the outer wings in the high field region traces of H addition radical formation (has already been identified in 7m BeF_2 matrix) can be detected from

which gets clearer at 140 K when the OH radical pattern decays and the H addition radical formation becomes clearer from the outer lines splitting (approx 4.0 mT) and can be specifically distinguished at 200 K (shown by the #). Traces of formation of C1'(-H) radical can be predicted at 140 K which might also present at 77 K directly after irradiation. Although it cannot be clearly observed at 77 K, but on annealing to 140 K OH addition radical at C6 of the FUdR base is observed. This becomes prominent after 190 K (as indicated by the arrows). The base anions produced at 77 K gets protonated at C6 positions (as observed in the wings) or at O4 positions and can be characterized from the conversion of a well defined doublet to a sharper asymmetric doublet structure and has been already identified in the previous results.

5-Fluoro-2'-deoxyuridine 5'-monophosphate (Na Salt) (FdUMP)

In **Fig. 5.1.15** annealling steps of 380 mM FdUMP in H_2O are shown which was irradiated with about 200 kGy of x- ray. At 77 K the lower field region is dominated by $OH^{\bullet}$ radical trapped in the aqueous matrix produced from the oxidation of water. Anion radical formation on th FdUMP base can be predicted from the doublet pattern of about 2.3 mT width. The high field region on amplification shows ESR signature which might be due to formation of OH (shown by arrow) as well as H addition (shown by #) radicals on C6 position of FdUMP base. Indication for the presence of C1'(-H) radical even at 77 K cannot be ignored (shown by +). On increasing the temperature of the system to 140 K, on magnification of the outer wings both H addition radical and OH addition radical at C6 position of the FdUMP becomes evident. The patterns of these radicals have already been identified in 7M BeF_2/H_2O matrix. With further increase in the temperature these patterns can be clearly noticed. At the centre of the spectrum at 200 K (**Fig. 5.1.15D**) peaks of about 5.7 mT spread becomes more clear which originate from C1'(-H) radical of deoxyribose part of FdUMP. The anion doublet visible at 77 K gets protonated and O4 protonated anion radical pattern takes over the central position of the spectra at higher temperature zone.

Discussion

From the annealing series of neat FUdR and FdUMP in H_2O it can be observed
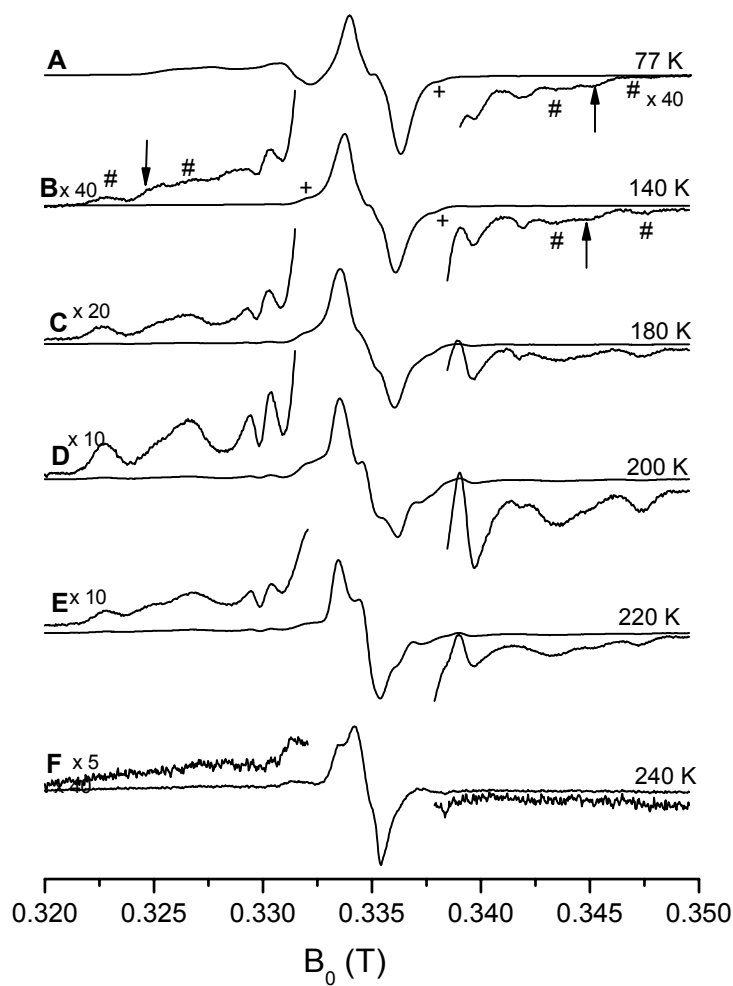
Fig. 5.1.15. ESR spectra obtained from the annealing series of 380 mM FdUMP in frozen aqueous system after irradiation with 20 kGy of x- ray. A) FdUMP at 77 K B) at140 K , C) 180 K, D) 200 K, E) 220 K, F) 240 K.

that at 77 K that the solvated electrons produced during irradiation react instantaneously with the substrates to form base anions which are similar to that found in 7M BeF_2/H_2O matrix. The OH$^•$ radicals are trapped in the matrix just as in BeF_2 glass. The formation of H addition radical at C6 position of nucleotide and nucleoside base was also observed in

the glassy matrix. Considering the direct model of irradiation the expected formation of FU base cation was not observed clearly in both of these FU derivatives. Although in Fig. 5.1.15 A at the right wing triplet pattern comparable to FU base cation was observed but a clear identification of this radical was not possible in the conditions applied here. But other evidences of oxidized radical formation at 77 K in frozen aqueous system were clear. Though there presence were moderately small in magnitude in frozen aqueous solutions but they were completely absent in the 7M BeF_2 glass system. The formation of the oxidized radicals at 77 K in frozen aqueous solution may be a result of direct irradiation. In order to enhance the presence of the oxidized species at 77 K further experiments are done by adding electron scavenging additives to the systems which has been discussed later. Another clear difference which is observed here is that even with the neat substrates the $OH^\bullet$ radical reactions are quite observable at temperature as low as 140 K which is prominent in BeF_2 matrix only after 170 K. Two factors can be responsible for this is that either the OH addition radicals are already formed at 77 K and show up more clearly at 140 K or may be in the ice matrix the presence of the hydrogen bonding scheme triggers the migration of the hole and their deprotonation to form $OH^\bullet$ radical at low temperature . At temperature range of 165-185 K the radical formation in FUdR and FdUMP in both the matrices are similar.

5-Fluoro-2'-deoxyuridine (FUdR) and $K_3Fe[CN]_6$

Fig. 5.1.16 shows the annealing series of a system containing FUdR and $K_3Fe[CN]_6$ in a molar ratio of 1:20 irradiated with a dose of 200 kGy. At 77 K (**Fig. 5.1.16A**) the $OH^\bullet$ radical patterns along with the H addition radical at C6 position of the base in FUdR can be observed. The middle portion of the spectrum shows almost total absence of the doublet pattern which was present in neat FUdR due to the formation of base anion radical. This shows very strong scavenging of the solvated electrons produced during irradiation in the system. A speculation can be made by very closely looking into the spectrum at 77 K that there might be some formation of C1'(-H) radicals at about 5.7 mT (shown by +) splitting and OH addition radical at C6 positon of the base (shown by arrow) due to oxidation process. With annealing the $OH^\bullet$ radical pattern decays and gets liberated from the matrix starts to react with the base moiety as well as with the sugar part of the substrate present in its near vicinity. Both OH addition radical via hydroxylation at 5,6 double bond of halopyriidine base and C1'(-H) radical formation through deprotonation on the sugar part are visible from the spectrum at 140 K. There is

formation of O4 protonated radical at the centre of the spectra which can be more clearly
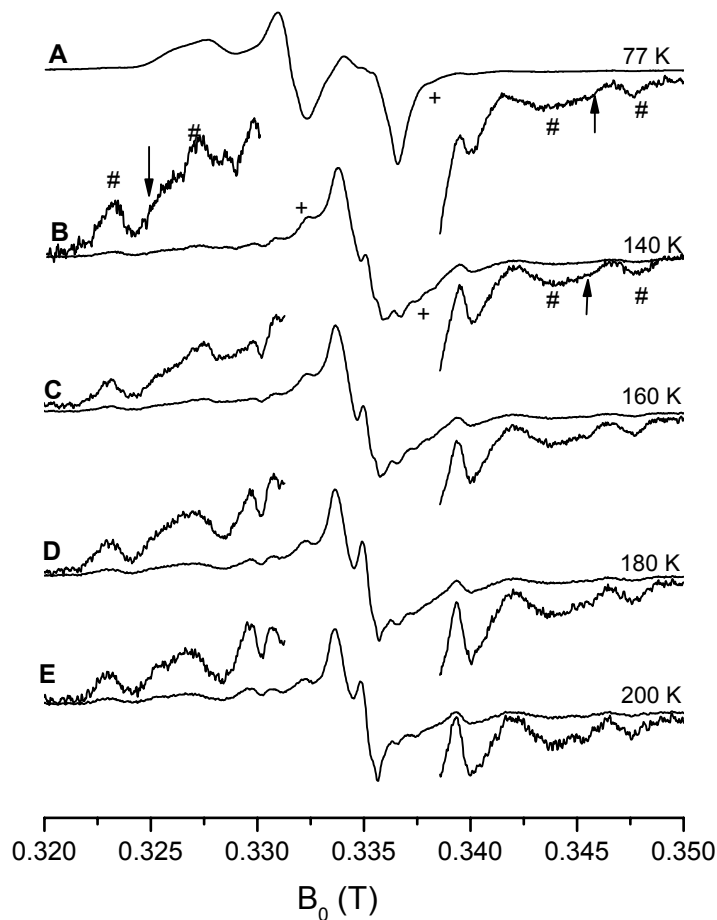
Fig. 5.1.16. ESR spectra obtained from the annealing series of a system containing $K_3Fe[CN]_6$ and FUdR in a molar ratio of 1:20 in frozen aqueous system after irradiation with 200 kGy of x-ray. A) at 77 K B) at140 K , C) 180 K, D) 220 K

followed with increasing temperature. Presence of large concentration of electron scavenger though reduces the formation of anion radicals drastically at 77 K and even if they are formed are instantly protonated to form H addition radical at C6 of FUdR base.

5-Fluoro-2'-deoxyuridine 5'-monophosphate (Na Salt) (FdUMP) and K₃Fe[CN]₆

Fig 5.1.17 represents the ESR spectra obtained by annealing the frozen aqueous sample containing $K_3Fe[CN]_6$ and FdUMP in a molar ratio of 1:20 which was irradiated with a x- ray dose of 200 kGy at 77 K.

It can be observed that at 77 K there is a very clear decrease in building of anion
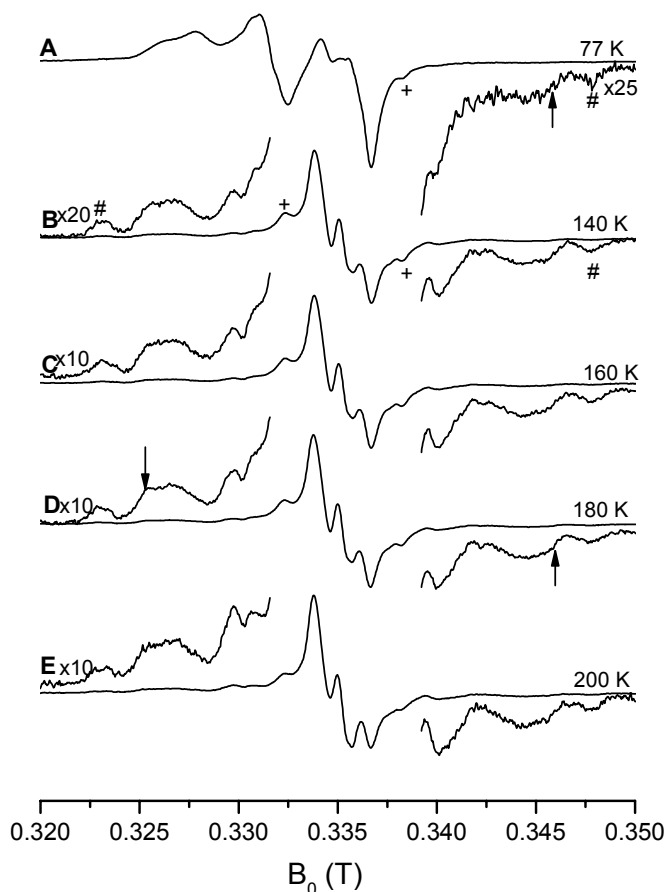
Fig. 5.1.17. ESR spectra obtained from the annealing series of a system containing $K_3Fe[CN]_6$ and FdUMP in a molar ratio of 1:20 in frozen aqueous system after irradiation with 20 kGy of X ray. A) at 77 K B) at140 K , C) 180 K, D) 200 K

radical as an effect of scavenging of the solvated electrons by $K_3Fe[CN]_6$. The OH• radical pattern can be easily detected at the left of the spectrum. The magnification of the high field region of the spectrum indicates again formation of both H• and OH• addition radical at C6 position of the FdUMP base (as shown by the arrow and # sign).

The middle of the spectrum also ensures the formation of C1'(-H) radical which was also traced in minute concentration in neat FdUMP. On raising the temperature of the matrix (> 140 K) and then measuring after re-cooling it to 77 K it can be observed that the H$^\bullet$ and OH$^\bullet$ radicals present in the ice matrix becomes mobile at react with the substrate molecules. With increase in the temperature the formation of O4 protonated anion becomes visible at the middle of the spectra.

Discussion

It can be clearly observed that by with addition of the electrophillic agent K$_3$Fe[CN]$_6$ the reduced species patterns are decreased in both the systems to a great extent. It is noteworthy to mention here that the triplet pattern which was observed at 77 K in irradiated frozen aqueous solution containing FdUMP was not observed anymore in the same system after addition of electron scavenger. To get more precise information about the formation of other oxidized radicals at 77 K under enhanced oxidized conditions, The OH$^\bullet$ radical pattern was subtracted from the spectra of FUdR and FdUMP containing K$_3$Fe[CN]$_6$ as an additive. **Fig. 5.1.18** shows the results of the subtraction, and it can be seen that there is a clear indication of formation of C1'(-H) radical. Though complete subtraction of the OH$^\bullet$ radical was not possible due to its very broad character but the peaks observed at about 8.7 mT appears to be arising from C2'(-H) radicals from the deoxyribose moiety of the nucleotide and nucleoside. Both the isolated radical patterns can be compared with the respective simulated spectra (**Fig. 5.1.18C and D**). The noise in the wings did not help to isolate the OH addition radical at C6 position of the base. In BeF$_2$ however at 77 K no substrate radicals were observed in the presence of very high concentrations of K$_3$Fe[CN]$_6$. With increase in the temperature the spectra obtained in frozen aqueous system from FUdR and FdUMP containing K$_3$Fe[CN]$_6$ the presence of C2'(-H) radical was not as prominent as was found for the same systems in BeF$_2$/H$_2$O matrix. It was not possible to isolate the C2'(-H) radical pattern by mere subtraction of the spectra obtained at different temperatures. Apart from these differences the radial balance and the nature of their decay was almost identical in the BeF$_2$ glass and frozen aqueous matrix.

The formations of OH addition radical at C6 of FUdR /FdUMP base moiety, the C1'(-H) radical and perhaps the C2'(-H) radical at 77 K in frozen aqueous system specifically in the presence of large concentration of electron scavenger shows that direct ionization does takes place on the substrate. The concentration of all these radicals are although very small as the subtracted spectra constitutes less than 30 % (from the DI value calculation) of the experimental spectra and it is also influenced by the presence of other radical patterns and in neat FUdR and FdUMP the main radical
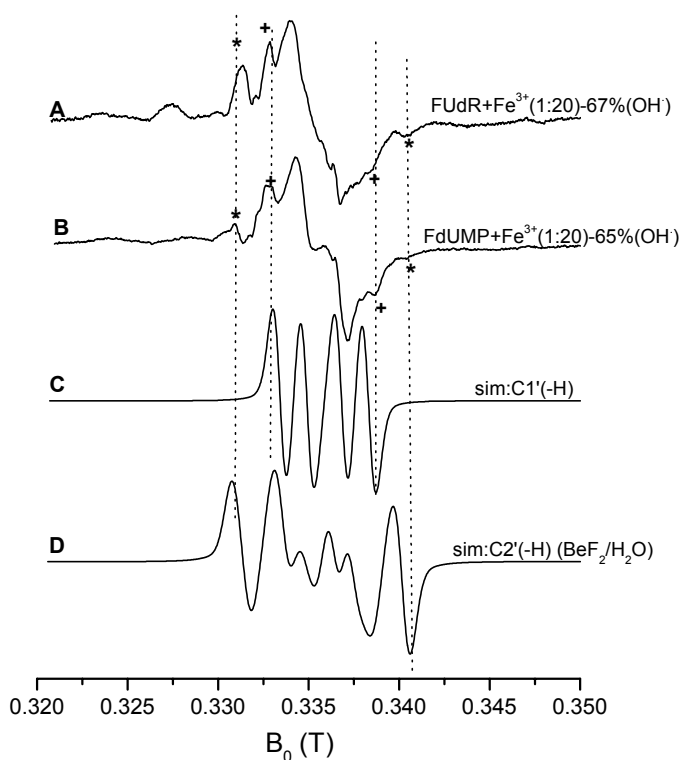
Fig. 5.1.18. A) Resultant pattern obtained after subtraction of 67% of OH radical pattern from that of $K_3Fe[CN]_6$:FUdR (1:20) received at 77 K in frozen aqueous system, Subtraction of 65% of OH radical pattern from the ESR spectrum of $K_3Fe[CN]_6$:FdUMP (1:20) resulted in spectrum B, C) Simulated pattern of C1'(-H) radical, D) Simulated pattern of C2'(-H) radical specific for BeF_2/H_2O glass matrix.

formed on the substrate is unequivocally the base anion. Although the model of direct irradiation proposes formation 50% oxidized radicals which are not the case here but the

undisputed presence of sugar radicals at 77 K specifically in frozen aqueous solutions do emphasize on the oxidation process in frozen aqueous system. Further results obtained by annealing the sample temperature are comparable to those obtained from the study of TMP and Cytosine and its derivatives when they were comparatively studied in both BeF_2 glass and ice matrix (Lange et. al.1995, Weiland et. al. 1996). It is observed in FU and in its derivatives also that the changes in the radical balance via annealing are similar in nature in both glass and frozen aqueous solutions. The scavenging effect of the electron scavengers is identical in both matrices as has been observed before. The sugar radicals formed at 77 K remain unchanged throughout the annealing series. The results obtained from frozen aqueous system containing FUdR and FdUMP along with $K_3Fe[CN]_6$ although did not provide a clear distinction in the FU base cation and OH addition radical at C6 of FU base but it is observed from these studies that the sugar radicals (C1' and perhaps C2') can be formed in FU derivatives at moderate doses by using strong electron scavengers and anaerobic conditions.

Formation of base and sugar radicals in pure and additive containing DNA in frozen aqueous DNA has been reported in the next section of this thesis. The results obtained in DNA are then compared with this model study.

5.2. Frozen Aqueous DNA Solution: Effect of Additives, Dose and Temperature on the Free Radical Formation

Ionizing radiation causes, in principle, indiscriminate damages, as a consequence of which each part of DNA molecule and those present in its environment like all four bases, sugar molecule, phosphate groups and surrounding water molecules in a hydrated or frozen aqueous system should be ionized. However, since DNA allows spin or charge transfer along its double stranded structure during the process of irradiation the final chemical damages are often detected at sites other than the initial ionization points. There have been several studies on the theoretical model and time scale of charge transfer along DNA (Wagenknecht 2005).

ESR spectroscopic studies of DNA in hydrated or frozen aqueous system have offered crucial knowledge about the formation of primary radicals on DNA at 77 K and about secondary radicals after annealing to higher temperatures. Recent reports on this topic mainly analyze the formation of sugar radicals on DNA after treating it with various doses specifically at 77 K (**section 3.1.2**).

Gregoli et. al. 1982 initially reported a two primary component model (guanine cation and thymine anion) for irradiated frozen aqueous DNA via direct irradiation mechanism. Several studies on dry DNA and hydrated DNA systems (Weiland and Hüttermann 1998, Shukla et. al. 2005) have been done since then. The scenario has improved by identification of few other free radicals like cytosine anions, C1' sugar radical but identification and percentage of all the radicals formed on DNA is still incomplete. The use of several electron and hole scavenging additives (Gregoli and Bertinchamps 1970, Boon et. al. 1985, Cullis et. al. 1985, Weiland and Hüttermann 1998) like $K_3Fe[CN]_6$, iodoacetamide, Mitoxantrone and $K_4Fe[CN]_6$ and iIncrease in dose of even low LET irradiation source (Shukla et. all 2005) can induce differences in the radical balance in DNA system at low temperatures. These section is dedicated to the identification of free radical ESR fingerprints in frozen aqueous DNA in pure form or along with electron scavengers like $K_3Fe[CN]_6$, Mitoxantrone (MX) and a hole scavenger like $K_4Fe[CN]_6$) (Shukla et. al. 2005) upon irradiation with different X ray doses. Both $K_3Fe[CN]_6$ and $K_4Fe[CN]_6$ upon irradiation are ESR silent at 77 K and irradiated MX gives very sharp singlet ESR fingerprint which could be easily subtracted from the DNA-

MX spectrum. For simplicity samples containing electron scavenger $K_3Fe[CN]_6$ are given the symbol 'Fe^{3+}/DNA' and for the hole scavenger $K_4Fe[CN]_6$) the form'Fe^{2+}/DNA' is used. The effect of temperature on the change in radical balance has also been studied. This can provide information regarding the stability of free radicals at higher temperatures. The difference of formation of guanine cation radical percentage in frozen aqueous DNA of about 40% vs.12% (Shukla et. al. 2005 and Burger 1999) and also to 7% guanine cation as observed in 76% hydrated (H_2O) DNA (Weiland and Hüttermann 1998) at 140 K is also reinvestigated in this section of the thesis for frozen aqueous DNA. An attempt has been made to disentangle the ESR finger print of group of deoxyribose sugar radicals formed upon irradiation. The question of mechanism of irradiation in frozen aqueous system is again dealt here through observing the formation of oxidized species. This study can therefore be looked upon as an extension of the work shown in **section 5.1** in the model compound fluorouracil and its derivatives where it has been observed that in frozen aqueous system although a clear evidence of base cation radical was not obtained but, specifically in the presence of electron scavengers other oxidized radicals (sugar radicals) were formed at 77 K in both FUdR and FdUMP. Oxidized sugar radicals at 77 K were on the other hand not observed for the same samples in 7 M BeF_2 /H_2O matrix.

5.2.1. Frozen Aqueous DNA: Effect of Electron and Hole Scavenging Additives and of X- Ray Dose

ESR spectra of frozen aqueous (in H_2O) samples of DNA were measured, after X ray irradiation at 77 K, then annealing to 140 K (**Fig. 5.2.1**) and 220 K (**Fig 5.2.2**) and further re-cooling to 77 K. **Fig 5.2.1A** shows the spectrum obtained at 140 K from pure DNA irradiated with 20 kGy which is expected to be consisting of both oxidized and reduced radical species. Along with a 'doublet-singlet mixed' type central region the magnified outer wings shows the presence of octet pattern originating from 5-thymyl radical (TH$^•$) (shown by asterisks) which has been among the first invented as well as undisputed radical in the DNA system (Lenherr and Ormerod 1971). The octet fingerprint becomes very prominent at 220 K as can be seen from **Fig. 5.2.2A**. The spectrum in **Fig. 5.2.1C** originates from DNA containing a very strong electron scavenger $K_3Fe[CN]_6$ in a molar ratio of 1 scavenger molecule per 20 nucleotide molecules (1:10 bp). This sample is expected to have considerably lower percentage of pyrimidine (T/C) one-electron-

reduced radicals than pure DNA. A decreased amount of octet pattern as seen from the magnified wings (and also at higher temperature **Fig. 5.2.2C**) and a predominant loss of doublet character of the spectrum in the central region (shown by an arrow) are observed. The singlet nature of the spectrum can be attributed to the presence of mainly the oxidized radicals like guanine cation also observed in earlier reports (Sevilla and Becker 1994, Weiland and Hüttermann 1998, Shukla et. al. 2005) and/or other neutral radicals.

The spectrum in **Fig. 5.2.1E** results from a sample of DNA in which a hole scavenger $K_4Fe[CN]_6$ has been added at a molar ratio of 1 scavenger to 20 DNA nucleotide molecules. This spectrum shows that the central region is composed of enhanced doublet nature in comparison to pure DNA irradiated with same dose as expected. The enhanced doublet character of the spectrum can be ascribed to be arising from the DNA anion radicals (from thymine and/or cytosine bases) and/or neutral radicals. On annealing this sample to higher temperature **Fig. 5.2.2E** the spectra consists mainly of octet fingerprint of 5-thymyl radical which is a secondary output from thymine anion radical ($T^{-\bullet}$) formed upon H addition to it from nearby water molecules.

Pure DNA, Fe^{3+}:DNA (1:20), Fe^{2+}:DNA (1:20) in H_2O were further subjected to higher irradiation dose to observe the effect of dose in frozen aqueous system. Visual inspection of spectra from **Fig 5.2.1B, D** and **F** shows that a higher dose causes an increase in doublet property of the composite spectrum of DNA at its central position irrespective of the systems used. The central doublet splitting in **B** is 2.5 mT while the similar looking doublet in **D** and **F** shows splitting of approximately 2.8 mT. Similar doublet patterns have been observed earlier in highly oxidized condition in frozen aqueous DNA as well as in hydrated DNA (76%) (Lange et. al. 1995, Weiland and Hüttermann 1998,). As the radical forming this large doublet cannot be scavenged even at higher scavenger concentration and since it is resistant to high radiation doses lead to the speculation that this radical is neutral in nature. Additional peaks (as shown by § and # in **Fig. 5.2.1A** and **B**) becomes more evident with higher dose in all three samples. After annealing to 220 K and then measuring at 77 K (**Fig. 5.2.2B, D, F**) the unnamed peaks (§, #) seems to dominate the total radical balance in the respective samples.
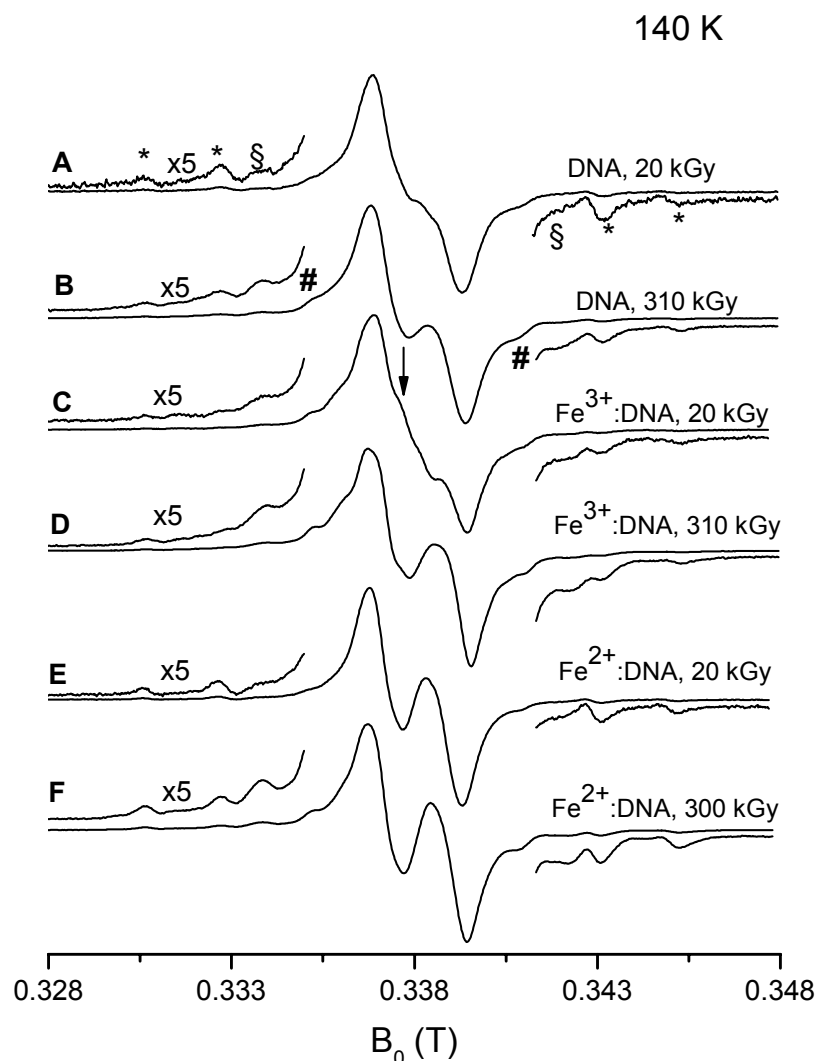
140 K

Fig 5.2.1. ESR spectra of frozen aqueous (H_2O) DNA samples X ray irradiated as indicated. The samples were annealed to 140 K to remove the hydroxyl radical signal and then were recorded at 77 K. The amplification (5 times) of outer wings for each spectrum shows the presence of octet pattern (see text) and other patterns too. (A-B) Neat DNA, (C-D) $K_3Fe(CN)_6$ plus DNA in molar ratio of 1 scavenger molecule per 20 DNA nucleotides, (E-F) $K_4Fe(CN)_6$ plus DNA in ratio 1:20.

All the radical patterns which will be isolated subsequently from different composite experimental spectra obtained at various conditions were already visible after annealing the frozen aqueous DNA (irradiated with moderate dose ~ 50 kGy) to 140 K (see **section 5.2.2**) and then measuring at 77 K. Owing to the overlap of many radical

patterns in a small region of g-factors it was essential to compare the ESR spectra of DNA after they are subjected to different conditions (doses, additives, temperature) and
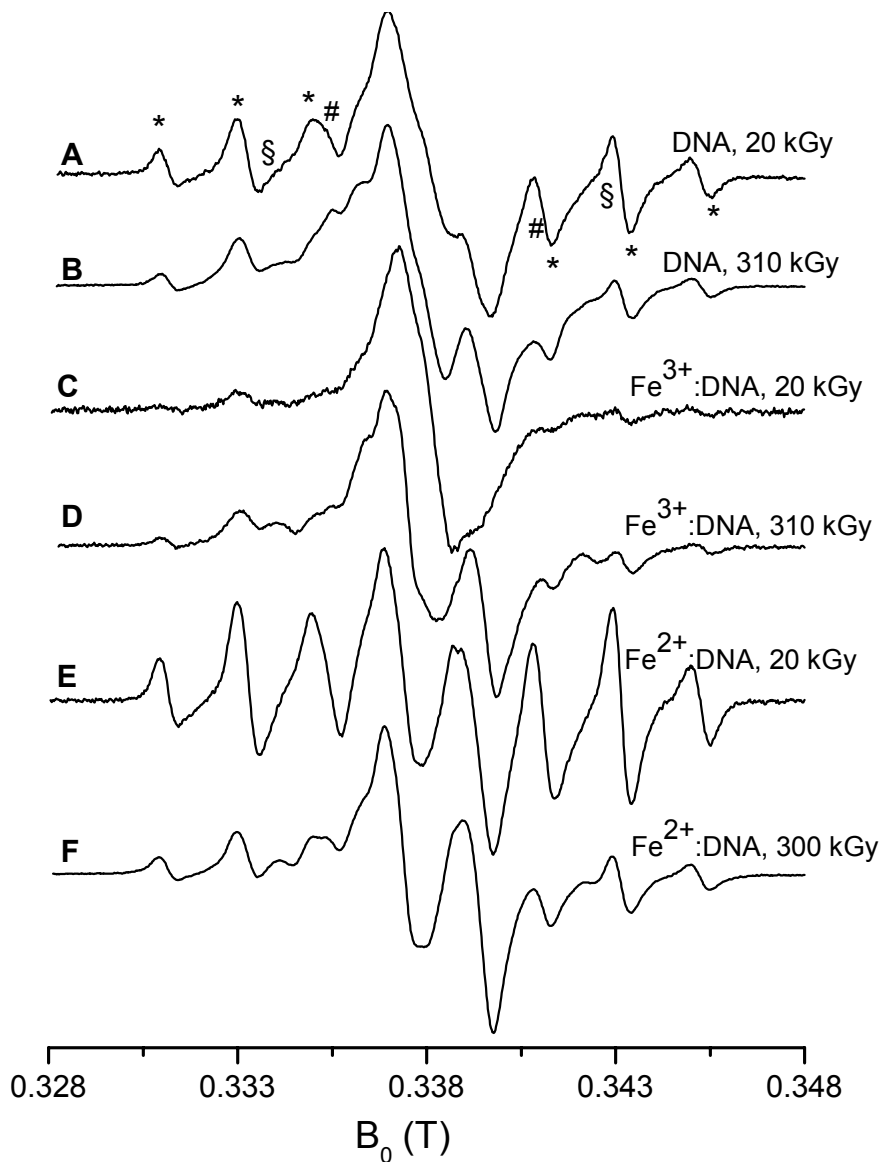
Fig 5.2.2. ESR spectra of frozen aqueous (H2O) DNA samples X ray irradiated as indicated. The samples were annealed to 220 K and then were recorded at 77 K. (A-B) Neat DNA, (C-D) $K_3Fe(CN)_6$ plus DNA in molar ratio of 1 scavenger molecule per 20 DNA nucleotides, (E-F) $K_4Fe(CN)_6$ plus DNA in molar ratio of 1:20.

then isolate the radical patterns (high quality) through spectral subtractions.

The use of selective scavengers in different concentration can modulate the formation of free radicals on DNA and thus provide a helpful direction towards step by step isolation of single radical patterns (Weiland and Hüttermann 1998, Cullis et. al. 1985, Cullis et. al. 1986). Various doses and annealing temperatures can also be used as a tool to disentangle the overlapping patterns of radical spectra produced on irradiated frozen aqueous DNA.

All these conditions were considered while isolation of radical patterns from the experimental spectra. The isolation methods were in most cases optimized to obtain a single component pattern using single step subtraction for noise reduction. Isolated single radical patterns can further be utilized for delineation of the complex experimental DNA spectra obtained at different conditions. Pure DNA radical patterns obtained from hydrated DNA or glass matrices are used for reconstruction of ESR spectra after examining their presence in experimental frozen aqueous spectra.

5.2.2. Isolation of ESR Spectral Components obtained from the DNA Spectra Series

Free Radicals in Aqueous Matrix

Solvated electrons e_{aq}, $H^\bullet$ and $OH^\bullet$ radicals are expected to be formed as a result of radiolysis of water at 77 K. The ESR spectrum of irradiated frozen aqueous DNA at 77 K only shows a broad pattern which arises due to formation $OH^\bullet_{ice}$ (bulk ice) from polycrystalline water molecules as shown in recording A of **Fig 5.2.3**.

This spectrum shows a low-field component near g=2.05 (shown by arrow in **Fig. 5.2.3B**) that corresponds to $g_\parallel$ along with characteristic 45 G doublet near g=2.01 (Brivati et. al. 1965, La Vere et.al.1996, Riederer 1981). Spectrum C and D shows the ESR spectrum of $OD^\bullet$ radical from the frozen aqueous matrix containing DNA with D_2O and only D_2O respectively. The triplet splitting (7 G) as observed in the central region arises due to nuclear spin 1 of the deuterium nucleus. The effect of the DNA hydration shells on ionization of DNA has been intensively studied in previous reports (Sevilla and Becker 1994, Becker et. al. 1994a). The ESR spectra of irradiated frozen aqueous pure DNA consist almost of 70% $OH^\bullet$ when measured at 77 K. The broad feature of $OH^\bullet$/ $OD^\bullet$ makes it difficult to subtract them from composite spectra of DNA at 77 K. These

patterns disappear on annealing the samples to 130 K without significantly disturbing the DNA spectra.

In this section the ESR spectra the samples are first annealed to 140 K and then re-cooled to 77 K and measured to obtain the free radical balance in the samples at low temperatures.

Isolation of Reduced DNA Radical Components at Low Temperature (<200K)

The spectrum containing large amounts of the hole scavenging additive Fe^{2+} ($1Fe^{2+}$ per 20 DNA nucleotides) shows nearly a pure doublet character (**Fig. 5.2.4A=5.2.1E**) in the middle but in order to minimize the presence of outer flanks coming mainly from octet pattern (TH$^\bullet$) (**see next**) another spectrum obtained from Fe^{2+}: DNA (**Fig. 5.2.4B**) has been subtracted from the first after normalization of outer wings. The doublet pattern (**Fig. 5.2.4C**) so obtained still shows presence of some other radical patterns in the outer wings. It was not possible to get rid of these outer lines through further subtraction due to its unchanged behavior with increasing dose at lower temperature. These outer lines are found to be originating from sugar radical patterns (see next). DNA in 7 M $LiBr/H_2O$ upon irradiation with X ray gives an ESR spectrum composed of only reduced species from DNA (combination of C^-/T^-) as the holes formed in the system are trapped at solvent matrix at 77K (**Fig. 5.2.4D**). This spectrum dominantly represents the DNA base radical components containing species reduced by one electron. Comparisons of **Fig. 5.2.4C**. and **5.2.4D** shows nearly identical central region. **Fig. 5.2.4D** is therefore used as a doublet component for the spectral reconstruction (see next sections).

More than one reduced base ions like of cytosine anion $C^{-\bullet}$ / $(C(N3H^+)^-{}^\bullet)$ **Str.5.2.1**) and thymine anion ($T^{-\bullet}$) (**Str.5.2.2)** are probable to form doublet patterns. Separation of this composite pattern into further components was not possible within the scope of this work. A quantitative estimation of each radical in this composite pattern cannot be given.
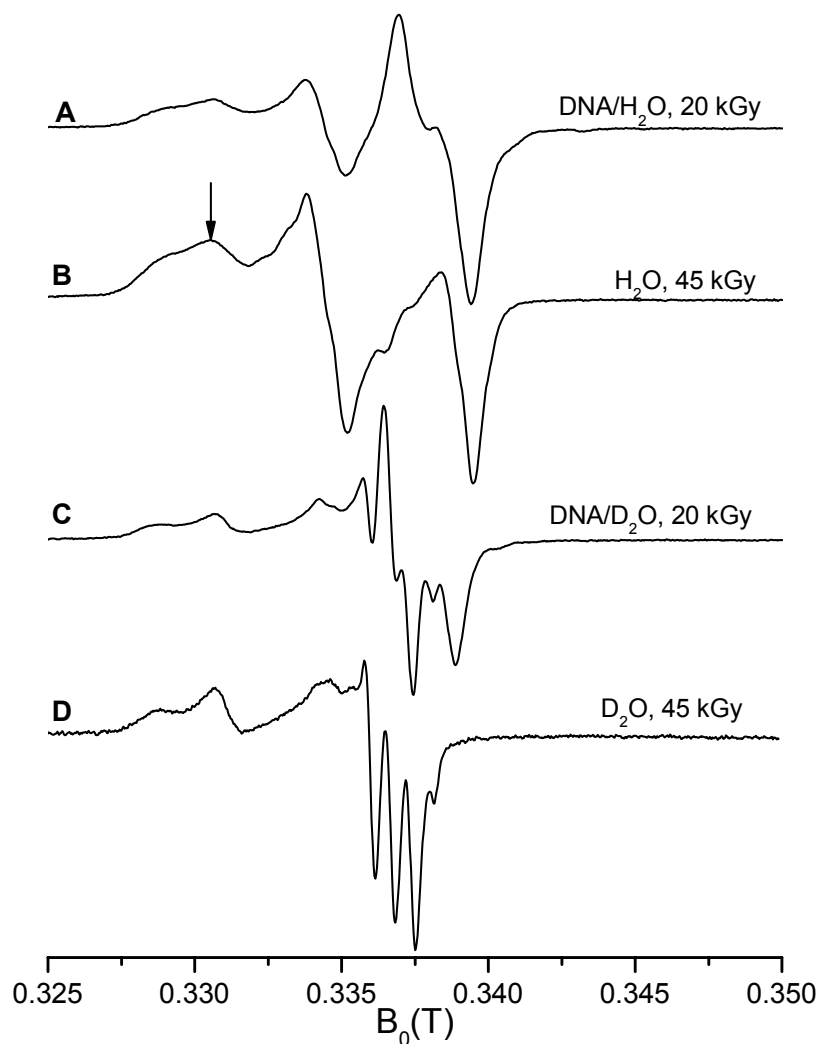
Fig. 5.2.3. ESR spectra of A) DNA/ H_2O (50mg/ml), B) water, C) DNA/ D_2O (50mg/ml), D) Deuterium oxide. All the samples are X irradiated and measured at 77 K.

It is noteworthy to mention here that this doublet pattern is about 2.6 Gauss broader than doublet pattern obtained in dry and hydrated DNA by subtraction of spectra obtained from pure DNA and Fe^{3+}:DNA(1:200) as reported in Weiland and Hüttermann 1998 (**Fig. 5.2.4E**).
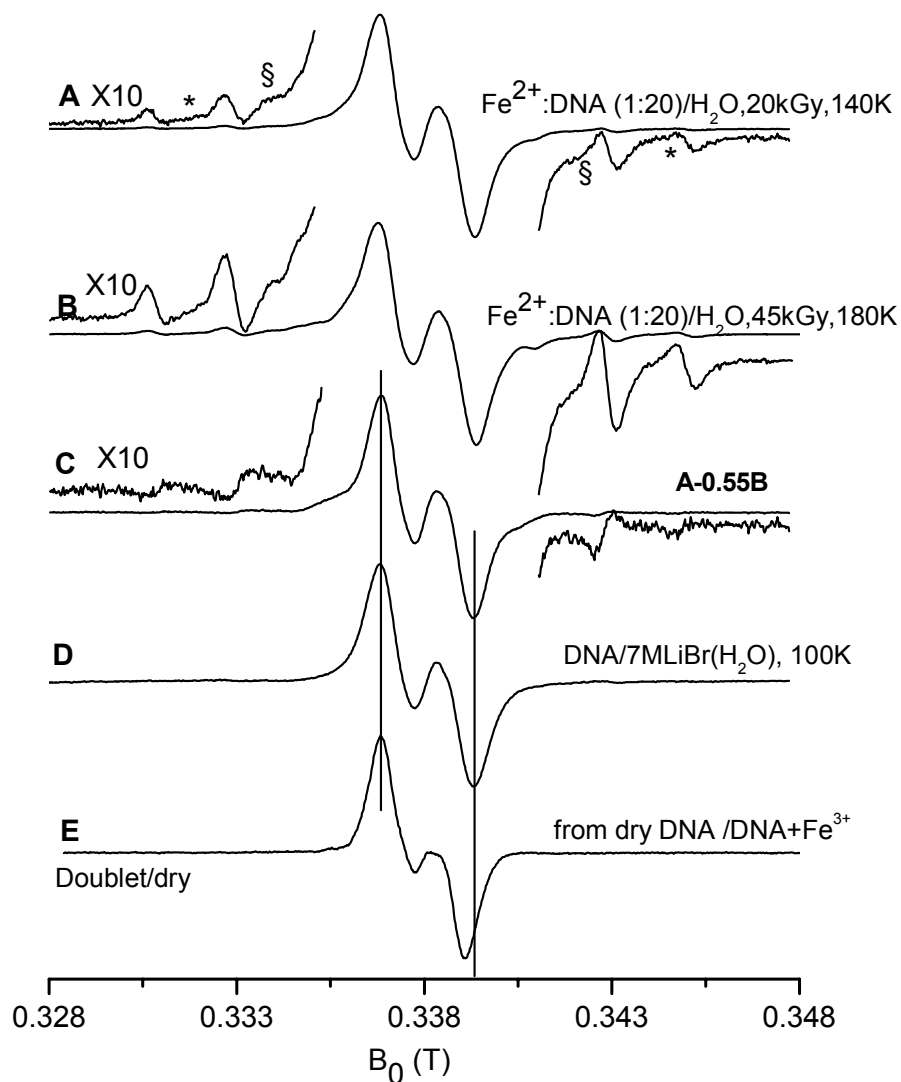
Fig. 5.2.4. Isolation of doublet pattern (C) at low temperature (till 180 K) formed by reduced base ions (T$^-$/C$^-$). This is obtained by subtracting the spectrum of pure DNA (B) from a spectrum of Fe^{2+}:DNA (1:20) (X ray 45 kGy) from (A) Fe^{2+}:DNA (1.20) (X ray 20 kGy) (same as in Fig. 5.2.1.E, for normalization of outer lines. D) Pattern for DNA pyrimidine anions as obtained in 7M LiBr/ H$_2$O matrix where the holes formed after irradiation are trapped by matrix radicals. E) Doublet pattern from the reduced base moieties obtained from lyophllized 'dry' DNA/H$_2$O (Weiland and Hüttermann 1998).

Str. 5.2.1. C$^{-\bullet}$/C(N3H$^+$)$^{-\bullet}$ **Str.5.2.2.** T$^{-\bullet}$
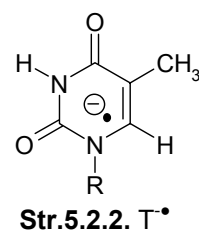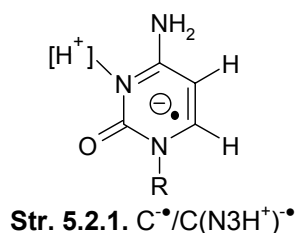
Isolation of Oxidized Radical Components on DNA at Low Temperature

Spectrum in **Fig. 5.2.5A (= Fig. 5.2.1C)** should contain mainly oxidized free radical species on DNA due to the presence of an electron scavenger and therefore can be utilized to isolate oxidized radical pattern formed on DNA. Subtracting a spectrum obtained after higher dose exposure of same system gives a neat singlet structure (**Fig. 5.2.5C**) and cancels the effect caused due to outer flanks (shown by arrows).

This component is nearly identical to **Fig. 5.2.5D** obtained from dry DNA also containing Fe^{3+} as an electron scavenger. This singlet structure is assigned to guanine radical cation (G$^{+\bullet}$) (**Str. 5.2.3**) in dry DNA and in other reports (Sevilla et. al 1991, Yan et. al 1992, Weiland and Hüttermann 1998). This pattern can also be obtained under oxidative conditions in glass matrices (Adhikary et. al. 2005) using dGMP as a substrate. **Fig. 5.2.5C** is used as a component for reconstruction of experimental spectra (See also **Appendix**).

Another component is mainly observed in oxidizing conditions typically in the case when high concentration of Fe^{3+} is used. The isolation of its pattern is shown in **Fig. 5.2.6**. With increase in irradiation dose quantity the doublet character in ESR spectrum frozen aqueous DNA increases. As depicted in **Fig. 5.2.6** subtraction of spectrum **B** from that of **A**, both of which contains equal scavenger concentration (1Fe^{3+} to 20 nucleotide) but were treated with different X ray doses. The subtraction results into a doublet pattern (**Fig. 5.2.6C**) which is broader than the reduced doublet species and has a splitting of approximately 2.8 mT. A similar pattern is also visible when frozen aqueous DNA contains very large scavenger concentration (5 Fe^{3+} to 1nucleotide) and X rayed with moderate dose of 45 kGy (**Fig. 5.2.4D**). **Fig. 5.2.6E** represents an identical pattern which was isolated in hydrated DNA (76%) on irradiation with moderate dose of X ray containing Fe^{3+} as an electron scavenger (Weiland and Hüttermann 1998); it was denoted ''doublet/ox''. In both spectra **Fig. 5.2.6C** and **D** there is apparently some interference from other radicals. Further operations on these spectra result into very

noisy spectra and therefore the doublet/ox pattern from 76% hydrated Fe^{3+}/DNA (**Fig. 5.2.6E**) has been used for spectral reconstructions having shown its unequivocal presence in frozen aqueous DNA. The assignment of this pattern to a certain radical is still not clear (Lange et. al. 1995, Weiland and Hüttermann 1998, Shukla et. al. 2005) although theoretical calculations (Close 1997) predict that both C4'$^\bullet$ or C5'$^\bullet$ sugar radicals can give rise to ESR doublets.
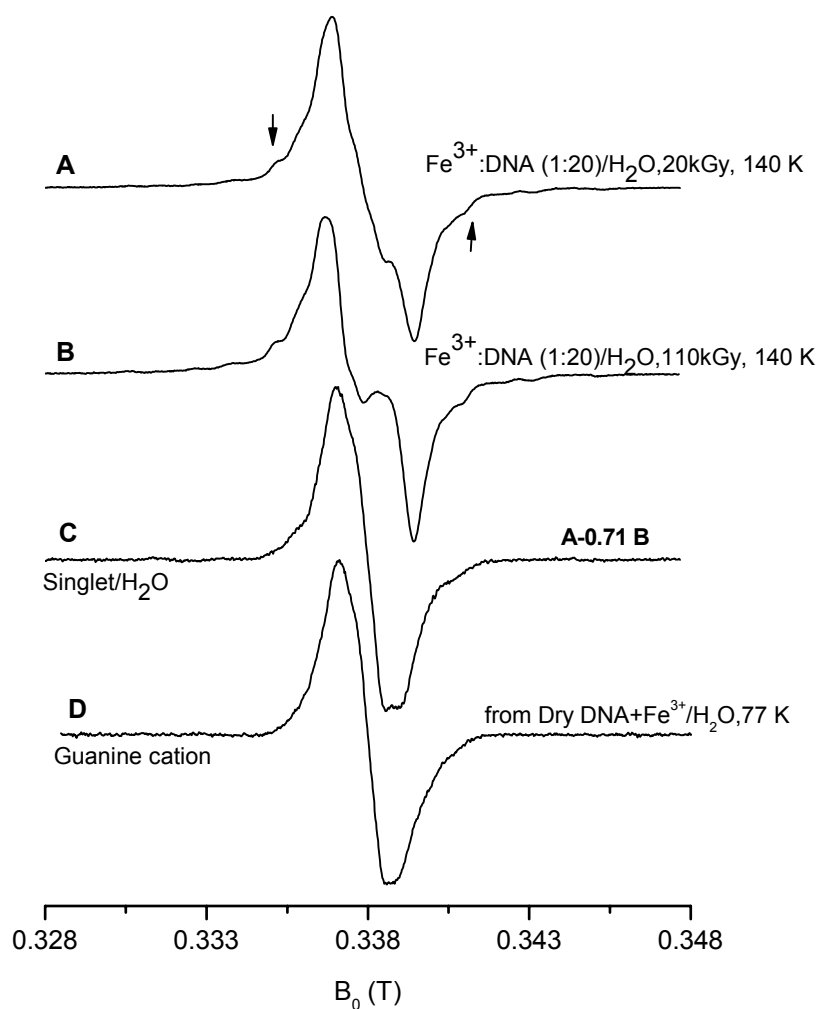
Fig. 5.2.5. Singlet pattern (C) as obtained by subtracting spectrum irradiated for longer period (B) from that of spectrum (A) obtained after low dose irradiation of sample containing electron scavenger in same molar ratio as indicated. D) Singlet pattern obtained in dry DNA +Fe^{3+}/H2O (Weiland and Hüttermann 1998) corresponds to singlet/H_2O (C)

Structures of both C4'$^\bullet$ (**Str. 5.2.4**) and C5'$^\bullet$ (**Str. 5.2.5**) sugar radicals are provided below.
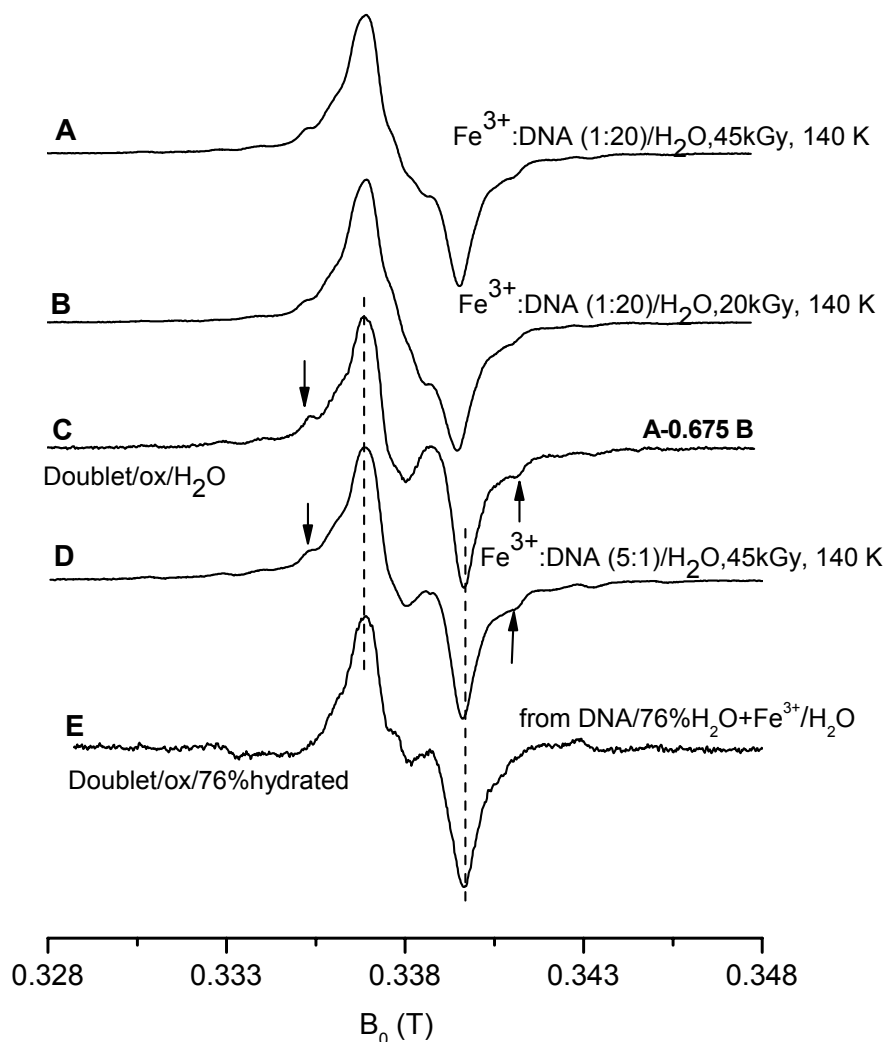
Fig. 5.2.6. Isolation of the ''doublet/ox'' pattern (C) by subtracting a spectrum obtained after X-irradiation of 20 kGy (B) from another which is x-irradiated 45 kGy (A) of frozen aqueous DNA plus $K_3Fe[CN]_6$ as electron scavenger (1Fe^{3*}to 20 nucleotides). The samples where annealed to 140 K and then measured at 77 K. D) X band ESR spectrum obtained after X irradiation of frozen aqueous DNA containing $K_3Fe[CN]_6$ (5Fe^{3+}:1 nucleotide) upon annealing to 140 K and then re cooling. E) Doublet/ox pattern obtained from DNA+Fe^{3+} system in 76% hydrated (H_2O) DNA after X ray irradiation (Weiland and Hüttermann 1998).

125

Isolation of Radical Components of DNA at Higher Temperature (> 200 K)

Further components comes into play in the spectrum obtained by exposing the frozen aqueous samples to higher temperature (200K-260K) and then re-cooling them to 77 K. The typical octet fingerprint of 5-thymyl radical (TH$^\bullet$) (**Str. 5.2.6**) whose minor presence was also observed at upon annealing to 140 K becomes most prominent at temperature above 200 K specially in pure DNA and DNA with hole scavenger $K_4Fe[CN]_6$. This hydrogen adduct species is fully accepted in literature because of its unambiguous ESR spectrum as a result of hyperfine splitting arising from sets of three and two hydrogen atoms with equivalent couplings (20.5 and 40.5 Gauss respectively) and was first observed as early as in 1965 (Pruden et. al. 1965). **Fig. 5.2.7** shows the experimental ESR spectra of pure DNA (X ray 20 kGy) acquired at 260 K which shows a principal presence of octet pattern (outer lines being 14.5mT apart) but as marked by the symbols like asterisk, plus and arrows there seems to be minor influences from some other components. The spectrum obtained from a DNA sample containing $K_4Fe[CN]_6$ (Molar ratio 1Fe^{2+}:20 DNA nucleotide) irradiated with same dose as pure DNA shows almost a pure octet pattern. This pattern has been taken further for spectral reconstruction. This octet pattern is about 2 gauss broader than the pattern which was used in reconstruction of DNA spectra in dry system (Weiland and Hüttermann 1998).

Str. 5.2.3. G$^{+\bullet}$ **Str. 5.2.4.** C4´$^\bullet$ **Str. 5.2.5.** C5´$^\bullet$

Str. 5.2.6. TH$^\bullet$ **Str. 5.2.7.** ROO$^\bullet$
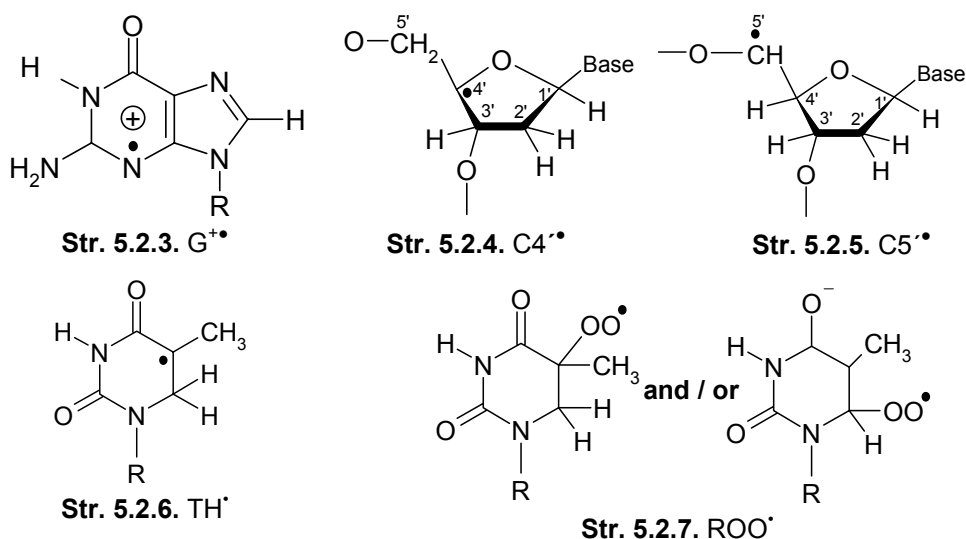
Another component which is present at low annealing temperature only in minute concentration but shows its clear presence at temperatures greater than 200 K is peroxy radical pattern. This pattern is specially observed in frozen aqueous samples prepared

under aerobic condition. **Fig. 5.2.8C** shows the isolated peroxy (ROO$^\bullet$) (**Str. 5.2.7**) component obtained from subtraction of two experimental spectra (190 K-180 K) of pure DNA which was prepared in aerobic condition. On preparation of frozen aqueous samples of DNA in anaerobic glove box the formation of peroxy radical upon irradiation is greatly reduced. Although in frozen aqueous DNA containing Fe^{3+} as an exception where in spite of maintaining anerobic condition ESR finger prints of peroxy radicals are observed on annealing the samples to higher temperatures (220 K).
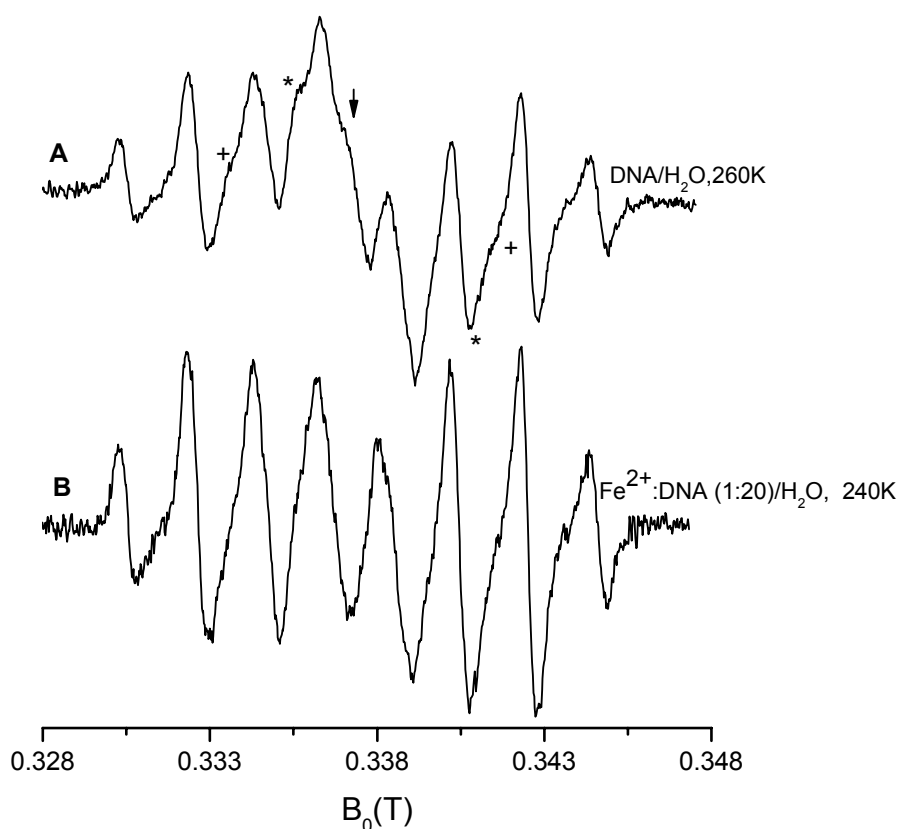
Fig. 5.2.7. X band ESR spectrum of frozen aqueous solution containing A) Pure DNA measured at 77K after being irradiated with X ray dose of 20 kGy and annealed to 260 K. B) $K_4Fe[CN]_6$ plus DNA (1:20) X rayed with 20 kGy and annealed to 240 K and measured at 77 K gives a pure octet fingerprint arising from 5-thymyl radical.

127

Fig. 5.2.8D shows presence of peroxy radical pattern in frozen aqueous sample of Fe^{3+}:DNA (1:20) irradiated with high dose of X ray on annealing up to 240 K before measuring at 77 K. Spectrum **5.2.8C** is considered as a component for spectral reconstruction owing to its noise free character.
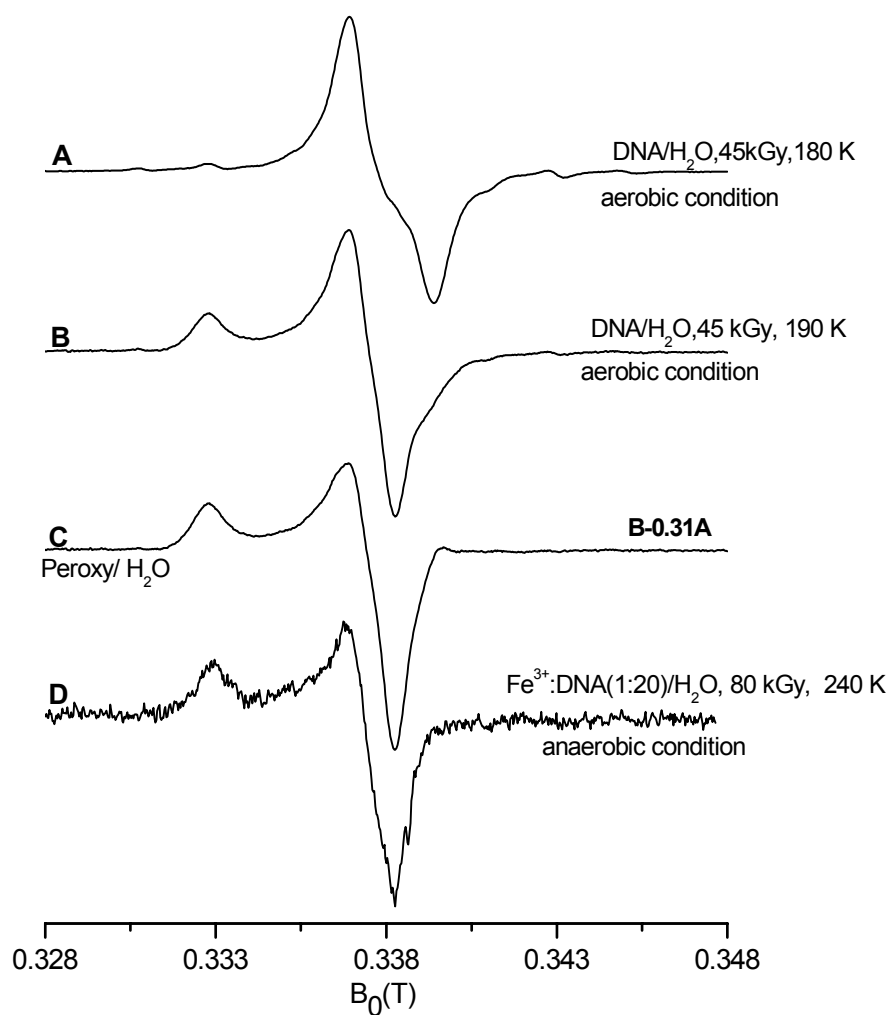
Fig. 5.2.8. Electron spin resonance spectra of frozen aqueous sample taken at 77 K of A) and B) Neat DNA dissolved in water under aerobic condition on irradiated and annealed as indicated. C) Isolated peroxy radical from subtraction and outer line normalization of B and A. D) Peroxy radical formation in frozen aqueous Fe^{3+}: DNA (1:20) sample in spite of its preparation inside an anoxic tent.

Isolation of DNA Radical Components at very High Dose and High Temperature

Fig. 5.2.9 shows the isolation of another pattern from annealing series of DNA irradiated with very high dose of 870 kGy. By subtraction of two spectra at temperatures 220 and 240 K (A and B) and then further subtracting the peroxy radical pattern from the resultant spectrum gives a quartet pattern (C) which can be treated as a single component. Quartet patterns obtained from hydrated DNA (95%) (D) and from dry DNA containing Fe^{3+} as an electron scavenger (E) are also shown in the figure for comparison. The quartet pattern from dry system is a mixture of two components but its outer lines matches with the quartet pattern found in frozen aqueous system. Quartet pattern of width 5.7mT arises from C1'$^{\bullet}$ sugar radical (**Str. 5.2.8**) formed due to dehydrogenation of sugar moiety and has been previously reported in model compounds irradiated in glass or frozen aqueous matrices (Malone et. al. 1995, Weiland et. al. 1996, Wang and Sevilla 1994b), in dry DNA containing electron scavengers (Weiland and Hüttermann 1998) and in frozen aqueous system after UV illumination of the γ-irradiated DNA (Shukla et. al 2004)

Fig 5.2.10 shows that subtraction of two ESR spectra obtained after annealing of DNA/H_2O to 240 K (A) and 260 K (B) irradiated with a dose of 870 kGy gives a pattern (E) the outer portion of which can be well correlated with allyl radical signature known from model compounds and from other studies with DNA (Hüttermann 1970, Hüttermann et. al. 1992a, 1992b, Malone et. al. 1993, Weiland and Hüttermann 1998). The central region of spectrum E as denoted by * is not well resolved. In order to get a better resolution the same experiment was performed by lyophilized DNA with D_2O and then solving 50 mg DNA in 1ml D_2O. The irradiation dose was 730 kGy. The samples were allowed to anneal to different temperatures and then re-cooled to 77 K for ESR measurements. Spectrum F shows a well resolved allyl radical (**Str. 5.2.9**) pattern after subtraction of spectra obtained at 260 and 270 K. This allyl/D_2O can be compared with that obtained from colyophilized DNA+Fe^{3+}/H_2O in dry system (**Fig. 5.2.10F**) (Weiland and Hüttermann 1998).
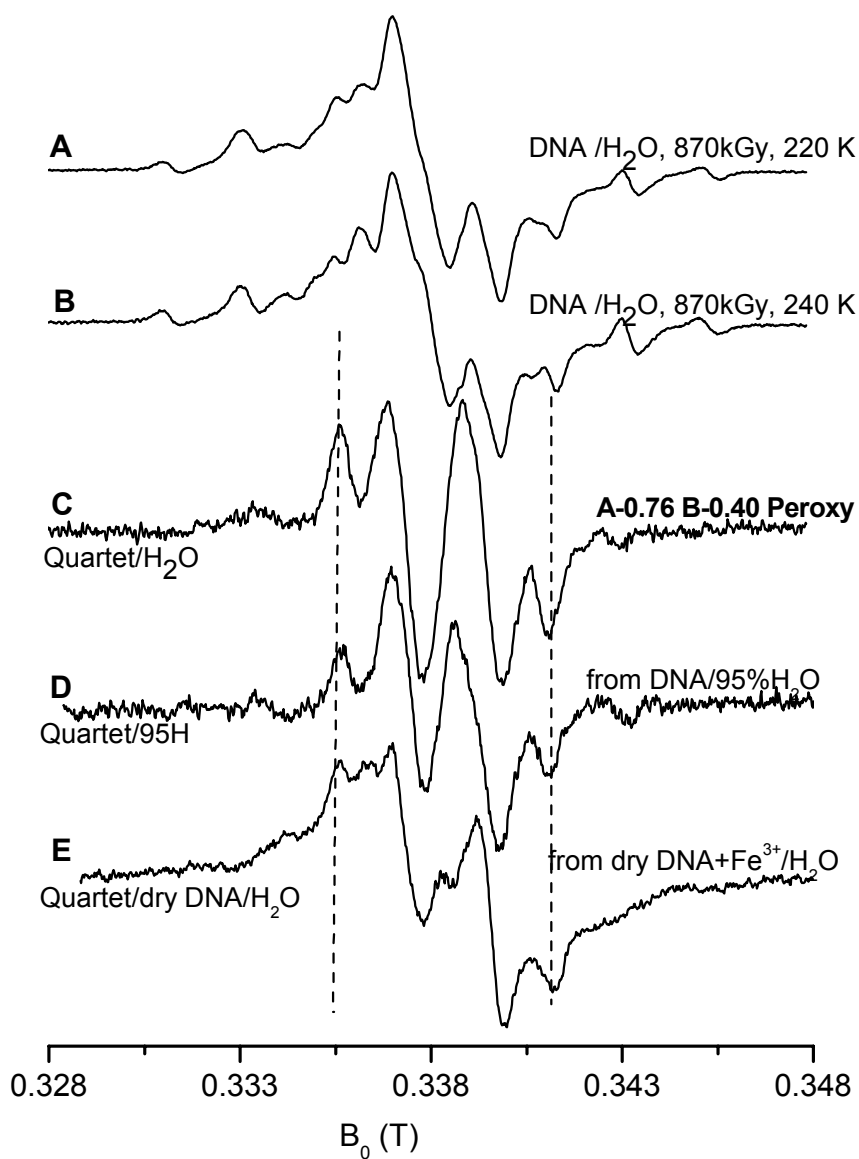
Fig. 5.2.9. Isolation of Quartet/ H_2O pattern (C) from subtraction of two spectra of pure DNA obtained upon annealing to temperatures 220 (A) and 240 K (B) and then re cooling to 77 K, (irradiation with 870 kGY of X ray), peroxy radical pattern was then subtracted from the resultant spectrum. D) Quartet pattern as obtained from 95% hydrated (56 H_2O/base pair) of pure DNA (Weiland 1999). E) Quartet pattern as obtained from colyophillized DNA and Fe^{3+}/H_2O (Dry state) (Weiland and Hüttermann 1998).
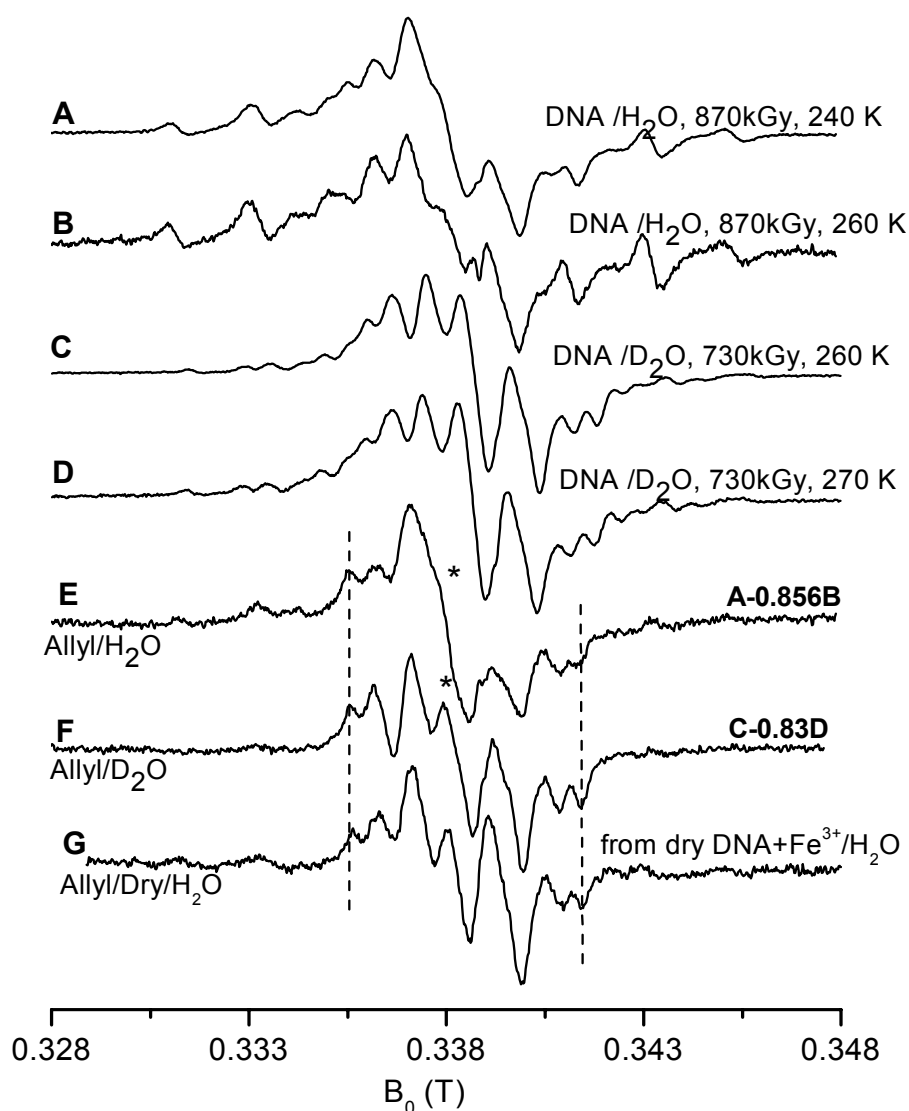
Fig. 5.2.10. Allyl radical like pattern (E) isolated by subtraction of 260 K spectrum (B) from that of 240 K (A) from pure DNA/ H_2O after irradiation with X ray of 870 kGY. To increase the resolution at the central portion (*) pure DNA lyophillized in D_2O has been irradiated with 730 kGY and on subtraction of ESR spectra obtained after annealing to higher temperatures 260 K and 270 K (C, D) Allyl/D_2O radical pattern (F) is obtained. G) Allyl radical pattern obtained from electron scavenger containing colyophilliszed DNA/H_2O (dry) after irradiating with moderate dose and annealing to 300 K (Weiland and Hüttermann 1998)

A minor indication of still another pattern is obtained even after irradiation of pure DNA for 20 kGy but this pattern could only be extracted at very high doses and at higher temperature like 240 K.
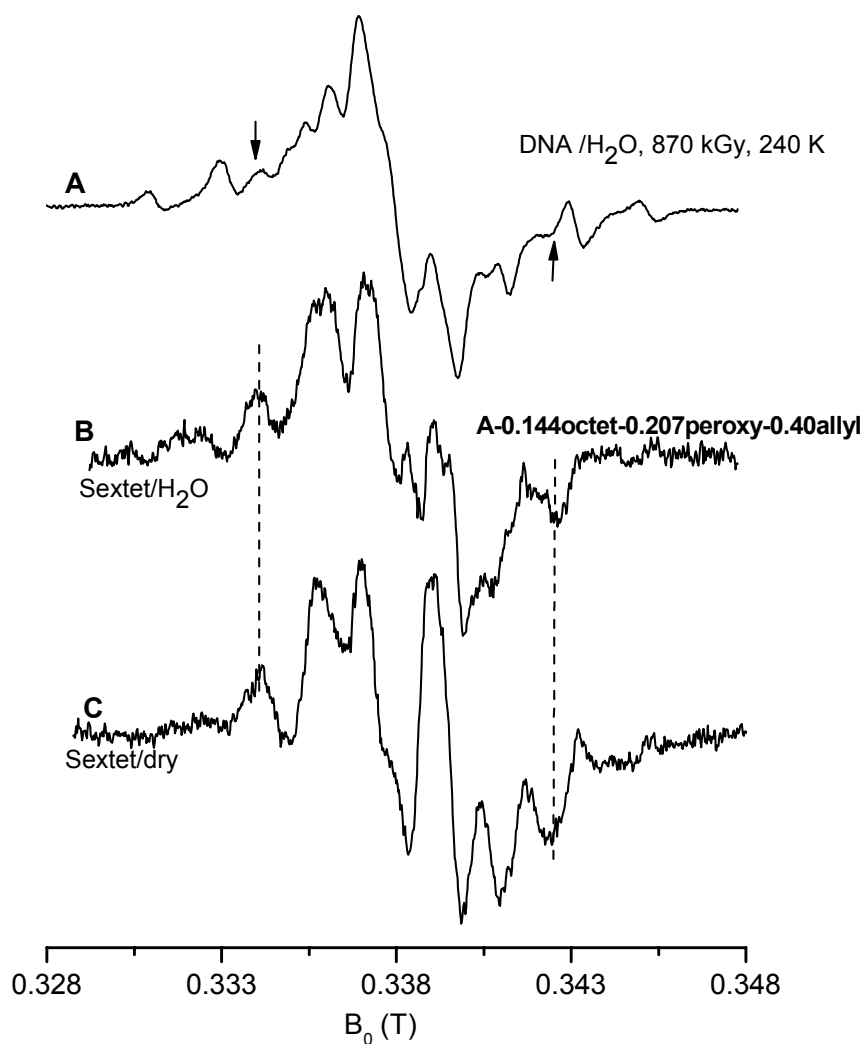
Fig. 5.2.11. Isolation of Sextet/ H_2O pattern (B) from subtraction octet, peroxy and allyl radical patterns from a spectrum of pure DNA obtained after X ray irradiation of 870 kGy and upon annealing to temperature 240 K (A). C) Sextet pattern obtained in dry DNA/H_2O (Weiland and Hüttermann 1998).

This pattern has total splitting of approximately 8.6 mT (peak to peak). In **Fig. 5.2.11** it has been shown by arrows in spectrum A. On subtraction of octet, peroxy and
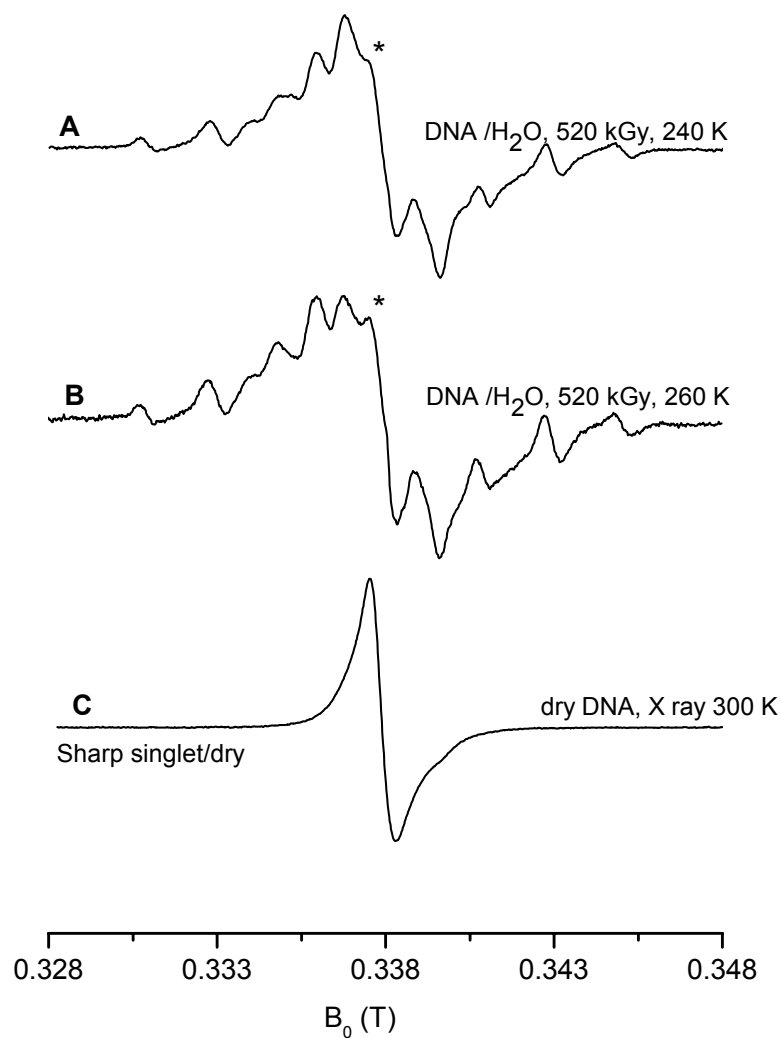
Fig. 5.2.12. Probable evidence of sharp singlet in ESR spectra (A-B) from frozen aqueous pure DNA, X ray irradiated for 520 kGy (shown by *) at 77 K and measured at same temperature after annealing to the given temperatures as compared to the sharp singlet pattern obtained from pure and lyophilized DNA/H_2O (dry) (Weiland and Hüttermann 1998) irradiated at room temperature and measured at 77 K .

allyl patterns from this spectrum a sextet structure is obtained which can be treated as a single component pattern (B). It closely resembles the sextet pattern tentatively assigned to the radical at the C3' or C4' position of the deoxyribose moiety obtained in dry DNA under high dose conditions (C) (Weiland and Hüttermann 1998) and on irradiation of dry DNA with heavy ions (Weiland and Hüttermann 1999). Similar pattern was also found in cytosine containing nuleosides and nucleotides (Malone et. al. 1995, Weiland et. al. 1996), in dGMP (Shukla et. al. 2004, Adhikary et. al.2005). In Shukla et al. 2005 the authors confirms this pattern to be originating from C3'• (**Str. 5.2.10**) or C4'• radical from H abstraction of sugar moieties.

One further component may come into play in the annealing series specifically in pure DNA irradiated treated with higher doses (>250 kGy) and on annealing above 220 K (**Fig. 5.2.12**) which is comparable with the ESR pattern of dry DNA obtained after irradiation at room temperature. This feature is called sharp singlet and has been correlated to radical N1-deprotonated radical cation from guanine (GN•) (**Str. 5.2.11**) in earlier works done with single crystals and powder spectra of dry DNA (Hüttermann and Voit 1987, Weiland and Hüttermann 1998).

Str. 5.2.8. C1'•

Str. 5.2.9. TCH$_2$•

Str. 5.2.10. C3'•

Str. 5.2.11. GN•

Str. 5.2.12. C3'•$_{dephos}$

Str. 5.2.13. C(N4H$^+$)•$^-$
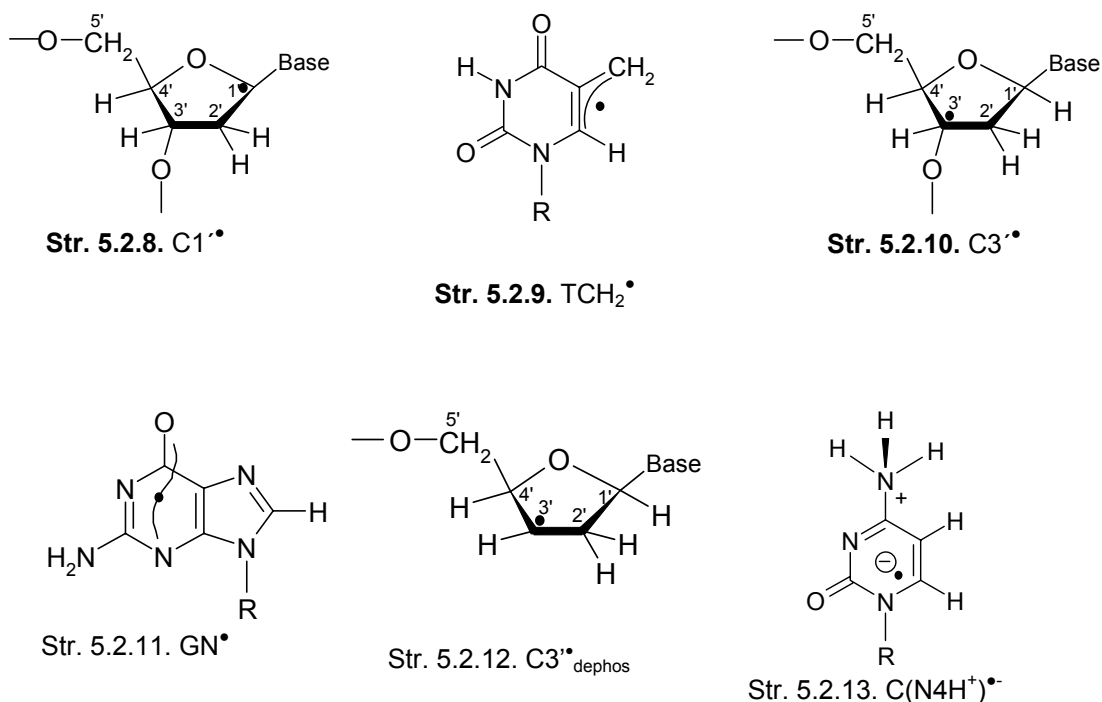
The process of isolation of the radical patterns from the composite experimental patterns is similar as has been done in previous reports e.g., Weiland and Hüttermann 1998. In frozen aqueous solution radical patterns like 'singlet' from guanine cation, 'sextet' from C3' or C4' sugar radicals, doublet/ox pattern tentatively from C4' or C5' sugar radicals and pattern from peroxy radical strongly similar to those found for irradiated dry or hydrated DNA systems. Other patterns like 'doublet' is originating from $C^{-\bullet}/(C(N3H^+)^{-\bullet})$ or $T^{-\bullet}$ and octet pattern from $TH^\bullet$ have different spectral width in frozen aqueous solutions. In this work the quartet pattern from C1' sugar radical and that of the allyl radical were separated in contrast to the combined 'Quartet' (C1' sugar radical and allyl radical) pattern used for the reconstruction of dry and 76% hydrated DNA (Weiland and Hüttermann 1998) and frozen aqueous DNA (Burger 1999). The two radical patterns used in their pure form for the reconstruction of the DNA spectra in this thesis.

It is necessary to mention here that in Shukla et. al. (2005) a broad sextet pattern is observed on irradiation of hydrated DNA with high doses. The outer components were 13.4 mT apart. This radical pattern was denoted to $C3"^\bullet_{dephos}$ radical (**Str. 5.2.12**) with four proton hyperfine coupling. This radical pattern could not be observed here in this thesis is spite of using very high doses of irradiation. This pattern is therefore not used for the reconstruction of the experimental spectra. A phosphate radical of the type $ROPO_2^{-\bullet}$ with very broad character was visible on irradiation of hydrated DNA with heavy ions like oxygen-ion (becker et. al. 1996) or argon –ion (Becker et. al. 2003) was not observed in this work.

In the report on lyophilized dry/H_2O and hydrated DNA H_2O by Weiland and Hüttermann 1998 one another pattern was used originating from $C(N4H^+)^{\bullet-}$ (**Str. 5.2.13**) which gives a 'triplet' fingerprint as shown in **Fig. 5.2.13** and contributed to about 10% to the total radical reconstruction for DNA. This pattern was also observed in frozen aqueous solution of 2' deoxycytidine 5'-monophosphate (dCMP) plus cysteamine (RSH) in H_2O after irradiation at 77 K and annealing to 140 K (Przybytniak et. al 1997). Shukla and coworkers (2005) did not consider this pattern since their work was in D_2O.

In this study of DNA in frozen aqueous solution this triplet pattern could not be isolated from the ESR spectra of frozen aqueous DNA by single step subtraction. The presence of triplet pattern could not be traced from the experimental spectra as could be done for doublet/ox pattern. Doublet/ox pattern could not be isolated from the
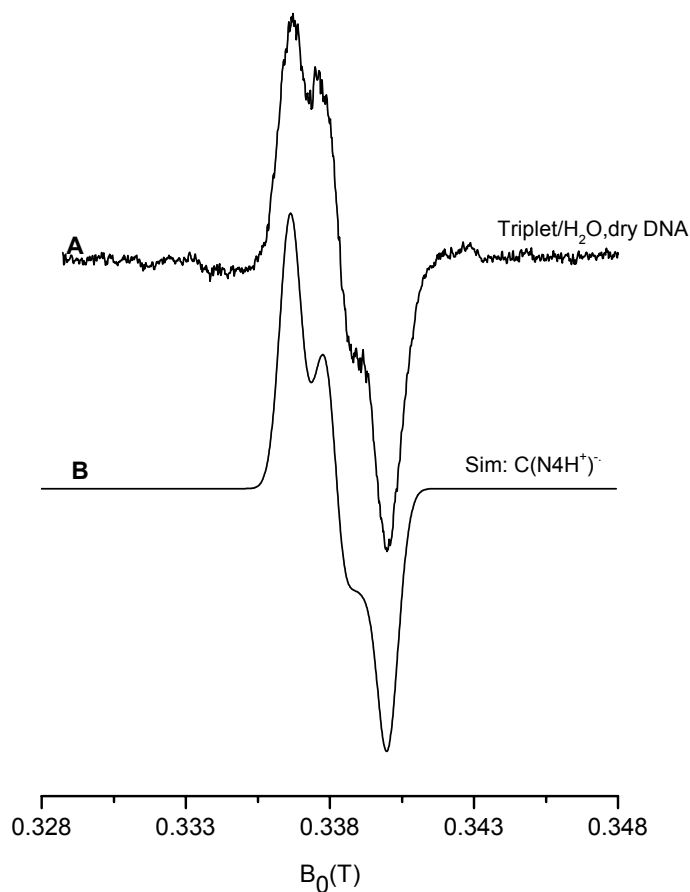
Fig. 5.2.13. A) Isolated pattern of 'triplet' from subtractions of experimental spectra of DNA (dry), B) Simulated triplet spectrum where A (mT) (x, y, and z) for H (C6) (-2.26, -0.73, -0.118), for N3 (0, 0, 0.44), for (N7 (0, 0, 0.5), for H (N7) (0.9, 0.9, 0.9), Line width (mT) (0.7, 0.7, 0.7) and g values are 2.0013, 2.00353 and 2.00237 respectively (Adapted from .Weiland 1999)

experiments but its clear presence could be traced in high scavenger concentration (DNA:K_3Fe[CN]$_6$ /5:1) or from subtraction of two spectra obtained after irradiation with two different doses at 140 K (**Fig. 5.2.6**).

In **Fig.5.2.14** the spectrum of pure DNA in H_2O is compared with those of pyrimidine nucleotides dCMP and CMP. It is found that the triplet character is reduced in the cytosine system if dCMP is considered, while in CMP the triplet pattern is prominent. The spectrum of DNA also shows more similarity with pure TMP (**Fig. 5.2.14D**) pattern obtained in aqueous medium, as far as the doublet hyperfine splitting is concerned.

In glass (7 MLiBr/H_2O) system also it can be observed that in pure DNA spectrum is doublet character is very prominent (arising both from $C^{-\bullet}/C(N3H^+)^{-\bullet}$) or $T^{-\bullet}$ and not
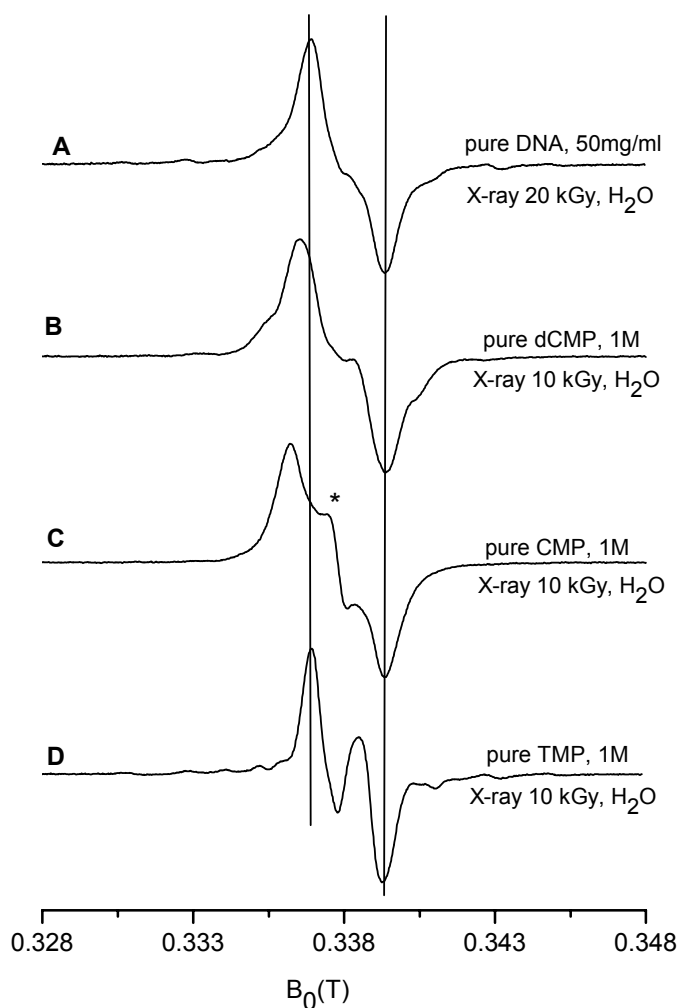
Fig. 5.2.14. ESR spectra of A) pure DNA in frozen aqueous system,B) dCMP, C) CMP and D) TMP in frozen aqueous solution measured at 77 K after annealing to 140 K. (Weiland 1999)

clue for the presence of triplet pattern (from $CN4H^+)^{\bullet-}$ is observed (as in Fig. 5.2.15B). Here also the doublet hyperfine splitting of pure DNA is comparable with the doublet pattern from pure TMP (Fig. 5.2.15C) in 7M LiBr/H_2O and no triplet character is observed in the DNA spectrum.

Considering these facts the triplet pattern has not been used in the reconstruction of the experimental spectra of pure DNA and DNA plus additive complexes in frozen aqueous solution in contrast to reconstruction in the respective reports (Burger 1999, Weiland and Hüttermann 1998).
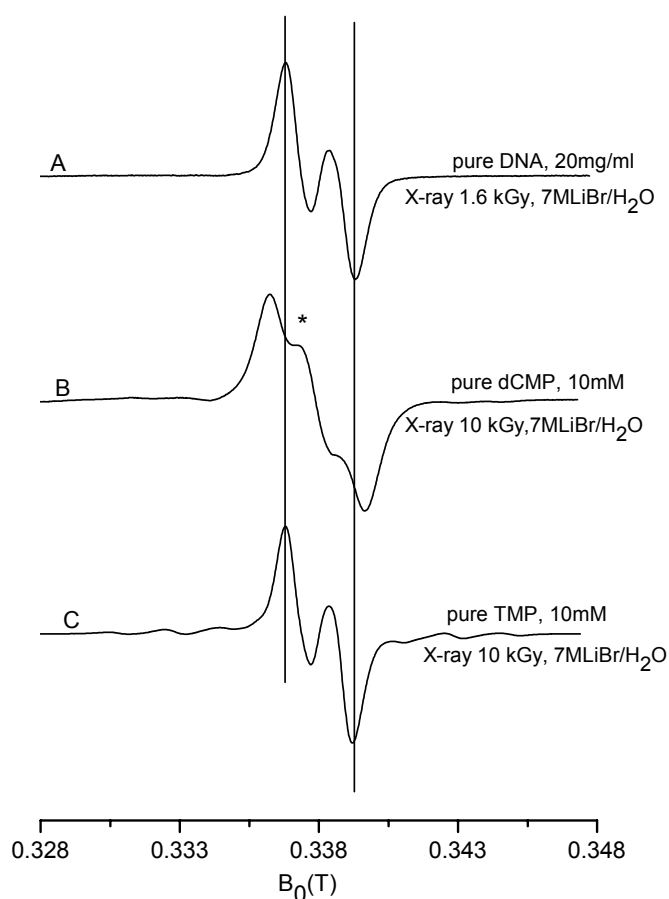
Fig. 5.2.15. ESR spectra of A) pure DNA, B) dCMP and C) TMP in frozen glass solution at 77 K.

The similarity between the ESR spectra of irradiated pure DNA in frozen aqueous and frozen glass system upon with those of pure TMP in identical matrices is clearly visible. It might be possible that thymine anions are present in major proportions in comparison to cytosine anion or N3 protonated cytosine anion in frozen aqueous or frozen glass DNA upon irradiation with low doses but a stringent quantitative analysis of this statement is not possible with the available results.

These isolated radical patterns are further used to reconstruct the ESR spectra obtained from measurement of pure DNA or DNA–additive systems in frozen aqueous matrix at different doses and temperatures (140 K onwards) conditions by using software known as APOLLO (Dusemund 1999). A general least-squares method was employed for analyzing the component contribution to composite DNA spectra, this involved solving the normal equations of the system by means of Gauß-Jordon elimination (Press et. al. 1992). The resulting weight of individual components (normalized to their respective double integrals) was used to produce reconstructed spectra (**See section 4.5.1**). With this process the relative percentage of each radical component present in a specific experimental spectrum can be calculated. Numerical contributions of temperature dependant radical components of ESR spectra from DNA under different dose conditions were normalized to total radical concentration at 140 K.

5.2.3. Effect of Increasing Dose and Temperature on the Radicals formed in Frozen Aqueous DNA/H$_2$O as Analyzed by Spectral Reconstruction

The spectral differences as observed in pure DNA after irradiation with low and high doses and at different temperatures (**Fig. 5.2.1 and Fig. 5.2.2**) can by analyzed by deriving the relative contributions of the components through reconstruction of the experimental spectra. The component patterns isolated in **section 5.2.2** are used for the reconstruction of the spectra. The relative contribution of each component has been portrayed in **Fig. 5.2.16** for annealing series of pure DNA from 140 K onwards after x - irradiation with 20 k Gy (A) or 310 k Gy(B). More than 70% of the total radicals stabilized at 77 K decays after annealing the samples to 240 K irrespective of the dose quantity. The contribution of singlet pattern denoted for G$^{+\bullet}$ almost reduces to half at 140 K when irradiation dose increases from 20 kGy to 310 kGy which explains the increase in doublet character in ESR spectra in **Fig.5.2.1A and B**.
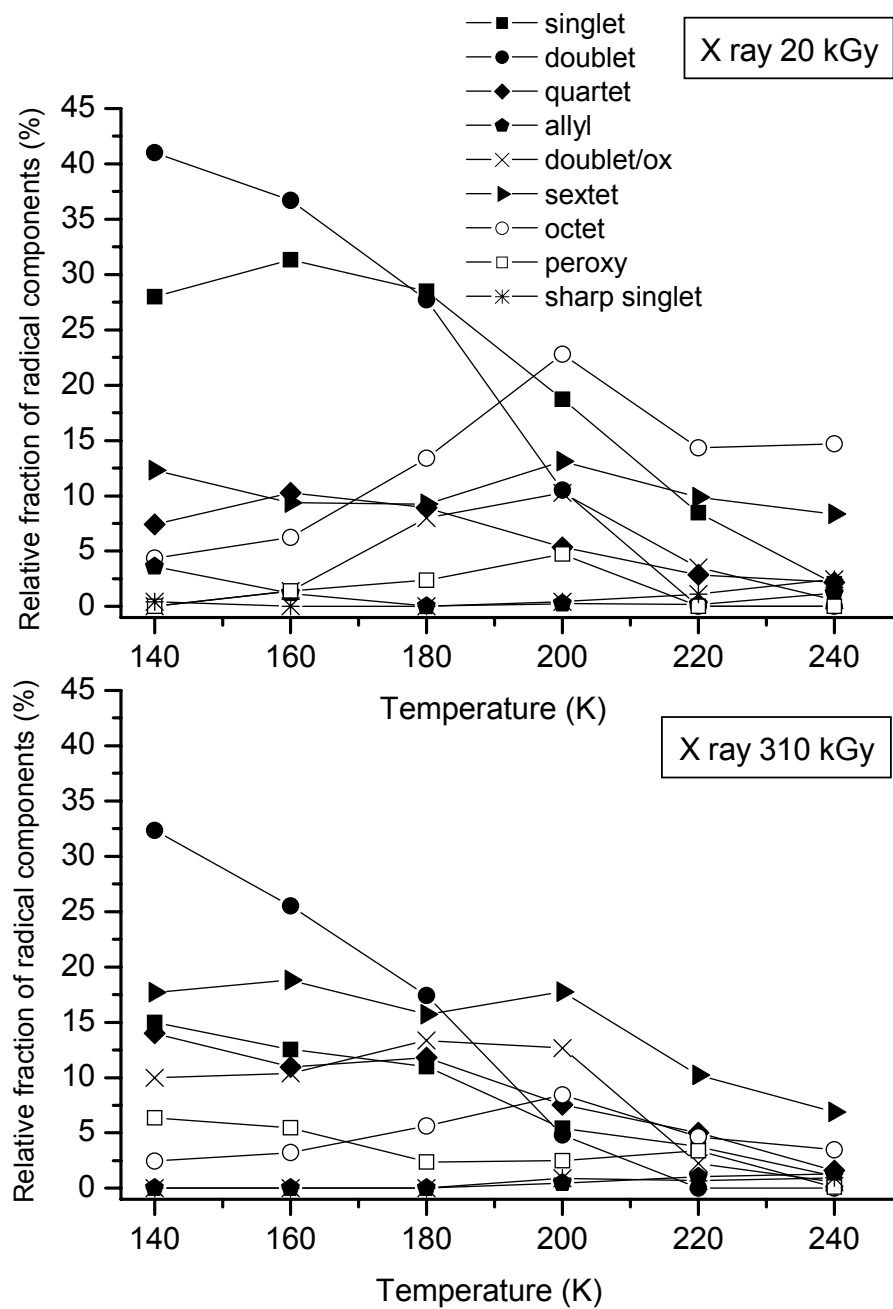
Fig. 5.2.16. The result of reconstruction of experimental spectra of irradiated frozen aqueous DNA (H$_2$O) by resolving set of linear equations for nine distinct components, denoted singlet, doublet, quartet, allyl, doublet/ox, sextet, octet, peroxy and sharp singlet (y axis) against temperature (x axis) for two different X ray doses A) 20 kGY and B) 310 kGy.

The doublet pattern arising from reduced species constitutes about 40% of 140 K spectrum in **Fig. 5.2.16A** but decreases by 7% with increasing dose. Radicals giving quartet and sextet patterns increase their presence with increase in dose from 10% to 15%. The peroxy, allyl and sharp singlet patterns are present in both cases in minute concentrations. The singlet and doublet component decays very steeply with temperature in both low and high dose conditions while the quartet, sextet components remains almost constant till 200 K and then decays. The doublet/ox component starts building up from 0% at 140 K to 10 % at 200 K in low dose irradiated DNA but is found to present at a stable concentration of 10% from 140K-200K in DNA treated with high dose. The octet pattern (TH$^\bullet$) shows its increase with temperature which is related with the estimated fall of doublet signal arising from T$^{-\bullet}$. A total decrease in octet contribution in 310 kGy irradiated system confirms the decreased formation of T$^{-\bullet}$ at 77 K also.

Fig. 5.2.17, 5.2.18 and 5.2.19 gives five sets of ESR spectra of pure DNA x-irradiated at 77 K with different doses then annealed to 140 K, 200 K and 240 K respectively before ESR measurement at 77 K along with their reconstructions from the above mentioned radical patterns. The numbers given for the reconstructed spectra represent the goodness-of-fit between experiment and reconstruction. Values between 0 and 1 represent a very good reconstruction (Dosemund 1998) as can also be verified by visual inspection. The reconstructed spectra at 240 K show a decreased goodness-of fit value. This can be explained considering that the sextet pattern which has been obtained by multiple subtractions poses relatively large noise and contributes to decrease in goodness-of-fit specifically at elevated temperature where its contribution enhances.

It is worth mentioning here that among all the radicals found at 140 K 20-40% of them are decayed at 200 K and only 20% of all radicals are left at 240 K (evaluated by normalization of total radical concentration i.e. Double Integral (DI) values obtained at 200 K and 240 K to the DI values at 140 K. **Fig. 5.2.20** gives an overview of the change in radical balance with increasing dose at three different temperature points (A: 140K, B: 200 K and C: 240 K). These figures distinctly show a constant decrease in base derived radial patterns like singlet, doublet and octet whereas the quartet, doublet/ox and sextet behave in an opposite manner proving their neutral character specifically at 140 and 200 K. At 240 K only octet and sextet pattern have a major contribution in the ESR spectra. It should be noted that there is almost 7-10% of absolute contribution (before normalizing

to the DI values of 140 K) of allyl radical to the ESR spectra at 240 K obtained after irradiation of pure DNA with 252 k Gy and more.
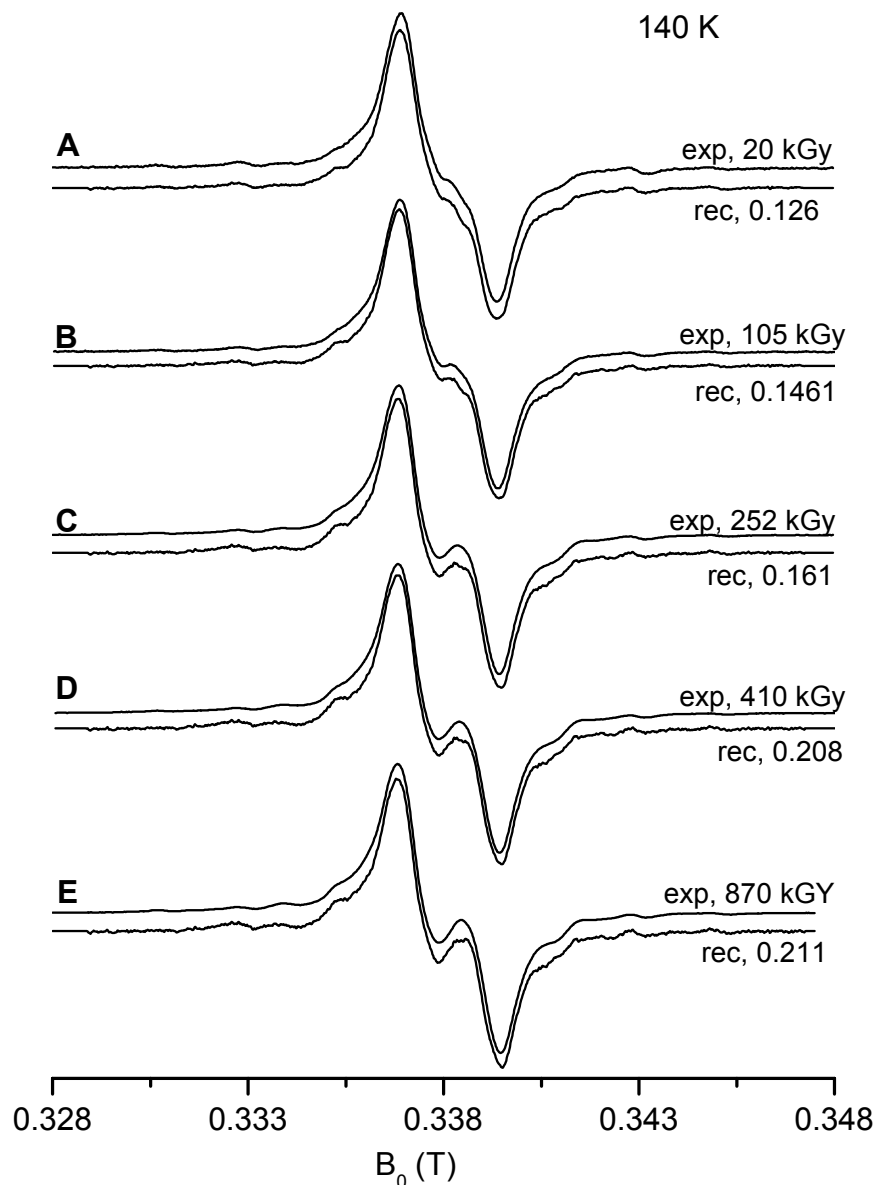
Fig. 5.2.17. Five sets of X-band ESR spectra of frozen aqueous DNA/H_2O X-irradiated with different doses (as indicated) and measured at 77 K after annealing to 140 K. The upper spectrum of each set gives the experimental recording while the lower spectrum is a reconstruction of the experimental spectra from the .isolated pattern. 'rec'. shows the value of goodness of fit for each reconstructed spectrum with the experimental spectrum (see text).
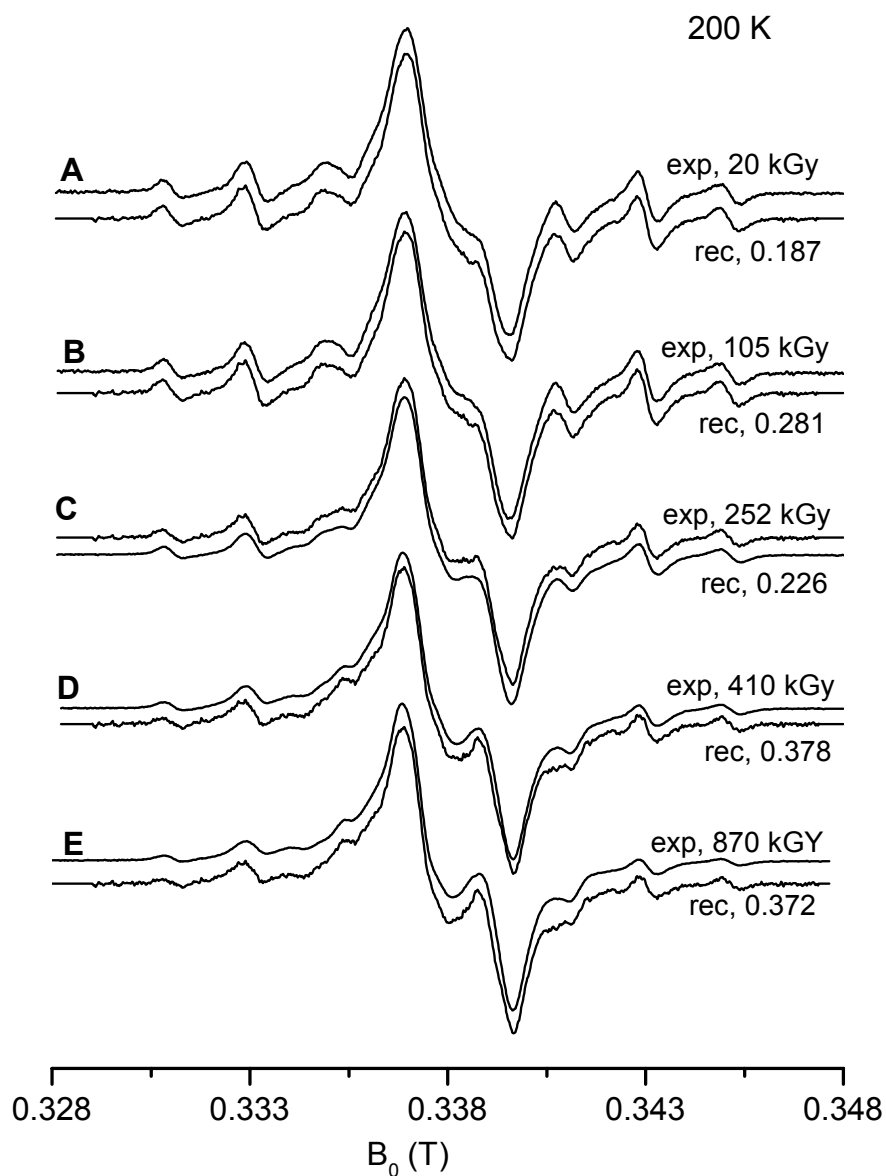
Fig. 5.2.18. Five sets of X-band ESR spectra of frozen aqueous DNA/H_2O x-irradiated with different doses (as indicated) and measured at 77 K after annealing to 200 K. The upper spectrum of each set gives the experimental recording while the lower spectrum is a reconstruction (see figure caption of Fig. 5.2.17).

The sharp singlet and peroxy radicals contribute to about 5-10% of absolute value in individual spectra at 240 K.
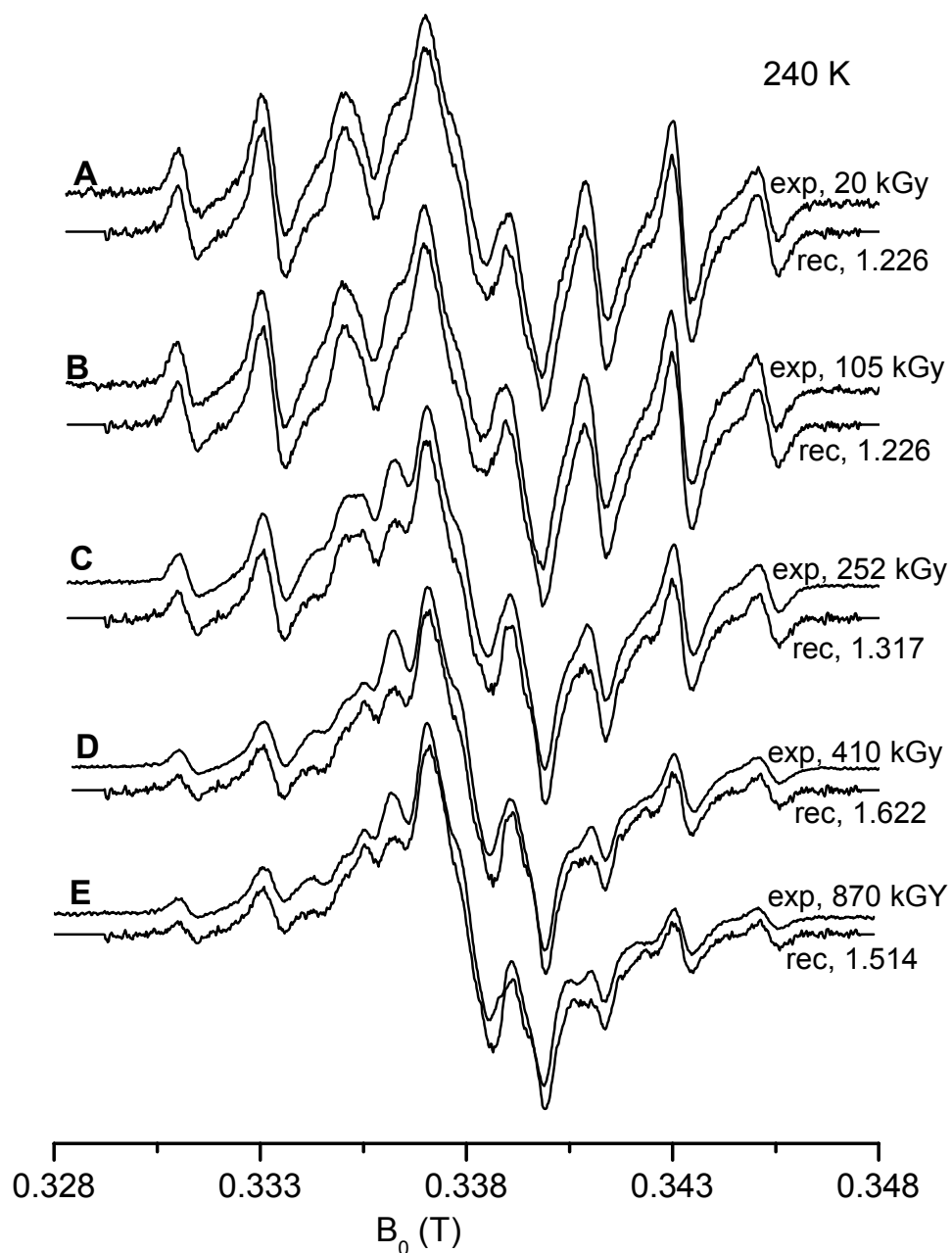
Fig. 5.2.19. Five sets of X-band ESR spectra of frozen aqueous DNA/H_2O X-irradiated with different doses (as indicated) and measured at 77 K after annealing to 200 K. The upper spectrum of each set gives the experimental recording while the lower spectrum is a reconstruction (see figure caption of Fig. 5.2.17).

The effect of these three radical patterns reduces when their normalized values are considered in **Fig. 5.2.20C**.
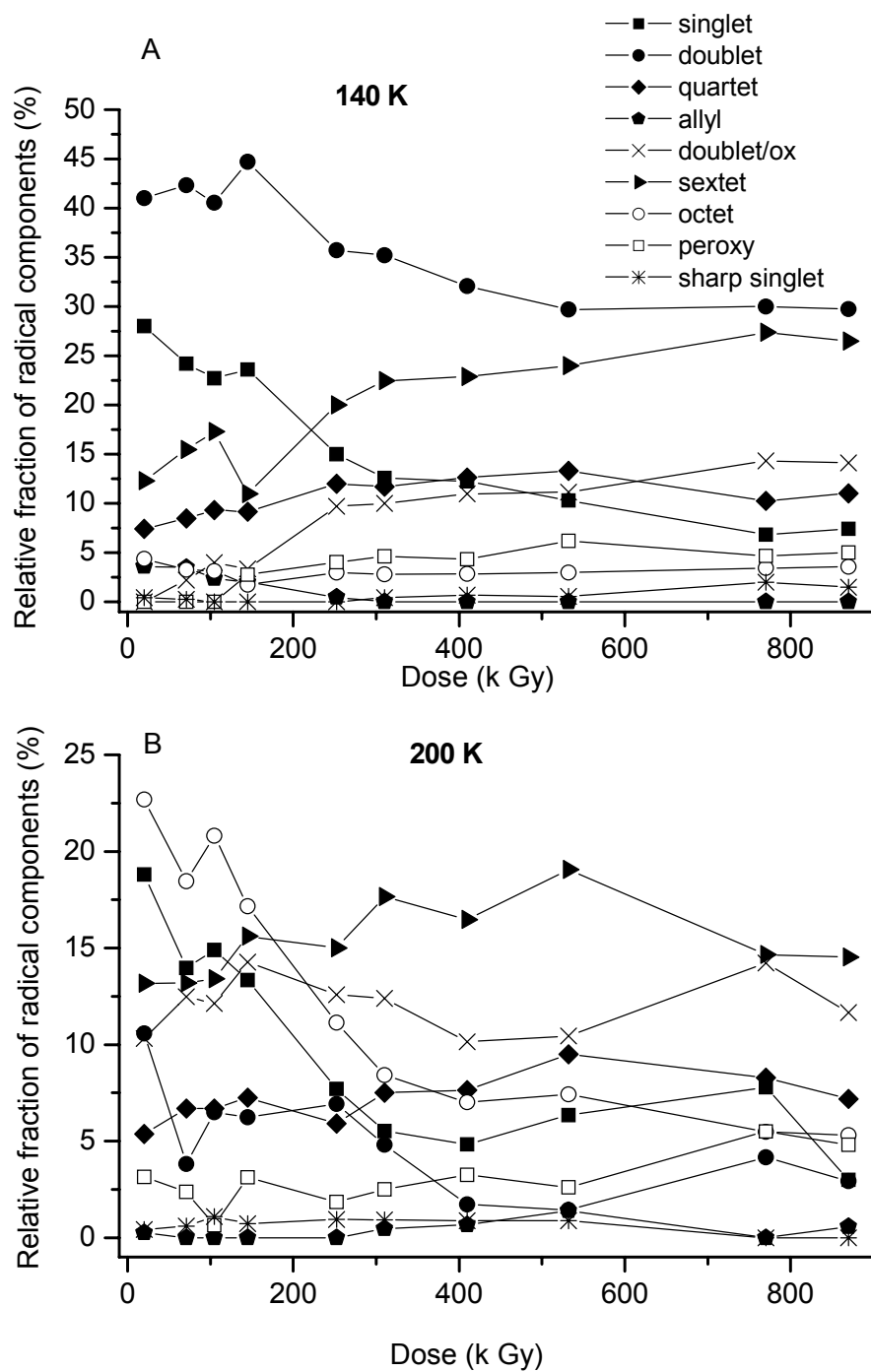
Fig. 5.2.20. The relative contributions of the radical patterns in frozen aqueous DNA after irradiation with different x- ray doses. After annealing to the temperatures A) 140 K, and B) 200 K.
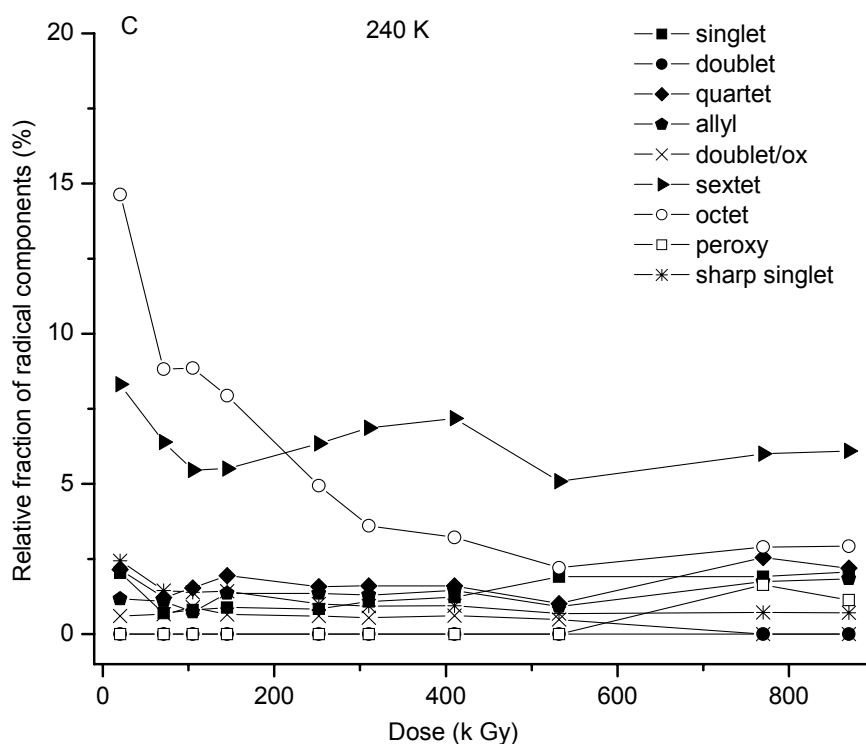
Fig. 5.2.20 C. The relative contributions of the radical patterns in frozen aqueous DNA after irradiation with different X ray doses at 240 K.

5.2.4. Effect of Increasing Dose and Temperature on the Radicals formed in Frozen Aqueous Solution of DNA Containing Various Additives

$K_3Fe[CN]_6$ and DNA

$K_3Fe[CN]_6$ have been used to study the oxidative radical pathway in frozen aqueous DNA in many investigations before (Lange et. al. 1995, Weiland and Hüttermann 1998 and Shukla et. al. 2005). Here the results from frozen aqueous system containing one $K_3Fe[CN]_6$ per 20 nucleotide are presented with a comprehensive account of all probable spectra components which were used in pure DNA after irradiation at 77 K and the analysis of their annealing behavior up to 240 K is attempted with respect to different dose values. **Fig. 5.2.21** gives the change in the nature of ESR spectra of Fe^{3+} plus DNA with increasing dose quantity. Addition of Fe^{3+} in DNA suppresses the formation anion radicals like T^-/C^- by successfully scavenging the electron produced by ionization, guanine cations and neutral radicals forms a major

portion of the ESR spectra at low irradiation dose, along with increase in dose quantity it can be seen that the ESR spectra again acquires a doublet character and remains so. This doublet character is similar in hyperfine splitting with that of doublet/ox pattern which is observed at low doses also but is more prominent in high dose and in presence of large additive concentration. A similar trend is observed at 200 K (**Fig. 5.2.22**) for same samples. With increasing dose (to 250 kGy) the broad doublet character which resembles closely to doublet/ox pattern becomes prominent in the ESR spectra and remains constant with further increase in dose.

Reconstruction of the experimental spectra was done using the radical patterns from pure DNA except the sharp singlet pattern. Presence of sharp singlet pattern was not observed in this series. **Fig. 5.2.23A** shows that there is a major suppression of the doublet pattern formed due to reduced anion radicals as expected, only 10% is present at 20 k Gy which reduces further with increase in dose. The singlet component produced by guanine cation constitutes about 32% of total experimental spectrum at 20 k Gy but reduces to zero with increasing dose, other major components are doublet/ox and sextet patterns which reaches a maximum value of about 30 % and remains constant with increasing dose quantity. The quartet patterns constitute about 10% and remain constant with dose. All other radical patterns have minor contributions (below 10%).

On annealing the samples to 200 K (**Fig. 5.2.23B**) the overall radical concentration decreases to 30-50% of that stabilized at 140 K (evaluated by normalization of the total radical concentration at 200 K to that of 140 K) and the radical patterns follow same trend as at 140 K. Octet patterns from 5-thymyl radical which were major constituents in pure DNA does not form here confirms the complete suppression of the thymine anion radicals by high scavenger concentration.

It is important to mention here that with increasing the annealing temperature to 220-240 K in the samples peroxy radical pattern emerges as the major constituent in the ESR spectra in spite of the fact that similar to all other frozen aqueous these samples were also prepared in strict anaerobic conditions.

140 K

A   exp, 20 kGy

rec, 0.358

B   exp, 110 kGy

rec, 0.980

C   exp, 255 kGy

rec, 1.154

D   exp, 422 kGy

rec, 1.068

E   exp,830 kGy

rec, 1.200

E   from DNA/76H+Fe^{3+}

Doublet/ox/76%H

0.328   0.333   0.338   0.343   0.348

B_0 (T)
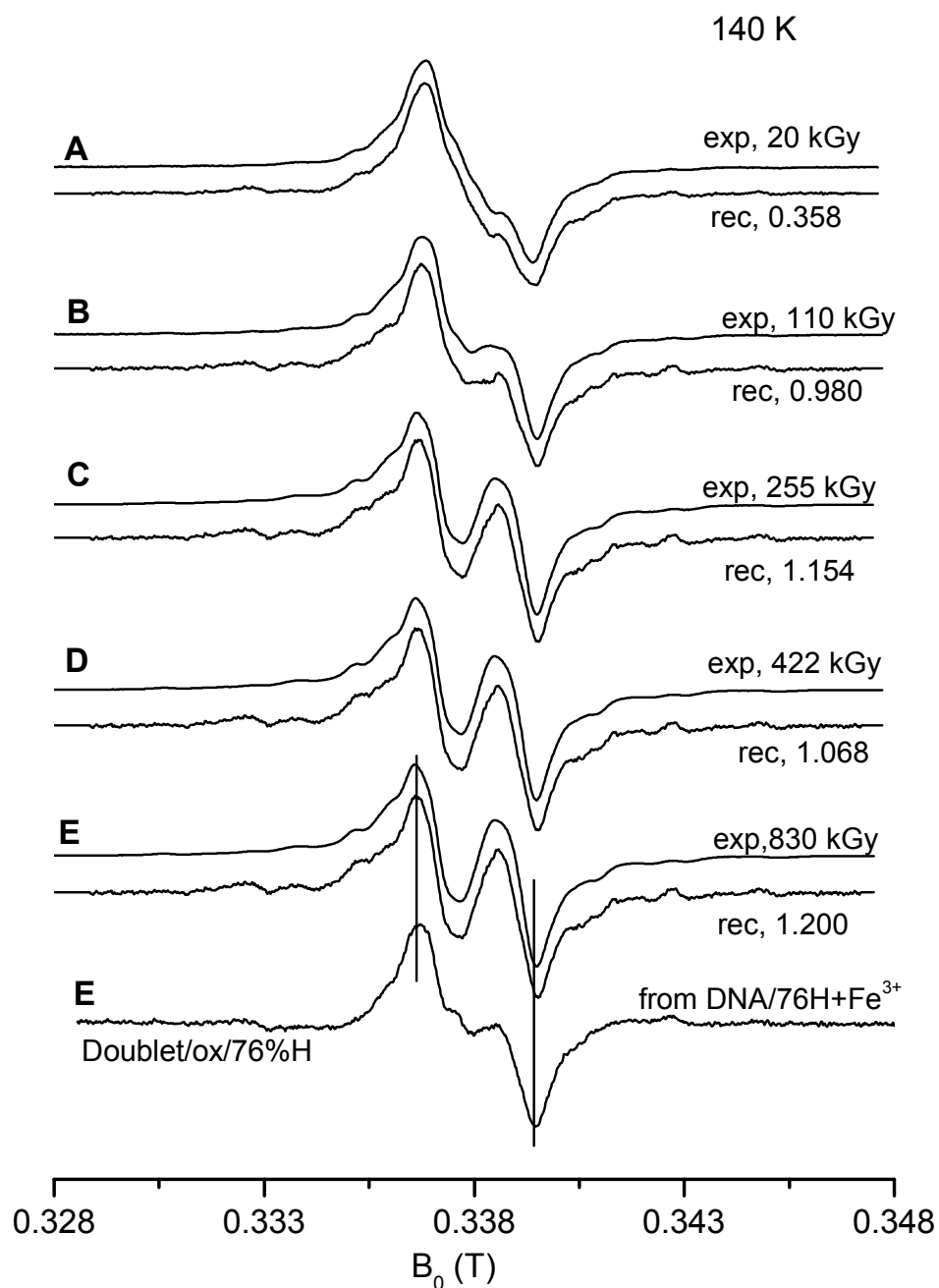
Fig. 5.2.21.(A-E) Five sets of X-band ESR spectra of $K_3Fe[CN]_6$ plus DNA (1:20) in frozen aqueous matrix, x-irradiated with different doses (as indicated) and measured at 77 K after annealing to 140 K. The upper spectrum of each set gives the experimental recording while the lower spectrum is a reconstruction. F) Doublet/ox pattern (Weiland and Hüttermann 1998), see also Fig. 5.2.6.
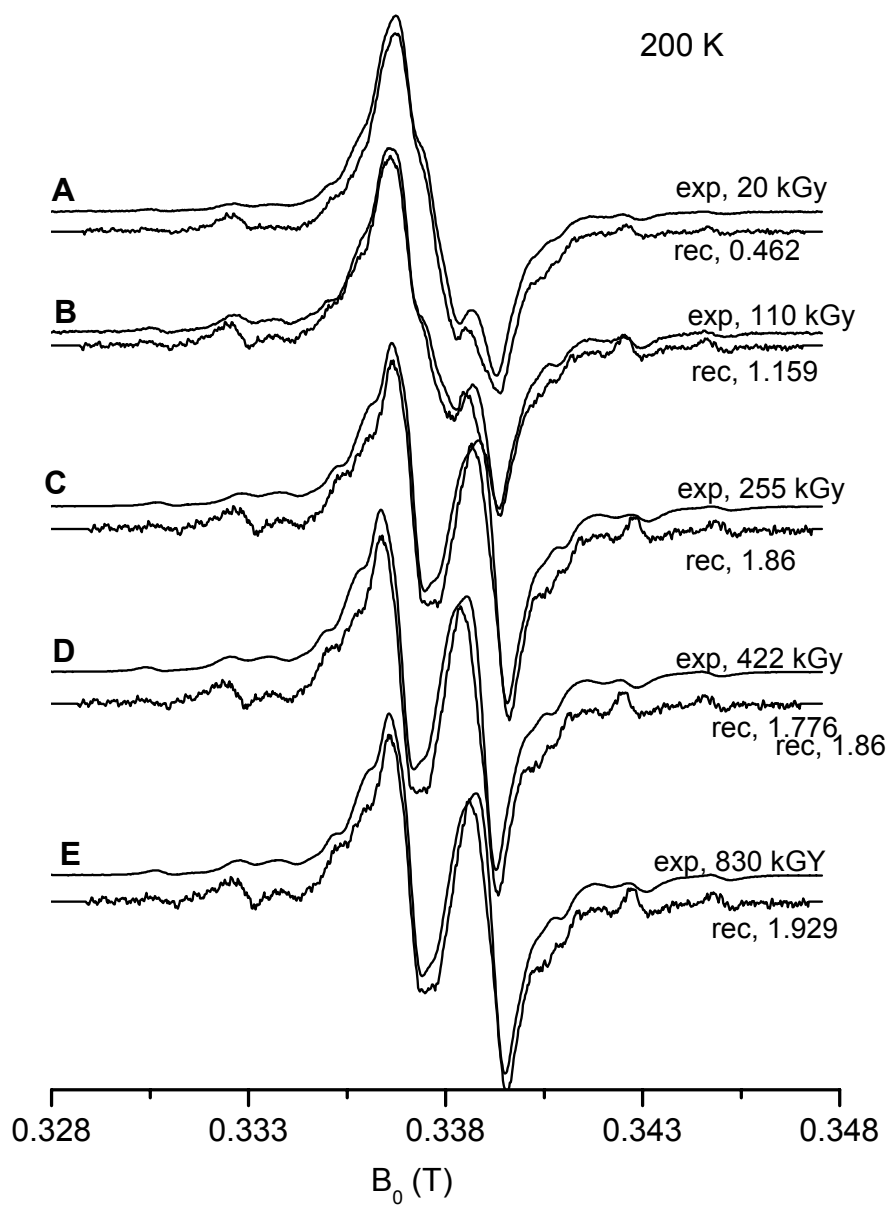
Fig. 5.2.22. Five sets of X-band ESR spectra of $K_3Fe[CN]_6$ plus DNA (1:20) in frozen aqueous matrix, x-irradiated with different doses (as indicated) and measured at 77 K after annealing to 200 K. The upper spectrum of each set gives the experimental recording while the lower spectrum is a reconstruction.
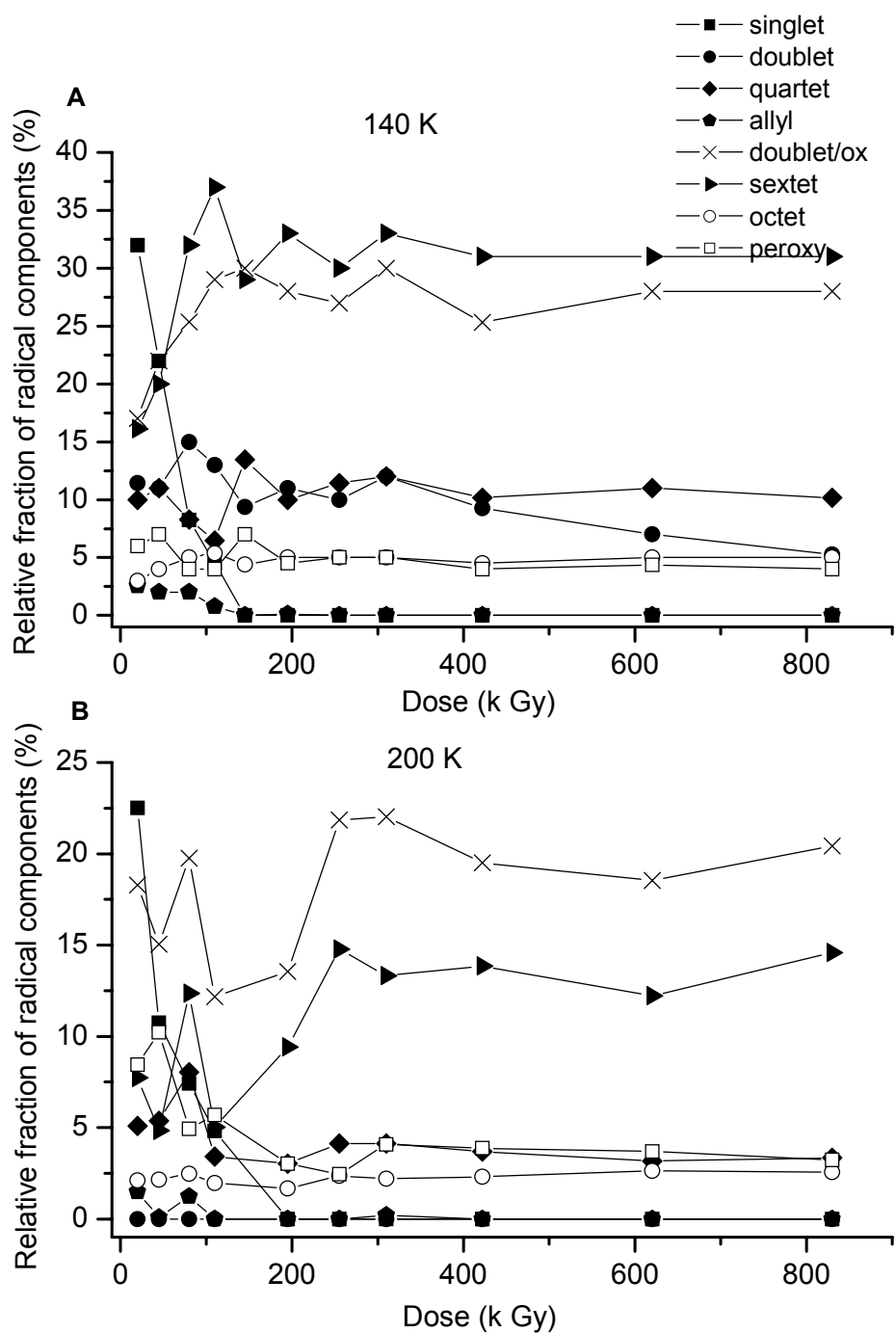
Fig. 5.2.23 The relative contributions of the radical patterns in Fe^{3+} and DNA in frozen aqueous matrix after irradiation with different X ray doses. Upon annealing to temperatures A) 140 K, B) 200 K.

$K_4Fe[CN]_6$ and DNA

$K_4Fe[CN]_6$ has been used as a hole scavenger in many previous reports (e.g Shukla et. al 2005). Like $K_3Fe[CN]_6$, Fe^{2+} does not give any ESR finger print at 77 K and can be conveniently used for understanding its influence on the radical balance produced on DNA after irradiation.

Fig 5.2.24 shows the experimental spectra of a frozen aqueous system containing one $K_4Fe[CN]_6$ per 20 DNA nucleotides at various doses along with their reconstructed spectra. The spectra obtained after annealing to 140 K and 200 K for samples treated with variable doses. $K_4Fe[CN]_6$ being a hole scavenger it is expected that guanine cation radicals will be considerably decreased here which is evident from the predominantly doublet character of the spectra. Although the other oxidized species originating from neutral sugar radicals are still observed. The spectrum so formed must be a resultant of DNA anion radicals and neutral radicals.

Radical component analysis Fe^{2+} plus DNA system irradiated with various doses shows (**Fig. 5.2.25**) that guanine cation is not formed in this system and doublet pattern produced by $T^{-\bullet}$ and / or $C^{-\bullet}$ constitutes almost 75% of the spectrum at low X ray dose (20 kGy). With increasing dose the anion radical pattern decreases and the neutral radical cohort increases in proportion.

With annealing to 200 K the radical concentration is 70% of that stabilized at 140 K (evaluated by normalization of the total radical concentration (DI) at 200 K to that of 140 K). At 200 K along with the anion doublet patterns the octet pattern is a major component especially for systems irradiated with low doses which decreases steadily with increasing dose. Doublet/ox constitutes about 20% and sextet patterns about 10% of the ESR spectra at 200 K.

ESR spectra obtained after annealing the variably irradiated samples to 240 K shows only the presence of octet patterns. This shows irreversible decay of all the neutral radicals at this temperature and secondary internal conversion of thymine radical anion radical to 5-thymyl radical. The 5-thymyl radical concentration decreases with increase in dose value, which is in line with the results obtained in pure DNA.
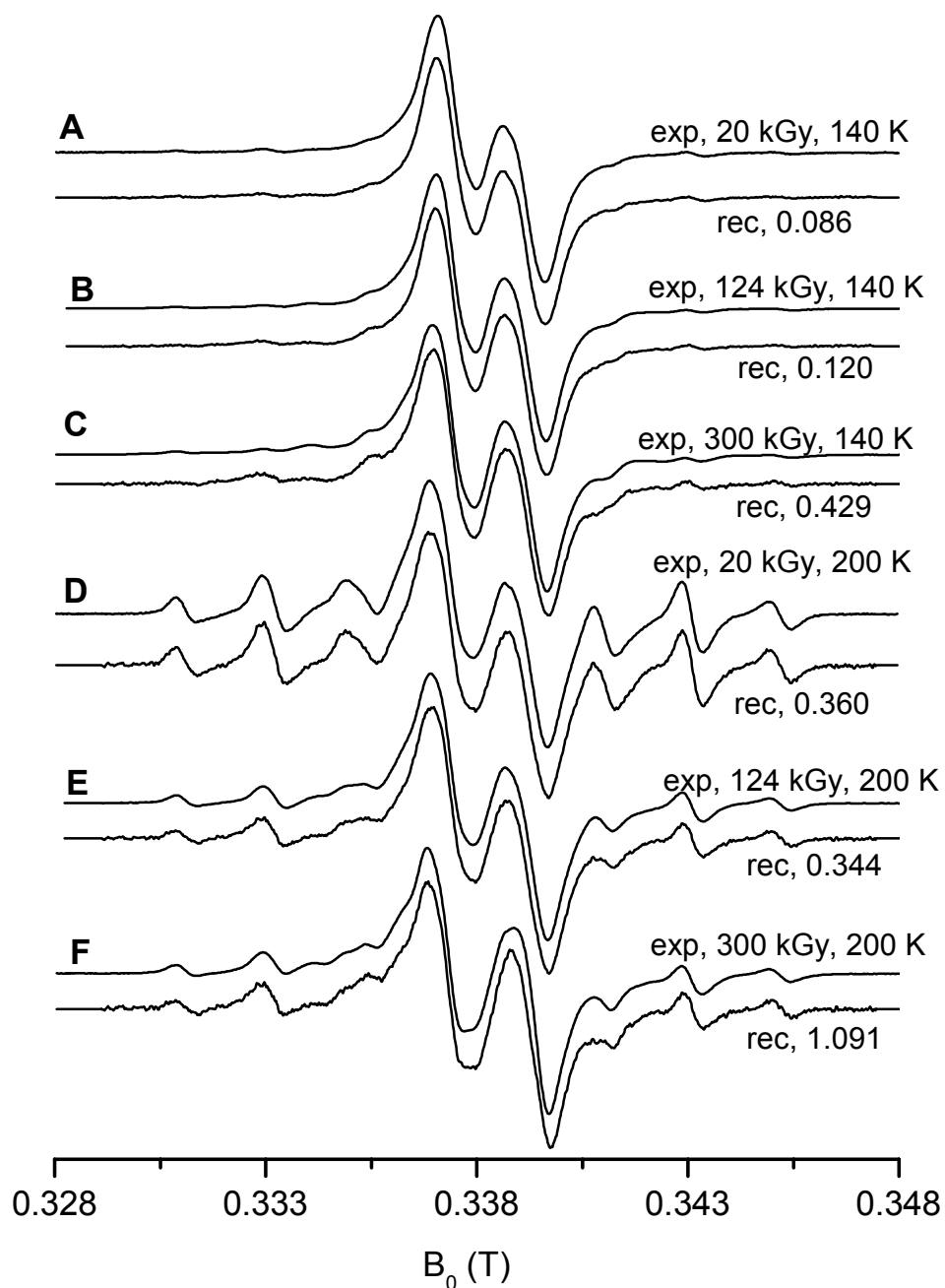
Fig. 5.2.24. Representative X-band ESR spectra of $K_4Fe[CN]_6$ plus DNA (1:20) in frozen aqueous matrix, X-irradiated with different doses (as indicated) and measured at 77 K after annealing to 140 K (A, B, C) and 200 K (D, E, F) respectively. The upper spectrum of each set gives the experimental recording while the lower spectrum is a reconstruction along with the 'rec' values showing goodness-of-fit.
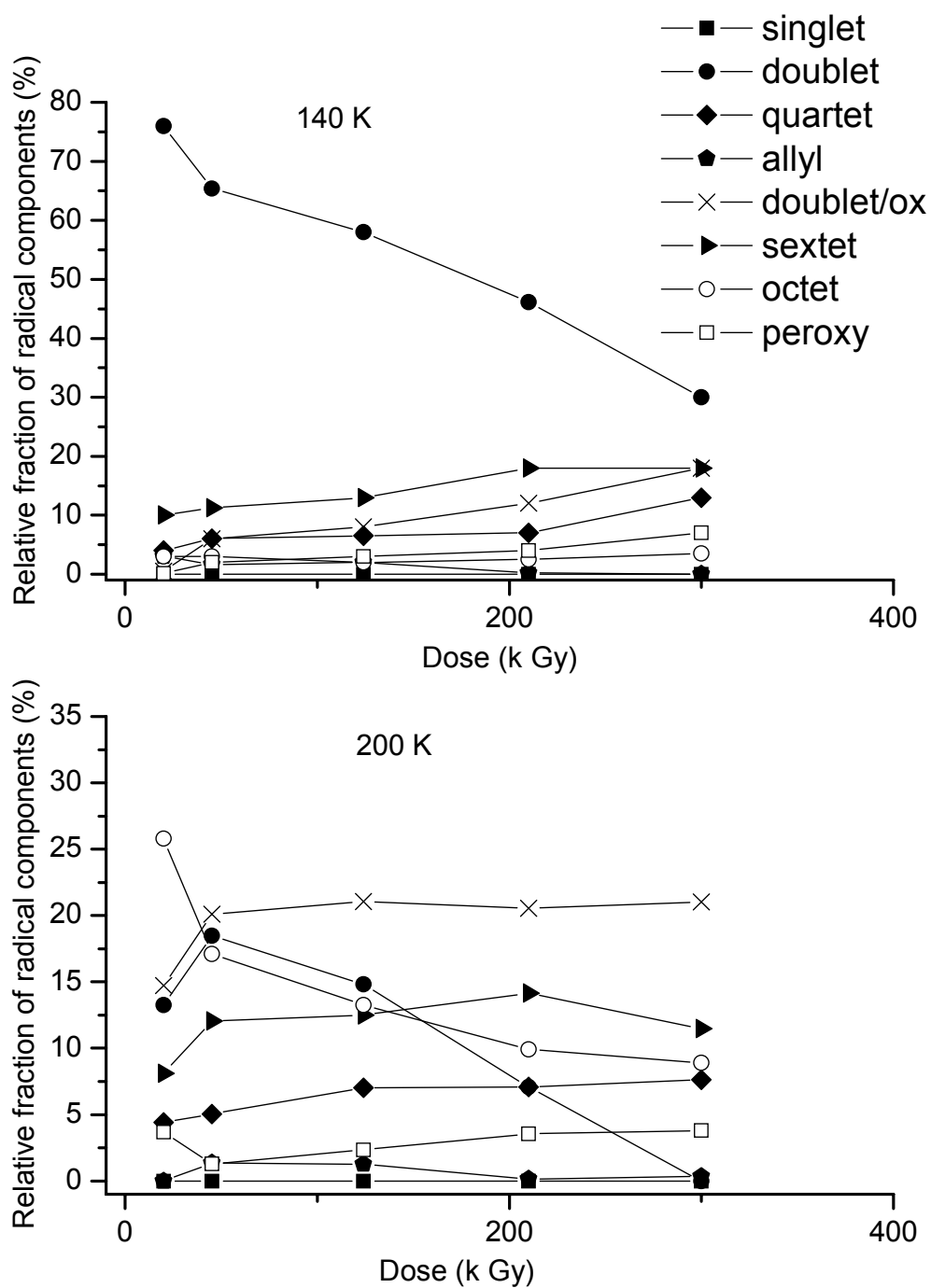
Fig. 5.2.25 The relative contributions of the radical patterns in Fe^{2+} and DNA in frozen aqueous matrix after irradiation with different X ray doses. Upon annealing to A) 140 K, B) 200 K.

Mitoxantrone (MX) and DNA

The main aim of this study was to probe the influence of electron affinic intercalator i.e. Mitoxantrone (MX) on the initial stages of radiation damage on DNA. Studies have been done on this system previously elaborating the distance traveled by ejected electrons (Pezeshk 1996), the extent of transfer of electrons via tunneling or electron hopping mechanisms from the DNA anions to the additive as a function of time after irradiation (Cai et. al. 2000) and inter double strand electron transfer possibilities in frozen aqueous and hydrated systems (Cai and Sevilla 2000). Mitoxanthrone (MX) is of considerable importance as a DNA affinic drug and being an intercalator attached in between the DNA double strands. The electron affinity of this additive is much higher than anion forming DNA bases like thymine and cytosine which can enhance the oxidative radical detection in the system. MX gives relatively narrow ESR singlet upon electron addition, with g-values close to the free-electron g-value and hence it is assumed that the additive spectrum will not interfere with the spectral components of radicals originating on DNA.

When low amounts of MX was incorporated into the DNA, i.e., 1MX:800 DNA nucleotides (equivalent to 1MX:400 DNA base pairs) there is an efficient scavenging of electrons by MX showing migration of electrons to a large distance through DNA double strands during irradiation. **Fig 5.2.26** reveals the representative ESR spectra of MX-DNA annealing series in frozen aqueous solution for two different doses (20 k Gy and 330 k Gy) along with their reconstructions from spectral patterns. The spectra shows a strong singlet associated with MX anion radical (shown by *) along with a shoulder (shown by arrow) from radicals produced on DNA giving a doublet like character at 140 K. With increase in annealing temperature the fingerprints of 5-thymyl radical becomes clear.

Reconstruction of the experimental ESR spectra are done by using the radical patterns used for reconstructing neat DNA (excluding sharp singlet pattern) and MX$^{-\bullet}$ pattern isolated from subtraction of two ESR spectra from MX:DNA (1:100) and MX:DNA (1:50) upon annealing to 140 K (irradiated with 45 kGy of x-irradiation) (**Fig. 5.2.28C**). Reconstruction of the spectra obtained after irradiation with various doses at annealing temperature 140 K (**Fig. 5.2.27**) shows that 20 % of MX derived radicals on irradiation with 20 k Gy of X ray. As a consequence the proportion of base anion species formed from DNA is lowered in comparison to neat DNA.
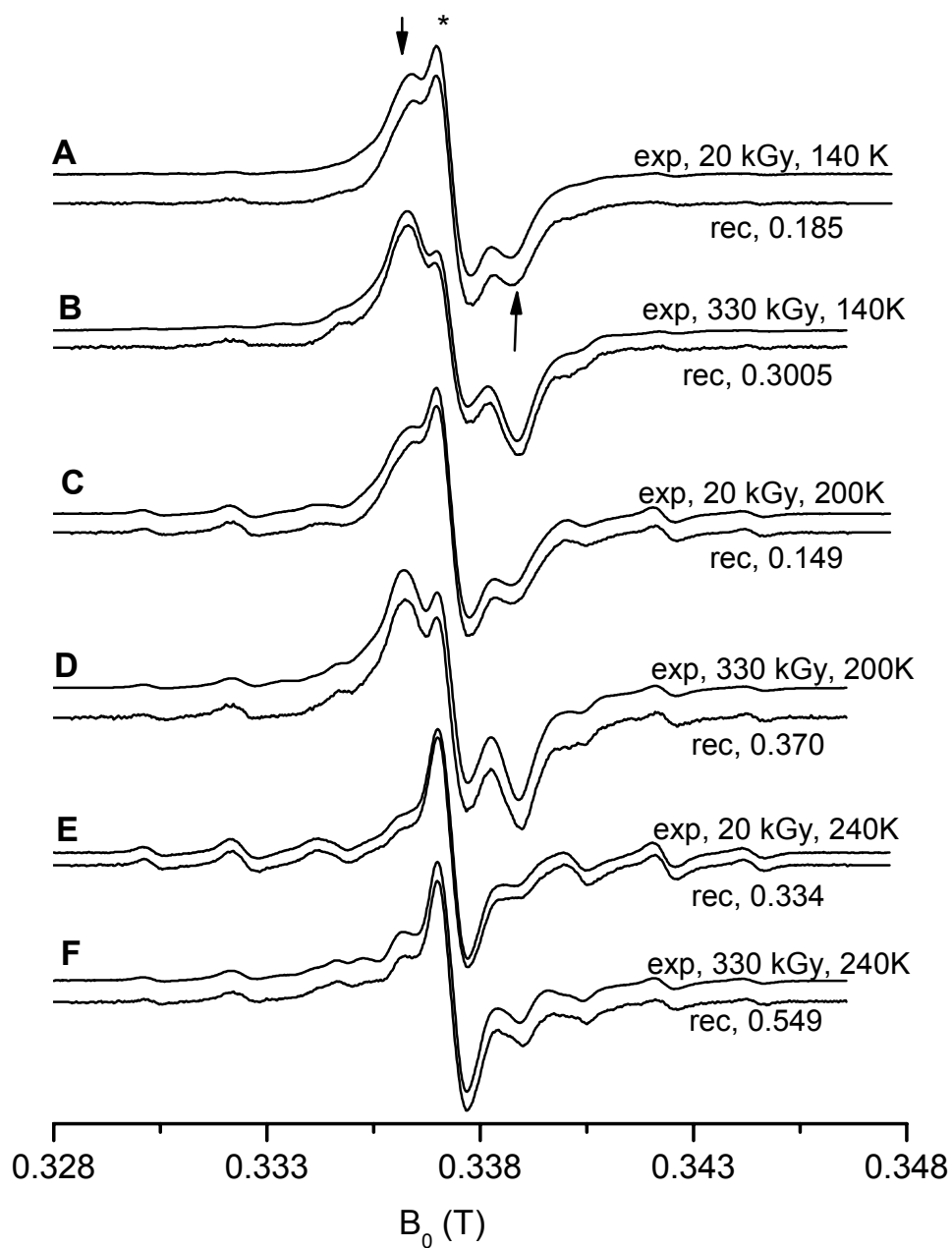
Fig. 5.2.26. X-band ESR spectra frozen aqueous system containing MX and DNA (1MX :800 nucleotides), x-irradiated with different doses (as indicated) and measured at 77 K after annealing to 140 K (A, B,) and 200 K (C, E,) and 240 K (E, F) respectively. The upper spectrum of each set gives the experimental recording while the lower spectrum is a reconstruction from the isolated patterns from DNA as well as from MX radical. The MX radical pattern used for reconstruction is shown in Fig. 5.2.28C.
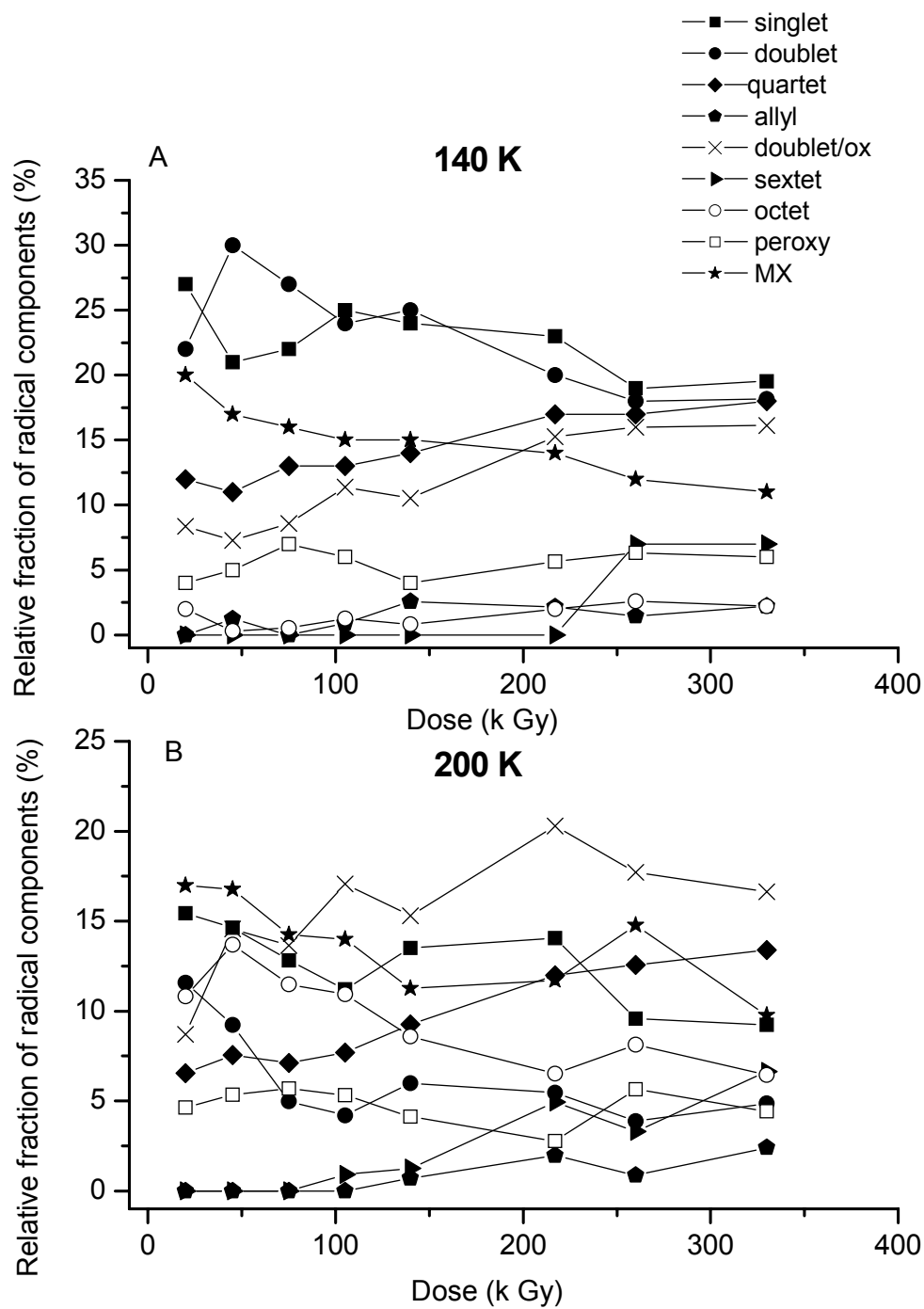
Fig. 5.2.27 The relative contributions of the radical patterns in MX and DNA (1:800) in frozen aqueous matrix after irradiation with different x ray doses. A) 140 K, B) 200 K.

The fraction of $G^{+\bullet}$ remains almost unchanged while formation of anion radicals is reduced in comparison to pure DNA. The $G^{+\bullet}$, $T^{-\bullet}/C^{-\bullet}$ and $MX^{-\bullet}$ radical components decrease steadily with increasing dose quantity. The quartet component and doublet/ox pattern increases with increasing dose similar to the effect observed in pure DNA.

After annealing to 200 K there is an average decay of 30% of total radical concentration as was observed upon annealing to 140 K (evaluated by normalization of the DI values). The octet pattern decreases with increasing dose as previously observed. Other charged radical species patterns decreases as expected. Among the neutral radical cohort the doublet/ox and quartet component constitute the major proportion and increases with increasing dose value. The sextet pattern component is formed in less percentage to what was observed in pure DNA or in Fe^{3+}/DNA or Fe^{2+}/DNA.
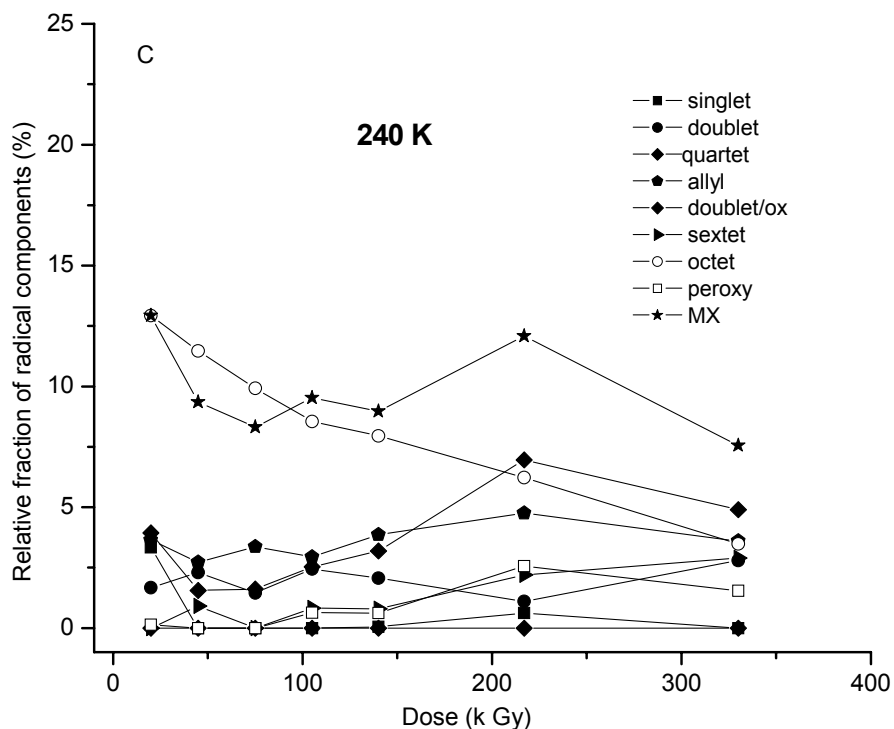
Fig. 5.2.27 C) The relative contributions of the radical patterns in MX and DNA (1:800) in frozen aqueous matrix after irradiation with different x ray doses. After annealing to 240 K.

Upon annealing to 240 K about 70% of the total radicals observed at 140 K are decayed (Evaluation by DI normalization). Along with the usual trend of decrease of charged radical patterns it is noteworthy to observe the presence of allyl radical (**Fig. 5.2.27C**).
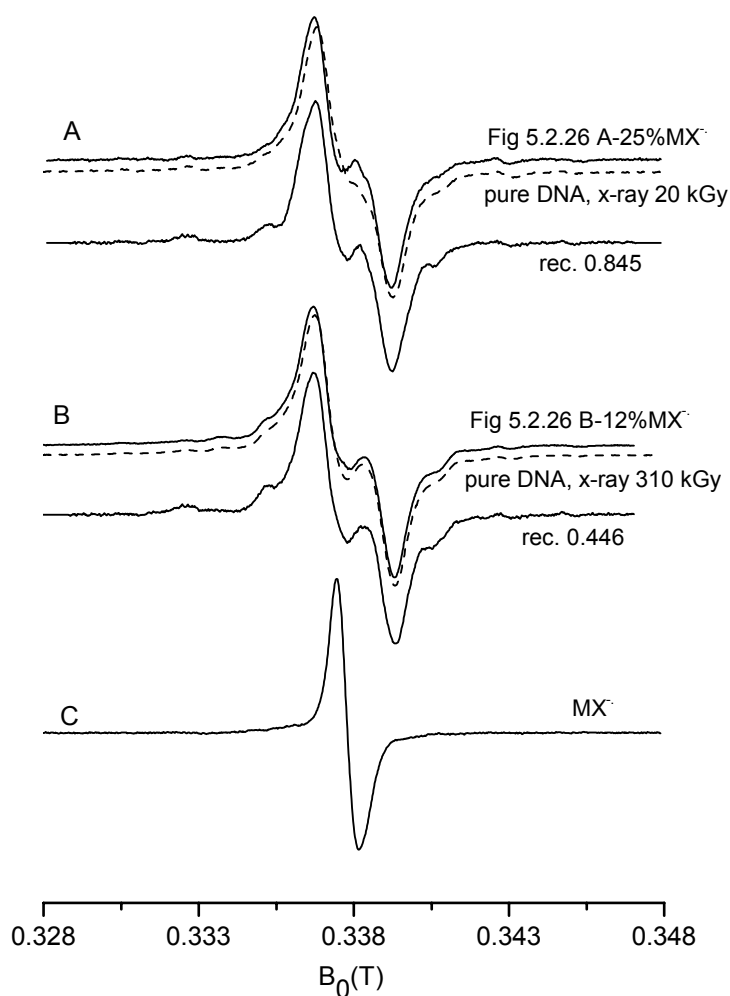
Fig. 5.2.28. Spectral pattern obtained after subtracting MX radical pattern from the experimental spectrum of MX:DNA (1:800) x ray irradiated by A) 20 kGY and B) 330 kGY respectively and measured at 77 K after annealing to 140 K , reconstructed spectrum is shown along with. C) MX radical pattern isolated from experimental spectra (see text). Dotted ESR spectra are the experimental ESR spectra obtained from pure DNA after irradiation with similar doses and measured under identical conditions.

For comparative reasons MX radical pattern was subtracted from the composite spectrum of MX:DNA (1:800) obtained at 140 K and then reconstruction of the resultant feature was performed using the radical patterns of DNA. Upon reconstruction the percentage of radical balance is found to be very much similar to that found in pure DNA (spectra shown by dashed lines) at 140 K. The subtracted spectra and MX radical pattern are shown in **Fig. 5.2.28.**

The percentage of MX radical pattern needed to be subtracted from MX:DNA complex spectra varied from 25% to 12% from dose 20 kGY to 330 kGY. The proportion MX radical component needed to be subtracted therefore decreased with increase in dose in a similar fashion to the change in percentage of MX radical pattern when reconstruction of the experimental MX:DNA complex spectra (**Fig. 5.2.27A**) were performed. The radicals behave in a similar manner for MX:DNA (1:800) as in pure DNA with respect to increasing dose after subtraction of the mitoxantrone pattern.
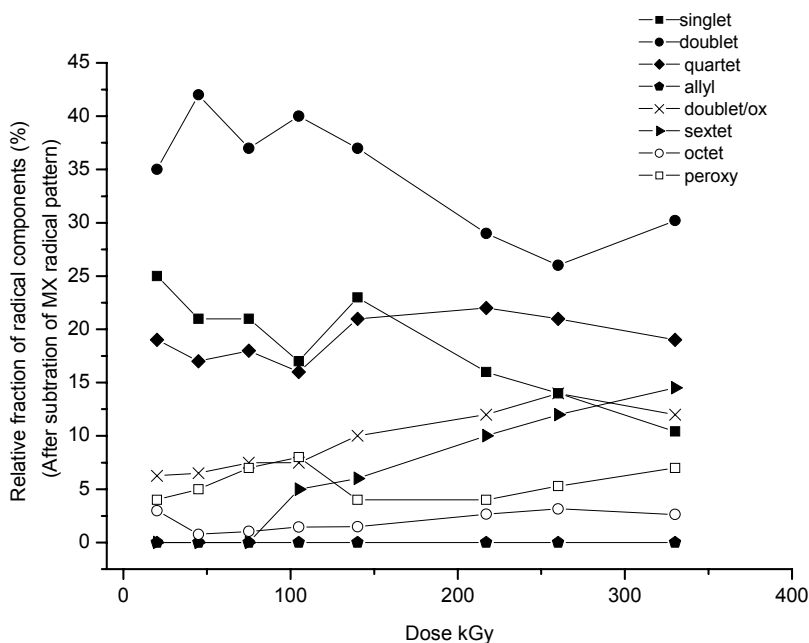
Fig. 5.2.29. The relative contributions of the radical patterns in a (MX:DNA /1:800) series of increasing dose where MX radial pattern has been subtracted and then reconstruction of the subtracted spectra has been done with the radicals patterns for DNA at 140 K.

Similar comparative analysis was not possible to do for systems at 200 K and 240 K. The change in the double integral (DI) values (hence the total concentration of radicals) of the subtracted spectra (at 200 K and 240 K) was not similar to the change of DI values of the experimental spectra obtained at 200 K or 240 K. This may be due to more noisy character of the subtracted spectra. Consequently proper normalization of the DI values to that of 140 K was not possible here.

When the concentration of MX was increased in the system for example to 1MX per 200 nucleotides (equivalent to 1MX:100 DNA bp) the radical balance altered in different manner after irradiation. **Fig. 5.2.30** shows the ESR spectra obtained from MX:DNA nucleotides (1:200) after irradiation with 20 k Gy and 440 k Gy at three different temperature point 140 K, 200 K and 240 K.

The reconstructions are compared with respective experimental spectra. In **Fig. 5.2.30** the spectra show the presence of sharp singlet originating from MX radical anion (shown by *) but the shoulder region (shown by arrow) specifically for low dose is decreased in comparison to 1MX:800 nucleotides.

The analysis of the reconstructions shows that at 140 K more than 55% (**Fig. 5.2.31A**) of mitoxantrone radicals are formed on irradiation upon 20 k Gy. Among the rest doublet pattern constitutes about 15-25%. Quartet pattern constitutes about 10% and remains constant through out the dose series. Singlet pattern from guanine cation is decreased which is not expected. The radical balance does not change so much with increasing dose quantity in comparison with the other systems studied. At 200 K 20-30% of the total radicals stabilized at 140 K are decayed. The formation of doublet/ox pattern especially at higher doses becomes clear but the sextet pattern is not formed like in pure DNA. Quartet and allyl pattern is present at a good proportion at this temperature point (**Fig. 5.2.31B**).

At 240 K 60% of the total radicals found at 140 K is lost. The MX radical pattern constitutes the major portion of the ESR spectra at 240 K which decreases with increasing dose. All other radicals are constituted to below 5% each. allyl radical forms to about 5 -7% and shows a nominal increase with increasing dose (**Fig. 5.2.31C**).
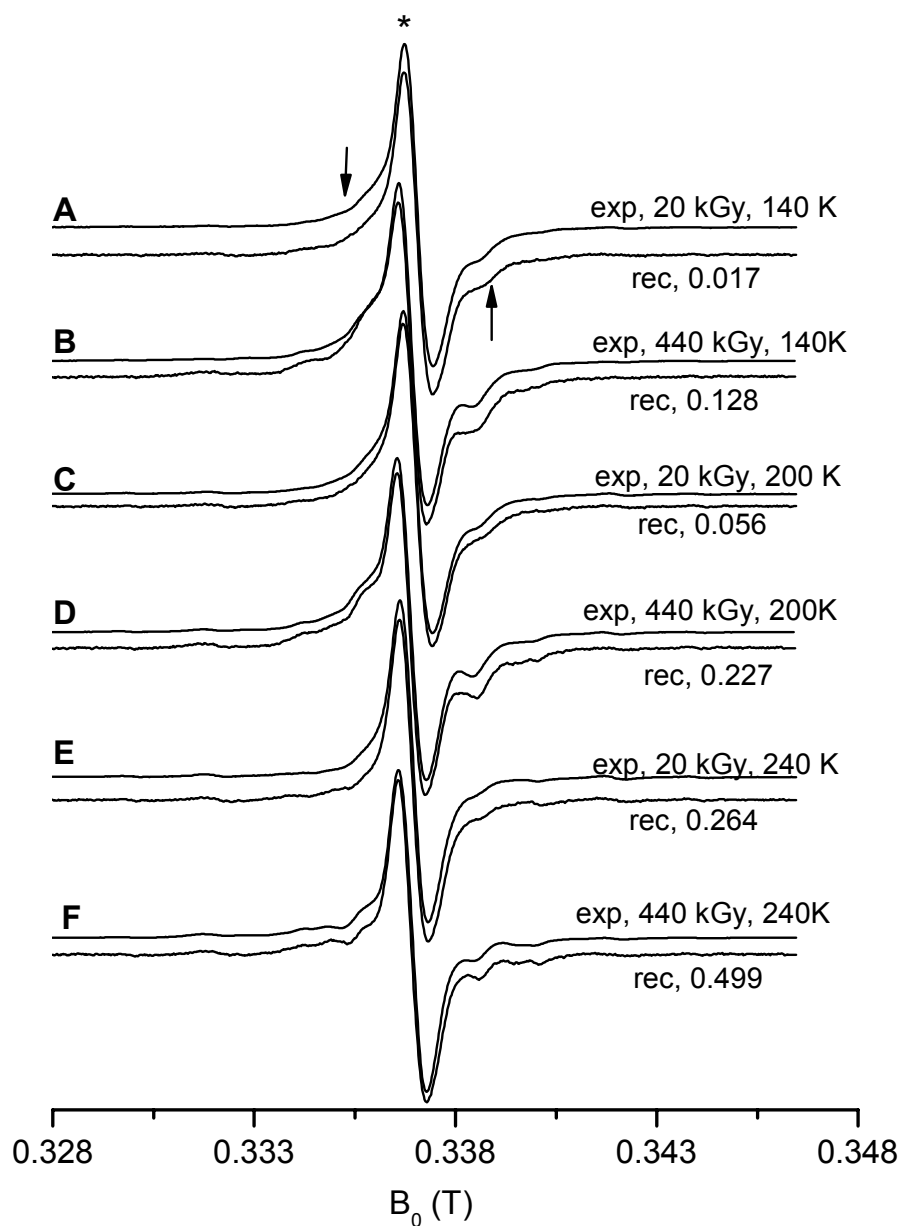
Fig. 5.2.30. X-band ESR spectra frozen aqueous system containing MX and DNA (1MX:200 nucleotides), X-irradiated with different doses (as indicated) and measured at 77 K after annealing to 140 K (A, B,) and 200 K (C, E,) and 240 K (E, F) respectively. The upper spectrum of each set gives the experimental recording while the lower spectrum is a reconstruction from the isolated patterns.
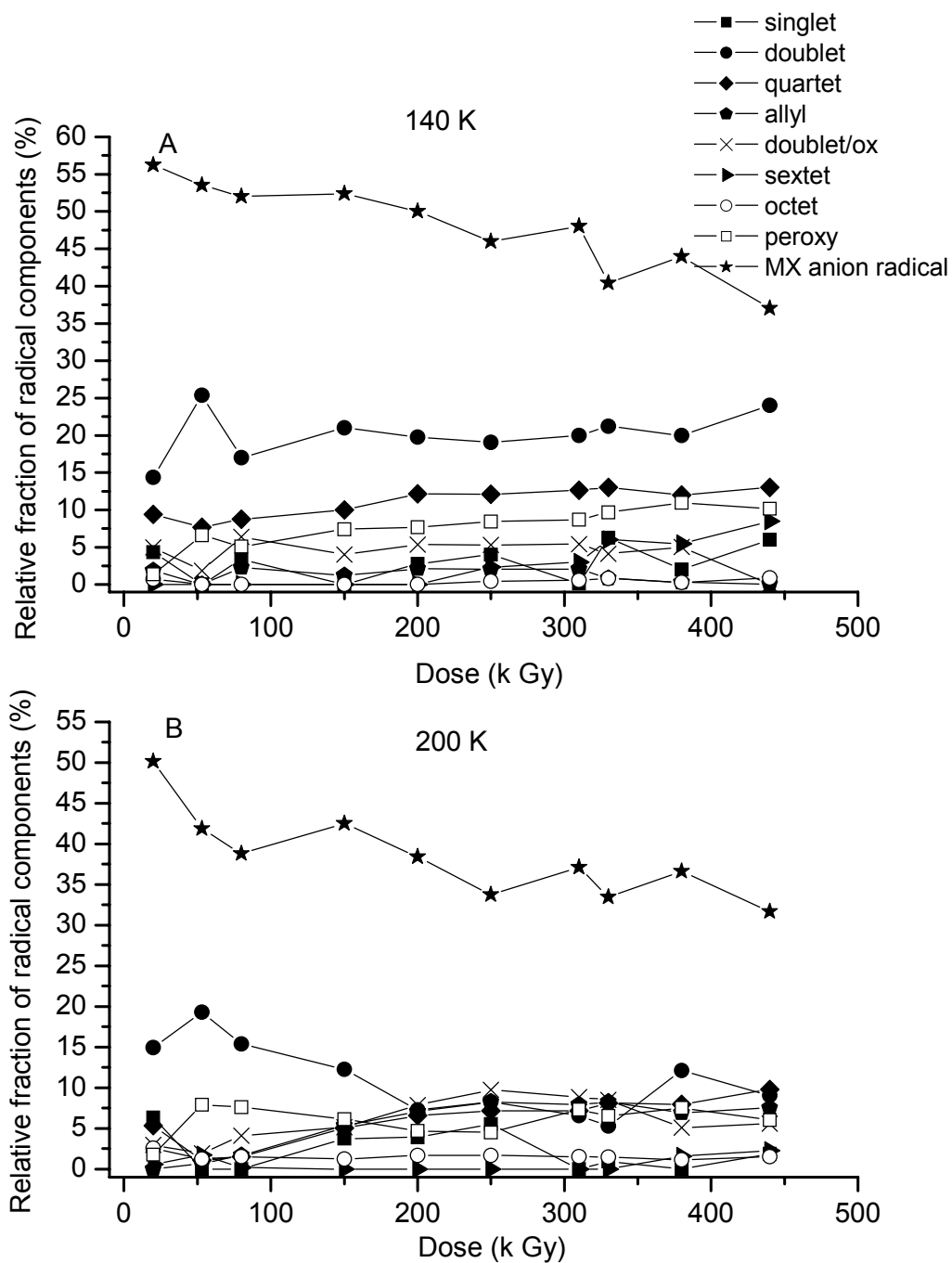
Fig. 5.2.31 The relative contributions of the radical patterns in MX and DNA (1:200) in frozen aqueous matrix after irradiation with different X ray doses. After annealing to A) 140 K, B) 200 K.

In order to understand clearly the remaining of the DNA part after subtracting the MX radical pattern as has been done for MX:DNA (1:800) system. It can be observed that the singlet character (owing to the presence of guanine cation radical) is not present in the subtracted ESR pattern (on comparing with the ESR spectra from pure DNA as shown by dashed lines). It was not possible to do deconvulute these subtracted spectra due to their high noise content (**Fig. 5.2.32**). The goodness of fit of the reconstructed spectra was more than 2 and cannot be considered as reliable value.
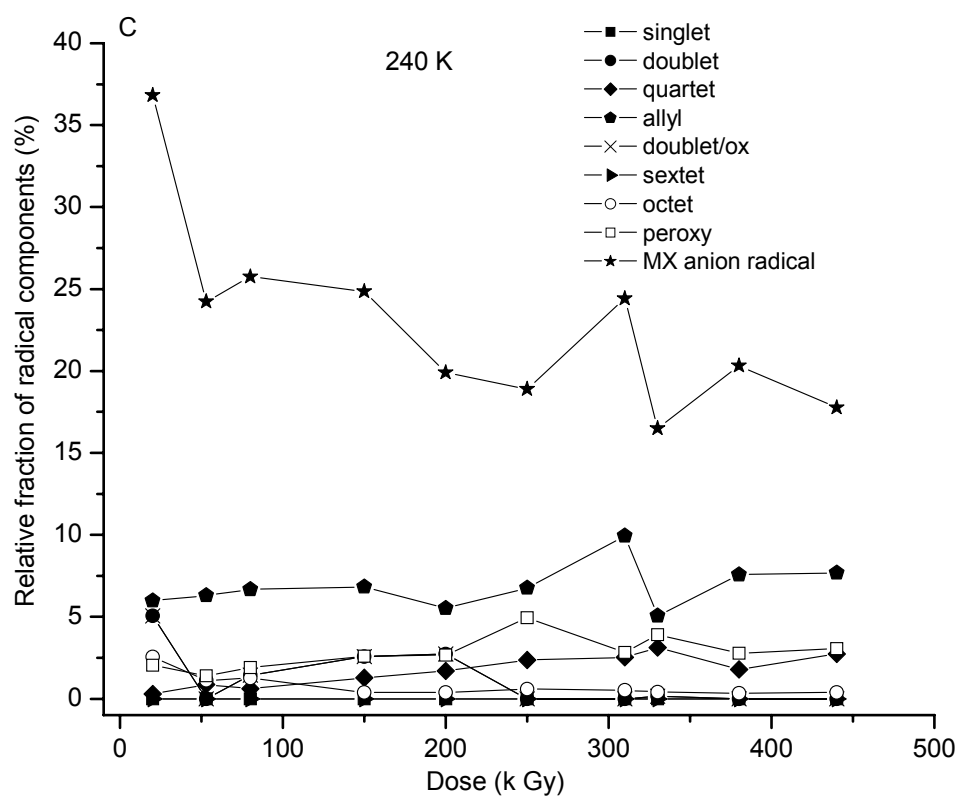
Fig. 5.2.31C The relative contributions of the radical patterns in MX and DNA (1:200) in frozen aqueous matrix after irradiation with different X ray doses. After annealing to 240 K.
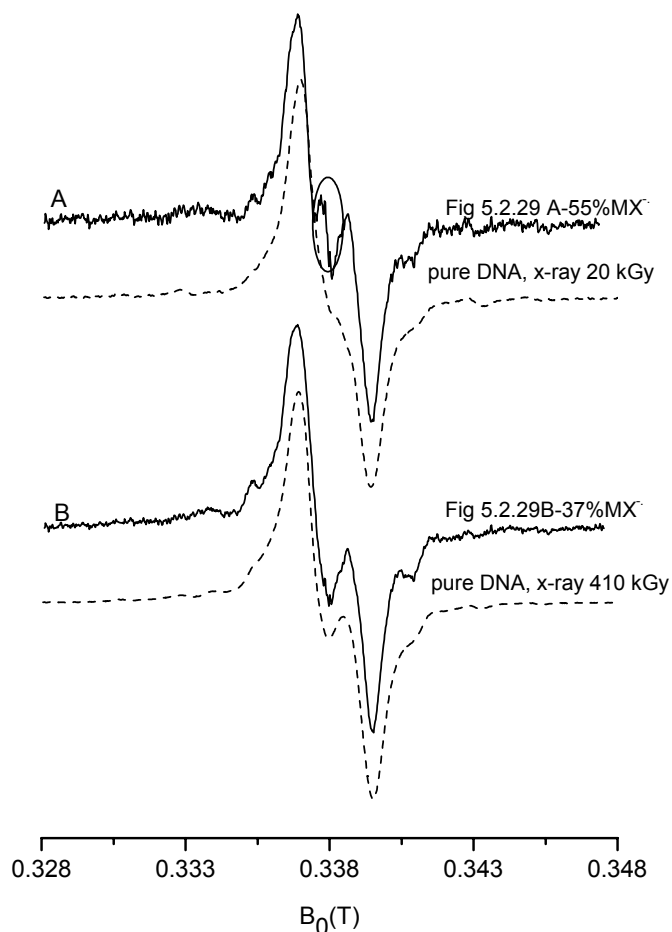
Fig. 5.2.32. Spectral pattern obtained after subtracting MX radical pattern from the experimental spectrum of MX:DNA (1:200) x ray irradiated by A) 20 kGY , the circle represents the presence of minor amount of MX pattern which could not be subtracted, and B) 440 kGY respectively and measured at 77 K after annealing to 140 K. Dashed ESR spectra are the experimental ESR spectra obtained from pure DNA after irradiation with similar doses and measured under identical conditions.

5.2.5. Discussion of the Free Radicals formed and on their Change in Contribution with Increasing Dose in Pure DNA and in DNA with Various Additives

The principal purpose of this work was to gain insight into the formation and change in concentration of primarily the oxidized radicals to gain more insight on the

mechanism of irradiation in frozen aqueous system with DNA as a substrate. For the first time both dose and temperature dependent studies are done on frozen aqueous (H_2O) system containing pure DNA or DNA and several additives ($K_3Fe[CN]_6$, $K_4Fe[CN]_6$ and Mitoxantrone). In order to understand the extent of direct irradiation in this system the hypothesis, was to examine the formation of guanine cation radical or if possible the deoxyribose radicals as they are formed via oxidation derived reactions. Complete analysis of the radicals from their ESR patterns at different temperatures, dose and with different additives was another task considered in this study. Although it was not possible from the scope of the work to differentiate between $T^{-\bullet}$ and $C^{-\bullet}$ radical patterns, and the doublet pattern used here is assumed to be consisting of both anion radical patterns. It is worth emphasizing here that all other isolated spectra used in reconstruction represent neat component patterns. It was primarily intended to isolate all the component patterns used for the reconstruction of the experimental spectra from the frozen aqueous system only. Doublet (from $T^{-\bullet}$ and $C^{-\bullet}/C(N3H^+)^{-\bullet}$) and doublet/ox pattern (either from $C4'^{\bullet}$ or $C5'^{\bullet}$) patterns could not be obtained in their pure form in frozen aqueous system and these patterns are taken from DNA in frozen glass or in 76% hydrated systems respectively.

In **Table 5.2.1** the contributions of each spectral patterns originating from one or a pair of particular radical species are summarized for all the systems after X ray treatment with 20 k Gy and annealing to 140 K before measurement at 77 K. It is very clear from this table that in pure DNA almost 50 % of the total radicals from oxidized species at low irradiation doses. With addition of electron scavenging additives like $K_3Fe[CN]_6$ at high concentrations enhances the oxidized radical formation to about 75% and suppresses the reduced species formation drastically. An opposite effect was observed on employing hole scavenger $K_4Fe[CN]_6$ with DNA in same concentrations. It is interesting to note that when MX is incorporated to DNA at very low concentrations (1MX:800 nucleotides) the proportion of oxidized vs. reduced radicals remains same like pure DNA only their internal distributions changes. With high concentrations of MX (1 MX:200 DNA nucleotides) although the fraction of doublet pattern originating from reduced anions decreases but a sharp decrease in guanine cation's spectral component is observed. MX itself scavenges more than 50% of the electrons during irradiation.

Table 5.2.1. Comparison of the relative proportions of the major spectral components from oxidized species vs. reduced species in different systems considered in this work upon annealing the samples to 140 K and then ESR measurement at 77 K.

		Oxidized radicals				Reduced radicals	
System	Dose (k Gy)	Singlet ($G^{+\bullet}$) (%), rel	Quartet ($C1'^{\bullet}$) (%), rel	Doublet/ox ($C4'^{\bullet}/C5'^{\bullet}$) (%), rel.	Sextet ($C3'^{\bullet}$) (%), rel.	Doublet ($C^{\bullet}$ or $T^{\bullet}$)(%), rel	Additive (%), rel.
Pure DNA	20	28	7.42	0	12.29	41	-
Fe^{3+}: DNA (1:20)	20	32	10	17.02	16.11	11.43	-
Fe^{2+}: DNA (1:20)	20	0	4	0.53	10	76	-
MX^- :DNA (1:800)	20	27	12	8.35	0	22	20
MX^- :DNA (1:200)	20	4.35	9.43	5	0	14.36	56

Comparison with other studies

Gregoli and co workers (1982) suggested for frozen aqueous solutions both direct type ionization on dry DNA skeleton and ionization of hydration water and transfer to DNA. They reported formation of two primary radicals $G^{+\bullet}$ and $T^{-\bullet}$ formed on DNA in frozen aqueous solution upon γ-irradiation at 77 K. Upon annealing $T^{-\bullet}$ was converted into secondary radical i.e. 5-thymyl radical through protonation at C6 position in anoxic conditions. In aerobic conditions at higher temperature a thymine located peroxyl radical was found. $G^{+\bullet}$ at neutral pH did not show any apparent transformation into a secondary radical at high temperatures. The authors although postulated the formation of $GOH^{\bullet}$ by addition of OH at C8 in alkaline conditions (pH 14) or in the presence of electron scavengers (iodoacetamide). The formation of a thymine based anion potentially in combination with a cytosine based anion radical and other thymine based radicals and guanine cation is observed also in this thesis as reported earlier by Gregoli and co workers. Although the formation of $GOH^{\bullet}$ radical could not be identified upon annealing in our study in spite using very high concentration of electron scavenger ($K_3Fe[CN]_6$). The formation of $GOH^{\bullet}$ was also not observed in another report using same electron scavenger (Cullis et. al. 1985). Gregoli and co workers also proposed approximately equal yield of formation for $G^{+\bullet}$ and $T^{-\bullet}$ upon irradiation of DNA at low temperatures. The

irradiation mechanism on frozen aqueous solution was refined by including an additional glass-like water shell in the immediate vicinity of the substrate and this effect was named as quasi direct irradiation mechanism (Symons 1991). Cytosine based anion radical C$^{-\bullet}$ was also proposed to be formed along with T$^{-\bullet}$ as primary radical in irradiated DNA by Hüttermann et. al. (1992a) and Lange (1994). No apparent successor was observed for the cytosine anion at higher temperature. Sevilla et. al. 1991 introduced another component i.e. adenine cation (less than 10%) supposed to be formed at 77 K in frozen aqueous DNA upon irradiation. This report and also Yan et. al. (1992) postulated transfer of electron from C$^{-\bullet}$ to thymine upon annealing from 77 K to 130 K, and then irreversible protonation at thymine shifts the anionic path to 5-thymyl radical (TH$^{\bullet}$). The possibility of electron transfer from T$^{\bullet -}$ to C on annealing from 77 K to 130 K does not influence the radical balance in this work as 140 K is taken as the first temperature point here to avoid the influence of OH radicals from the ESR spectra of irradiated DNA. The reports of Sevilla et. al. (1991), Yan et. al. (1992) done on frozen aqueous DNA in D$_2$O and another report on hydrated/deuterated DNA samples (Γ>18) (Wang et. al. 1994) estimated formation of 39% C$_D^{\bullet}$, 22% T$^{-\bullet}$ and 40% G$^{+\bullet}$ at 77 K upon irradiation with low doses (approx. 50 kGy) after annealing the DNA samples to 130 K. Thus it was proposed that hydrated DNA with Γ>18 (95% hydration) behaves in a similar manner like frozen aqueous DNA (Hüttermann et. al. 1992a). In a recent report (Shukla et. al. 2005) these values were modified to 38% C(N3)H$^{\bullet}$ which is more stable than C$^{-\bullet}$ due to protonation of C$^{-\bullet}$ at N3 (Wang et. al 1993), 10% T$^{-\bullet}$, 40% G$^{+\bullet}$ and 12% of sugar radicals for frozen aqueous DNA irradiated with 27 k Gy and annealed to 130 K before ESR measurement at 77 K. Lange and Hüttermann (1995) argued that the competition for scavenging electrons between DNA bases (thymine and cytosine) and the electron scavengers present in the system is a property seen more commonly in dilute solutions and frozen glasses. They proposed that therefore it is possible that in frozen aqueous solutions indirect effect of irradiation prevails. In their study they did not find any guanine based cation species and found similar electron scavenging efficiency of electron scavengers in both frozen aqueous and frozen glass solutions containing DNA and K$_3$Fe[CN]$_6$ in identical concentration. It should be noted that in dry DNA (a model for direct irradiation mechanism) plus K$_3$Fe[CN]$_6$ systems strong electron scavenging effect of K$_3$Fe[CN]$_6$ was observed (Weiland nd Hüttermann 1998) and that the scavenging efficiency of the additives cannot be the only factor to understand the mechanism of

irradiation in frozen aqueous system. Burger (1999) found formation of 10% of guanine cation radicals DNA in frozen aqueous solution and also observed formation of N1 deprotonated guanine cation at higher temperature The percentage of guanine cation as reported in this thesis is about 28% for pure DNA on irradiation with low dose of 20 k Gy which is little altered in the presence of electron scavenger like $K_3Fe[CN]_6$ or low concentrations of MX (1MX:800 DNA). With high concentrations of MX (1 MX:200 DNA nucleotides) though a sharp decrease in guanine cation's spectral component is observed. In the literature there are evidence that the secondary nitrogen on the side chain of the MX reacts with the N-2 exocyclic amino of guanine to form adduct with DNA (Parker et. al. 2004). But a clear explanation of this result is still not known. The percentage of 28% $G^{+\bullet}$ is in between the numbers observed in earlier results. The studies done in this thesis shows that guanine cation is primarily formed in pure DNA at low temperatures (140 K) but undergoes a sharp decay with increase in dose.

The doublet ESR pattern obtained in this thesis from strong reducing conditions (Fe^{2+} and DNA (1:20), (20 kGy)) is similar to that obtained from doublet pattern from DNA in reducing glass (7 M $LiBr/H_2O$) and is supposed to consist of both $C^{-\bullet}$/ $C(N3)H^{\bullet}$ and $T^{-\bullet}$. The doublet pattern of DNA in glass (consisting of all base derived reduced species in irradiated DNA) shows a close proximity with the hyperfine splitting of the doublet pattern ($T^{-\bullet}$) (at low dose conditions) (**Fig. 5.2.15**) obtained under same condition; nonetheless, a contribution from $C^{-\bullet}$ cannot be excluded, a quantitative separation of $C^{-\bullet}$ and $T^{-\bullet}$ radical patterns was not possible from the composite spectrum obtained. The percentage of reduced species in our work is found to be of 41% in pure DNA and about 76% in Fe^{2+}/DNA (1:20) both irradiated with 20 kGy annealed to 140 K and then measuring at 77 K. In the presence of electron scavengers Fe^{2+} and MX the reduced species were strongly reduced. The doublet pattern is also found to be reduced with increasing dose at 140 K in pure DNA

We consider first the fate of base derived primary charged radicals with increasing dose at three representative temperature points. It has been explained previously that because of coulombic attractions, charged radicals are more susceptible to recombination from holes and electrons produced by radiation (Shukla et. al. 2005 and references therein). This explains the decline of singlet and doublet pattern with increasing dose as they initiate from potentially charged guanine and cytosine/thymine

bases, respectively. The singlet pattern from guanine cation decays faster than the doublet spectral component, this phenomenon has been observed before and has been attributed to the prevalence of an overall reducing environment due to excess electrons in the system at 77 K. An earlier proposal made by Hüttermann and coworkers (1992b) may also be considered here for explaining the faster decay of guanine cation both in pure and additive containing DNA which suggests that in frozen aqueous system the electrons formed in bulk ice may migrate through the phase separation to the DNA while the holes remains trapped in the ice phase.

In the Fe^{3+} /DNA system (**Fig. 5.2.2.3**) the amount of $G^{+\bullet}$ increases only nominally at low dose systems but the decay of $G^{+\bullet}$ radical's spectral pattern with increase in irradiation dose is much faster than in pure DNA. It has been discussed in a previous report (Shukla et. al. 2005) that after accepting electrons from the system Fe^{3+} is converted into Fe^{2+} which itself is a strong hole scavenger and thus leads to destruction of guanine cation. The specific mechanism of this proposal is not yet known. It has also been observed that UV – illumination of guanine cation at 77 K results into formation of $C1^{'}$ sugar radical via hole transfer (Shukla et. al. 2004). It has been also observed that in dry DNA system containing additives like $K_3Fe[CN]_6$ or Azomycin the guanine cation pattern converts into quartet pattern (consisting of C1' sugar and allyl radical component) at a certain temperature (private communication) which may also be due to hole transfer from guanine moiety to a nearby C1' sugar molecule. This process may also be one reason for the fast decay of guanine cation with dose. Although in our studies a direct correlation between decay in guanine cation and an increase in $C1'^{\bullet}$ sugar radical is not observed. In the frozen aqueous DNA solution Fe^{2+} acts as a strong hole scavenger as has been reported earlier (Shukla et. al. 2005). Gunaine cations are heavily scavenged in the presence of Fe^{2+} as expected. This shows the close association between the DNA and the scavenger molecules. An unanticipated effect observed here was absolute decrease in the formation of guanine cation radical when the high amount of MX was used with DNA (1MX:200DNA nucleotide). This can be directly observed from the overlap of spectrum obtained by subtraction of MX radical pattern from MX:DNA (1:200) upon irradiation with 20 kGy with that of pure DNA. The reason behind such reduction in guanine cation radical may be due to the binding nature of MX. It might be possible that due to adduct formation between MX and guanine there is formation of MX cation radical in this system The MX cation radical does also have

same sharp singlet structure (Cai et. al. 2001) and separation of MX anionic species from that of MX cation radical was not possible in this study. It was not possible to understand the exact reason behind this result.

The proportion of doublet pattern from anionic base moieties reduces to great extent in the presence of the electron scavengers. Fe^{3+} is only closely associated to DNA and is found to be strongly effective when it is present in large ratio of 1 Fe^{3+} to 20 DNA nucleotides. MX can bind with DNA via intercalation and therefore is found to effectively scavenge 20 % of the electrons when only 1 MX is present for 800 DNA nucleotides. At molar ratio of 1MX:200 DNA the electron scavenging capacity of MX is equivalent to 1Fe^{3+}:20 DNA.

Hüttermann et. al. (1992a) showed the formation of allyl radical in 95% hydrated DNA prepared from in both H_2O and D_2O. The allyl radical is found to form by net H abstraction of methyl group present in thymine. It can be formed via both direct irradiation and indirect irradiation. They did not analyze the exact concentration of this radical. Weiland and Hüttermann (1998) also isolated allyl radical in dry Fe^{3+}/ DNA system but they used combined pattern of C1' sugar radical and allyl radical for spectral reconstruction. Burger (1999) also used same method for reconstruction of ESR spectra from frozen aqueous DNA solutions and about 40% of this combined pattern was found even at annealing temperature of 140 K. Although the allyl radical is found to be more prominently observed at high temperatures with D_2O containing matrices, Shukla et. al. (2005) did not report formation of these radicals may be because of working only at low temperatures where less than 5% of allyl radical formation is observed in our studies. It becomes prominent after 200 K in all systems studied here but can be distinctly isolated only at 240-260 K. In pure DNA formation of allyl radical is observed at high dose, high annealing temperature. The identification of fully resolved allyl radical pattern in these experimental spectra was not possible due to overlap from several other spectral patterns. In MX-DNA (1:200) system at 240 K octet pattern is not found at higher temperature although an average of 20% of doublet spectral component was observed at 140 K. Instead a clear indication of allyl radical is obtained in this system at higher temperatures. **Fig. 5.2.33** shows the experimental evidence (shown by asterisks) of formation of allyl radical for the first time in frozen aqueous MX:DNA (1:200) in H_2O at 260 K. It can be seen that the formation of allyl radical enhances with increasing dose which is expected due to its neutral character
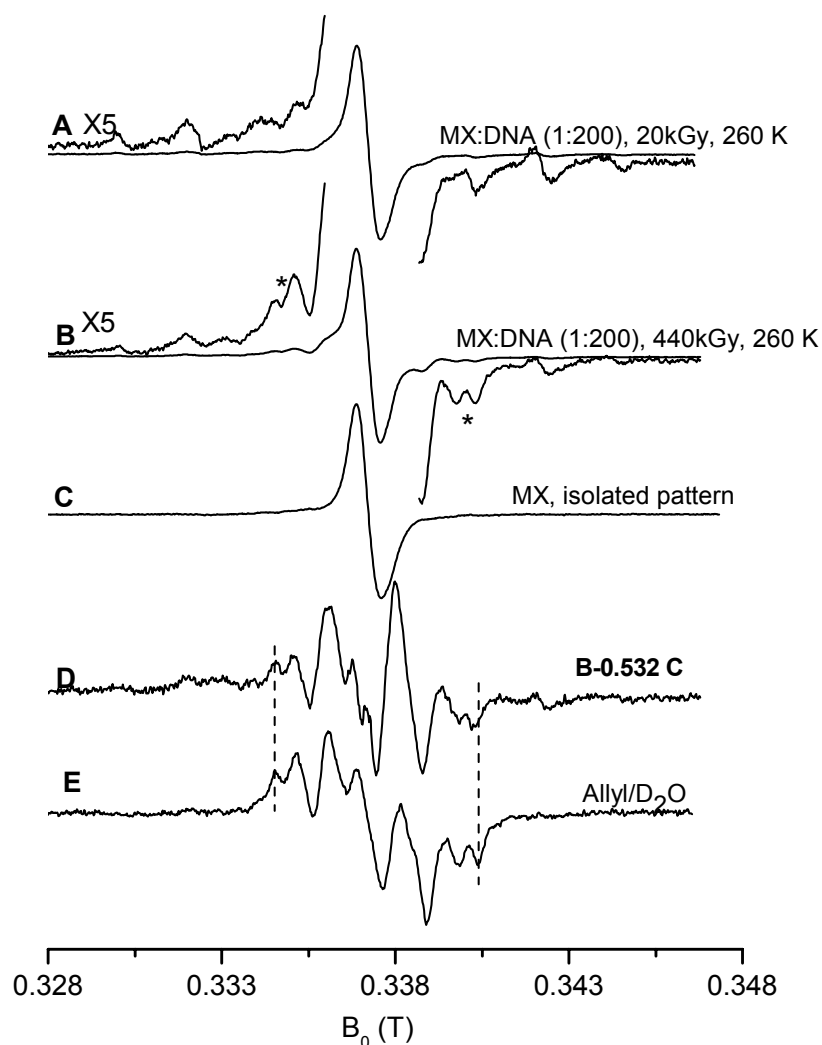
Fig. 5.2.33. X band ESR spectra of ice plugs of MX:DNA (1:200) (50 mg/ml H_2O) upon A) X ray irradiation with 20 k Gy, annealed to 260 K, B) X ray irradiated with 440 k Gy, annealed to 260 K, C) Isolated pattern of MX (same as in 5.2.28C), D) Spectrum obtained from subtraction of isolated MX pattern from ESR spectrum of MX:DNA (1:200) irradiated with 440 k Gy annealed to 260 K, showing the presence of allyl radical, E) Allyl radical pattern isolated from X ray irradiated pure DNA dissolved in D_2O (same as in 5.2.10F).

Characterization of the sugar radicals in irradiated DNA with low doses at low temperature has been a challenge due to its formation in small fraction and because of the variety of sugar radical confomations defined by the pseudo –rotation cycles (Sänger 1984). Cullis et. al. (1985 and 1986) proposed the formation of sugar radicals (denoted as 'X') via H-abstraction from various sites of deoxyribose units but they could not

identify the radical based on sugar moieties. They also connected these sugar radicals to be responsible for with double strand break in DNA upon irradiation. Wang et. al. (1994) obtained a bench mark spectra of sugar radical ($S^{\bullet}$) from irradiated 5'-deoxyphosphate sugar and showed that the fraction of this $S^{\bullet}$ increases with increasing hydration level and increasing dose giving a strong indication of their formation through $OH^{\bullet}$ attack from the hydration layer. Lange et. al. (1995) pointed out formation of a broad doublet (denote as doublet/ox) in frozen aqueous DNA in the presence of high electron scavenger ($K_3Fe[CN]_6$) concentration. This doublet/ox pattern was also identified at high temperature (200 K) in 76% hydrated DNA containing Fe^{3+} and was proposed to be a sugar radical component preferably on C4' or C5' position of deoxyribose moiety (Weiland and Hüttermann 1998). This broad ESR finger print is also observed in the recent report by Shukla et. al (2005) but whether its origin is from $C4'^{\bullet}$ /$C5'^{\bullet}$ or from $C5'^{\bullet}_{dephos}$ (about 30% is found) is not understood. The formation of same doublet/ox is observed in our studies also particularly in DNA containing very high concentration of electron scavenger and on treatment with high doses. It was not possible to isolate this pattern in pure state form our studies. The doublet/ox pattern obtained from 76% hydrated Fe^{3+}/DNA is used in this study for spectral reconstruction. The doublet/ox pattern is found to be present in minor quantities (< 5%) at 140 K upon irradiation of frozen aqueous DNA with moderate dose (45-145 kGy) but its proportion increases with increase in irradiation dose (~15`%). This radical pattern constitutes major proportion in the Fe3+/DNA (1:20) (>15%) and MX:DNA (1:800) (varies from 10-20%) systems specifically in high dose high annealing temperature conditions. In MX:DNA (1:200) the ESR pattern is dominated by MX radical and presence of doublet/ox pattern is not well observed. In Fe^{2+}/DNA (1:20) solutions the proportion of doublet/ox increases with increasing dose at 140 K and at high annealing temperatures. A plausible identification of the $C3'^{\bullet}$(or $C4'^{\bullet}$) in oxygen 16 irradiated hydrated DNA was made by Becker et. al. (1996). Weiland and Hüttermann also observed same pattern (1999) in dry DNA after irradiation with heavy ions. In the recent study done by Shukla et. al (2005) only 4% of this radical pattern is reported to be formed in hydrated DNA/D_2O upon irradiation with 152 kGy of γ-irradiation This sextet pattern is confirmed to be from $C3'^{\bullet}$ by Adhikary et. al. (2005). In this thesis the formation of sextet pattern is observed even at very low dose irradiation of DNA and at low annealing (140 K) temperature. This radical pattern constitutes major proportion of total radical balance in DNA upon irradiation with high doses and also in Fe^{3+}:DNA and MX:DNA (1:800). An unexpected effect observed here

is that upon irradiation with low doses of X ray that at high concentrations of Fe^{2+} ($1Fe^{2+}$:20 DNA nucleotides) the guanine cations are completely scavenged but the oxidized radicals originating from C3'/C4' could still be observed from the ESR spectra. Formation of neutral radical cohort under similar conditions was also observed by Shukla et. al. (2005). Considering the direct and quasi-direct effect of irradiation mechanism in frozen aqueous solutions they have explained that the cation radical precursor ($DNA^{+\bullet}$) produced upon irradiation will prefer to undergo deprotonation (faster process takes few picoseconds) to form a neutral sugar radical in comparison to hole transfer from the cation precursor to nearby Fe^{2+} (1-100μs). In MX:DNA (1:200) systems again the minor formation of sextet pattern is only observed at high doses. C1'$^{\bullet}$ sugar radical have been identified in dry and hydrated DNA in high oxidizing conditions previously (Weiland and Hüttermann 1998). Formation of this sugar radical has also been observed by photoexcitation of previously stabilized guanine cation in frozen aqueous DNA (Shukla et. al. 2004). Shukla et. al. 2005 showed presence of 6% of Ci'$^{\bullet}$ radical pattern after irradiation of hydrated DNA with high doses. In this thesis C1'$^{\bullet}$ sugar radical pattern can be very well isolated by single subtraction step from DNA irradiated with high doses. It is found to be formed to be 7-10% in all the systems studied and is only moderately affected with increasing dose and annealing temperature. This result is in close agreement with Shukla et. al. 2005. It is important to mention here that Weiland and Hüttermann (1998) used a 'quartet' pattern (combination of C1'$^{\bullet}$ and allyl radical) (**Fig. 5.2.9E**) and found about 28% of these pattern in 76% hydrated DNA while Burger (1999) used the same pattern in reconstruction of frozen aqueous DNA spectra obtained after irradiation with moderate dose. At 140 K 40% of this quartet pattern was observed by Burer (1999) which is a high representation of C1'$^{\bullet}$ as formation of allyl radical is observed only in negligible amounts at low annealing temperature. We would like to mention the presence of the flanges at the outer wings of the 'quartet' pattern (**Fig. 5.2.9E**) used by Weiland and Hüttermann (1998) and Burger (1999) correlates with the sextet patterns and that might be the reason behind the disagreement of their result with us.

TH$^{\bullet}$ is obtained as a prominent secondary (200K) radical (derived from protonation of T$^{-\bullet}$) in DNA and Fe^{2+}:DNA at low doses (20-25%) but it decreases with increasing dose as its precursor T$^{-\bullet}$ also decreases.

Peroxy radical consisted 5-10% of the total radical concentration in most of the cases shows minor presence of oxygen in the systems studied. This radical can form from addition of O_2 on the C5 position of C6 protonated thymine anion or from direct addition on non protonated thymine anion (Gregoli et. al. 1982). In Fe^{3+} plus DNA systems the annealing series always ended up giving only peroxy radical patterns (240K) at all doses irrespective of the fact that samples where prepared in the strict anaerobic conditions. This phenomenon is not observed in any other additive-DNA combined systems. It can be that the Fe^{2+} formed after electron capture by Fe^{3+} may be responsible for its formation through reaction with hydrogen peroxide formed after water radiolysis (Henle and Linn 1997).

Triplet pattern arising from $C(N4H^+)^{\bullet-}$ has been observed in irradiate frozen aqueous solution of dCMP (Przybytniak et. al. 1997), in dry DNA (Weiland and Hüttermann 1998). This radical pattern could not be isolated from the series of spectra obtained during our study. Shukla et. al. (2005) reported formation of 8% $C3"^{\bullet}_{dephos}$ in their study with outer line component at about 13.4 mT apart. This broad spectral pattern was not observed in our work in spite of using very high dose of 870 kGy. A phosphate radical of type $ROPO_2^{-\bullet}$ was reported to be formed in hydrated DNA on irradiation with heavy ions (Becker et. al. 1996 and 2003). It was not possible to observe this radical in our set up because the irradiation source was always X ray.

This study offers a detailed knowledge about the formation of DNA based radicals in irradiated frozen aqueous solutions of DNA. More than the only two primary radicals proposed by Gregoli et. al. (1982) could be isolated here from the experimental spectra. Formation of oxidized radicals on guanine cation radical is confirmed even in pure DNA. Radicals derived from deoxyribose moieties are also observed similar to the irradiated frozen aqueous solutions of FU derivatives specifically in the presence of electron scavenger. This provides evidence for direct irradiation effect in frozen aqueous DNA. There are differences in the percentage of formation of radicals from the previous reports (Shukla et. al. 2005). It is necessary to mention here that Shukla et. al. (2005) have used deuterated samples, different doses of γ-irradiation, different level of hydration and they have used benchmark spectra obtained from neucleotides or simulated patterns for reconstruction of the experimental spectra. It can be generalized that the formation of a radical on DNA upon irradiation is very much dependent on the

chemical environment, hydration level, irradiation dose, irradiation quality, annealing temperature and additives used in a system.

5.3. Study of Temporal Behavior of Radicals formed on DNA or on its Mixtures with Electron Scavenging Additives in LiBr Glass at Low Temperatures[2]

In this part of the thesis, the time dependent behavior of radicals formed on DNA or in a mixed system containing DNA and electron scavenging additives mitoxantrone (MX) or riboflavin (RF) with respect to time has been discussed. Messers et. al. in 2000 postulated that the possibility of *post irradiation* electron transfer in from DNA to intercalating additives (for example MX or Ethidium bromide) both present in frozen glass matrix through single step electron tunneling process at very low temperature. On the contrary, it has been previously observed in this laboratory that although spins transfer from protein (histone) to DNA *during* irradiation but the radicals once formed on each compartments tend only to protonate or deprotonate within their vicinity of the primary radicals without having any intermolecular interaction and decay independently with increasing temperature of the system (Weiland and Hüttermann 2000) **(see 3.1.3)**. This led us to reinvestigate temporal effect on radicals formed on DNA or DNA – additive colyophillised mixture system in frozen glass matrix (7 M LiBr/D_2O) after X-ray irradiation. Observations were done on neat DNA and neat additive (MX and RF) systems as well as on their colyophillised mixtures. DNA –MX systems were irradiated with different x–ray doses (800 Gy, 1.6 kGy and 10 kGy) to investigate the effect of irradiation dose. In order to get into more details we widened our investigation with deoxyribonucleotide systems like thymidine 5'-monophosphate (sodium salt) (TMP) and 2'-deoxycytidine 5' – monophosphate (sodium salt) (dCMP). MX and RF are used as electron scavenging additives which have different binding mode with DNA. MX intercalates with DNA (Messers et. al. 2000) and RF forms a close association in the vicinity of guanine residues (Ito et. al. 1993). In order to control the quantitative ESR measurements a stable free radical, TEMPOL (4-hydroxy-2,2,6,6-tetramethylpiperidine-1-oxyl) was used as an external standard for all the measurements. Neat 7 M LiBr/D_2O samples was also irradiated and measured for baseline corrections. **Fig. 5.3.1** gives the structure of the electron scavenging additives and TEMPOL used in this work. Because

---

[2] The major parts of results and discussion on the study of temporal behavior of radicals produced on DNA and its mixture in frozen glass system has been published in Pal and Hüttermann (2006).

of quantitative nature of the study the experiments were performed more than once for reproducibility.
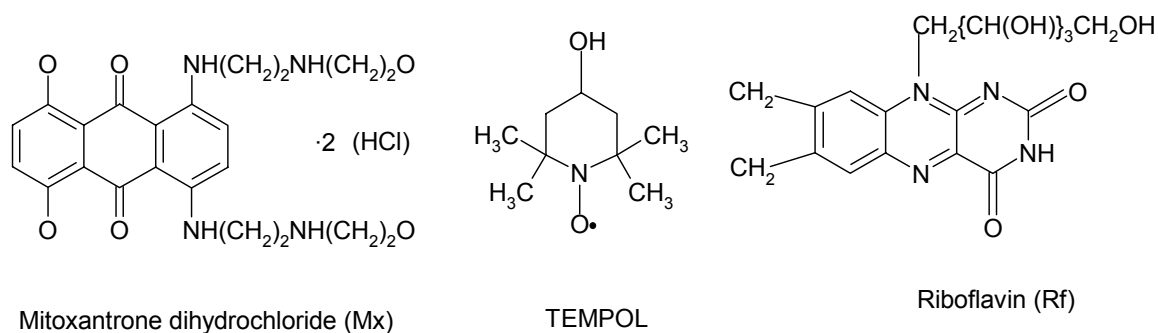
Fig. 5.3.1. Structures of electron scavenging additives and TEMPOL as employed in this work.

5.3.1. Reaction and Products in LiBr Frozen Glasses

Addition of 7 M LiBr in D_2O produces ions which forms salvation shells around them and forbid the aqueous medium to form polycrystalline matrix upon freezing. Frozen 7 M LiBr/ D_2O produces amorphous transparent glassy matrix. Adding low concentration of substrates (DNA / deoxynucleotides or/ and additives) at room temperature and then on freezing it, a transparent solid is formed. Upon x-ray irradiation of neat 7 M LiBr/ D_2O glass at 77 K holes and electrons are produced. Holes are scavenged by bromide ions to give $Br_2^{-\bullet}$. This species gives a very broad (approximately 120 mT) ESR spectrum which has a baseline type character. The electrons trapped can also be observed. The presence of the substrates upon irradiation results into scavenging of electrons formed on the matrix and producing their electron adducts selectively. These electron adduct formation can be very well monitored by ESR spectroscopy. The ESR character of the matrix remains unchanged in the time frame of measurement at constant temperature.

5.3.2. Mitoxantrone and DNA

Representative ESR spectra of irradiated frozen LiBr glass sample containing DNA together with two different loadings of randomly interspaced MX are shown in **Fig. 5.3.2** and **5.3.3**. Recordings from A-C are for concentration of one molecule of MX per 100 DNA nucleotides (denoted 1:100) and the spectra D-F are for 1:50 ratio. The first two
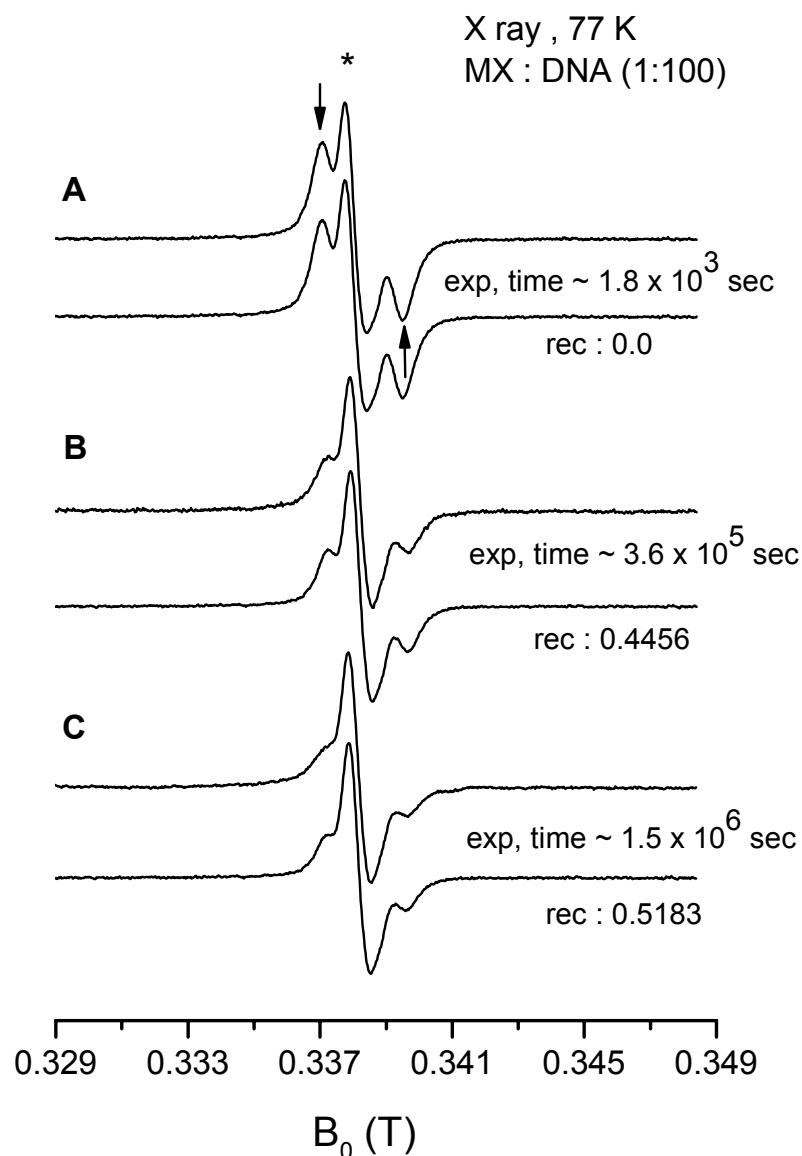
Fig. 5.3.2. A-C) Temporal development at 77 K of first derivative ESR spectra (X-band ~ 9.5 GHz) of 20 mg/ml of a MX:DNA mixture in 1:100 in 7 M LiBr/ D_2O glass. Each experimental spectrum is accompanied by respective reconstructed spectrum (denoted as rec.) from neat DNA and MX patterns along with their goodness of fit value (see text). The parts originated from MX and DNA in the composite mixture spectrum has been denoted by an asterisk and an arrow. The time of measurement of each spectrum after irradiation has been indicated.

spectra of the series (recordings A and D, respectively) were taken at about 30 minutes after irradiation.
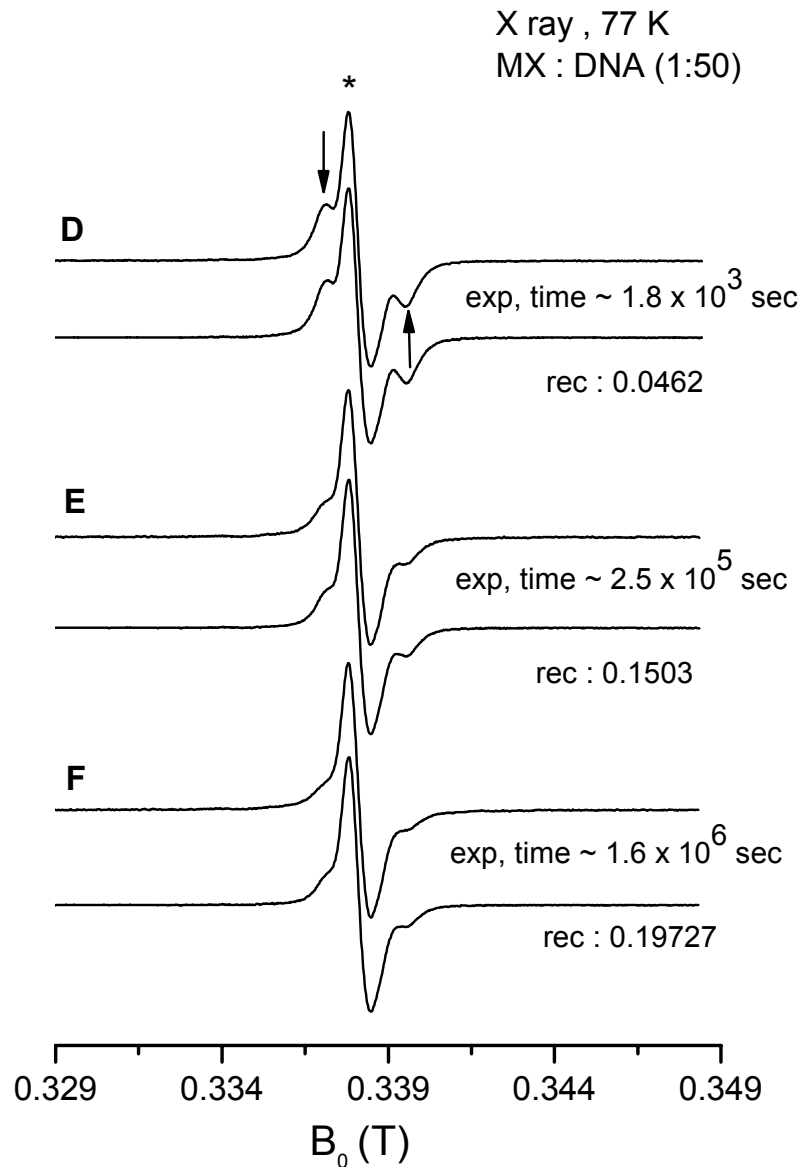
Fig. 5.3.3. D-F) Temporal development at 77 K of first derivative ESR spectra (X-band ~ 9.5 GHz) of 20 mg/ml of a MX:DNA mixture in 1:50 in 7 M LiBr/ D_2O glass. Each experimental spectrum is accompanied by respective reconstructed spectrum (denoted as rec.) from neat DNA and MX patterns along with their goodness of fit value (see text). The parts originated from MX and DNA in the composite mixture spectrum has been denoted by an asterisk and an arrow. The time of measurement of each spectrum after irradiation has been indicated.

The subsequent ESR spectra (B-F) were obtained at different time frames as indicated in the figures. The spectra were reconstructed from neat patterns of DNA and of MX (shown later). The sharp MX and broad DNA anion radical part in the composite spectra in **Fig 5.3.2** and **Fig. 5.3.3** has been indicated by an asterisk and an arrow. The reconstructed spectra are given beneath each experimental one along with the goodness of fit value. From the reconstructions the relative contribution of the MX anion radical pattern produced is found to be 30% and 45% respectively, in the initial spectra A and D of systems 1:100 and 1:50 (MX:DNA nucleotides). MX acts as a strong electron scavenger under these conditions as the radical yields are significantly higher than expected from the molar ratio. The relative concentration of MX anion radical seems to increase with increasing time period and on evaluation it can be found that after about 18 days (spectra C and F, respectively) the fraction of MX located radicals has increased to about 47% and 62% for the 1:100 and the 1:50 concentration ratios. The DNA – related contribution has decreased from 70% to about 53% at the ratio of 1:100 and from about 55% to 38% when the ratio of MX was increased to 1:50.

The time dependent variation of the weight of the components associated with MX and DNA in the spectra is dose dependent. The above analysis was performed for three doses (800 Gy, 1.6 kGy and 10 kGy respectively) for both additive concentrations. The dose value 800 Gy corresponds closely to that used by Messers et. al. 2000. It is observed that the independent component (MX and DNA) weights changes more significantly with time in low doses than with 10 kGy. The values are represented for each dose used in MX:DNA systems for both ratios in **Table 5.3.1**. For all doses and additive concentrations, however the trend is similar i.e. the apparent (or relative) contribution of MX radicals to spectra increases significantly with time. This finding formed the basis of suggesting post irradiation electron transfer with time from DNA to MX under these conditions (Messers et. al. 2000).

However, the analysis of the total radical concentration of the same set of experimental spectra over the same time period of time displays a considerable decay of radicals at 77K. The corresponding data are shown in **Fig. 5.3.4 (top)**. For the two concentrations of MX vs. DNA as discussed above, the total amount of free radicals are given as the respective double integral value of the baseline corrected experimental spectra. Data included are only from 800 Gy and 10 kGy dose analysis to avoid overcrowding of the data points but all three cases are discussed in text. The

normalization for each set of data is to the first spectrum taken after irradiation (at about 30 minutes). Normalized spin control (Double integral value) of TEMPOL standard is used as a control and is found to be constant with time as expected.

Table 5.3.1. Relative concentration (%) of [MX$^{\bullet}$] and [DNA$^{\bullet}$] radicals at 77 K with increasing time in frozen LiBr glass irradiated at 77 K.

MX:DNA nucleotide (Molar ratio)	dose (kGy)	time (sec)	MX$^{\bullet-}$ (%)	DNA$^{\bullet-}$ (%)	goodness of fit
1:100	0.8	1.8 x 103	29	71	0
		1.95 x105	53	47	0.035
		1.3 x 106	61	38	0.207
	1.66	2.9 x 103	31	69	0.1111
		1.9 x105	50	50	0.3017
		1.6 x 106	62	38	0.0818
	10	1.8 x 103	30	70	0.0
		3.6 x 105	42	58	0.4456
		1.5 x 106	47	53	0.5183
1:50	0.8	1.8 x 103	45	55	0
		1.9 x 105	63	37	0.0799
		1.2 x 106	69	31	0.0926
	1.66	3 x 103	50	50	0
		1.9 x 105	67	33	0.0132
		1.6 x 106	73	27	0.0992
	10	1.8 x 103	44	56	0.0462
		2.5 x 105	56	44	0.1503
		1.3 x 106	62	38	0.1972

The decay of the radicals with time at 77 K appears to exhibit approximately two different regimes under all conditions (concentration, dose) which could be termed a ''fast'' and a ''slow'' decay regime. The first is responsible for the loss of about 35% of the initial radical population within approximately 2 days of time. Though small differences are seen relating to MX and DNA concentration ratios and the irradiation doses, but the overall picture remains unchanged by these factors. About 50-60% of the initial radical population is lost within the total time of study. This is new and essential information for MX/DNA studied in glass system at low temperature. This observation necessitates additional detailed exploration of the system since the presumed electron transfer from DNA anions to MX must be weighed against total radical decay. Accordingly as an alternative of electron transfer, the reason behind observed relative shift in fraction of MX and DNA located radicals with time in the experimental spectra

could be differential decay behavior of the two constituting radical parts in the aqueous low temperature LiBr glass matrix (see next).
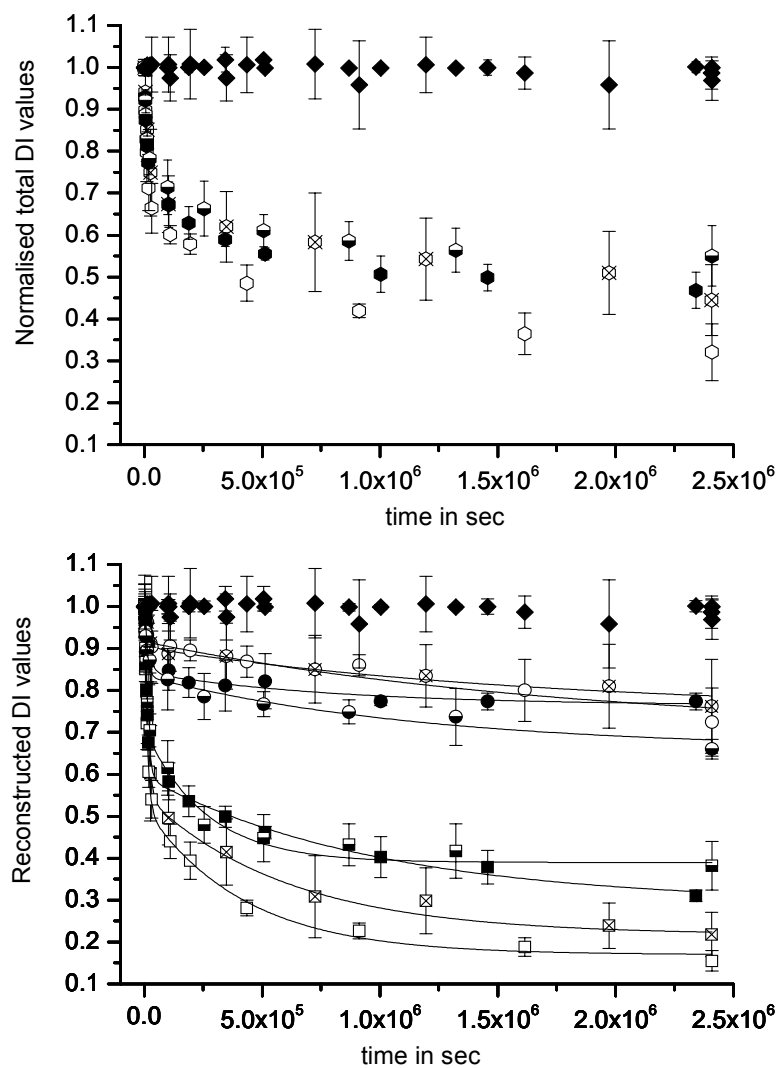
Fig. 5.3.4. (Top) Change in total radical concentration with time of MX:DNA mixtures at 77 K given as double integral (DI) values normalized to the first measurement ~ 30 minute after X-ray irradiation in comparison with an external standard TEMPOL (closed rhombic points). Daata from two experiments are shown: 1:100/ 800 Gy (open hexagons); 1:50/ 800 Gy(crossed hexagons); 1:100/ 10 kGy (filled hexagons); 1:50/ 10 kGy (half filled hexagons). (Bottom) Delineation of the above data into MX and DNA radical components and their change with time using the patterns from pure DNA and MX systems. The conventions are kept same only hexagons have been changed into circles. The solid line represents the bi - exponential fit to the experimental data.

The decay of free radicals from neat DNA in the LiBr glass under the same condition has been considered first. The initial and final ESR spectra at 77 K obtained in the time period of study from pure DNA after irradiation at two different doses (800 Gy and 10 kGy) are shown in **Fig. 5.3.5 (top)**. The nature of the pattern remains same with time but the signal to noise ratio decreases in both cases. The bottom part of Fig. 5.3.5 shows the decay of DNA radical concentration as a function of time. Similar to the MX/ DNA systems discussed above a fast and slow component of decay is observed here also. About 70-80% of DNA-located free radicals are lost with in the period of observation.

The comparable results obtained from neat MX in LiBr glasses are shown in **Fig. 5.3.6**. Like in DNA, the shape of the spectra of MX radical is found to be stable with time and independent of irradiation dose as shown in **Fig. 5.3.6 (Top)**. The concentration of MX radical also shows decay with time although at a lower rate in comparison to neat DNA system. About 30-40% of total radicals are lost over the study period with a similar division of fast and slow decay regime.

Discussion

The fast and slow decay regimes observed in the nature of change of radical concentration in all the cases observed above can by analyzed numerically through the following equation where x represents the time and y the radical concentration.

$$y = y_0 + A_1(\exp(-x/t_1)) + A_2(\exp(-x/t_2))$$

(5.3.1)

The respective fitting parameter A and t obtained for the DNA system irradiated at three different doses are shown in **Fig 5.3.5 (Bottom)**. The values are listed in **Table 5.3.2**. The respective value of t_1 and t_2 varies by about a factor of 40-70 thus supporting the validity of bi-exponential analysis

The same analysis for MX decay data gives the fitting results shown for the three doses in the bottom part of **Fig. 5.3.6**. The respective time constants and the other parameters are listed in **Table 5.3.2**. In MX the two values of t differ by a factor of 30-40 magnitude only. Most importantly, the constants and the weight for the fast and the slow components for DNA and for MX differ noticeably.
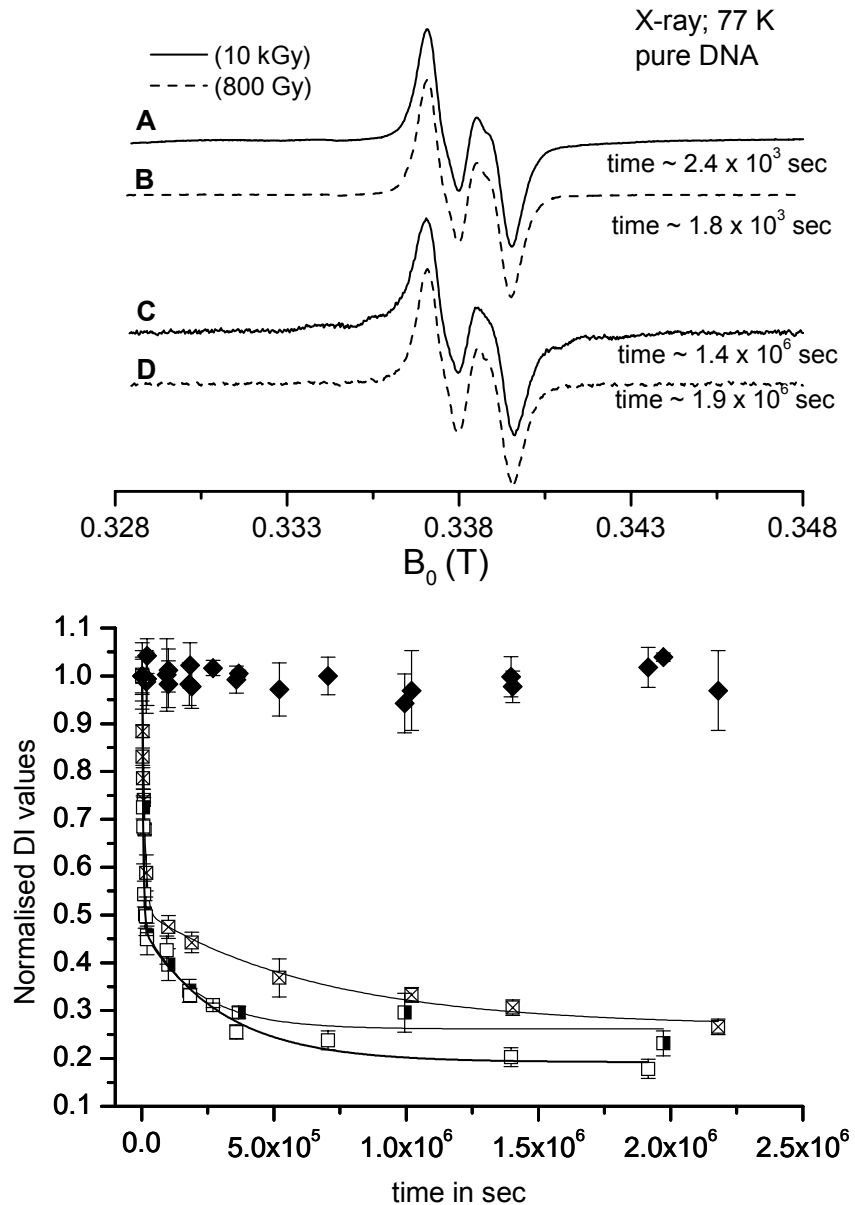
Fig. 5.3.5. (Top) Initial (A, B) and final (C, D) ESR spectra of pure DNA (20 mg/1ml of 7 M LiBr/D_2O) irradiate at 77 K with 10 kGy (Solid lines) or 800 Gy (dotted lines). The time of measurement after irradiation has been indicated against each spectrum. (Bottom) Development of the total DNA radical concentration with time at 77 K. Data are shown for irradiation doses: 800 Gy (open squares); 1.6 kGy (half filled squares) and 10 kGy (crossed squares). The external standard (TEMPOL) data are shown by filled rhombic points. The solid line represents the bi-exponential fits to the data.

DNA radicals seem to decay at much faster rates than radicals formed on MX. Therefore if the two components in the mixed DNA/MX system would decay independently (i.e., with the same constants as in the neat systems), an increasing predominance of MX located electron adducts with time would be expected.
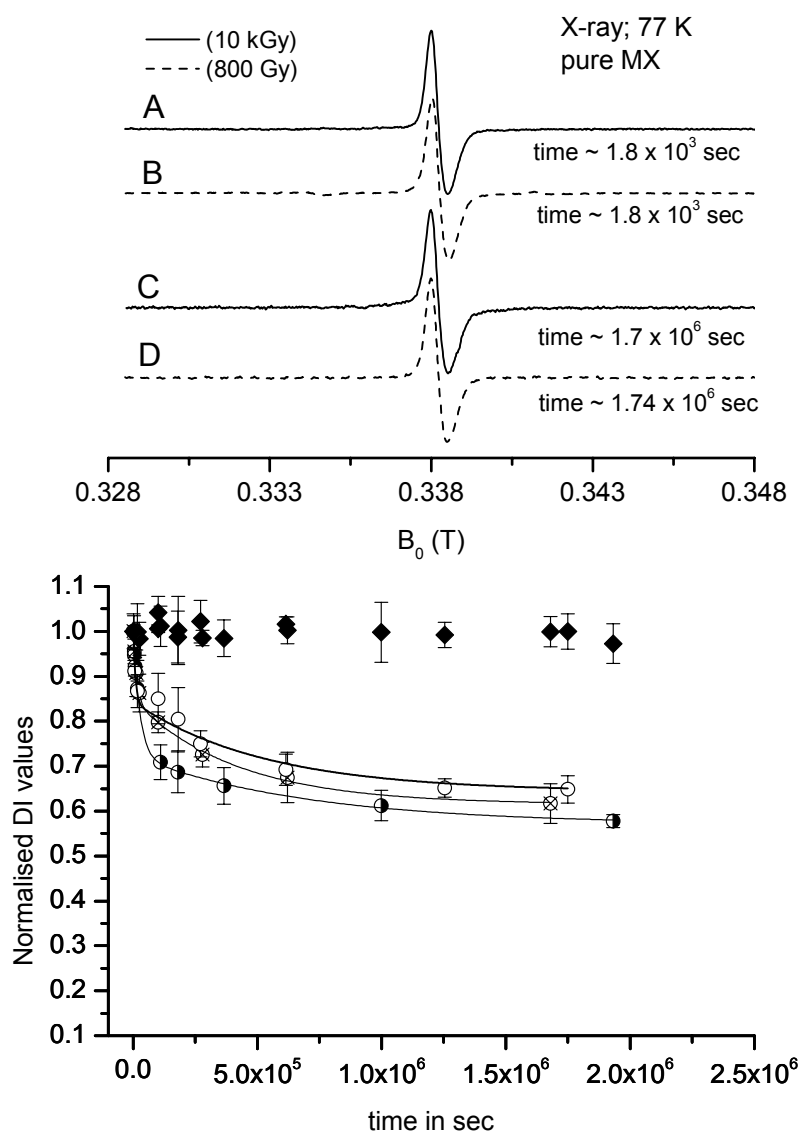
Fig. 5.3.6. (Top) Same as in Fig. 5.3.5 but for pure MX (1mg/ml). (Bottom) Data are accumulated in same fashion as in Fig.5.3.5 but for pure MX systems.

Table 5.3.2. Parameters A_1, t_1, A_2, t_2 obtained from fitting the experimental time dependent decay data at 77 K to y = y_0 + A1(exp(-x/t_1)) + A2(exp(-x/t_2)) for the DNA and the additive radical fractions in pure systems[1,2].

System	dose (kGy)	A_1 (%err)	t_1 (sec) (%err)	A_2 (%err)	t_2 (sec) (%err)
Pure DNA	0.8	0.787 (6%)	4522 (13%)	0.284 (7.4%)	296581 (15%)
	1.66	0.787 (6.5%)	4470 (15 %)	0.212 (11.3%)	203999 (23%)
	10	0.543 (5%)	9492 (12%)	0.241 (9%)	671485 (18.6%)
Pure MX	0.8	0.192 (18%)	8272 (34%)	0.2 (12.5%)	527794 (17%)
	1.66	0.291 (6.2%)	26306 (17%)	0.152 (9.2%)	699965 (21.6%)
	10	0.177 (9%)	13567 (22%)	0.231 (6.5%)	416383 (12%)
Pure RF	10	0.260 (20%)	4107 (25.2%)	0.195 (9.7%)	219310 (24.5%)

[1]The relative error in (%) for each parameter is shown in parentheses as calculated from absolute errors obtained from nonlinear least squares fitting routine used by ORIGIN. [2] The R^2 values showing goodness of fit of between several experimental repeats ranges from 0.992 ± 0.00734.

Spectra reconstruction method was used for the analysis of the decay behavior of MX/ DNA (1:100 and 1:50) systems. Each experimental spectrum was numerically reconstructed by using neat patterns of DNA and MX components. This finally gives the fraction of DNA and MX located radicals present in the respective spectrum. The entirely different characteristics of the two constituent spectra enabled it to delineate the composite MX/DNA spectra into their components perfectly. The reconstructed spectra along with their goodness of fit values are shown in **Fig. 5.3.2** and **Fig. 5.3.3** for MX/DNA nucleotide 1:100 and 1:50 respectively. The breakdown of total dataset as shown in **Fig. 5.3.4 (Top)** into component contributions for the two concentrations of MX/DNA when irradiated with two different doses are shown in bottom part of **Fig. 5.3.4**. The line show the curve fitted to **equation 5.3.1** for the two components under each

experimental condition. The numerical values for the decay time constants gained from analysis are listed in **Table 5.3.3**.

Table 5.3.3. Same as in table 5.3.2 but for MX/DNA system in 7 M LiBr/ D_2O[3].

MX:DNA nucleotide (Molar ratio)	dose (kGy)	radical fractions	A_1 (%err)	t_1 (sec) (%err)	A_2 (%err)	t_2 (sec) (%err)
1:100	0.8	DNA	0.552 (4%)	11560 (10%)	0.352 (5.4%)	422606 (11%)
		MX	0.117 (32%)	5622 (28%)	0.216 (5%)	1833463 (15.7%)
	1.66	DNA	0.514 (11%)	6392 (24%)	0.370 (8%)	197196 (13.8%)
		MX	0.152 (7.2%)	9303 (30%)	0.089 (12.3%)	1012195 (34%)
	10	DNA	0.465 (4%)	11802 (8%)	0.301 (4%)	981732 (10%)
		MX	0.171 (9%)	17953 (17%)	0.078 (9%)	808241 (24%)
1:50	0.8	DNA	0.519 (5%)	14305 (12%)	0.319 (6%)	706909 (12%)
		MX	0.111 (16%)	16742 (36%)	0.152 (8%)	1690474 (18%)
	1.66	DNA	0.595 (13%)	5112 (23%)	0.372 (6%)	207066 (13.4%)
		MX	0.144 (21%)	9798 (35%)	0.187 (7.5%)	663608 (18%)
	10	DNA	0.360 (10%)	8376 (26%)	0.318 (10%)	257182 (18.2%)
		MX	0.193 (8%)	10491 (26%)	0.175 (7.4%)	1175019 (18%)

[3]The R^2 value ranges from 0.98998 ± 0.01129.

The comparison of the numbers as well as the fitted lines shows that the decay behavior of the separate components in the mixed system (MX/DNA) strongly resembles to that of each respective component in its neat state. Although small errors may have been introduced due to different experimental sample sets as well as because of numerical reconstructions but the alignment of the decay constants between the individual and the combined system is so close that the decay of each component can be warranted to independent from the presence of another constituent in the mixed systems. The observed shift in fraction of components with time in **Fig. 5.3.2** and **Fig. 5.3.3** can be ascribed to result dominantly from differential radical stability for DNA and

MX located radicals respectively. In post irradiation period no communication of charges within the DNA-scavenger system is involved.

5.3.3. Riboflavin and DNA

To increase the understanding of the post irradiation behavior of DNA radicals in low temperature glasses, another system consisting of DNA and different loadings of Riboflavin (RF) were chosen. This is does not intercalate with DNA but forms close association with it. So no electron transfer (intrastrand transfer) is expected in this case from the very beginning, and the independent component decay within a mixture should perhaps prevail. The time dependent experimental ESR spectra obtained after irradiation (10 kGy) of a system containing 1RF per 100 DNA nucleotides are shown in **Fig. 5.3.7** and that for 1RF per 50 DNA nucleotides are shown in **Fig. 5.3.8**. The molar ratio between RF and DNA is same as has been used in the case of MX/DNA. The numerical reconstructions of each experimental spectrum are shown. The reconstructions are done using neat DNA (as has been used in MX/DNA) and RF spectra.

Table 5.3.4. Radical fractions of [DNA$^{\bullet}$] and [RF$^{\bullet}$] in RF/DNA systems in 7 M LiBr/D$_2$O glass.

RF:DNA nucleotide (Molar ratio)	time (sec)	RF$^{\bullet-}$ (%)	DNA$^{\bullet-}$ (%)	goodness of fit
1:100	1.8×10^3	28	72	0.0882
	5.0×10^5	47	53	0.1769
	1.5×10^6	56	44	0.1533
1:50	1.8×10^3	40	60	0.0464
	4.5×10^5	60	40	0.1832
	1.6×10^6	65	35	0.3353

Unlike in the case of MX/DNA in RF/DNA systems the initial spectra (A and D respectively in **Fig. 5.3.7** and **5.3.8**) shows very negligible influence of additive RF. Contrary to the visual evidence the quantitative reconstruction shows that about 28% of the radicals are located on RF in spectrum A and about 40% in spectrum D. These values are very close to that found in MX/DNA systems. Also with increasing time interval at 77 K the spectra changes in RF/DNA systems and additive located radical fraction increases. At the end of the observation series, about 60% of the radicals are on the additive RF for the concentration ratio 1:100 (spectrum C). The respective value for

the 1:50 concentration is 65% (spectrum F) (**Table 5.3.4**) and is therefore similar to the values obtained from MX/DNA systems (compare with **Table 5.3.1**). In an overall
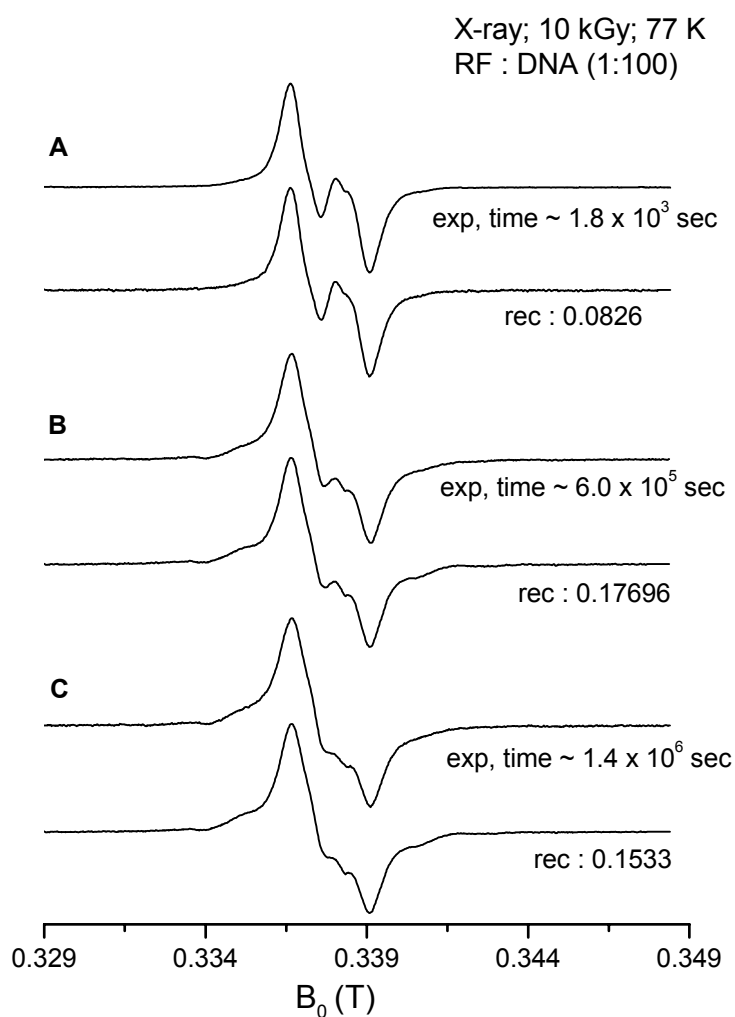
Fig. 5.3.7. A-C) Temporal development at 77 K of first derivative ESR spectra (X-band ~ 9.5 GHz) of 20 mg/ml of a RF:DNA mixture in 1:100 in 7 M LiBr/ D_2O glass. Each experimental spectrum is accompanied by respective reconstructed spectrum (denoted as rec.) from neat DNA and RF patterns along with their goodness of fit value (see text).

manner the non intercalating additive RF participates like an evident electron scavenger during irradiation.
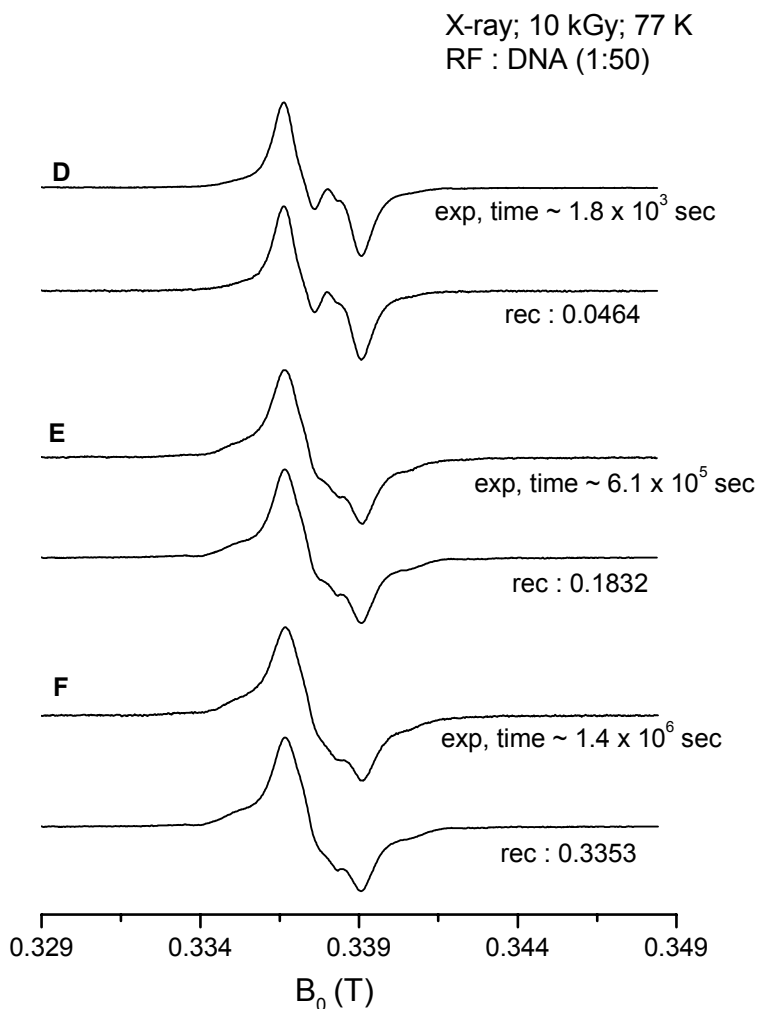
Fig. 5.3.8. D-F) Temporal development at 77 K of first derivative ESR spectra (X-band ~ 9.5 GHz) of 20 mg/ml of a RF:DNA mixture in 1:50 in 7 M LiBr/ D_2O glass. Each experimental spectrum is accompanied by respective reconstructed spectrum (denoted as rec.) from neat DNA and RF patterns along with their goodness of fit value (see text).

The initial spectra obtained in both 1:100 and 1:50 systems are not significantly different from pure DNA. An ESR spectrum of pure riboflavin in 7 M LiBr/ D_2O taken after 30 minutes is shown in **Fig. 5.3.9 (Top)**. It can be seen that the unlike pure MX, the spectrum of RF is a broad one with some shoulders. Due to this width of signal small change in amplitudes will result in large double integral variations. Time dependent decay patterns of the RF derived radicals in 7 M LiBr glass has been shown in bottom part of **Fig. 5.3.9**. The data points can be well fitted to a bi-exponential curve (Equation

5.3.1) yielding similar fast and slow component of decay of the RF radicals. The results of the numerical analysis are listed in **Table 5.3.2**.
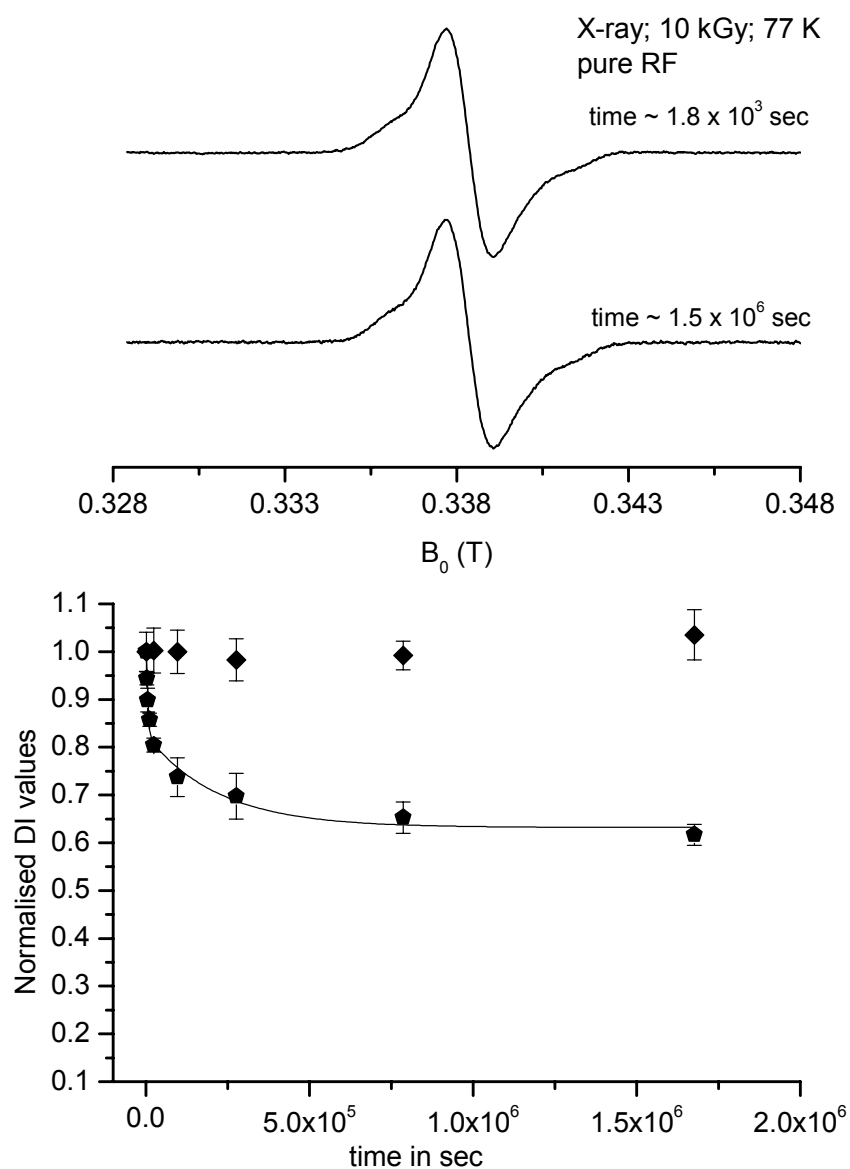
Fig. 5.3.9. (Top) X-band ESR spectra of pure RF (1mg/ml of 7 M LiBr/D_2O), both x-ray irradiated (10 kGy) and measured at 77 K. The qualitative feature of the spectra shows no variance with dose or time. (Bottom) Development of concentration of pure RF radicals in frozen LiBr glass at 77 K with time. The bi exponential fit to the experimental points is shown as a solid line. The external standard data (TEMPOL) are shown by rhombic points (filled).

The change in total radical concentration in the system containing both DNA and RF is shown in **Fig. 5.3.10 (Top)**. As observed previously in MX/DNA systems considerable fading is observed with time at 77 K which displays a fast and slow component, the former leading to a loss of 35% of the radical population within first day. Following the procedure described previously for MX/DNA, the individual component fading was analyzed from reconstructions of the experimental spectra as shown in the bottom part of **Fig. 5.3.10**.

Discussion

The rate of fading of radicals (**Fig.5.3.10, Top**) is independent of RF concentration ratio which is 1:100 nucleotides and 1:50 respectively. As formerly seen the fading of DNA (**Fig. 5.3.10, Bottom**) radicals in RF/DNA mixture is faster and more efficient than RF derived radicals. Hence again differential radical stability is the origin of the enhanced fraction of RF radical with time. The time constants for DNA derived from the bi exponential decay fitting are listed in **Table 5.3.5** and are found to be approximately same as those found in the MX/DNA mixture and in neat DNA as well. This ensures again that the dominant process governing the spectral changes of the mixed system in the post irradiation is differential radical decay.

Table 5.3.5. Parameters A_1, t_1, A_2 and t_2 by fitting equation 5.3.1 to the fading of radical fractions in RF:DNA systems (dose 10 kGy)[4].

RF:DNA nucleotide (Molar ratio)	radical fractions	A_1 (%err)	t_1 (sec) (%err)	A_2 (%err)	t_2 (sec) (%err)
1:100	DNA	0.524 (6%)	6631 (15%)	0.285 (8%)	301781 (16.4%)
	RF	0.187 (9%)	9774 (21%)	0.160 (7.5%)	766002 (20%)
1:50	DNA	0.579 (8%)	4116 (19%)	0.311 (9%)	104427 (16.2%)
	RF	0.220 (14%)	9955 (36%)	0.141 (15%)	657725 (34%)

[4]The R^2 value ranging from 0.992± 0.00853.
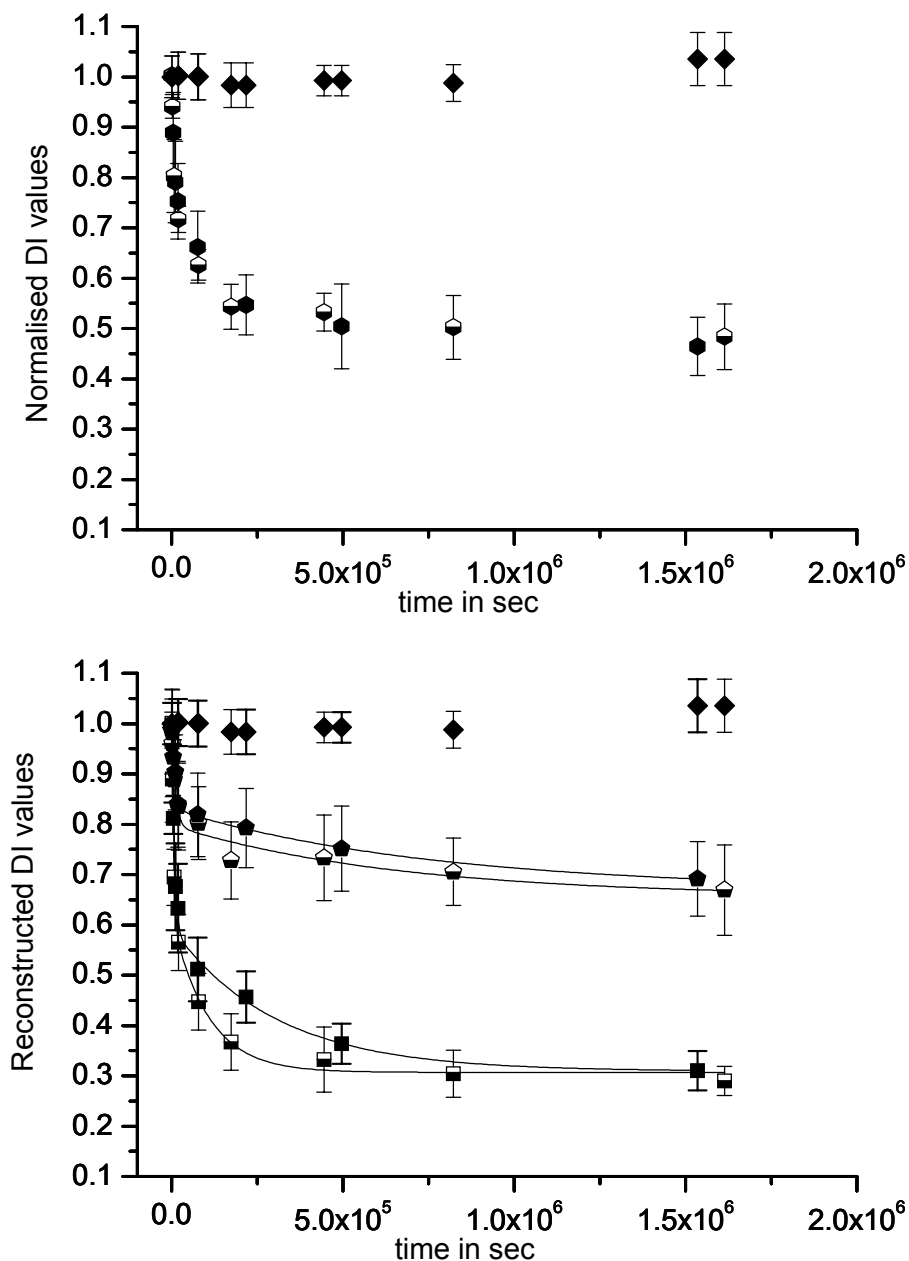
Fig. 5.3.10. (Top) Development of total radical concentration with time of RF:DNA mixtures at 77 K given as double integral (DI) values normalized to the first measurement ~ 30 minute after X-ray irradiation in comparison with an external standard TEMPOL (closed rhombic points). Data from experiments with two different loadings are shown: 1:100 (closed hexagons) 1:50 (half filled hexagons). (Bottom) Delineation of the above data into RF and DNA radical components and their change with time using the patterns from pure DNA and MX systems. The conventions are kept same only hexagons have been changed into circles. The solid line represents the bi - exponential fit to the experimental data.

5.3.4. Deoxyribonucleotides and MX

Another investigation was done with combination of MX with deoxyribonucleotides TMP and dCMP. The prior expectations are that the radicals formed on each component will certainly decay independently as deoxyribonucleotide is not a big molecule like DNA and there should in principle be no association between either substrate. These two model DNA constituents were chosen since their anions are expected to be formed in DNA in the low temperature glass (Messers et. al. 2000).

The ESR spectra obtained are shown in **Fig. 5.3.11** for TMP and **Fig. 5.3.12** for dCMP. Three groups of spectra are shown. One is the neat compound and the others are for the concentration ratios 1:50 and 1:10 molecules (MX:pyrimidine). For each case the initial spectrum is taken about 30 minutes after irradiation whereas the second spectrum reflects ESR spectra obtained after about one month of storage time. For both deoxyribonucleotide it is noted that the initial spectra have hardly any MX radical contributions. The contributions of MX radicals as listed in **Table 5.3.6** indeed shows resemblance with their stoichiometric values.

Table 5.3.6. Relative fraction of deoxyribonucleotide derived radicals and MX radicals with increasing time in MX:deoxyribonucleotide (TMP/dCMP) irradiated with 10 kGy.

MX:Nucleotide	molar ratio	time (sec)	MX$^{\bullet-}$ [%]	Nucleotide$^{\bullet-}$ [%]	goodness of fit
MX:TMP	1:50	2.4×10^3	4	96	0.072
		2.7×10^6	12	88	0.45
	1:10	1.8×10^3	12	88	0
		2.5×10^6	26	74	0.238
MX:dCMP	1:10	1.8×10^3	8	92	0
		2.7×10^6	7	93	0.078
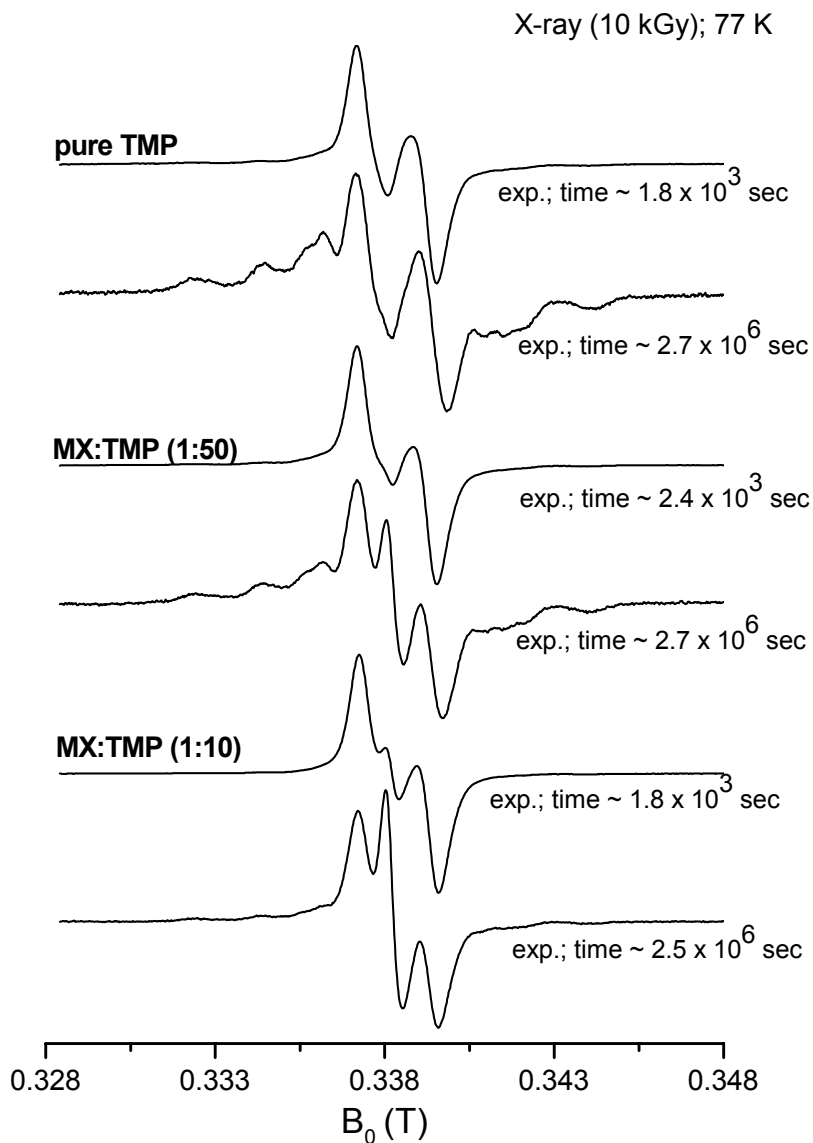
Fig. 5.3.11. The initial 30 minutes and final (after ~ one month) first derivatives ESR spectra of time series of spectra obtained after X ray irradiation (10 kGy) from pure TMP (Top), a mixture of MX:TMP of 1:50 (middle) and at 1:10 molecular ratio.

In the 1:10 mixture for TMP the MX radical amounts to 12% and in 1:50 mixture to about 4.3%. Similar results are obtained in dCMP and its mixture with MX.
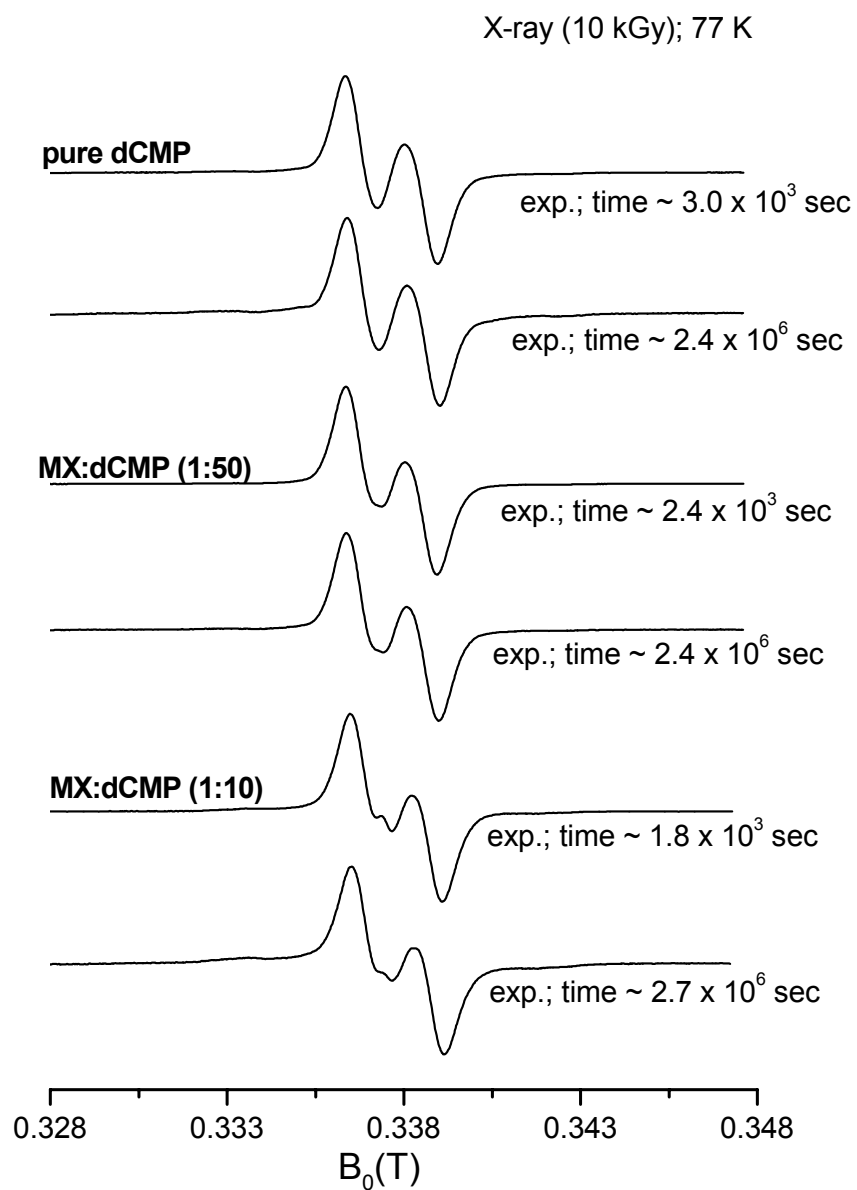
Fig. 5.3.12. The initial 30 minutes and final (after ~ one month) first derivatives ESR spectra of time series of spectra obtained after X ray irradiation (10 kGy) from pure dCMP (Top), a mixture of MX:dCMP of 1:50 (middle) and at 1:10 molecular ratio.

The decay of total radical concentration in the same samples of TMP with time is shown in **Fig. 5.3.13**. Again loss of radicals at 77 k in terms of fast and slow components is observed. The difference between neat TMP and the mixtures with MX in the ratio 1:50 and 1:10 respectively are seen to be small. In total about 70% of the initially detected radicals are lost at the end of the time series. The reconstruction of the mixtures between TMP and MX in terms of individual components decay gives the results displayed in the bottom part of **Fig. 5.3.13** (see also **Table 5.3.7**).

Table 5.3.7. Parameters A_1, t_1, A_2 and t_2 for deoxyribonucleotides TMP and dCMP and for their mixtures with MX (dose 10 kGy)[5].

system	molar ratio	fractions	A_1 (%err)	t_1 (sec) (%err)	A_2 (%err)	t_2 (sec) (%err)
Pure TMP	-	TMP	0.632 (2.4%)	6731 (6.2%)	0.194 (6%)	446932 (10%)
MX:TMP	1:10	TMP	0.418 (11%)	9742 (25%)	0.408 (7.5%)	750571 (16%)
		MX	0.077 (31%)	6192 (28%)	0.2425 (2%)	949923 (5.2%)
Pure dCMP	-	dCMP	0.271 (10.33%)	12880 (20%)	0.273 (6.2%)	962421 (13.2%)
MX:dCMP	1:10	dCMP	0.285 (11.2%)	8104 (21%)	0.287 (7%)	568649 (12.35)
		MX	0.278 (13.3%)	7053 (27%)	0.284 (10%)	322705 (16.4%)

[5] The R^2 value ranging from 0.99347 ± 0.00344

The rate of decay of TMP located radicals are significantly faster than that of the MX leading to an enhanced visibility of the latter group in the spectra with time as can also be predicted from the experimental spectra (**see Fig. 5.3.11**).
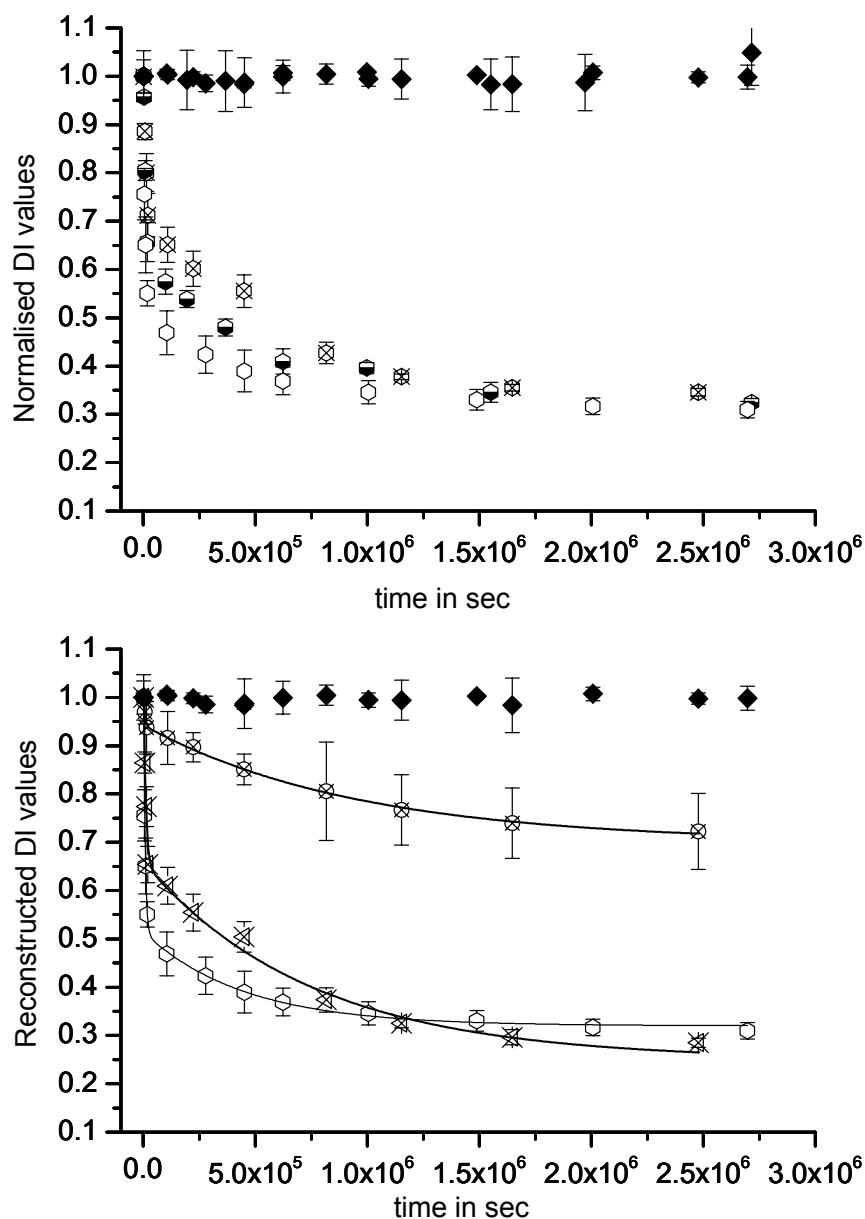
Fig. 5.3.13. (Top) Development of total radical concentration with time of TMP and MX:TMP at 77 K given as double integral (DI) values normalized to the first measurement ~ 30 minute after X-ray irradiation in comparison with an external standard TEMPOL (closed rhombic points). Pure TMP (open hexagons); MX:TMP(1:50)(half filled hexagons); MX:TMP (1:10) crossed hexagons. (Bottom) Delineation of the above data for MX:TMP (1:10) into TMP (crossed triangle) and MX (closed circles) radical components and their change with time using the patterns from pure TMP and MX systems. The conventions are kept same only hexagons have been changed into circles. The solid line represents the bi - exponential fit to the experimental data The data for pure TMP is included for comparison.

The results obtained from dCMP are different. The experimental spectra of **Fig. 5.3.12** showed almost no significant difference between the initial spectra and the final spectra taken at the end of the time frame both in pure dCMP and in mixtures with MX. The decay of total radical is also quantitatively different. As can be seen from **Fig. 5.3.14**, the loss of radicals is found to be only about 20% on the first day and settles at about 50% at the end of the observation time. This decay behavior is independent of the presence of MX present in the mixed system. The reconstruction analysis shown in the bottom part gives about the same decay behavior for dCMP and MX for the 1:10 concentration.

Discussion

These results in deoxyribonucleotides (both in TMP and dCMP) imply that there is no influence of MX on the free radical distribution in these systems even during irradiation. This situation is completely different from that observed in the case of DNA – additive systems. These findings, in retrospect, supports the assumption implicitly made previously that there is a very close association between the DNA and the additives MX and RF.

Considering the decay results of pure TMP, pure dCMP and their mixtures with MX it is a new finding that although TMP related radicals do decay much faster than MX at 77 K but dCMP does have similar rates of decay like MX. There are no signs of electron transfer from deoxyribonucleotide electron adducts to MX in the post irradiation time period.

5.3.5. Post Irradiation Radical Decay Behavior: The Mechanistic Aspects

When associated with DNA, radical fractions derived from both additives MX and RF measured immediately after irradiation at 77 K is much larger (about a factor of 20-30) than expected from their stoichiometric ratio. Irrespective of different modes of interaction of the additives with DNA the enhancement is comparable in both cases. In this case therefore the close association with DNA is more important. Similar results are found in solid, lyophilized DNA containing the respective additive or in frozen aqueous solutions. This type of intra irradiation transfer of spins between DNA bases and closely associated additives has been has been known in this field of study for a long time (Gregoli et. al. 1970) and has been since then reported several times for different
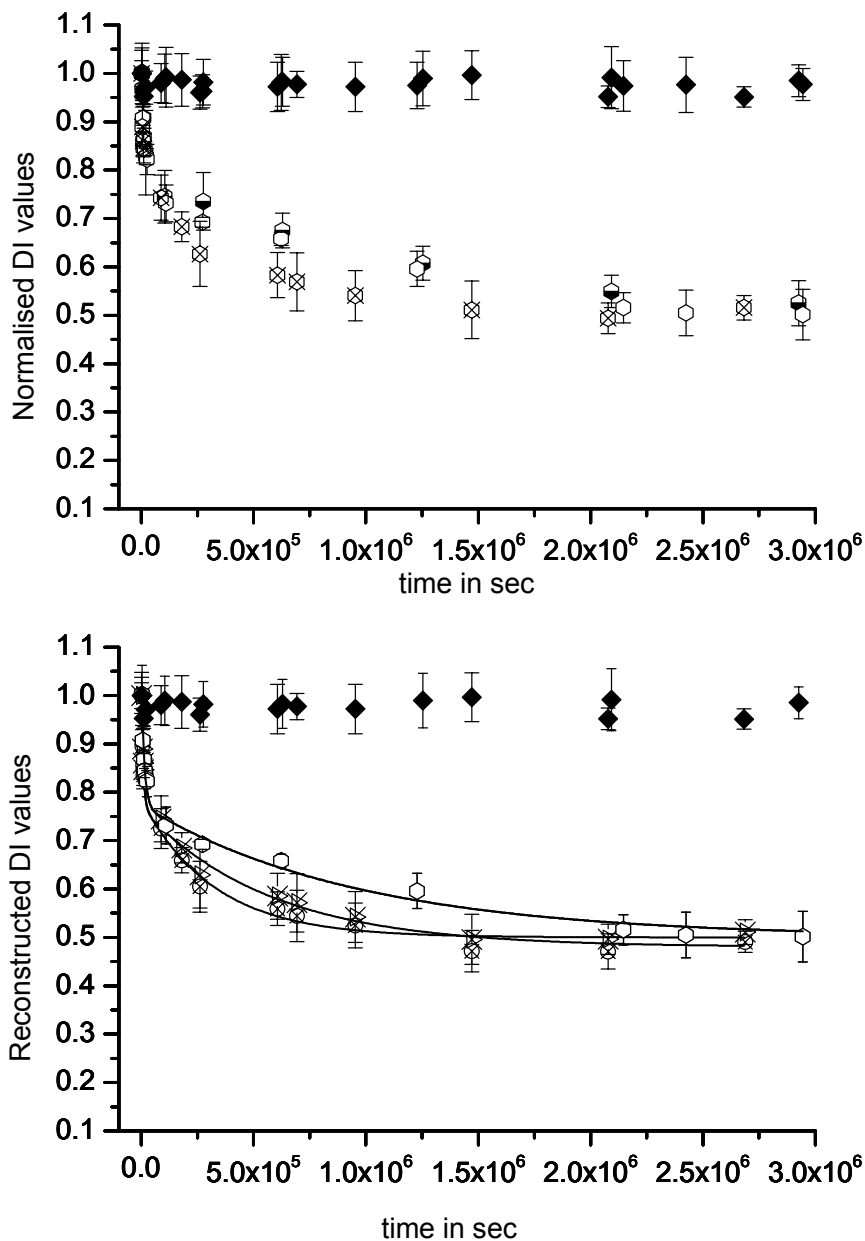
Fig. 5.3.14. (Top) Same plot as in Fig. 5.3.13 (Top) but for dCMP and its mixtures with MX. Nomenclature and symbols have same meanings. (Bottom) Same delineation of MX and nucleotide radical contributions for MX:dCMP (1:10) as in Fig. 5.3.13 (Bottom) but for dCMP as deoxyribonucleotide. The data fro pure dCMP are included for comparison (open hexagon)

additives. A recent report deals with the mixture of DNA with histones in chromatin in which DNA takes up about a factor of two more radicals than expected from the mass ratio (Weiland and Hüttermann, 2000).

Other recent examples concern the efficient and selective hole trapping by minute amounts of thio-substituted nucleic acid bases doped into single crystals of the corresponding unsubstituted base (Herak et. al. 2000) or doping 5-methylcytosine into the cytosine crystalline lattice (Kripokavic and Sagstuen, 2003). In spite of so many investigations the details of the mechanisms controlling the radical distribution between DNA located radicals and additive radicals during the process of irradiation are still not completely clear.

The main interest of this report is however the absence of significant net electron transfers with time at 77 K from DNA to the additives in the post irradiation period. This finding is in complete conflict with earlier interpretations (Messers et. al. 2000), of the same system and is also unexpected as electron transfer, e.g., in proteins is very well established (Gray and Winkler 1996, Gray and Winkler 2005). Besides, the considerable amount of radical decay, especially of the DNA located electron adducts in the glass, clearly shows that post irradiation processes occur with time, e.g., at 77 K, which modulate the observed radical balance with respect to time.

To our knowledge, no mechanism has been put forward until now to explain the observed decay of radicals. Oxidation of electron adducts on DNA and on the additives by $Br_2^{-\bullet}$ might be considered: which means that the trapped holes are having some kind of mobility at 77 K and even at lower temperature. Typically, the $Br_2^{-\bullet}$ species become mobile and react from about 140 K onwards, but they might be partially detrapped at lower temperature too. An alternative scheme which is considered here is that apart from the electrons which are added to DNA (typically pyrimidine bases), to the additives and apart from the holes trapped by LiBr glass another fraction of electron and holes do exist. These are denoted as "defects", they are supposed to remain trapped in the matrix after the irradiation is complete. This fraction can play a pivotal role in the post irradiation decay processes which has been dominantly observed in all the cases studied so far.

These matrix trapped defects must have three properties to explain the results; first, they must be ESR mute and remain undetectable at the applied conditions. Second, their energy should be such that they are unable to form new radicals but rather capable of destroying them. Third they are present in larger numbers in the matrix than the free radicals stabilized on the substrates at 77 K.

A simple model picture evolves here that storage of the irradiated samples at 77 K leads to liberation of the defects from their (shallow) matrix – located traps with time. Apart from recombination which goes unnoticed by ESR, their reactions then lead to the observed decay of the ESR-active free radical population. This process then should be dominating the post-irradiation time profile of radicals. The one proposed earlier, electron transfer from a DNA pyrimidine radical anion to MX or another additive via some kind of transport structure (Messers et. al. 2000) may perhaps occur but has, if at all, a negligible quantitative effect on the ratio of free radical types detected. A recent work by Barton and O' Neil 2004, has also proposed that charge transfer in a glassy matrix at 77 K does not occur in DNA due to lack of motional flexibility of the polymer which although have used different techniques but do comply with the results found in this report. With this model the well established general picture of electron transfer remains unconcerned. Only, its contribution is insignificant in an environment loaded with trapped radiation-produced defects.

In order to establish the above proposed model it is essential to see the behavior of the solvent molecules and the effect of temperature during the period of study of the substrate radicals.

We consider first the behavior of $Br_2^{-\bullet}$ in the post-irradiation phase. It can be tested by using TEMPOL as an ESR-active monitor. **Fig. 5.3.15 (part A)** gives a spectrum (a) for the (stable) TEMPOL radical (1 mM) measured at 77 K. When irradiated to a dose of 30 kGy, its ESR-activity is apparently fully abolished (spectrum b) by reaction with radiation-produced electrons whereas the holes form $Br_2^{-\bullet}$ as usual. After about 30 days, the typical time range used in the above radical decay studies, a very minute TEMPOL activity was gained back (not shown). After 65 days of storage at 77 K some additional ESR-activity of TEMPOL was found to be restored (spectrum c). From a dilution series of TEMPOL a concentration of roughly 5 to 8 µM can be assigned to this latter spectrum (reference spectrum d), a number which must be dealt with reservation due to the large errors involved in double integration of the weak signals. Nevertheless, $Br_2^{-\bullet}$ apparently cannot reactivate the TEMPOL radical within up to about 65 days at 77 K to a significant extent. This is not due to lack of oxidative power which can be derived from the data given in **Fig. 5.3.15 (B)**. Irradiation of TEMPOL with doses lower than 30 kGy yields only partial loss of the ESR activity; e.g.at 600 Gy a spectrum corresponding to about 60% of the control activity is obtained. Storage of this sample at 77 K leaves the ESR-activity

unchanged over a period of 30 days (data not shown). Thus, both the active TEMPOL fraction as well as its ESR-mute product produced from irradiation are highly stable against any reaction in the post-irradiation time regime at that temperature. However, when annealing to higher temperatures, reactions do occur in the sample. First, between 125 and 160 K a sizeable decay of TEMPOL activity (up to about 20% loss) is observed. More important, further annealing enhances the ESR-activity. Both processes can be ascribed to reactions of $Br_2^{-\bullet}$. The decay could involve oxidation of the radicals, whereas the formation of TEMPOL radicals should be expected to involve oxidation of the diamagnetic product formed upon irradiation. In any case, $Br_2^{-\bullet}$ is seen to react when it becomes mobile and therefore it should not be connected to a significant extent with the decay observed for DNA and additive radicals at 77 K.

One further argument leads to the same conclusion. If $Br_2^{-\bullet}$ were to react with the solute radicals at 77 K one has to expect, apart from their decay, new free radicals from oxidation of solute molecules which were not yet converted to free radicals by irradiation. Thus, patterns other than those of the electron adduct radicals discussed above should be observed. There is little indication of this process since mostly the patterns remain stable throughout the decay period. Only TMP (**Fig. 5.3.11**) is seen to display a change in ESR pattern; some smaller change is also seen in DNA at the end of the storage time. The effect in both cases is so small that it cannot be analyzed quantitatively. The dominant process is just pattern decay. In the same context one can argue that the differential decay of the different free radicals should rule out an involvement of $Br_2^{-\bullet}$ Apparently, DNA radicals decay more efficiently than those on mitoxantrone or TEMPOL. If $Br_2^{-\bullet}$ were involved one would expect indifferent oxidation perhaps modulated by differential accessibility but not by radical stability.

Also, potential alternative mechanisms for the free radical decay at 77 K and lower temperatures (see below) in the glass matrix must be considered. Radical-radical recombination between solute radicals must be discarded under these conditions. Therefore, not considered before in the literature, it appears likely that there must be species in the glass which can destroy free radicals with time at 77 K and which are indeed ESR-mute as discussed above. A prominent example for an ESR-mute species is the solvated electron in ice at neutral pH and at 77 K. Only at alkaline pH a sufficiently deep trap structure appears to have evolved allowing for the species to become ESR
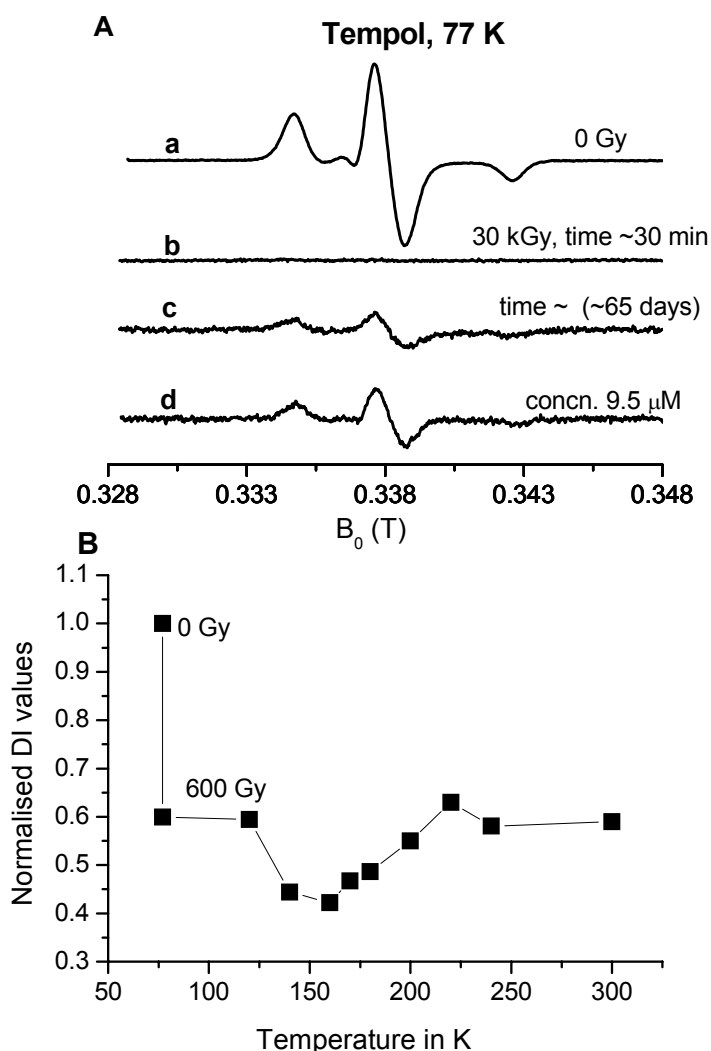
Fig. 5.3.15. (A) X–band (~ 9.5 GHz) ESR spectra of (a) 1mM TEMPOL frozen in 7 M LiBr/ D_2O, (b) same sample X-irradiated with 30 kGy and measured after 30 minutes, (c) sample as in (b) measured after 65 days, (d) 9.5 μM frozen TEMPOL in 7 M LiBr / D_2O as reference. X-irradiation, ESR measurement and storage were always done at 77 K. (B) Loss of ESR activity of TEMPOL (1 mM in 7 MLiBr / D_2O) after X-irradiation (600 Gy) and measurement at 77 K in LiBr glass with respect to control; effect of thermal annealing of the irradiated sample to the temperatures indicated and subsequent measurement at 77 K on the ESR-activity (double integral value) of TEMPOL showing reactions of $Br_2^{-\bullet}$.

visible (Eiben, 1970, Schulte-Frohlinde and Eiben 1962). A similar situation might apply to the matrix defects discussed here.

One aspect of the "defect" mechanism which can be tested experimentally concerns the influence of the temperature on the post-irradiation time profile of free

radicals. Unlike electron tunneling processes, radical decay should be temperature dependent if the picture of de-trapping matrix-trapped defects were reasonable. Only preliminary results are given here for the nucleotide TMP and for DNA. After irradiation at 77 K, the samples were kept at 77 K and at lower temperatures. **Fig. 5.3.16** gives the results. For TMP (top) the samples were kept at 10 K and at 40 K whereas the DNA (bottom) was probed at 14 K in addition to 77 K; the temperatures below 77 K were chosen in order to gain high temperature stability under the given experimental conditions since otherwise the results would show a large scatter. Also, the total time interval applied in this case was only about 10 hrs so that only part of the 'fast component' of decay after irradiation was probed; measurements for longer time periods under these conditions i.e. with the sample being within the helium cryostat in the ESR-apparatus are not feasible. Nevertheless, the results clearly show that the decay efficiency is temperature dependent for both TMP and DNA; storage temperatures below 77 K reduce the loss of radical activity with time.

Interestingly the effect of the temperature reduction on the decay efficiency is larger in TMP than in DNA, although most of the DNA radicals probably are located on TMP sites if judged from the difference in the decay efficiency of the neat nucleotide TMP as compared to dCMP (cf. **Figs. 5.4.13 and 5.3.14**). This could imply that the accessibility of the free radicals to the defects when liberated from their matrix traps is larger in the isolated deoxyribonucleotide than it is in DNA. The accessibility factor in both systems, TMP and DNA can be tested, although probably not fully independent from the other parameters like trap-depth, by changing the matrix. We have probed the system of frozen aqueous solutions which have been studied quite intensely in the past (Sevilla and Becker 2004). Roughly, it was proposed that the solute in this case should be confined in 'puddles' formed by exclusion from water during its freezing and that these regions were surrounded by bulk-phase ice. As a consequence, the distribution of the solute over the sample volume is considered to be highly inhomogeneous, in contrast to the situation in the glass. Therefore, we expect that the accessibility of the solute free radicals for defects in this situation should be much smaller and thus defect recombination in the bulk ice phases should be the dominant post-irradiation process. This is indeed observed experimentally for TMP and DNA. The radical decay for both compounds during the fast decay period (first day) in the glass is much less efficient in the frozen aqueous solution at the same temperature (i.e. 77 K). It can, of course, not be
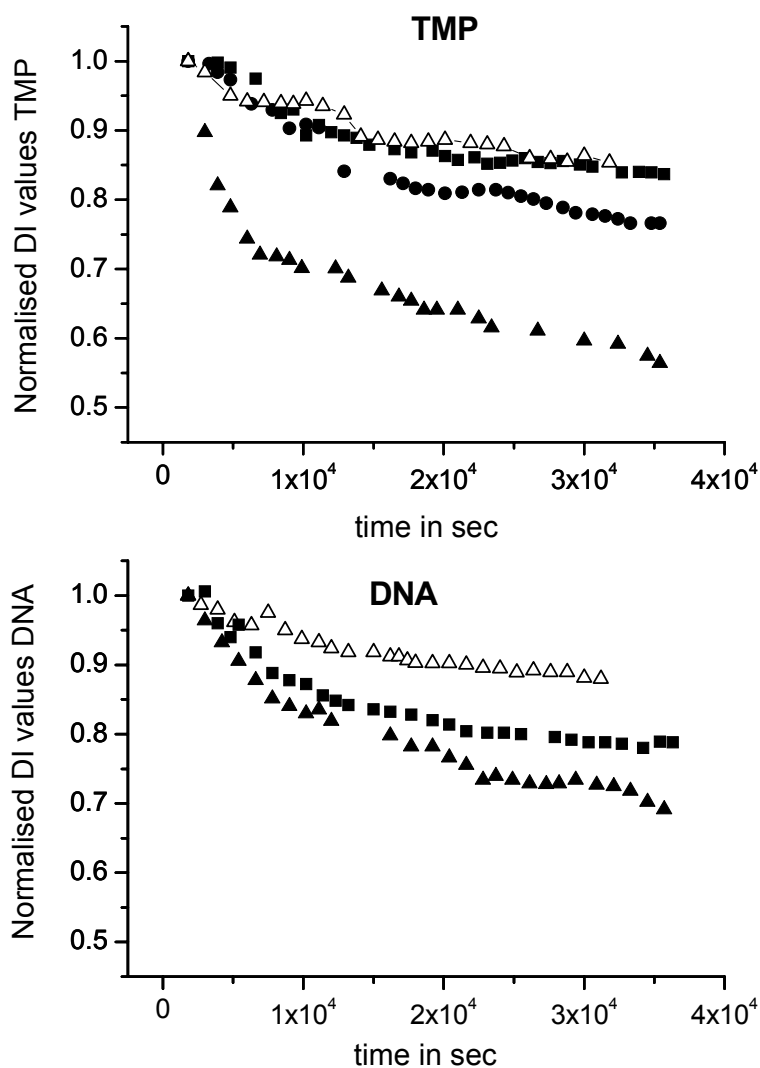
Fig. 5.3.16. (Top): Temporal development of ESR-spectra intensity from frozen glass samples of pure TMP (20 mg/1ml in 7 MLiBr (D$_2$O)), X-ray irradiated (10 kGy) at 77 K and measured at 10 K (filled squares), 40 K (filled circles) and 77 K (filled triangles), respectively. The open triangles are for TMP in frozen aqueous solutions (50 mg / 1ml in D$_2$O), X-ray irradiated (20 kGy) at 77 K and measured at the same temperature after irradiation. (Bottom): Temporal development of ESR-spectra intensity from frozen glass samples of neat DNA (20 mg / 1ml in 7 MLiBr (D$_2$O)), X-ray irradiated (10 kGy) at 77 K and measured at 14 K (filled squares) and at 77 K (filled triangles), respectively. The open triangles are for DNA in frozen aqueous solutions (50 mg/1ml in D$_2$O) measured at 77 K after irradiation at that temperature.

excluded, that this effect is also related to a difference in the trap depth of the two systems.

Although there is little work available in the literature which can be compared with the present results, some reports seem to be related. For example, the apparent bi-exponential decay behavior of the fading profiles in all samples tested is not without precedent. A case which could be closely related with the present findings involves a small trapped ESR active species, the hydrogen atom. Very early on in the field of radiation chemistry the decay kinetics of hydrogen atoms trapped in irradiated sulfuric acid glasses were studied in detail. At 77 K a clear separation between a rapid and a slow decay phase of this species was observed in the post-irradiation period which involved time ranges comparable to those used here. It was analyzed in terms of two traps of different depth rather than in terms of non-random distance distribution between the H-atom and its reaction partner (Sprague and Schulte-Frohlinde 1973). It could be that, under our conditions, both the apparent fast and the slow components might comprise some distribution of trap energies. Nevertheless, the partition into two phases appears to be operationally a sensible approach.

Another early work with potential relevance to the present findings is a study of the decay of radiation produced organic free radicals in solid samples by heat. The time period of measurement applied in that work was only of the order of one hour or less. Under these conditions, mono-exponential decay was found for solid samples of organic acids or amino acids which were irradiated at 300 K and subsequently heated from 100 to 150 °C (373 to 423 K). It was proposed that mobile charges were induced by heat in the organic solid, unnoticeable by ESR perhaps due their low concentration. These charges were suggested to interact with the organic free radicals in terms of destruction by site hopping (Horan et. al. 1968). The picture of radiation produced defects in the solid responsible for free radical decay was not elaborated but can, in our view, also explains the above results.

6. Conclusions and Outlook

One main objective of this thesis was to understand the numbers, relative distribution and the structures of the free radicals formed in X irradiated frozen aqueous DNA under the influence of several parameters like dose, annealing temperature and additives (electron and hole scavengers). Special emphasis was on identification of the structures of oxidation derived radicals. The oxidized radicals formed on DNA base or deoxyribose sugar moieties can provide knowledge about the extent of direct, quasi direct or indirect mechanism of irradiation in frozen aqueous solutions. Fluoruracil and its derivatives were used as model compounds to gain more insight about the mechanism of irradiation in frozen aqueous solutions. The study was then extended to frozen aqueous solutions of DNA.

Another aim of this thesis was to re-investigate the postulated electron transfer phenomena from DNA radicals to the added scavenger molecules as a function of time after irradiation in frozen glass solutions.

X-band ESR spectroscopic measurements at mainly at 77 K were performed to obtain the ESR spectra from the radicals produced on DNA or nucleotides upon X-ray irradiation.

Considering all the results obtained from the low temperature ESR measurements of irradiated fluorouracil and its derivatives in three different matrices namely 5 M H_2SO_4 glass containing large concentrations of $Na_2S_2O_8$, 7 M BeF_2/H_2O glass and frozen aqueous solutions it can be said that, as assumed, fluorouracil and its derivatives proves to be very suitable system for the purpose of understanding the mechanism of radiation action in the frozen aqueous system. In 5 M H_2SO_4 containing large concentrations of $Na_2S_2O_8$ in FU N1 deprotonated radical was observed undisputedly. In FUdR and FdUMP in addition to the N1 base cation radicals and the FUdR_C6(SO_4^-) radical as found previous reports (Riederer and Hüttermann 1982), formation of C2'• radical from the C2' of the deoxyribose part was observed for the first time in this glass matrix. Another sugar based radical observed in FudR or FUR at 165 K was tentatively assigned to C5'• species (C5' position of deoxribose moiety) but clear identification of this radical was not possible owing to overlapping of several other patterns. An asymmetric doublet with very close correlation to O4 protonated FU anion radical was

found to be the thermally most stable component in all the substrates. In 7 M BeF_2/H_2O containing neat FU and derivatives formation of FU anions and 5-yl radicals were observed as major low temperature components along with the trapped OH radical pattern at 77 K. With increase in annealing temperature (> 165 K) minor formation of OH addition radical at C6 position of FU base was observed along with the asymmetric doublet (might be from O4 protonated anion) as observed in 5 M H_2SO_4 glass. In FUdR and FdUMP formation of C1'$^\bullet$ sugar radical and C2'$^\bullet$ sugar radical were predicted to be formed via OH$^\bullet$ attack at higher annealing temperatures. On addition of high concentration of electron scavenger ($K_3Fe[CN]_6$) in the system base anions were not formed at all at 77 K giving signal of only trapped OH$^\bullet$ and H$^\bullet$ radical. Upon annealing both species get released and disappeared forming 5-yl radical and FU_C6(OH) radicals were formed. Although N1 deprotnated radical or base cation was not observed but C1'$^\bullet$ and C2'$^\bullet$ sugar radicals could be observed more clearly than in pure derivatives. C5'$^\bullet$ formation was predicted in FdUMP but its isolation was not possible. In frozen aqueous solutions FU could not be used because of its poor solubility in water and therefore only FUdR and FdUMP were studied. In this matrix along with the FU anion radical and 5-yl radical clear evidence of formation of C1'$^\bullet$ radical was observed even at 77 K in both FUdR and FdUMP. C1'$^\bullet$ was not observed at 77 K in 7 M BeF_2/H_2O containing FUdR and FdUMP. Also in frozen aqueous solutions patterns arising from OH addition radical was already observable at 140 K in contrast to its observation in 7 M BeF_2 only after annealing to 170 K. On addition of high concentration of $K_3Fe[CN]_6$ formation of FU based anion was greatly reduced. Clear presence of C1'$^\bullet$ and C2'$^\bullet$ were observed and there outer lines could be identified by the subtraction of the broad OH$^\bullet$ radical pattern from complex spectrum obtained from FUdR/ FdUMP and electron scavenger at 77 K. Formation of these oxidized radicals at 77 K were not observed in 7 M BeF_2 where only indirect effect of irradiation prevails. This difference is an evidence of direct or quasi-direct irradiation mechanism in frozen aqueous solutions.

On extending the study to the irradiated DNA in frozen aqueous matrix it has been observed oxidized radicals are formed at low temperature upon irradiation both on DNA base, guanine cation (G$^{+\bullet}$) and sugar moieties (C1'$^\bullet$, C3'$^\bullet$ and C4'$^\bullet$/C5'$^\bullet$). Reduced radicals are mainly cytosine and thymine based C$^{-\bullet}$/ C(N3H$^+$)$^{-\bullet}$ and T$^{-\bullet}$. On annealing secondary radicals like 5-thymyl radicall (TH$^\bullet$), thymine allyl radical (TCH$_2$$^\bullet$) were observed. This study has extended the number of isolated radical patterns in frozen

aqueous DNA from that was proposed by Gregoli and co workers (1982) and Cullis et. al. (1985). This study gives for the first time a detailed analysis of the influence of dose and temperature together on the distribution of free radicals formed on frozen aqueous DNA. Increase in dose induced decay in the contributions of charged radical species while the neutral sugar radicals remained constant. Upon annealing octet pattern from 5-thymyl radical was mainly observed in low dose irradiated samples. Allyl radical pattern and sharp singlet pattern from $GN^\bullet$ were observed on irradiation of DNA with high doses. 5-thymyl radical pattern was found to be decreased in most cases with higher doses due to reduced formation of its precursor $T^{-\bullet}$ in DNA.

The electron scavenger $K_3Fe[CN]_6$ and hole scavenger $K_4Fe[CN]_6$ were used (as in Shukla et. al. 2005). Expected reduction of anion radicals in presence of $K_3Fe[CN]_6$ and guanine cation in presence of $K_3Fe[CN]_6$ were observed. The guanine cation radical was found to decay much faster with increasing dose in the presence of electron scavenger then in pure DNA. Although there are probabilities of guanine cation radical behaving as a precursor to $C1'^\bullet$ sugar radicals formation or that Fe^{2+} formed after acceptance of one electron by Fe^{3+} can further act as hole scavenger and destroys guanine cation radical however there is no clear mechanism for this observation. The Sugar derived radicals (from $C1'^\bullet$, $C3'^\bullet$ and $C4'^\bullet/C5'^\bullet$) remained unscavenged even in the presence of hole scavenger showing formation of sugar radicals (via oxidation) is faster than scavenging of holes by the closely associated $K_4Fe[CN]_6$ molecules. Temperature annealing studies showed that peroxy radical remains as the final radical in DNA-$K_3Fe[CN]_6$ system irrespective of the dose of irradiation. Octet pattern from 5-thymyl radical is found to be the final radical formed at 240 K in DNA-$K_4Fe[CN]_6$ system where the concentration of octet decreases with dose.

There has been no dose dependent study done on MX:DNA system in frozen aqueous solution till now. A study by Cai et. al. 2001 estimating the effects of hydration, aliphatic amine cations, and histone proteins in MX:DNA (1:400 base pairs) system reported formation of 18% MX. 30.3% of $G^{+\bullet}$, 31.7% of $CD^\bullet$, 20.2% of $T^{-\bullet}$. A direct comparison of the formation of the radicals with our system cannot be done as the irradiation dose used by Cai. et. al. 2000 was very low (2.6.k Gy) and hydrated system in D_2O matrix was used. The authors reported minor formation of sugar radicals but were ignored due to their minor presence. In our study for irradiated 1MX:800 DNA it was

observed that about 20% of MX based radicals were formed showing possibility of long range electron transfer in DNA during irradiation. The distribution of the DNA based radicals with increasing dose and temperature were similar to that observed in pure DNA. Formation of sugar radicals are observed even when low irradiation was used. In 1MX:200DNA system unexpected drop of guanine pattern is observed along with large reduction in the reduced species even at low doses. More than 50% MX derived radicals are found to be formed. A clear mechanism of this observation cannot be given although it might be possible that MX cation radical (having similar ESR pattern as MX anion radical) are formed here thus lowering the formation of guanine cation. At high doses and high temperature (260 K) formation of allyl radical is clearly observed in the experimental spectrum in frozen aqueous solutions. Formation of guanine cation and unscavangable sugar derived radicals in irradiated frozen aqueous DNA ensures the direct irradiation effect in frozen aqueous system.

In the system of DNA associated with additives like MX and RF in the low temperature glasses 7 M LiBr, the response to ionizing radiation can be divided into two phases, the intra- and the post-irradiation period. In the former, there is a strong influence of the additives on the distribution of radicals between the DNA and the additive component observed by ESR-spectroscopy in favor of the additive. The post-irradiation phase, on the other hand, is governed by processes which induce net decay of the free radical population with time. Differential stability of the radicals against the decay then changes the relative contribution of DNA vs. additive radicals in the post-irradiation period. Electron tunneling from DNA to the additive, unlike earlier suggestions in the literature, is not a process involved in this change to any significant amount. A detailed mechanistic description of the decay process is still not possible. A proposal has been given here which involves detrapping of matrix-stabilized ESR-mute defects formed upon ionizing irradiation. Some of the potential parameters connected with such a mechanism have been tested and the results have shown the feasibility of this proposal but further studies are needed for detailed quantitative assessments.

In future it will be interesting to understand the effect of heavy ions on the formation of radicals in model compounds or on DNA in frozen aqueous solution as still now heavy ion irradiation has been proved to be very useful in understanding and isolating the sugar radical formation on DNA nucleotides and dry DNA. Working on frozen aqueous solution it self is a challenge for heavy ion irradiation sources as high

vacuum conditions are necessary to maintain during irradiation and also the maintenance of low temperature is very difficult in these set up which is very crucial in case of radicals formed in frozen aqueous solutions. The patterns from $C^{-\bullet}$/ $C(N3H^+)^{\bullet-}$ and $T^{-\bullet}$ and could not be separated owing to their similar hyperfine splittings. More studies on DNA irradiated with different doses using high field ESR techniques might provide better insight to this question. In 7 M LiBr glass matrix the time dependent study on the radical decay in MX-DNA systems have showed the presence of shallow defects in the glass matrix whose identification would be an interesting task to accomplish in the future. More knowledge on the formation of sugar radicals can be obtained by using other sources of irradiation like photoionization for deoxyribonucleiotides and DNA in pure form or in the presence of suitable additives.

References:

Adhikary, A., Malkhasian, A. Y. S., Collins, S., Koppen, J., Becker, D., Sevilla, M. D., 2005, UVA-visible photo-excitation of guanine radical cations produces sugar radicals in DNA and model structures. Nucleic Acids Research, 33, 5553-5564.

Adhikary, A., Becker, D., Collins, S., Koppen, J., Sevilla, M. D., 2006, C5'-and C3'-sugar radicals produced via photo-excitation of one-electron oxidized adenine in 2'-deoxyadenosine and its derivatives, Nucleic Acids Research, 34, 1501-1511.

Adhikary, A., Collins, S., Khanduri, D., Sevilla, M. D., 2007, Sugar radicals formed by photoexcitation of guanine cation radical in oligonucleotides, The Journal of Physical Chemistry B, 111, 7415-7421.

Alexander, P., Lett, J. T. and Ormerod, M. G., 1961, Energy transfer in irradiated deoxyribonucleic acid and nucleoprotein. Biochimica et Biophysica Acta, 51, 207-209.

Ambroz, H. B., Kemp, T. J., Rodger, A. and Przybytniak, G., 2004, Ferric and ferrous ions: binding to DNA and influence on radiation-induced processes, Radiation Physics and Chemistry, 71, 1023-1030.

Bansal, K. M., Patterson, L. K. and Schuler, R., 1972, Production of halide ion in the radiolysis of aqueous solutions of the 5-halouracils, The Journal of Physical Chemistry, 76, 2386-2392

Bansal, K. M. and Fessenden, R. W., 1978, Radiation-chemical studies of the reaction of $SO_4^\bullet$ with Uracil and its derivatives, Radiation Research, 75, 497-507.

Becker, D., La Vere, T. and Sevilla, M. D., 1994a, ESR Detection at 77 K of the hydroxyl radical in the hydration layer of gamma-irradiated DNA. Radiation Research, 140, 123-129.

Becker, D., Razskazovskii, Y., Callaghan, M. U. and Sevilla, M. D., 1996, Electron spin resonance of DNA irradiated with a heavy-ion beam ($^{16}O_8$): evidence for damage to the deoxyribose phosphate backbone. Radiation Research, 146, 361-368.

Becker, D. and Sevilla, M. D., 1993, The chemical consequences of radiation damage to DNA. Advances in Radiation Biology, 17, 121-179.

Becker, D., Summerfield, S., Gillich, S. and Sevilla, M. D., 1994b, Influence of oxygen on the repair of direct radiation damage to DNA by thiols in model systems. International Journal of Radiation Biology, 65, 537-548.

Becker D. and Sevilla, M. D., 1998, Radiation damage to DNA and related biomolecules. In: Specialist Periodical Reports - Electron Paramagnetic Resonance, Vol. 16. Publisherr: B. C. Gilbert, N. M. Atherton and M. J. Davis (Royal Society of Chemistry, Cambridge) pp. 79-115.

Becker, D., Bryant-Friedrich, A., Trzasko, C. A. and Sevilla, M. D., 2003, Electron spin resonance study of dna irradiated with an argon-ion beam: evidence for formation of sugar phosphate backbone radicals, Radiation Research ,16, 174-185.

Becker, D. and Sevilla, M. D., 2004, ESR Studies of radiation damage to DNA and related biomolecules, Specialist Periodical Reports of Electron Paramagnetic Resonance, 79-115.

Becker, D., Adhikary, A., and Sevilla, M. D., 2007, Charge migration in DNA, Springer Berlin Heidelberg, 139-175.

Bernhard, W. A.,1989, Sites of electron trapping in DNA as determined by ESR of one-electron-reduced oligonucleotides. The Journal of Physical Chemistry, 93, 2187-2189.

Bhatia, K., Schuler, R. H., 1973, Uracilyl radical production in the radiolysis of aqueous solutions of the 5-halouracils, The Journal of Physical Chemistry, 77, 15, 1888-1896.

Boon, P. J., Cullis, P. M., Symons, M. C. R. and Wren. B. W., 1984, Effects of ionising radiation on deoxyribonucleic acid and relatied systems. Part 1. The role of oxygen. Journal of the Chemical Society. Perkin Transactions II, 1393-1399.

Boon, P. J., Cullis, P. M., Symons, M. C. R. and Wren. B. W., 1985, Effects of ionising radiation on deoxyribonucleic acid and relatied systems. Part 2. The influence of

nitroimidazole drugs on the course of radiation damage to aqueous deoxyribonucleic acid. Journal of the Chemical Society. Perkin Transactions II, 1057-1061.

Cai. Z. and Sevilla, M. D., 2000, Electron spin resonance study of electron transfer in DNA: Inter-double-strand tunneling processes. The Journal of Physical Chemistry B, 104,6942-6949.

Cai, Z., Gu, Z. and Sevilla, M. D., 2000, Electron spin resonance study of the temperature dependence of electron transfer in DNA: Competitive processes of tunneling, protonation at carbon, and hopping, The Journal of Physical Chemistry B, 104, 10406-10411.

Cai, Z., Gu, Z. and Sevilla, M. D., 2001, Electron spin resonance study of electron and hole transfer in DNA: Effects of hydration, aliphatic amine cations, and histone proteins. The Journal of Physical Chemistry B, 105, 6031-6041.

Cai, Z., Li, X., Sevilla, M. D., 2002, Excess electron transfer in DNA: effect of base sequence and proton transfer, The Journal of Physical Chemistry B, 106, 2755-2762.

Cai, Z., Sevilla, M. D., 2004, Studies of excess electron and hole transfer in DNA at low temperature, Topics in Current Chemistry, 237, 103–128.

Close, D. M., 1993, Radical ions and their reactions in DNA constituents: ESR/ENDOR studies of radiation damage in the solid state. Radiation Research, 135, 1-15.

Close, D. M., 1997, Where are the sugar radicals in irradiated DNA? Radiation Research, 147, 663-673.

Cullis, P. M., Symons, M. C .R. and Wren, B. W., 1985, Effects of ionising radiation on deoxyribonucleic acid, part 3-The effect of iodoacetamide. Journal of Chemical Society : Perkin Transaction 2, 1819-1825.

Cullis, P. M., Symons, M. C. R., Sweeny M. C., Jones, G. D. D., and Mc Clymont, 1986, The effects of ionising radiation on deoxyribonucleic acid, part 4- The role of hydrogen peroxide, Journal of Chemical Society Perkin Transaction 2, 1671-1676,

Cullis, P.M., Mc Clymont, J. D. and Symons M. C. R., 1990, Electron conduction and trapping in DNA. Journal of Chemical Society Faraday Transaction, 86, 591-592.

Cullis, P. M., Jones, G. D. D., Lea, J., Symons, M. C. R. and Sweeney, M, 1987a, The effects of ionizing radiation on deoxyribonucleic acid. Part 5. The role of thiols in chemical repair. Journal of the Chemical Society. Perkin Transactions II, 1907–1914.

Cullis, P. M., Jones, G. D. D., Symons, M. C. R. and Lea, J. S., 1987b, Electron transfer from protein to DNA in irradiated chromatin. Nature, 330, 773-774.

Cullis, P. M., McClymont, J. D., Malone, M. E., Mather, A. N., Padmore, M. C., Sweeney, M. C. and Symons, M. C. R., 1992, Effects of ionising radiation on deoxyribonucleic acid. Part 7. Electron capture at cytosine and thymine, Journal of the Chemical Society. Perkin Transactions II, 1695-1702.

Debije, M. G., Strickler, M. D., and Bernhard, W. A., 2000, on the efficiency of hole and electron transfer from the hydration layer to DNA: an EPR study of crystalline dna X-irradiated at 4 K, Radiation Research, 154, 163-170.

Debije, M. G., Milano, M. T. and Bernhard, W.A., 1999, DNA Responds to ionizing radiation as an insulator, not as a" molecular wire'', Angew Chem Int Ed Engl, 38, 2752-2756.

Dusemund, B., 1999, ESR-spektroskopische Untersuchungen strahleninduzierter freier Radikale in polykristallinen Nukleotiden und Nukleotidgemischen. Einfluss der Strahlenqualität. Dissertation, Universität des Saarlandes.

Fujita, S., Steenken, S., 1981, Pattern of OH radical addition to uracil and methyl- and carboxyl-substituted uracils. Electron transfer of OH adducts with N, N, N', N'-tetramethyl-p-phenylenediamine and tetranitromethane, The Journal of American chemical Society, 103, 2540-2545.

Faucitano, A., Buttafava, A., Martinotti, F. and Pedraly-Noy, G., 1992, ESR study of the direct radiolysis of DNA, DNA-Histones and DNA-intercalator complexes. Radiation Physics and Chemistry, 40, 357-364.

Flossman, W., Zehner, H., and Westhof, E., 1979, The Protonation of the 5-thymyl radical in single crystals of thymine derivatives: E.S.R. and INDO Evidence, 36, 577-586.

Galla, H., J., 1988, Spektroscopische Methoden in der Biochemie. Thieme Verlag, Stuttgart, New York.

Gräslund, A., Ehrenberg, A., Rupprecht, A. and Ström, G., 1971, Ionic base radicals in γ-irradiated DNA, Biochimica et Biophysica Acta, 254, 172-186.

Gatzweiler, W., Hüttermann, J. and Rupprecht, A., 1994, Free radicals from oriented DNA fibers after irradiation at 77 K: continuous-wave and pulsed electron paramagnetic resonance spectroscopy from D2O-equilibrated specimens. Radiation Research, 138, 151-164.

Gray, H. B. and Winkler, J. R., 1996, Electron transfer in proteins, Annual Review of Biochemistry, 65, 537-561.

Gray, H. B. and Winkler, J. R., 2005, Long-range electron transfer (Special Feature) Long-range electron transfer. Proceedings of National Academy of Science, 102, 3534-3539

Geimer, J., 1994, Diplomarbeit, Universitaet des Saarlandes

Gregoli, S., Olast, M. and Bertinchamps, A., 1970, Electron-transfer in gamma-irradiated complexes between DNA nucleotides and proflavine. International Journal of Radiation Biology, 18, 577-585

Gregoli, S., Olast, M. and Bertinchamps, A., 1974, Free radicals in γ-irradiated frozen solutions of deoxyadenosine-5'-monophosphate. A computer analysis of temperature-dependent ESR spectra. Radiation Research, 60, 388-404.

Gregoli, S., Olast, M. and Bertinchamps, A., 1976, Free radical formation in deoxythymidine-5'-monophosphate γ-irradiated in frozen solution. A computer-assisted analysis of temperature-dependent ESR spectra. Radiation Research, 65, 202-219.

Gregoli, S., Olast, M. and Bertinchamps, A., 1977a, Free-radical formation in deoxyguanosine-5'-monophosphate γ-irradiated in frozen solution. A computer-assisted analysis of temperature-dependent ESR spectra. Radiation Research, 72, 201-217.

Gregoli, S., Olast, M. and Bertinchamps, A., 1977b, Charge migration phenomena in γ-irradiated costacking complexes of DNA nucleotides. I. A computer-assisted ESR analysis of dAMP.dTMP complexes in frozen solution. Radiation Research. 70, 255-274.

Gregoli, S., Taverna, C. and Bertinchamps, A., 1979, Charge migration phenomena in γ-irradiated costacking complexes of DNA nucleotides. II. An ESR study of various complexes in frozen solution. Radiation Research, 77, 417-431.

Gregoli, S., Olast, M. and Bertinchamps, A.,1982, Radiolytic pathways in gamma-Irradiated DNA: Influence of Chemical and Conformational Factors, Radiation Research, 89, 238-254.

Herak, J. N. and Hüttermann, J., 1991, Long-range hole migration in irradiated crystals of nucleic acid bases. An EPR study. International Journal of Radiation Biology, 60, 423-432.

Herak, J. N., Sankovic, K., Krilov, D. and Huttermann, J., 1991, An EPR study of the transfer and trapping of holes produced by radiation in guanine (thioguanine) hydrochloride single crystals. Radiation Research, 151, 319-324.

Herak, J. N., Sankovic, K., Sankovic, K., Hole, E., O., and Sagstuen, E., 2000, ENDOR study of a thiocytosine oxidation product in cytosine monohydrate crystals doped with 2-thiocytosine, X-irradiated at 15 K. Physical Chemistry Chemical Physics, 2, 4971-4975.

Herak, J. N., Sankovi K., Hole, E. O., Sagstuen, E. and Matter, S., 2001, ENDOR study of the chlorinated thiocytosine radical in a crystal matrix, Physical Chemistry Chemical Physics, 3 4926-4931.

Henle, E. S. and Linn, S., 1997, Formation, prevention, and repair of DNA damage by Iron/Hydrogen Peroxide, The Journal of Biological Chemistry, 272, 19095-19098.

Hole, E.O., nelson, W. H., Sagstuen, E. and Close, D. M., 1992, Free radical formation in single crystals of 2'- deoxyguanosine 5'-monophosphate tetrahydrate disodium salt: An EPR/ENDOR study, Radiation Research, 129, 119-138.

Hutchinson, F. and Köhnlein, W., 1980, The photochemistry of 5-bromouracil and 5-iodouracil in DNA. Progr. Molecular Subcellular Biology, 7, 1-42.

Hüttermann, J., 1970, Electron spin resonance of radiation-induced free radicals in irradiated single crystals of thymine monohydrate. International Journal of Radiation Biology, 17, 249-259.

Hüttermann, J., Ward, J. F. and Myers, Jr., L. S. 1971, Electron spin resonance studies of free radicals in irradiated single crystals of 5-methyl cytosine. International Journal of Radiation Physics and Chemistry, 3, 117-129.

Hüttermann, J., Bernhard, W.A., Haindl, E., Schmidt, G., 1977, Reactions of radiation induced free radicals in solid halodeoxyuridines single crystals of 5-Chloro-and 5-Bromodeoxyuridine, The Journal of Physical Chemistry, 81, 228-232.

Hüttermann, J., 1982, Solid-state radiation chemistry of DNA and its constiuents. Ultramicroscopy, 10, 25-40.

Hüttermann, J., Voit, K., Oloff, H., Köhnlein, W., Gräslund, A. and Rupprecht, A., 1984, Specific formation of electron gain and loss centres in X-irradiated oriented fibres of DNA at low temperatures, Faraday Discussions of the Chemical Society, 78, 135-149.

Hüttermann, J., and Voit, K., 1987, Free radicals from direct action of ionising radiation in DNA: Structural assignments from EPR spectroscopy. In: Electronic Magneti Resonance of the Solid State. Publisher: J. A. Weil (The Canadian Society for Chemistry, Ottawa), 267-279.

Hüttermann, J., 1991a, DNA-radicals as structural monitors of direct radiation action: Sensitization by incorporation of 5-halouracils. Radiation and Environmental Biophysics, 30, 71-79

Hüttermann, J., 1991b, Radical ions and their reactions in DNA and its constituents. In: Radical Ionic Systems. Publisher: A. Lund and M. Shiotani (Kluwer Dordrecht). 435-462.

Hüttermann, J., Ohlmann, J., Schaefer, A. and Gatzweiler, W., 1991c, The polymorphism of a cytosine anion studied by electron paramagnetic resonance spectroscopy. International Journal of Radiation Biology, 59, 1297-1311.

Hüttermann, J., Röhrig, M., and Köhnlein, W., 1992a, Free radicals from irradiated lyophilized DNA: Influence of water of hydration, International Journal of Radiation Biology, 61, 299-313.

Hüttermann, J., Lange, M. and Ohlmann, J. 1992b, Mechanistic aspects of radiation induced free radical fomation in frozen aqueous solutions of DNA constituents: consequences for DNA? Radiation Research, 131, 18-23.

Jortner, J., Bixon, M., Langenbacher, T. and Michel-Beyerle, M. E., 1998, Charge transfer and transport in DNA, Proceedings of National Academy of Science(U.S.A.) 95, 12759-12765.

Ito, K., Inoue, S., Yamamoto, K., Kawanishi, S., 1993, 8-Hydroxydeoxyguanosine formation at the 5'site of 5'-GG-3'sequences in double-stranded DNA by UV radiation with riboflavin. 268, 13221-13227.

Kelley, S. O. and Barton, J. K., 1999, Electron transfer between bases in double helical DNA, Science, 283, 375-381.

Krivokapic, A., and Sagstuen, E., 2003, Hole transfer and differential radical recombination in x-irradiated doped crystalline DNA model systems. The Journal of Physical Chemistry A, 107, 9561-9566.

Kuwabara, M., Minegishi, A., Ito, A. and Ito, T., 1986, A study of aqueous solutions of nucleic acid constituents exposed to monochromatic 160 nm vacuum-UV light by spin-trapping method. Photochemistry Photobiology, 44, 265-272.

Kuwabara, M., Kato, S. and Yoshii, G., 1974, Effects of Ca++ ion on the formation of free radicals in irradiated deoxyribonucleoprotein. Journal of Radiation Research, 15, 219-222.

Lange, M., 1994, ESR-Untersuchungen und Strangbruch-Analysen der DNA und ihrer Untereinheiten nach Einwirkung dünn-ionisierender Strahlung in der gefrorenen, wässrigen Lösung. Dissertation, Universität des Saarlandes.

Lange, M., Weiland, B. and Hüttermann, J.,1995, Influence of electron scavengers on the radical formation in thymidine-5'-monophosphate and DNA in frozen aqueous solution and glasses. International Journal of Radiation Biology, 68, 475-486.

Lenherr; A. D. and Ormerod, M. G., 1971, Electron reactions with thymidine in γ-irradiated frozen aqueous glasses. Proceedings of the Royal Society of London. Series A, Mathematical and Physical Sciences, 325, 81-99.

Malone, M. E., Cullis, P. M., Symons, M. C. R. and Parker, A. W., 1995, Biphotonic photoionization of cytosine and its derivatives with uv radiation at 248 nm: an epr study in low-temperature perchlorate glasses. The Journal of Physical Chemistry, 99, 9299-9308

Malone, M. E., Symons, M. C. R. and Parker, A. W., 1993, An EPR study of photoionised thymine and its derivatives at 77 K, Journal of the Chemical Society. Perkin Transactions 2, 2067-2075.

Marcus, R. A., Sutin, N., 1985, Electron transfers in chemistry and biology, Biochimica et Biophysica Acta, 811, 265-322.

Mroczka, N., and Bernhard, W. A., 1993, Hydration effects on free radical yields in DNA X-irradiated at 4 K, Radiation Research, 135, 155-159.

Messer, A., Carpenter, K., Forzley, K., Buchanan, J., Yang, S., Razskazovkii, Y., Cai, Z. and Sevilla, M. D., 2000, Electron spin resonance study of electron transfer rates in DNA: Determination of the tunneling constant for single-step excess electron transfer. The Journal of Physical Chemistry B, 104, 1128-1136.

Moens, P., De Volder, P., Hoogewijs, R., Callens, F. And Verbeeck, R., 1993, Maximum-likelihood common-factor analysis as a powerful tool in decomposing multi-component EPR powder spectra. Journal of Magnetic Resonance, Series A, 101, 1-15.

Murphy, C.J., Arkin, M. R., Jenkins, Y., Ghatlia, N. D., Bossmann, S. H., Turro, N. J.,and Barton, J. K., 1993, Long-range photoinduced electron transfer through a DNA helix, Science, 262, 025-1029.

Nelson, W. H., 2005, Dose response relationships for radicals trapped in irradiated solids. Radiation Research, 163, 673-680.

Neumüller, W., Hüttermann, J., 1980, Radiation damage in solid 5-halouracils: free radicals in single crystals of 5-fluorouracil, International Journal of Radiation Biology, 37, 49-60.

Ohlmann, J., Hüttermann, J.,1993, Reactions of water radiolysis intermediates with pyrimidine and purine bases in aqueous BeF_2 Glasses: An EPR Study, International Journal of Radiation Biology, 63, 427-436.

Oloff, H. and Hüttermann, J., 1977, Radiation –induced free radicals in solid halouracil derivatives: Single crystals of 5-Chlorouracil and –uridine, Journal of Magnetic Resonance, 27, 197-200.

Oloff, H., Riederer, H. and Hüttermann, J., 1984, Free radical probes of condensed-phase aspects of radiation damage mechanisms in DNA constituents:5-Halouracils, Ultramicroscopy, 14, 183-194.

Ormerod, M. G., 1965, Free-radical formation in irradiated deoxyribonucleic acid. International Journal of Radiation Biology, 9, 291-300.

O'Neill, M. A. and Barton, J. K., 2004, DNA-mediated charge transport requires conformational motion of the DNA bases: Elimination of charge transport in rigid glasses at 77 K. Journal of American Chemical Society, 126, 13234-13235.

Parker, B. S., Buley, T., Evison, B. J., Cutts, S. M., Neumann, G. M., Iskander, M. N., Phillips, D. R., 2004, A molecular understanding of Mitoxantrone-DNA adduct

formation: Effect of cytosine methylation and flanking sequences, Journal of Biological Chemistry, 279, 18814-18823.

Pal, C. and Hüttermann, J., 2006, Postirradiation electron transfer vs differential radical decay in X-Irradiated DNA and iIts mixtures with additives. Electron spin resonance spectroscopy in LiBr Glass at low temperatures. The Journal of Physical Chemistry B, 110, 14976-14987.

Pezeshk, A., Symons, M. C. R. and Mc Clymont, J. D., 1996, Electron movement along DNA strands: Use of intercalators and EPR spectroscopy. The Journal of Physical Chemistry, 100, 18562-18566.

Porath, D., Cuniberti, G. and Di Felice, R., 2004, Long-range charge transfer in DNA. In: Topics in Current Chemistry, Publisher: Springer, Heidelberg, 183–227.

Pruden, B., Snipes, W. and Gordy, W., 1965, Electron spin resonance of an irradiated single crystal of thymidine. Proceedings of the National Academy of Science, 53, 917-924.

Przybytniak, G., Hüttermann, J., Ambroz, H. and Weiland, B., 1997, The influence of cysteamine on free radical formation in frozen aqueous matrices containing dCMP. Nukleonika, 42, 323-332.

Purkayastha, S. and Bernhard, W.A., 2004, What is the initial chemical precursor of DNA strand breaks generated by direct-type effects? The Journal of Physical Chemistry. B,108, 47, 18377-18382.

Purkayastha, S., Milligan, J. R., Bernhard, W. A., 2005a, The role of hydration in the distribution of free radical trapping in directly ionized DNA, Radiation Research, 166, 1-8.

Purkayastha, S., Milligan, J. R., Bernhard, W. A., 2005b, Correlation of free radical yields with strand break yields produced in plasmid DNA by the direct effect of ionizing radiation, The Journal of Physical Chemistry. B, 109, 16967-16973.

Razskazovskii, Y., Swarts, S. G., Falcone, J. M., Taylor, C. and Sevilla, M. D., 1997, Competitive electron scavenging by chemically modified pyrimidine bases in

bromine-doped DNA: Relative efficiencies and relevance to intrastrand electron migration distances, The Journal of Physical Chemistry B, 101, 1460–1467.

Riederer, H., Hüttermann, J. and Symons, M. C. R., 1981, Matrix-isolation of free radicals from 5-halouracils. 2. Electron spin resonance of hydrogen atom reactions in acidic glasses. The Journal of Physical Chemistry, 85, 2789-2797.

Riederer, H., 1981, Molekulare Mechanismen der Wirkung ionisierender Strahlung auf Nukleinsäuren: freie Radikale in 5-halogenierten Urazilderivaten nach Reaktion der Radiolyseprodukte des Wassers in Tieftemperaturgläseren. Dissertation, Universität Regensburg.

Riederer, H. and Hüttermann, J., 1982, Matrix isolation of free radicals from 5-Halouracils. 3. Electron spin resonance of base oxidation in aqueous acidic glasses. The Journal of Physical Chemistry, 86, 3454-3463.

Riederer H., Hüttermann, J., Boon, P. and Symons, M. C. R., 1983, Hydroxyl radicals in aqueous glasses: Characterisation and reactivity studied by ESR spectroscopy. Journal of Magnetic Resonance, 54, 54-66.

Saenger, W., 1984, Principles of nucleic acid structure. Springer Verlag, New York, Berlin, Heidelberg, Tokyo.

Sankovic, K., Krilov, D. and Herak, J. N., 1991, Postirradiation long-range energy transfer in a single crystal of cytosine monohydrate: An EPR Study. Radiation Research, 128, 119-124

Sagstuen, E., Close, D. M., Vågane, R., Hole, E. O. and Nelson, W.H., 2006, Electron transfer in amino acid· nucleic acid base complexes: EPR, ENDOR, and DFT Study of X-irradiated N-Formylglycine·cytosine complex crystals. The Journal of Physical Chemistry A, 110, 8653-8662.

Schulte-Frohlinde, D., Simic, M. G. and Gorner, H.,1990, Laser-induced strand break formation in DNA and polynucleotides. Photochemistry Photobiology, 52, 6, 1137-1151.

Sprague, E. D. and Schulte-Frohlinde, D.,1973, Electron spin resonance investigation of the disappearance of trapped hydrogen atoms in. gamma.-irradiated sulfuric acid glasses. The Journal of Physical Chemistry, 77, 1222-1225.

Schaefer, A., Hüttermann, J. and Kraft, G., 1993a, Free radicals from polycrystalline pyrimidines and purines upon heavy ion bombardment at low temperatures: an electron spin resonance study. International Journal of Radiation Biology, 63, 139-149.

Schaefer, A., Hüttermann, J. and Kraft, G., 1993b, Free radicals induced in solid DNA by heavy ion bombardment. Radiation Effects and Defects in Solids, 126, 381-384.

Scheffler, K. and Stegmann, H. B., 1970 Electron spin resonanz: Grundlagen und Anwendungen in der organischen Chemie, Springer-Verlag Berlin, Heidelberg.

Sevilla, M. D., Engelhardt, M. L., 1977, Mechanisms for radiation damage in DNA constituents and DNA. Reactions of the N-substituted thymine-cation radicals, Faraday Discussion Chemical Society, 63, 255-263.

Sevilla, M. D., 1972, Electron spin resonance study of the photoionization of thymine. Thymine cation and anion radicals. The Journal of Physical Chemistry, 75, 626-631

Sevilla, M. D. , 1976, Electron spin resonance study of N-Substituted thymine π-cation radicals. The Journal of Physical Chemistry, 80, 1898-1901.

Sevilla, M. D., Becker, D., Yan, M. and Summerfield, S. R., 1991, Relative abundance of primary ion radicals in γ-irradiated DNA: cytosine vs thymine anions and guanine vs adenine cations. The Journal of Physical Chemistry, 95, 3409-3415.

Sevilla, M. D. and Becker D., 1994, Radiation damage in DNA. In: A Specialist Periodical Report - Electron Spin Resonance, Vol. 14. Publisher: N. M. Atherton, M. J. Davis and B. C. Gilbert (Royal Society of Chemistry, Cambridge). 130-165.

Sevilla, M. D. and Becker, D., 2004, ESR Studies of radiation damage to DNA and related biomolecules. In: A Specialist Periodical Report - Electron Spin Resonance, Vol.

19. Publisher: M. J. Davis, B. C. Gilbert and Murphy, D., M., (Royal Society of Chemistry, Cambridge), 243-278.

Sevilla, M. D;., D'Arcy, J. B., Morehouse, K. M. and Engelhardt, M. L. ,1979, An ESR study of π-cation radicals in dinucleoside phosphates and DNA produced by photoionization, Photochemistry Photobiology, 29, 37-42

Sevilla, M. D., Swarts, S., Riederer, H. and Huettermann, J., 1984, Electron Spin Resonance investigation of the 5-halouracil and 5-halocytosine π-cations produced by attck of the Cl_2^- radical, The Journal of Physical Chemistry, 88, 1601-1605.

Sevilla, M. D., Suryanarayana, D., Morehouse, K. M., 1981, ESR study of DNA base cation radicals produced by attack of oxidizing radicals, The Journal of Physical Chemistry, 85, 1027-1031.

Shields, H. and Gordy, W., 1959, Electron-spin resonance studies of radiation damage to the nucleic acids and their constituents. Proceedings of the National Academy of Science, 45, 269-281.

Shukla, L. I., Pazdro, R., Huang, J., DeVreugd, C., Becker, D., and Sevilla, M. D., 2004, The formation of DNA sugar radicals from photoexcitation of guanine cation radicals, Radiation Research, 161, 582-590.

Shukla, L. I., , Adhikary, A., Pazdro, R., Becker, D., Sevilla, M. D., 2004, Formation of 8-oxo-7, 8-dihydroguanine-radicals in γ-irradiated DNA by multiple one-electron oxidations, Nucleic Acids Research, 32, 6565-6574.

Shukla, L. I., ,Pazdro, R., Becker, D. and Sevilla, M. D., 2005, Sugar Radicals in DNA: Isolation of Neutral Radicals in Gamma-Irradiated DNA by Hole and Electron Scavenging, Radiation Research, 163, 591-602.

Sieber, K., Hüttermann, J., 1989, Matrix-isolation of H·-induced free radicals from purines in acidic glasses, International Journal of Radiation Biology, 55, 331-345.

Spalletta, R. A. and Bernhard, W. A.,1992, Free radical yields in A: T polydeoxynucleotides, oligodeoxynucleotides, and monodeoxynucleotides at 4 K, Radiation Research, 130, 1, 7-14.

Swarts, S. G., Sevilla, M. D., Becker, D., Tokar. C. J., and Wheeler, K. T., 1992, Radiation induced DNA damage as a function of hydration I. Release of unaltered bases. Radiation Research, 129, 333-344.

Symons M.C.R. 1990, ESR spectra for protonated thymine and cytidine radical anions: their relevance to irradiated DNA. International Journal of Radiation Biology, 58, 93-96.

Symons, M. C. R., 1991, The role of radiation induced charge migration with DNA: ESR studies. In: The early effects of radiation on DNA, NATO ASI Series H, 54. Publisher: E. M. Fielden and P. O'Neill (Springer Verlag Berlin), 111-124.

Symons, M. C. R., 1997, Electron movement through proteins and DNA. Free Radical Biology and Medicine, 22, 1271-1276.

Tao, N. J., Lindsay, S. M. and Rupprecht, A., 1989, Structure of DNA hydration shells studied by raman spectroscopy. Biopolymers, 28, 1019-1030.

Tubiana, M., Dutreix, J., Wambersie, A., 1990, Introduction to Radiobiology, Taylor & Francis. London, 1-21.

Vere, T. L., Becker, D. and Sevilla, M. D., 1996, Yields of ·OH in gamma-irradiated DNA as a function of DNA hydration: Hole transfer in competition with ·OH formation, Radiation Research, 145, 673-680.

Voit, K., Oloff, H., Hüttermann, J., Köhnlein, W., Gräslund, A. and Rupprecht, A., 1986, Anionradicals from 5-halouracil substituted oriented DNA after X-irradiation at low temperatures. Radiation and Environmental Biophysics, 25, 175-181.

Von Sonntag, C., 1987, The chemical basis of radiation biology, Taylor&Francis, London.

Wang, W., Becker, D. and Sevilla, M. D., 1993, The influence of hydration on the absolute yields of primary ionic free radicals in γ-irradiated DNA at 77 K I. Total radical yields, Radiation Research, 135, 146-154.

Wang, W., Yan, M., Becker, D. and Sevilla, M. D., 1994, The influence of hydration on the absolute yields of primary free radicals in gamma-irradiated DNA at 77 K. II. Individual radical yields, Radiation Reseacrh, 137, 2-10.

Wang, W. and Sevilla, M. D., 1994a, Protonation of nucleobase anions in gamma-irradiated DNA and model systems. Which DNA base is the ultimate sink for the electron? Radiation Research, 138, 9-17.

Wang, W. and Sevilla, M. D., 1994b, Reaction of cysteamine with individual DNA base radicals in γ-irradiated nucleotides at low temperature. International Journal of Radiation Biology, 66, 683-695.

Wagenknecht, H. –A., 2005, Principles and Mechanisms of Photoinduced Charge Injection, Transport and Trapping in DNA. In Charge Transfer in DNA: From Mechanism to Application, Willey-VCH Verlag, Weinheim, 1-26.

Wardman, P., 1991, Chemical properties of 'radiation modifiers' of DNA damage and their radiobiological effects. In: The Early Effects of Radiation on DNA, NATO ASI Series, Vol. H 54. Publisher: E. M. Fielden and P. O'Neill (Springer Verlag Berlin, Heidelberg), 249-264.

Weiland, B., Hüttermann, J. and van Tol, J., 1997a, Primary free radical formation in randomly oriented DNA: EPR spectroscopy at 245 GHz. Acta Chemica Scandinavica, 51, 585-592.

Weiland, B., Hüttermann, J. and van Tol, 1997b, Highfield EPR (8.7 T, 245 GHz) of free radicals from nucleotides and DNA after irradiation with X-rays and heavy ions at low temperature. Radiation Research, 148, 510-511.

Weiland, B., Hüttermann, J., Malone, M. E. and Cullis, P. M., 1996, Formation of C1' located sugar radicals from X-irradiated cytosine nucleosides and -tides in BeF_2 glasses and frozen aqueous solutions. International Journal of Radiation Biology, 70, 327-336.

Weiland, B. and Hüttermann, J., 1998, Free radicals from X-irradiated 'dry' and hydrated lyophilized DNA as studied by electron spin resonance spectroscopy: analysis

of spectral components between 77K and room temperature. International Journal of Radiation Biology, 74, 341-358

Weiland, B.and Hüttermann, J.,1999, Free radicals from lyophilized'dry'DNA bombarded with heavy-ions as studied by electron spin resonance spectroscopy. International Journal of Radiation Biology, 75, 1169-1175.

Weiland, B., 1999, Elektronspinresonanz-Spectroskopie bei 9,5 und 245 GHz an strahleninduzierten, freien Radikalen in DNA: einfluss von Hydratwasser, Additiven, Histonen und Strahlenqualität, Dissertation, Universität des Saarlandes.

Weiland, B., Hüttermann, J., 2000, Spin transfer from protein to DNA in X-irradiated 'dry'and hydrated chromatin: an electron spin resonance investigation of spectral components between 77K and room temperature, International Journal of Radiation Biology, 76, 1075-1084.

Wertz, J. E. and Bolton, J. R., 1972, Electron Spin Resonance: elementary theory and practical applications, McGraw-Hill, New York.

Yan, M., Becker, D., Summerfield, S., Renke, P. and Sevilla, M.D., 1992, Relative abundance and reactivity of primary ion radicals in γ-irradiated DNA at low temperatures. Single-vs double stranded DNA, The Journal of Physical Chemistry, 96, 1983-1989.

Zell, I., Hüttermann, J., Graslund, A., Rupprecht, A. and Kohnlein, W.,1989, Free radicals in irradiated oriented DNA fibers: results from B-form DNA and from deuterated DNA samples. Free Radical Research Communication, 6, 105-106.

Zimbrick, J. D., Ward, J. F. and Myers, L. S., 1969, Studies on the chemical basis of cellular radiosensitization by 5-bromouracil substitution in DNA, I. Pulse and steady state radiolysis of 5-bromouracil and thymine, International Journal of Radiation Biology, 16, 505-523.

Appendix

A1.1. Anion and Cation Radicals of DNA Components in Glasses

Frozen aqueous glasses provide a model for indirect radiation action and also glasses can sometimes be used as a medium for analyzing the reaction of electron or hole selectively. Neutral aqueous glasses like 12 M LiCl along with oxidising agents (like $K_3Fe(CN)_6$) or 8M $NaClO_4$ were used to study oxidative reactions in thymine and its derivatives both by photolysis and radiolysis (Sevilla 1971, Sevilla et. al. 1981). Thymine base was found to produce the N_1 deprotonated cation which was also confirmed in acidic glasses (Riederer et. al. 1981) while N_1 substituted derivatives of thymine showed formation of cations or OH addition at C_6 position (Sevilla and Engelhardt 1976). Further detailed analysis with thymine and a variety of derivatives was done in perchlorate glass treated with photoionization showed presence of radicals like $T^{-\bullet}$, $TCH_2^{\bullet}$, $TH^{\bullet}$, or $TD^{\bullet}$ in D_2O. In TMP after annealing to 240 K a quintett pattern with splitting 1:4:6:4:1 was observed which was suggested in this work to be the result of cyclization or dimerization. This quintet pattern in TMP was also observed earlier in frozen aqueous system by Gregoli and co workers (1976) and was assigned as $T(C6)OH^{\bullet}$ which was discarded. More research in this field was done using thymine, thymidine TMP and several other related components in BeF_2 glass (Ohlmann and Hüttermann 1993), and in frozen aqueous system and it was observed that allyl radical and presence of sugar phosphate precursor are the essential precursors for quintet pattern formation (Lange et. al. 1995).

In BeF_2 glasses using cytosine and its derivatives as target molecules (Ohlmann and Hüttermann 1993), most electron adducts were observed at 77 K which were protonated at the exocyclic nitrogen. On annealing to higher temperatures H addition radicals to C5 and C6 were found in acidic glasses (Sieber and Hüttermann, 1989). $OH^{\bullet}$ addition species were observed on further annealing in case of cytosine. Quartet patterns were observed in the cytosine base (due to $OH^{\bullet}$ addition at the C5 or C6 position) as well as in 2′-deoxycytidine (CdR), 5′-dCMP and CMP. C1′ and C3′ radicals on the sugars were identified done in later research done on perchlorate glass treated with biphotonic ionization containing cytosine base, its nucleoside and nucleotides (Malone et. al. 1995) and then by Weiland et al (1996) in BeF_2 and D_2O matrices. The radioprotective agent like cysteamine was used in another work to see its effect on

formation of the C1$'$ radical in 5$'$dCMP in BeF$_2$ and in aqueous ice (Przybytniak et. al. 1997).

In low temperature glasses, photoionisation of guanine give rise to singlet type spectra for π-cation radical in the LiCl system (Sevilla et. al. 1978). Sieber and Hüttermann (1989) have studied H$^{\bullet}$ and OH$^{\bullet}$ addition on purine systems, their ribosides and deoxyribosides (-tides). Formation of H addition radical at C2 was observed for guanine and at C2 and C8 for adenine. H$^{\bullet}$ attack on C1$'$, C2$'$ and C5$'$ positions were observed in deoxyribosides and -tides while probable formation of C3$''^{\bullet}$ in ribosides was suggested. Extension of this work in BeF$_2$ glass (Ohlmann and Hüttermann 1993) showed that for adenine at 77 K the N3 protonated adenine anion is formed.

Recent approaches in this field mainly tried to accumulate knowledge regarding radiation induced damage of sugar phosphate backbone as they play a critical role in radiation induced biological damages. Various nucleosides and nucleotides of guanine and adenine were investigated for this purpose. The irradiation of the substrate in LiCl glass containing high concentrations of electron scavenger at 77 K was performed and then the glass was annealed to the temperature (~155 K) where Cl$_2^{-\bullet}$ oxidizes the purines to produce base cations. These base cations were identified by ESR spectroscopy; these were then exposed to visible lights of different wavelengths which led to the formation of sugar radicals on excitation of the base cation. These works showed presence of C1$'^{\bullet}$, C2$'^{\bullet}$, C3$'^{\bullet}$ and C5$'^{\bullet}$ in the systems studied by deprotonation of the sugar moiety. Influence of different pH and wavelengths of visible lights were studied. These studies could not detect the presence of C4$'^{\bullet}$ in both guanine and adenine systems though theoretically it was shown to have similar stability like other sugar radicals. 5$'$-TMP and 5$'$-dCMP were reported to form respective cation radicals on annealing in glass but identification of sugar radicals was not possible after visible light illumination because of highly overlapping nature of the radicals (Shukla et. al. 2004, Adhikary et. al. 2005, Adhikary et.al. 2006).

At this phase a comparative study is needed to be done with all the four neucleotides (dGMP, dCMP, TMP and dAMP) in a neutral aqueous glass (frozen) medium like 7 M LiBr/H$_2$O. In this matrix the reduced species are formed on the nucleotides upon irradiation and holes are trapped by the solvent matrix. Upon annealing (step-wise) the samples to higher temperatures and then ESR measurements at 77 K

information can be obtained about the reactions of the mobilized holes (from the solvent matrix) with the substrates. This study can also help to understand how the presence of an electron scavenging additive and increase in temperature together can modulate the formation of free radicals in these irradiated substrates.

A1.2. Identification of Free radicals formed upon x-ray irradiation on the deoxy-ribonucleotides in frozen aqueous 7M LiBr/H2O glasses

In this section the formation of free radicals in frozen aqueous glasses (7M LiBr/ H_2O) containing the deoxyribonucleotides 2′-Deoxycytidine 5′-monophosphate (Na Salt) (dCMP), Thymidine 5′-monophosphate (Na Salt) (TMP), 2′-Deoxyguanosine 5′-monophosphate (Na Salt) (dGMP) and 2′-Deoxyadenosine 5′-monophosphate (Na Salt) (dAMP) is studied upon x-ray irradiation at 77 K. The structures of the deoxyribonucleotide used in this study are given below in **Fig. A1**. In 7 M LiBr glass matrix the holes produced on ionization are scavenged by bromide moieties leaving only the electrons to react with the substrate (Messer et. al. 2000, Pal and Hüttermann 2006). This glass matrix therefore provides an efficient medium to exclusively study the electron reaction in DNA components at 77 K. With increment of temperature the trapped holes in the matrix get destabilized and might react with the substrate (Adhikary et. al. 2005).

In recent years many works are focused on the topic of elucidation of sugar radicals as they are critical to understanding their damaging effects in DNA via photo excitation at elevated temperatures of the free radicals formed on various DNA bases, deoxynucleosides and deoxynucleotides containing high concentrations of electron scavengers upon gamma irradiation at 77 K in frozen glasses (Adhikary et. al 2005, Adhikary et. al. 2006, Adhikary et. al. 2007). This work on the other hand emphasis on the isolation and identification of free radicals formed on purine and pyrimidine deoxyribonucleotides immediately after x-ray irradiation and whether formation of sugar based radicals can be observed in these systems or not. It has been explained in **section 5.3** that addition of substrates (Nucleic acid bases/deoxyribonucleotides in pure form or with electron scavengers are used in this section) in LiBr glass matrix results into formation of electron adduct selectively upon irradiation.
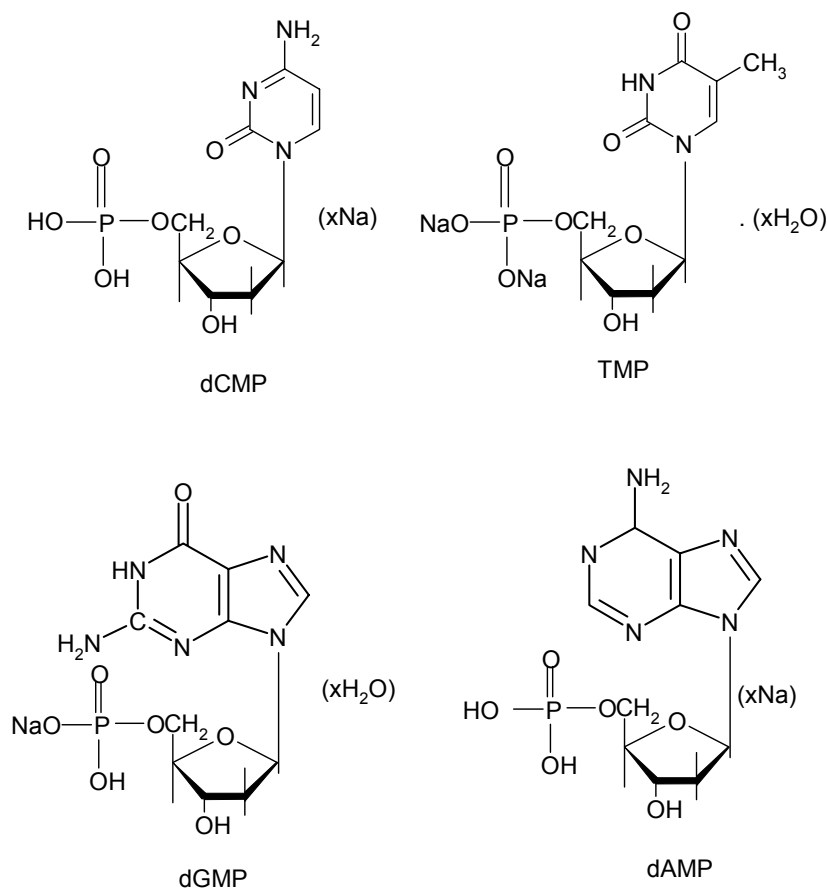
Fig. A.1. Structures of the deoxyribonucleotides (Sodium salts) used in this study.

Pyrimidines

Fig. A.2 represents the series of spectra obtained upon irradiation (10 kGy) of dCMP (10 mM) with annealing between 77 K and 170 K in 7M LiBr/ H_2O. A strong triplet feature is observed at 77 -160 K. As electron is mobile at 77 K therefore this feature can be assigned to an electron adduct. This triplet pattern has been previously observed (Cullis et. al. 1989, Hüttermann et. al. 1991c) and has been assigned to the electron adduct of the base protonated at the amino group denoted as $C^-(N4H^+)^{\bullet-}$ (**Str. A.1**). There are some outer wings (as shown with the arrows) just after irradiation at 77 K. With increase in annealing temperature the electron adduct starts decaying and a sextet pattern remains at 170 K.

When a strong electron scavenger like $K_3Fe[CN]_6$ is added to dCMP in equivalent stoichiometric amounts and the sample is on irradiatied with same dose at 77 K, the ESR measurement at 77 K shows that the triplet pattern at the center is no more present but only the sextet structure is formed (**Fig. A.3.A**). This pattern is a sextet in nature but its spectral width is much larger than the sextet observed to be formed from C3'/C4' sugar radical on DNA (**Fig. A.3.C**). In order to understand the origin of this pattern; the same experiment was repeated with cytosine (25 mM) along with Fe^{3+} (in 1:1 molar ratio) as an additive. The resultant spectrum showed formation of a similar pattern. In both cases the pattern remains unchanged with annealing and is the final radical pattern when the samples started to melt. This pattern can be correlated with C6-H radical formed by H-addition to the 6-position of the 5, 6-double bond of cytosine as shown by simulated spectrum (**Fig. A.3.F**).

Str. A.1.C⁻ (N4H⁺)•⁻

Str. A.2. C_(C6H)
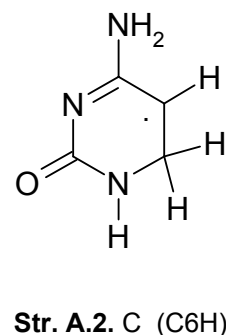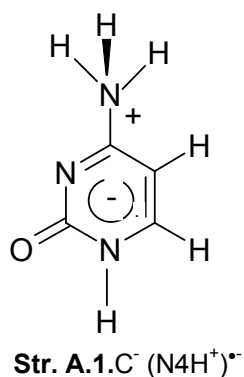
Table A.1. Parameters of proton hyperfine interaction (mT) used in simulation of dCMP_C6H.

dCMP_C6H (Ohlmann and Hüttermann) 1993)				In this work			
A(mT); g	x	y	z	A(mT); g	x	y	z
H (C5)	-1.78	-2.67	-0.72	H (C5)	-2.28	-3.07	-0.72
H(C6)	4.90	4.90	4.90	H(C6)	5.2	5.2	5.2
H(C6)	4.30	4.30	4.30	H(C6)	4.8	4.8	4.8
				Line width	0.8	0.8	0.8
g	2.002	2.002	2.003	g	2.002	2.002	2.003

The simulated C_C6H (**Str. A.2**) pattern is obtained by using the parameters given in **Table A.1**.
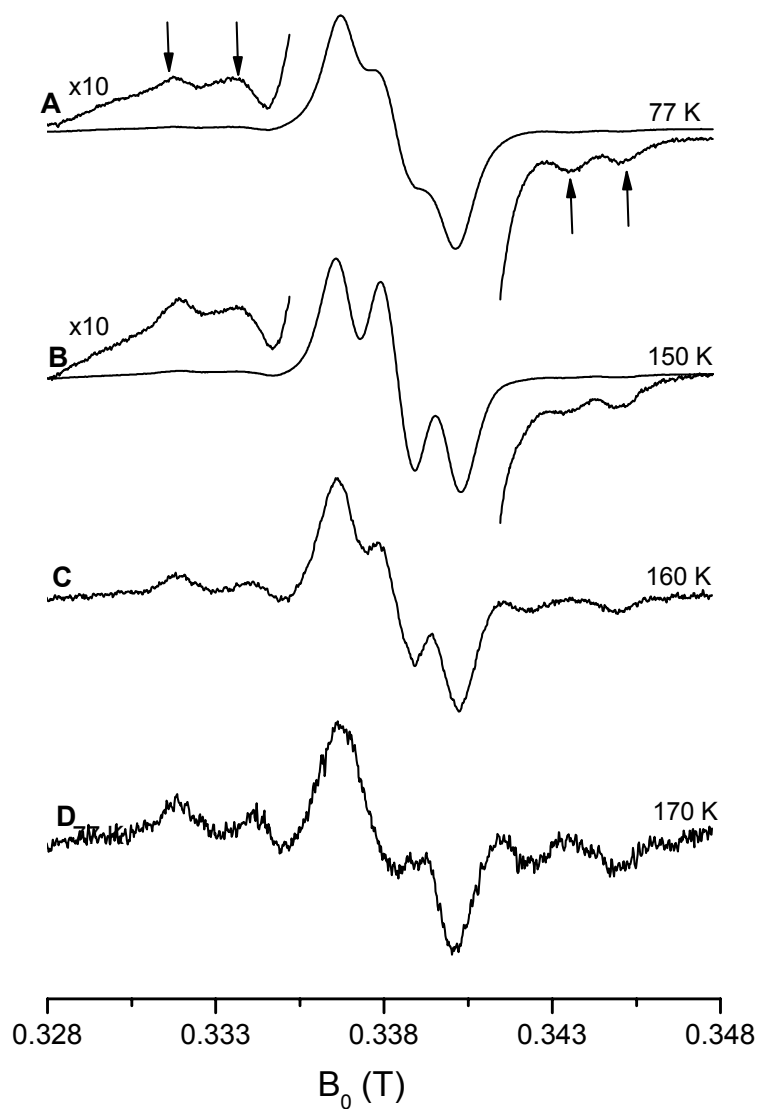
Fig.A.2. Sequence of ESR spectra from dCMP (10mM) in 7M LiBr/ H_2O glasses irradiated at 77K (10 kGy), annealed to the temperatures as indicated, and measured at 77K. The presence of outer wings at 77 K has been shown by proper magnification.
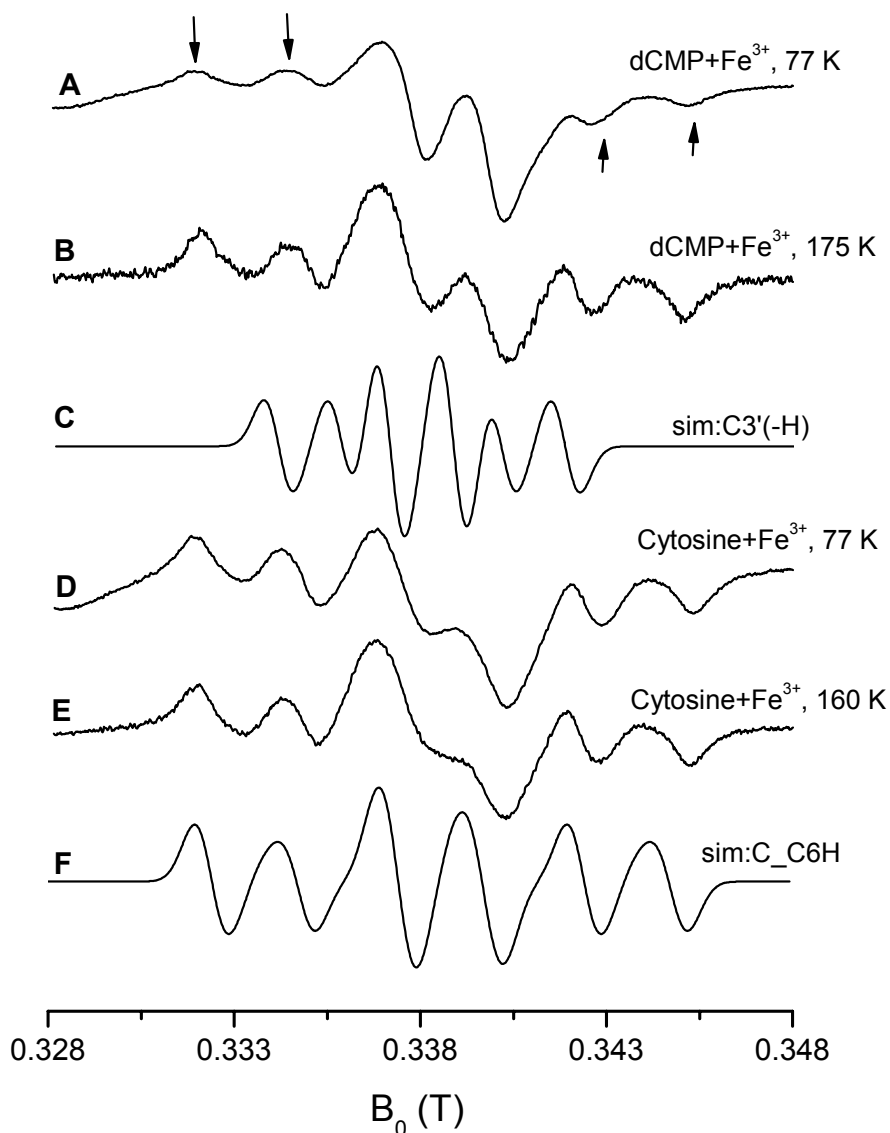
Fig.A.3. ESR spectra obtained from A) Fe^{3+}:dCMP (1:1) in 7M LiBr/ H_2O glasses irradiated at 77K (10 kGy) and measured at 77 K, B) Same sample annealed to 175 K and measured at 77 K. C) Simulated sextet pattern assuming two β-protons with A_{iso} =3.0 mT and one β-proton with A_{iso} =1.7 mT, g factors are 2.0033, 2.0028 and 2.0034, line width= 0.7 mT. This is tentatively assigned to a radical at the C3' or C4' position of the deoxyribose moiety. (D) Fe^{3+}: Cytosine (1:1) in 7M LiBr/H_2O matrix irradiated with 10 kGy of X-ray and measured at 77 K. (E) On annealing to 160 K and measuring at 77 K. (F) Simulated pattern for H addition radical on C6 of Cytosine (parameters given in table A1).

The spectra of relevant temperature stages in annealing of TMP in 7M LiBr/H$_2$O are shown in **Fig. A.4**. Again as expected, in **Fig. A.4.A** the electron adduct T$^-$ at 77 K can be characterized by the doublet pattern at 77 K which decays upon annealing. At high temperatures the well known octet pattern arising from 5-yl radical is most prominent, although its indication is there at 77 K also. At high temperature there is a presence of other lines (shown by arrows) which does not belong to any of these two radical patterns. At 175 K the sample melts with formation of peroxy radical pattern. After adding electron scavenger K$_3$Fe[CN]$_6$ in a molar ratio of 1:1 to TMP the formation of electron adduct at thymine base reduces drastically at 77 K, the spectrum is predominated by octet pattern from H addition radical at C6 (TH$^\bullet$) and another radical pattern (arrows). Changing the matrix from H$_2$O to D$_2$O clarifies the presence of thymine allyl radical (TCH$_2$$^\bullet$) which has also been previously observed in BeF$_2$/H$_2$O glass matrix (Ohlmann and Hüttermann 1993). The presence of multiplet from D addition to C6 could not be observed very prominently in this system may be owing to the difficulty in deuteration of the 6H to 6D on thymine completely. The structures of the radicals are shown in **Str. A.3-A.5**.

Str. A.3. T$^-$ **Str. A.4.** TH$^\bullet$ **Str. A.5.** TCH$_2$$^\bullet$
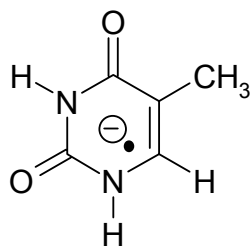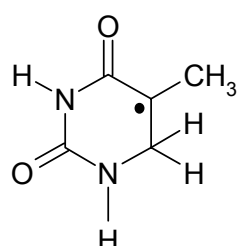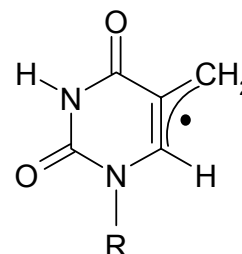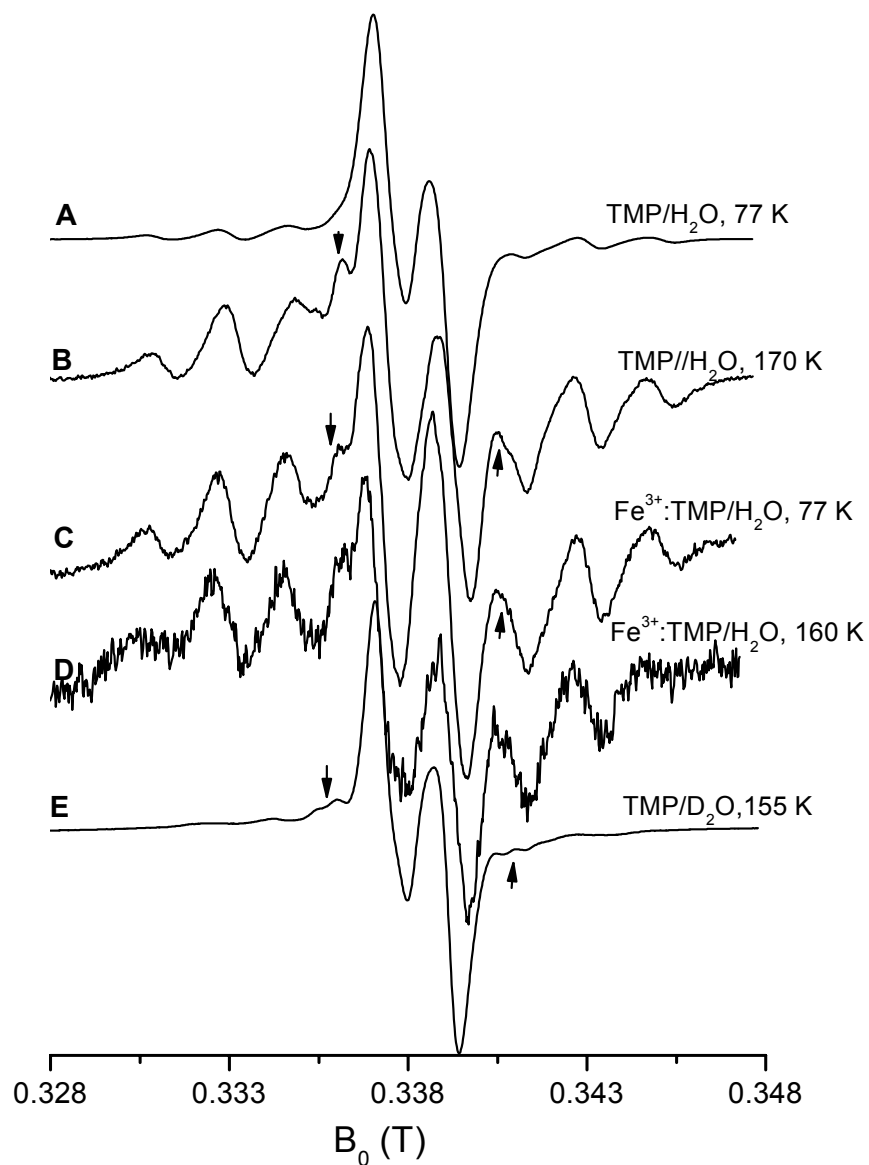
Fig.A.4. A-B) Sequence of ESR spectra from TMP in 7M LiBr/ H_2O glasses irradiated at 77K (10 kGy), annealed to the temperatures as indicated, and measured at 77K. C-D) Fe^{3+}:TMP (1:1) treated similarly as pure TMP, E) TMP/D_2O X-rayed to 10 kGY and annealed to 155 K before ESR measurement at 77 K.

Discussion

The basic chemical structure of most of the radicals formed from electron addition and from subsequent reactions is already known from previous studies on single crystals as well as on other glass matrices. Among the two pyrimidines cytosine is more sensitive and forms protonated electron adduct in H_2O. Formation of H-addition radicals is also prominent. It should be noticed that in both cases at 77 K there is a genuine presence of $H^\bullet$-addition radicals. Presence of high electron scavenger concentration decreases the electron adduct formation to a large extent but the H addition radicals i.e. C_C6H and $TH^\bullet$ or $TCH_2{}^\bullet$ which are formed during irradiation remains unaltered at 77 K. With increasing temperature also the anion radical concentration decreases in both pure dCMP and TMP. Formation of C_C6H is observed in dCMP, this pattern can be confirmed from the pattern obtained from cytosine base, and formation of C_C5H is not observed in this case (Ohlmann and Hüttermann 1993). Unlike in BeF_2/H_2O matrix (Ohlmann and Hüttermann 1993) no oxidation reaction was observed at higher temperature in spite of the fact that holes trapped at LiBr matrix at 77 K upon irradiation do get released at higher temperature. In TMP the final radicals are mainly $TH^\bullet$ and $TCH_2{}^\bullet$ radical as has been observed previously in other reports (Ohlmann and Hüttermann 1993). No spin transfer between the radicals is observed after the irradiation is completed. Sugar derived radicals were also not observed at higher temperatures.

Purines

Fig. A.5 gives representative spectra of the annealing series of dGMP in pure state and with additives in $7MLiBr/H_2O$ matrix after irradiation with 10 kGy of X-ray. **Fig.A.5A** and **B** shows the ESR spectra obtained from pure dGMP at 77 K just after irradiation and then on annealing to 160 K.

The correlation of the outer wings of the spectrum at 77 K can be done with simulated pattern of H addition radical on C8 position of dGMP base (Sieber and Hüttermann 1989). The parameters for this simulation are given in **Table A.2**. The structure of the H addition radical at C8 of guanine base is shown in **Str. A.6**.

It can be observed that with increasing temperature the triplet character of the experimental spectrum is lost and a singlet is obtained. When Fe^{3+} is used as electron scavenging agent (1Fe^{3+}:1dGMP) the nature of the spectrum remains basically the same with that of pure dGMP at 77 K only the concentration decreases to a large extent. In
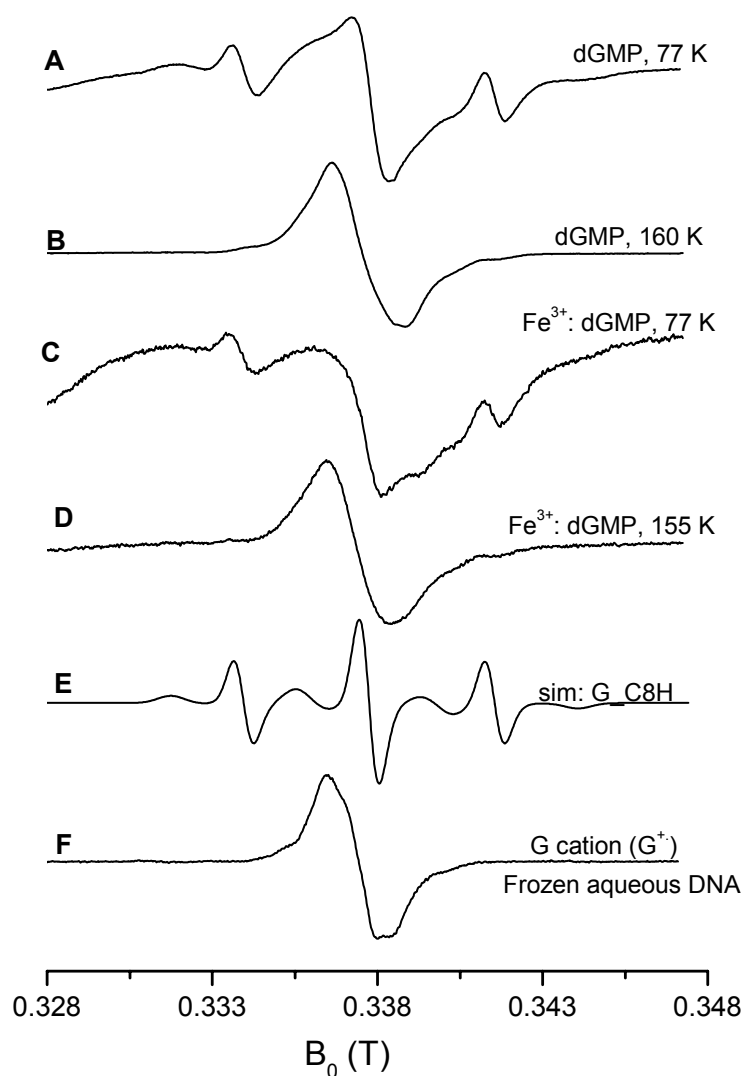
Fig.A.5. A-B) Sequence of ESR spectra from dGMP in 7M LiBr/ H_2O glasses irradiated at 77K (10 kGy), annealed to the temperatures as indicated, and measured at 77K. C-D) Fe^{3+}:dGMP (1:1) treated similarly as pure dGMP, E) Simulated pattern of radical formed on dGMP by H addition on C8, F) Guanine cation radical pattern derived from Fe^{3+}:DNA (1:20) in frozen aqueous solution (H_2O).

this system annealing leads to the formation of singlet pattern. This pattern arises due to formation of guanine cation via hole transfer from the matrix to the substrates as increase in temperature releases the trapped holes from the matrix. The spectra obtained from pure dGMP and Fe^{3+}:dGMP at higher temperatures (>150 K) can be well compared with the guanine cation (**Str. A.7**) pattern obtained from irradiated DNA in frozen aqueous solution or that from DNA (Weiland and Hüttermann 1998).

Table A.2. Parameters of proton hyperfine interaction (mT) used in simulation of dGMP_C8H.

dGMP_C8H (Weiland 1999)				In this work			
A(mT); g	x	y	z	A(mT); g	x	y	z
N7	0	0	2.4	N7	0	0	2.4
2xH(C8)	3.65	3.65	3.65	2xH(C8)	3.8	3.8	3.8
Line width	0.5	0.5	0.5	Line width	0.5	0.5	0.5
g	2.0051	2.0032	2.0029	g	2.0051	2.0032	2.0029
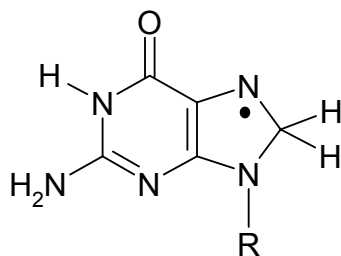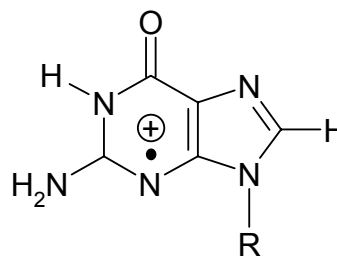
Str. A.6. G_C8H   **Str. A.7.** G$^{+\bullet}$

Fig. A.6 represents the ESR spectra of pure dAMP obtained after X-ray irradiation with 10 kGy. The spectra do not show any major change with increasing temperature except that the triplet character of the spectra increases at the central position.

As observed earlier (Ohlmann and Hüttermann 1993) the spectrum at 77 K for
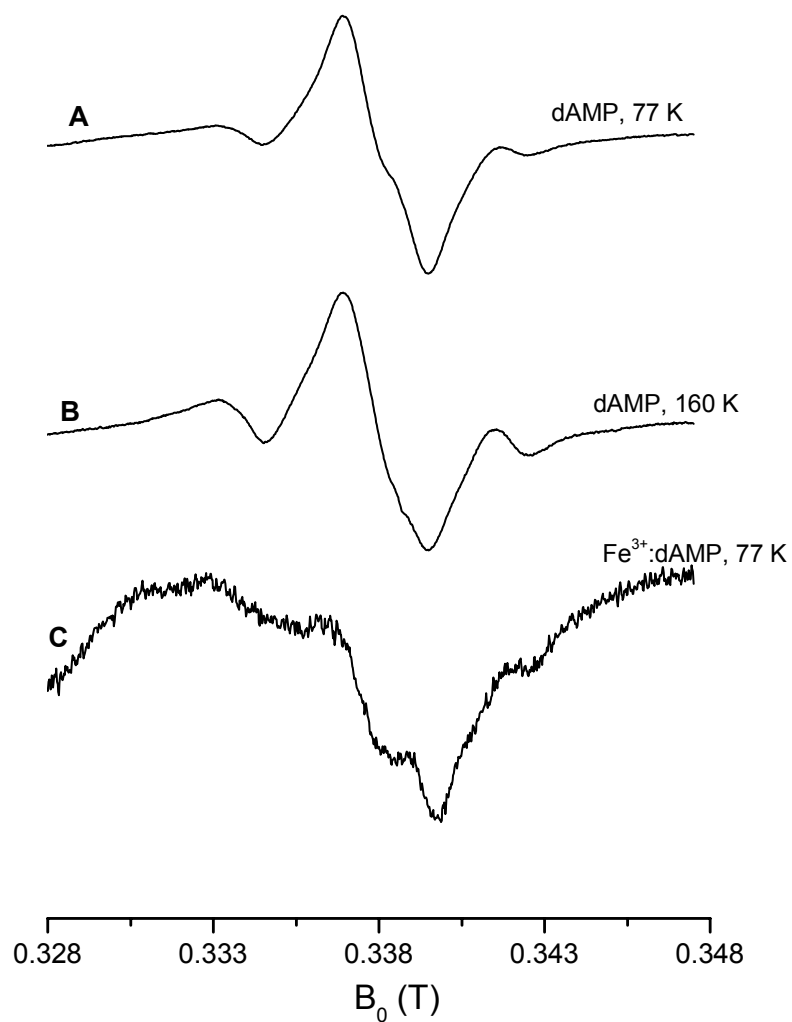
Fig.A.6. A-B) Sequence of ESR spectra from dAMP in 7M LiBr/ H_2O glasses irradiated at 77K (10 kGy), annealed to the temperatures as indicated, and measured at 77K. C) Fe^{3+}:dAMP (1:1) x rayed and measured at 77 K. (H_2O).

neat dAMP may be due to formation of N3 protonated adenine anion (**Str. A.8**) which gives a singlet pattern and minor amounts of H addition radical at C2 or C8 (**Str. A.9, Str. A.10**) of dAMP which produces a triplet pattern. The separation of these two radical

patterns was not possible by subtraction of the experimental spectra due to very noisy character of the spectra.
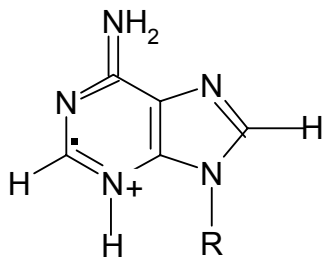
Str. A.8. A_anion (A⁻(3H⁺))
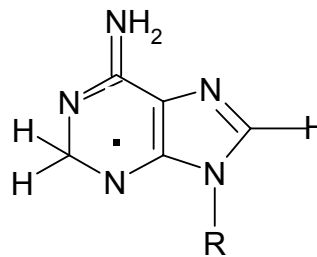
Str. A.9. A_C2H
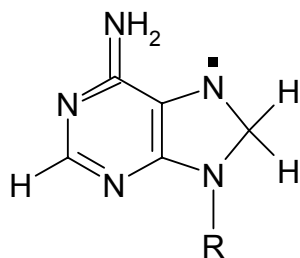
Str. A.10. A_C8H

With increasing temperature triplet pattern remained as the final radical product. No ESR finger print due to formation of sugar radicals were observed in pure dAMP. On adding Fe^{3+} with dAMP in frozen glass solution in a molar ratio of 1:1 relation the ESR spectrum at 77 K reduced in quantity to a large extent (**Fig. A.6C**) and on further annealing till 160 K (melting point of the glass matrix) only decay of the ESR spectra were observed.

Discussion

The annealing series of dGMP and and dGMP with $K_3Fe[CN]_6$ was important to observe whether increasing temperature of the matrix leads to any sugar radical formation as has been observed earlier (Adhikary et. al. 2005 and 2006) via photo excitation of glass matrix containing guanine and its derivatives along with electron scavenger. There was no formation of sugar derived radicals only upon annealing of irradiated pure or Fe^{3+} and dGMP systems. The oxidation of the H• addition radical at C8 formed at 77 K does occur with attaining higher temperature from the holes trapped in

the matrix to non irradiated guanine molecules. No further spin transfer from guanine cation radical to the sugar moieties are observed in the given circumstances.

In dAMP the ESR spectra obtained are not very well resolved and could not be disentangled into further radical patterns. Sugar radicals were not observed also no oxidized species were observed on the adenine base at higher temperature. The triplet pattern from H addition radical on C2 reduces to doublet character when the same experiment is performed in D_2O (spectrum not shown here). Similar results were obtained for adenine in BeF_2 glass (Ohlmann and Hüttermann 1992).

The annealing series of nucleotides dCMP, TMP, dGMP and dAMP obtained in 7M LiBr glass/H_2O upon irradiation with 10 kGy in neat form or with additive Fe^{3+} showed no sugar radical formation at elevated temperatures via oxidation of reduced base radicals by the mobile holes from the solvent matrix. In all cases addition of Fe^{3+}reduces the formation of anions but the neutral reduced species which are formed during irradiation at 77 K remains unaltered. In all cases the H addition radicals at formed at different C positions of the nucleotide base after being formed at 77 K, also remained unaltered at higher temperature except in dGMP where guanine cation was formed via oxidation of H addition radical from matrix holes.

ACKNOWLEDGEMENT

The thesis presented here has taken its shape only after constant and consistent encouragement, support and inspiration provided by a large number of people. I express my enormous gratitude to all of them.

First and foremost I would like to express my indebted acknowledgement to my supervisor Prof. Dr. J. Hüttermann for his immense patience and constant encouragement for my work. I also acknowledge him for the financial support and the extent of freedom he had given me for my work. His experienced overview in this subject has greatly enriched the subject of my work.

I am immensely thankful to Dr. R. Kappl for a continuous help in all respect of my staying in Germany, from professional to personnel matters. He always found time for answering my all kinds of queries. Discussions with him regarding all kinds of scientific problems have provided new light to the matter under study. I am also grateful to Ms. R. Kaleja for her endless help for all kinds of official formalities throughout my stay in Germany.

I owe very much to Mr. J. Marx for the technical support he has always provided, especially for X ray irradiation. I am thankful to G. Rothaar and R. Stumpf for providing me immediate hand of technical help whenever I needed it.

I want to pay my thanks to Mr. E. Arnd and to Mr. G. Barcic for the smooth computational facilities they have maintained in this group.

I am especially thankful to my colleagues who have substantially contributed to the development of this work. Special thanks go to Ms. H. Luxenburger who has introduced me to this subject and helped me to learn the technical details of ESR spectroscopy. She has always helped me with all kinds of discussions regarding my research. I am also grateful to Mr. C. Müller and Mr. T. Dell for being very supportive colleagues.

I would like to thank ex-colleagues of mine specially Dr. Peter Schmidt, Mr. M Elbeweiser, Dr. K. Ranguelova for providing a very friendly and helpful scientific atmosphere to me.

Besides I would like to acknowledge all those friends of mine who were once there in Saarbruecken or homburg and now are spread in different parts of this world. I would also like to thank Dr. A. Singh and Dr. M. Rale for their constant support and encouragement.

I give my hearty thanks to the child care systems (Caritus, Saarbruecken and AWO, Homburg) without whose helping hands to look after my child I would not be able to finish this big task. I acknowledge the help of Ms. C. Ngassam who looked after my daughter during my long days at laboratory in Homburg.

I owe a very special thanks to my husband Dr. Sudip Roy for being so supportive, encouraging and understanding for all these years. I have no words to pay my gratitude to my little daughter Adwitiya (Jiya) whose small moves, cheerful smiles and never ending curiosities have always brought me more closure to my motivations.

I finally pay my acknowledgements to my grand parents and parents (Mr. B. K. Pal and Mrs. K. Pal), my brother Bhaskar and sister Gourismita, my parents-in-law (Mr. S. Roy and Mrs. N. Roy) and all other family members who have smilingly and patiently waited for us and encouraged us through all these years to fulfil our dreams.

Eidesstattliche Versicherung

Hiermit versichere ich an Eides statt, dass ich die vorliegende Arbeit selbstständig und ohne Benutzung anderer als der angegebenen Hilfsmittel angefertigt habe. Die aus anderen Quellen oder indirekt übernommenen Daten und Konzepte sind unter Angabe der Quelle gekennzeichnet. Die Arbeit wurde bisher weder im Innoch im Ausland in gleicher oder ähnlicher Form in einem Verfahren zur Erlangung eines akademischen Grades vorgelegt.

Ort, Datum   (Unterschrift)